Australian National University

Inside And Out: Virtual Anatomy and Cerebrocranial Evolution of The Temporal Regions in Anthropoid Primates

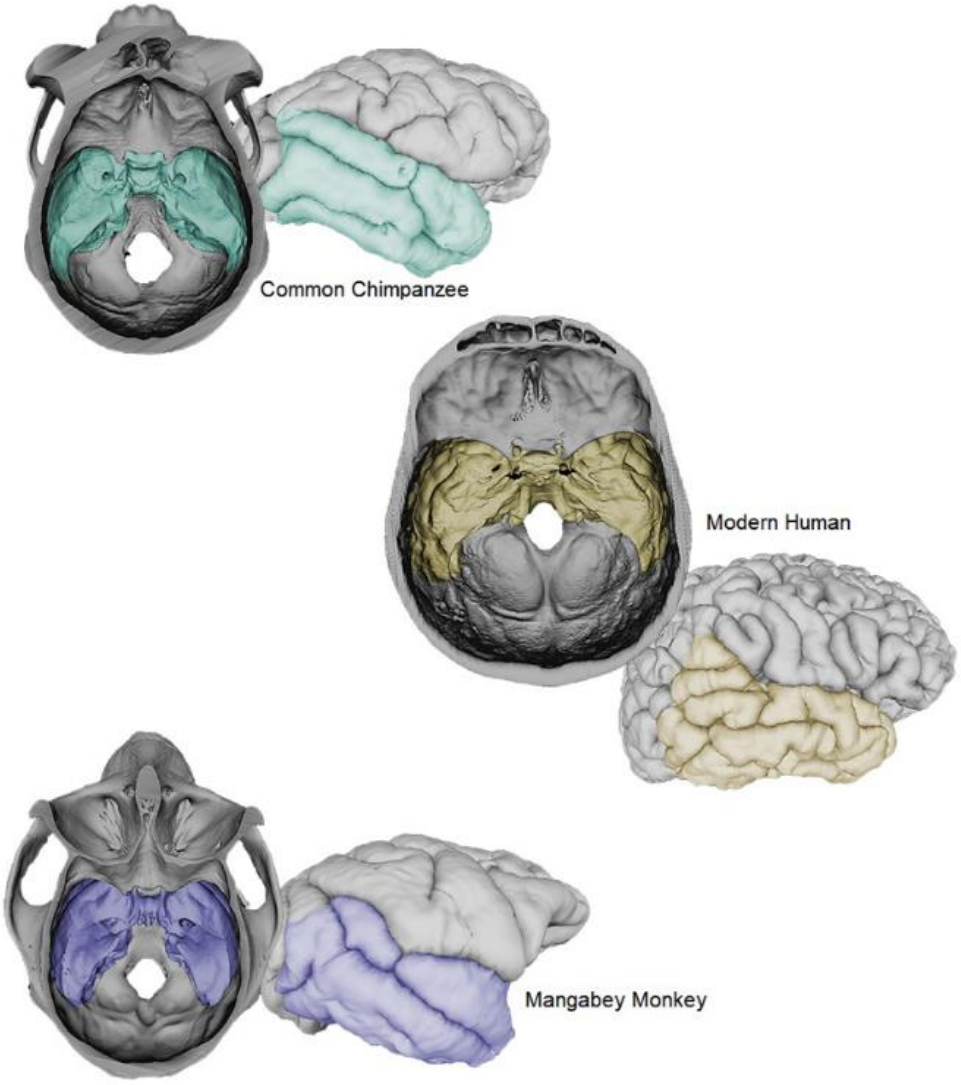

Alannah Kirsty Pearson

December 2023

A thesis submitted for the degree of Doctor of Philosophy of The Australian National University.

Department of Biological Anthropology, School of Archaeology and Anthropology

© Copyright 2023

Statement of Originality

The work presented in this thesis is, to the best of my knowledge and belief, original and my own work, except where acknowledged. This material has not been submitted either in whole or in part, for a degree at this or any other university.

Alannah Kirsty Pearson

At the time of submission, Chapter 3, 4, 5 and Chapter 6 were published. Chapter 7 is also now published at the time of corrections submission.

Chapter 3

Pearson, A., Polly, P. D., & Bruner, E. (2020). Is the middle cranial fossa a reliable predictor of temporal lobe volume in extant and fossil anthropoids? *American Journal of Physical Anthropology*. 172(4),698-713. doi:10.1002/ajpa.24053

Chapter 4

Pearson, A., Polly, P.D. & Bruner, E. (2021) Temporal lobe evolution in Javanese *Homo erectus* and African *Homo ergaster*: Inferences from the cranial base. *Quaternary International*, 603:5-21.

Chapter 5

Pearson, A., Bruner, E., Polly, P.D. (2023a) Updated imaging and phylogenetic comparative methods reassess relative temporal lobe size in anthropoids and modern humans. *American Journal of Physical Anthropology*,180(4) 768-776.

Chapter 6

Pearson, A., & Polly, P.D. (2023b) Temporal lobe evolution in extant and extinct Cercopithecoidea, *Journal of Mammalian Evolution*, 683–694.

Chapter 7

Pearson, A., & Polly, P.D. (2024) Temporal lobe evolution in Hominidae and the origin of human lobe proportions. *American Journal of Biological Anthropology* (early online view).

Acknowledgements

This dissertation is dedicated to Emeritus Professor Colin Groves (1942-2017) who provided so much wisdom, inspiration, knowledge and shared his passion for primatology with me. I am grateful to have been his student and for the guidance in designing the initial concepts of this dissertation including Dr Emiliano Bruner who shared his enthusiasm for Paleoneurology. I am forever appreciative to my supervisory panel: Professor Alison Behie (ANU), Professor P. David Polly (IU, Bloomington), Associate Professor Laura Wilson (ANU) for their enthusiasm for incredible support throughout this dissertation. I am forever grateful to Associate Professor Raymond Garrick, Professor Andrew Carr and my family and friends who have supported and encouraged me constantly throughout my dissertation. I'm in debt for hours of canine support from Master Ditto, Greta Munchkin and Lord Ciaran the Cuddly throughout this dissertation. Lastly, for the encouragement provided by the Biological Anthropology Labs at ANU, The Hominid Paleoneurology Lab at the CENIEH and the Polly Lab at IU.

Abstract

The brain does not preserve in the fossil record making any study of brain evolution reliant on endocasts or moulds of the inside of the skull. While endocasts are not the brain but retain neuroanatomical features preserved as imprints on the endocranium including the middle cranial fossae (MCF) which is in close spatial proximity to the temporal lobe of the brain where many cerebral features are retained on the surface of the MCF. Unfortunately for palaeoneurologists, the superior-posterior border of the temporal lobe cannot be defined on endocasts or the external surface of the brain but rely on internal neuroanatomy only observable from dissections or magnetic resonance imaging (MRI) of the brain. The temporal lobe its important in anthropoid evolution where it functions as a multimodal association cortex and is associated with many memory-related tasks, auditory and visual processing, and speech comprehension in modern humans.

The methodology includes virtual anatomy techniques such as computed tomography (CT) and micro-computed tomography (µCT) of the skull in extant anthropoids (n= 135) and magnetic resonance imagining (MRI) of the brain in extant anthropoids (n = 78) and CT and µCT in extinct anthropoids (n= 38) with a total sample size for extant and extinct anthropoids (N = 251).

I present, a new approach to predict temporal lobe volume (TLV) in extant and extinct anthropoids from the middle cranial fossa (MCF) using seven linear metrics I developed which are biologically homologous in the extant and extinct anthropoid taxa studied to allow for the first time, the quantification of temporal lobe size and middle cranial fossa (MCF). The findings presented in this thesis relate to five research aims. The prediction of (TLV) from any of the seven MCF metrics within +/- 1. S.E in the anthropoid taxa studied (Aim 1); for the first time,

the ability to predict TLV in fragmentary fossil remains noting species-specific differences between *Homo erectus* and *Homo ergaste*r (Aim 2); a reassessment of a foundational study using updated imaging and phylogenetic comparative analyses found contrary that modern humans did not have disproportionately large temporal lobe size but fit the general anthropoid trend (Aim 3); the prediction TLV relative to brain size in fossil catarrhines and extant cercopithecines indicated a relative increase in TLV associated with paleoenvironmental shifts from arboreal fossil catarrhines to semi-terrestrial cercopithecoids with potential increased social complexities (Aim 4); the comparison of absolute and relative TLV and proportions in extant hominids and fossil hominins where the greatest changes occurred in *Australopithecus*, *Paranthropus* and extant *Pan* species potentially reflecting the absolute, relative and temporal lobe size and proportions of the last common ancestor between chimpanzees and fossil hominins (Aim 5). This thesis examined the anthropoid trend over 40 million years of cerebrocranial temporal region evolution, the eco-behavioural trajectories for some anthropoid lineages and the application of phylogenetic comparative methods and virtual anatomy to examine the cerebrocranial temporal regions and enable future study directions for cerebral reorganisation in anthropoid primate evolution.

Table of Contents

Chapter 1: Introduction

This chapter outlines the thesis format, primary research aim to examine size changes in the cerebrocranial temporal region in extant and extinct anthropoids and details the subsequent secondary research aims and concludes with the ethics and permissions for this dissertation research.

1.1. Research Aims

The aim of this thesis was to determine the cerebrocranial association between the size of the temporal lobe of the brain and the middle cranial fossa of the skull in anthropoid primates. I adopt a unique approach combining medical imagining techniques including Computed tomography (CT) and Magnetic Resonance Imaging (MRI) for 11 extant anthropoids for individuals of the same species for the sample and micro-CT (μCT), laser surface scanning and close-range photogrammetry for fossil taxa to generate three dimensional (3D) virtual models. I relied on a combination of anatomical analyses, evolutionary analyses, advanced statistical regressions and phylogenetic comparative methods. I provide a new contribution to anthropoid primate brain evolution by the following research aims to predict temporal lobe volume and size-related changes:

1) Confirming the association between temporal lobe volume of the brain and middle cranial fossa size in anthropoids, to provide a reliable prediction of temporal lobe size in fossil anthropoids with application for examining cerebral reorganisation.
2) The application of a limited number of middle cranial fossa metrics to predict temporal lobe size in fragmentary fossil skulls.

3) Confirming whether modern humans have disproportionately large temporal lobes compared to other anthropoids using updated imaging and phylogenetic comparative methods.
4) Determining the relative difference of temporal lobe to brain size in extinct and extant old-world monkeys (Cercopithecoidea) and if potential cerebral reorganisation was associated with socio-behavioural shifts and paleoenvironmental changes over time.
5) Examining the evolutionary shifts in temporal lobe proportion in extant and extinct Hominidae and Hominini.

1.2. Thesis Overview

Chapter 1introduces this dissertation aims of examining cerebrocranial temporal lobe evolution in extant and fossil anthropoids.

Chapter 2 provides the background details on anthropoid primate neuroanatomy and endocranial anatomy. An overview of primate brain evolution, paleoneurology and implications for cerebral reorganisation among primates. A description of the virtual techniques employed, and the phylogenetic comparative method used before an overview of anthropoid taxonomy with a summary of extant anthropoid morphology and socio-behaviour before a description of extinct anthropoid taxonomy and a summary of the extinct taxa studied.

Chapter 3 (Aim 1) quantifies for the first time the association between the temporal lobe of the brain and the middle cranial fossa of the skull in extant anthropoids using seven linear metrics which I developed and are homologous among all anthropoid taxa studied. Each of seven metrics of the MCF provided statistically reliable to +/- 1 S.E and predict TLV in extant and extinct anthropoid including highly fragmented fossil remains.

Chapter 4 (Aim 2) uses three of the seven MCF metrics that are consistently present even in highly fragmented fossil crania in from African *Homo ergaster* and Javanese *Homo erectus* to predict TLV. The species differences were tested whether there was as much variation within Javanese *H. erectus* and African *H. ergaster* as observed in extant *Homo sapiens*. Species-specific differences were found in the relative temporal lobe size between African *H. ergaster* and Javanese *H. erectus*.

Chapter 5 (Aim 3) was to re-assesses the foundational research study whether temporal lobe size in modern humans was disproportionally large compared to other anthropoids using newer phylogenetic comparative methods, imaging techniques and a larger sample size The findings indicate the temporal lobe was not disproportionally large in modern humans compared to other extant anthropoids as previously found.

Chapter 6 (Aim 4) uses 7 MCF metrics to predict a single TLV for stem-anthropoids and extant cercopithecines. The relative temporal lobe size to brain size in fossil and extant old-world monkeys (Cercopithecoidea) indicated changes in temporal lobe size associated with shifts in socio-behavioural ecology from arboreal to semi-terrestrial monkeys and paleoenvironmental changes over a time span of 36 million years.

Chapter 7 (Aim 5) uses all 7 MCF metrics to predict a single TLV for extant great apes and fossil hominins with absolute, relative TLV and temporal lobe proportions for the Hominidae including fossil hominins and the Tribe Hominini alone. This first assessment of absolute and relative temporal lobe changes in the Hominidae indicated that temporal lobe proportion in modern humans and fossil hominins followed the same general trend for the Hominidae (all great apes) with greatest changes occurring in *Australopithecus*, *Paranthropus* and species of *Pan* examined within the framework of three main brain evolution hypotheses

(social, functional craniology and environmental) and may reflect the temporal lobe proportions and size of the last common ancestor between fossil hominins and chimpanzee lineages.

Chapter 8 provides a discussion synthesis of each of the research aims within the context of anthropoid brain evolution and the future avenues for research into cerebrocranial temporal lobe evolution in anthropoids and cerebrocranial changes in other regions of the brain beyond the temporal lobe and extension into other primate lineages and, more broadly, into other mammalian taxa.

Appendix A contains a thorough description of extant anthropoid taxa studied including classification systems, morphology, habitat diet, and social organisation.

Appendix B provides a description of the extinct anthropoid taxa studied including fossil site details, classification systems, general cranial morphology, estimated dating and endocranial descriptions.

Appendix C provides the sample composition for the anthropoid taxa studied including the imaging modality, specimen IDs and the museum sources.

1.3. Ethics and Permissions

All Magnetic Resonance Imaging (MRI) data was provided from published sources which adhered to human and animal ethics guidelines at the time of original publication. Access to Computed Tomography (CT) and micro-CT (μCT) were attained through museum agreements or permissions through online databases such as Morphosource.org and Nespos.org. The full digital acknowledgements are provided at the end of this thesis with

Appendix C containing the specimen collection IDs and source information for the digital sample.

Chapter 2: Background Information

2.1. Introduction

The following chapter will cover the discussion of the cranial and cerebral anatomy and functions of the cerebrocranial temporal regions including the middle cranial fossae and temporal lobe of the brain; virtual anatomy methods including computed tomography, magnetic resonance imaging, 3D laser surface-scanning and 3D close range photogrammetry; statistical analyses and phylogenetic comparative methods. An overview of primate brain evolution and the implications for socio-behaviour and cerebral reorganisation will conclude with a taxonomic listing of the extant and fossil anthropoid taxa studied in this thesis and conclusion. More detailed information on the extant and fossil anthropoid species and fossil specimens is provided in Appendices A-C.

2.2. Function and Evolution of the Cerebrocranium

Any consideration of cerebrocranial anatomy is dependent on the development and growth of the skull tissues and cerebral matter. Relevant to these factors are the studies of modularity, the biological process of how the skull develops and grows to form modules including the splanchnocranium (facial skeleton), neurocranium (vault) and basicranium (base). From an evolutionary perspective, modularity is an important foundation to understand how cranial anatomy may differ between and within species and to note that traits of these modules are not singular isolated skeletal element but can occur at different life stages according to species-specific growth and development factors which facilitate an evolutionary trait change (Enlow and Hans, 2008). The cerebrocranium is a logical extension of the cranial

modules to include the cerebral or brain matter. By this logic, cerebral tissue develops and grows with similar species-species changes and life stages and as the cerebrum is contained within the bony confines of the cranium, the cranium and cerebrum interact and influence each other during expansion and contraction of cranial elements and cerebral regions (Richtsmeier & Flaherty 2013).

2.2.1. Growth and Development of the Skull

The growth and development of these three cranial modules occurs at different stages throughout the development with cranial sutures of the basicranium fusing into a module before the neurocranium, and lastly, the facial skeleton. The study of cranial modules and how they interact as semi-autonomous bony regions is investigated by Enlow and Hans (2008) In the primary volume of growth and development of the human cranium.

The development of the skull from cartilaginous precursors (Thorgood,1993) comprises part of the basis for the concept that the skull develops in a modular manner in the skull. Further investigations into the phylogenetic relationships and cranial modules conducted by Cardini & Elton (2008), Cardini et al., (2015), Cardini & Polly (2013) and Adams et al., (2011) have yielded varying conclusions about whether cranial modules are consistent in mammals in an evolutionary context. There is also evidence that the complexity of cranial modules and differing evolutionary patterns and traits in the skull may yield it to grow in an integrated manner where each cranial module forms a semi-independent structure in an evolutionary context (Klingenberg, 2013).

In this thesis, the evolutionary context of anthropoid primates was accommodated through the Functional Craniology hypothesis proposed by Moss and Young (1960) which applies concepts of modularity and cranial integration arguing that cranial form may restrict

brain form. The interaction between cranial modules does not occur in isolation and all three endocranial fossae are involved in the growth of the cranium (Moore, 2009). The endocranial fossae are assumed to play primary roles influencing the morphology of the brain with the facial, vault and cranial base allowing for the expansion or constriction of the brain (Bruner, 2017). The middle cranial fossae are particularly important in the integration of the facial, vault and cranial base and potential expansion or constriction of the temporal lobes (Bastir et al., 2008).

2.2.2. Paleoneurology

Paleoneurology is the study of brain evolution. In the fossil record, the soft-tissue brain does not preserve, and brain morphology must be indirectly inferred from endocasts, physical or virtual moulds of the endocranial cavity (Holloway, 2018). The discoveries and descriptions of anthropoid primate fossil endocasts and inferences of anthropoid brain evolution predate the more commonly focused works from palaeoanthropology highlighted by Raymond Dart on *Australopithecus africanus* the 1920s with descriptions on the size and morphology of the endocasts (Dart, 1926). Later studies in investigated brain size and organisation in early hominins, including *Australopithecus africanus* which were based on endocranial impressions from the convolutional details of the brain Falk, 1980; 1983, 1989, 2009; Holloway, 1973, 1975, 1984, 1985, 1988, 1991). The Taung fossil of *Australopithecus africanus* comprises a natural hemi-endocast, or one where brain form has fossilised by geological matrix infill into the cranial cavity to preserve brain form and create an endocast (Neubauer et al., 2012). More commonly, endocasts must be created using either plaster or latex moulds on the inside of the skull to create a physical endocast (Holloway, 2018) or using virtual anatomy techniques which

employ computed tomography (CT) scans to generate a three-dimensional (3D) virtual endocasts (Zollikofer & Ponce de Leon, 2005) (see Figure 2.2.2.1).

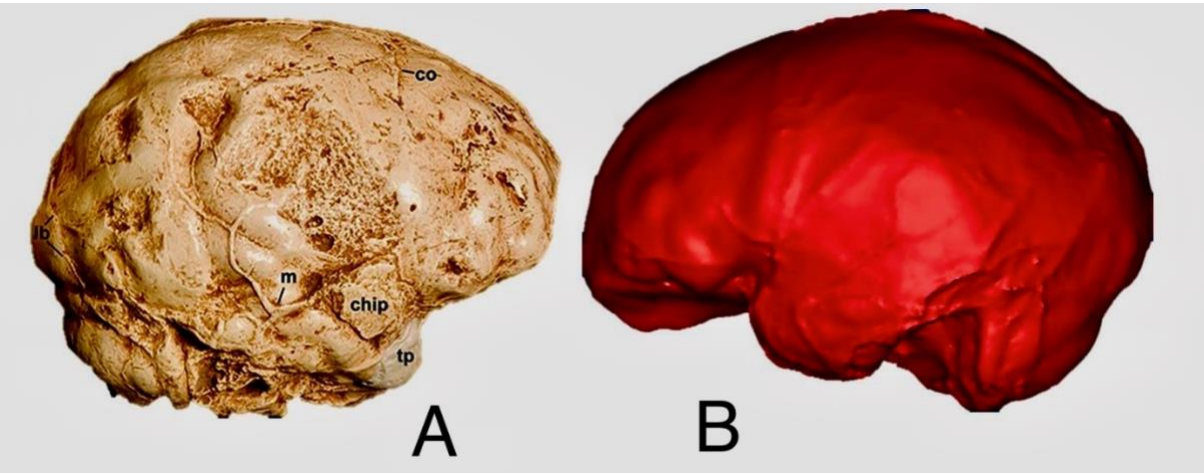

Figure 2.2.2-0-1. *A comparison of A) physical plaster endocast from the right lateral view and B) a virtual endocast from the left lateral view in a modern human. Image © Alannah Pearson.*

The development of paleoneurology is not limited to only palaeoanthropology. The investigations of fossil anthropoids excluding the extinct hominins, has a longer and more detailed history. Some of the earliest examinations of early primate endocasts include the genera *Tetonius homunculus* (Cope, 1884; Conroy, 1990) and *Adapis parisiensis* (Neumeyer, 1906) with descriptions and endocranial volumes by Gurche (1982) in adapoids *Adapis parisiensis*, *Notharctus tenebrosus* and *Smilodectes gracilis* but also extending into the omomyoids including *Tetonius homunculus*. More recent investigations of some of these genera using 3D virtual anatomy techniques by Harrington et al. (2016). A thorough discussion of early primate paleoneurology and descriptions of early ancestral primate endocasts is provided by Silcox et al. (2023).

Investigations in paleoneurology of stem-anthropoids includes descriptions and quantification of cranial and endocranial form in *Apidium* (Simons, 1995a), *Proteopithecus*

sylviae (Simons, 1997) and *Parapithecus grangeri* (Simons, 2001; Bush et al., 2004). The descriptions and quantification of stem-catarrhine absolute and relative endocranial volume was conducted using 3D virtual endocasts of *Aegyptopithecus zeuxis* by Simons et al. (2007) and cranial descriptions of *Catopithecus browni* by Simons & Ramussen (1996).

Paleoneurology in stem-platyrrhines has included descriptions of the endocranial morphology in *Homunculus patagonicus*, *Dolichocebus gaimanensis* and *Tremacebus harringtoni* where relative optic canals and orbit size as well as the olfactory fossa may suggest a similar nocturnal ecology in some extinct stem-platyrrhines with nocturnal extant platyrrhines such as *Aotus* (Kay et al., 2008; Kay et al., 2004; Kay et al., 2012; Fleagle & Tejedor, 2002; Kay & Simmons, 2008; Dominy 2004). Extensive discussions of the platyrrhine fossil record have been provided by Fleagle & Rosenberger (1990), Rosenberger (2002), Fleagle & Tejedor (2002) and Miocene northern neotropical taxa (Hartwig & Meldrum, 2002) and the extinct platyrrhines from Antilles and Brazil (McPhee and Horovitz, 2002) with more recent paleoneurological discussions on platyrrhine endocast asymmetry by Gonzles et al. (2022).

In stem-catarrhines and extant catarrhines, paleoneurological studies of absolute endocranial size and convolutional details between extant and extinct catarrhines by Radinsky (1974) and later Falk (1978). Descriptions and comparisons of relative and absolute endocast and cerebral reorganisation has also been provided extensively in fossil cercopithecoids including *Victoriapithecus macinnesi* (Benefit, 1999; Benefit & McCrossin, 2002; Gonzales et al., 2005) and comparison with extinct and extant cercopithecines and relative temporal lobe volume by Pearson and Polly (2023b).

2.2.3. Anatomy of the Endocranial Fossae

The endocranium comprises the anterior cranial fossa (ACF) which is associated with the frontal lobe of the brain, the posterior cranial fossa (PCF) associated with the cerebellum and occipital lobes and the middle cranial fossa (MCF) associated with the temporal lobes of the brain (Borden, Forseen, & Stefan, 2016) (see Figure 2.2.3.1.)

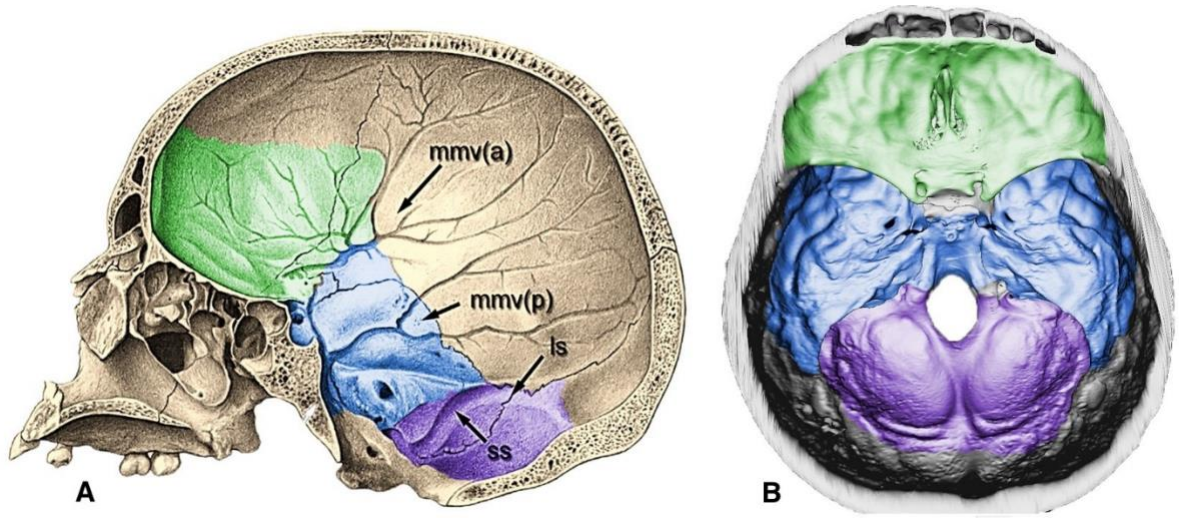

Figure 2.2.3-1. A depiction of the endocranium in A) midsection lateral aspect and B) superior angle showing the three endocranial fossae in a modern human skull with the anterior cranial fossae ACF (green), the middle cranial fossae or MCF (blue) and the posterior cranial fossae PCF (purple). Figure modified from Bruner (2017). Image © Alannah Pearson.

The frontal lobes of the of the brain fit closely within the anterior cranial fossae (ACF). On either side of the midline in the ACF is the cribriform plate which is part of the ethmoid bone and transmits the olfactory nerves ascending into the mucus membrane lining the surface of the upper nasal cavity. The olfactory bulb and tract lie adjacent to the cribriform plate and trauma to this region results in the loss of smell (Romanes, 2012). The optic canal is located medially to the sellae turcica and beneath the projection of the lesser wings of the sphenoid bone which along with the greater wings of the sphenoid, enclose the orbital region (Moore, 2009; White et al., 2011). The optic canal transmits the optic nerve and the ophthalmic artery

to the orbital cavity. In the case of the optic nerve, this passes directly into the eyeball. The central artery of the retina of the eye passes within a dural sheath that encloses the optic fibres. Any trauma received to this region can cause swelling of the optic sheath and the optic nerve within compressing the nerve fibres and vessels to potentially cause blindness (Romanes, 2012).

The temporal lobes of the brain are located within the middle cranial fossae (MCF). The superior orbital fissure conducts the oculomotor, trochlea, ophthalmic, the first division of the trigeminal, and the abducens nerves (Nolte, 2009; Romanes, 2012). The superior orbital fissure is located just beneath the edge of the anterior cranial fossa and receives the nerves as they project anteriorly into the orbital cavity. The foramen rotundum conducts the maxillary second division of the trigeminal nerve in an interior direction as it proceeds toward the upper teeth, nasal cavity, and face (Nolte, 2009). The foramen ovale transmits the mandibular or third division of the trigeminal nerve where it enters the infratemporal fossa just in front and below the ear but deep within the mandible and is responsible for innervating several of the muscles for mastication (Romanes, 2012).

The cerebellum fits within the posterior cranial fossae (PCF). The internal auditory meatus is located on the lateral wall of the petrous portion of the temporal bone and receives the facial nerves and vestibulocochlear nerves. Located inferiorly to the internal auditory meatus, the jugular foramen transmits the glossopharyngeal, vagus, cranial and spinal root of the accessory nerves (Nolte, 2009). These nerves share a foramen with the jugular vein which emerges from the sigmoid sinus where the jugular vein is responsible as one of the primary vascular vessels to drain blood from the brain (Nolte, 2009; Nolte 2013; Borden et al., 2016). Located within the PCF, the paired hypoglossal canals are positioned on either side of the

foramen magnum and conduct the hypoglossal nerve to be received at the base of the tongue (Nolte, 2009; Nolte 2013). The internal auditory, jugular, and hypoglossal nerves are arranged along the lateral aspects of the lower brainstem in a descending line with the foramen magnum the largest of the cranial foramina and transmits the spinal cord, vertebral arteries and the anterior and posterior spinal branches and the spinal roots of the accessory nerve where these enter or leave the cranium (Romanes, 2012).

2.2.4. Anatomy of the Cerebrocranial Temporal Regions

In this thesis, I have defined the middle cranial fossa (MCF) as comprising the squamous and petrous parts of the temporal bone and the greater wings of the sphenoid which are bound anteriorly by the lesser wings of the sphenoid and laterally by the squamous part of the temporal bone and posteriorly by the petrous part of the temporal bone (Lieberman et al. 2000a, 2000b; Lieberman, 2011; McCarthy, 2001).

The close spatial correspondence between the temporal lobe and the middle cranial fossa is most noticeable on the surface of the MCF, where sulcal imprints from the temporal lobe are retained on the lateral, anterior and inferior bony surfaces (Falk, 1978, 1980, 2014; Falk et al., 2018; Gonzales et al., 2015; Rosas et al. ,2014) as per Figure 2.2.4.1. and Figure 2.2.4.2. The extension of the Functional Craniology hypothesis into an evolutionary context is discussed by Bruner (2015) where reciprocal changes to skull and brain form are associated with the development and growth of both the brain and skull. The retention of sulcal imprints from the convolutions of the temporal lobe are particularly noticeable on the surface of MCF (Pearson et al., 2020; Labra et al., 2023).

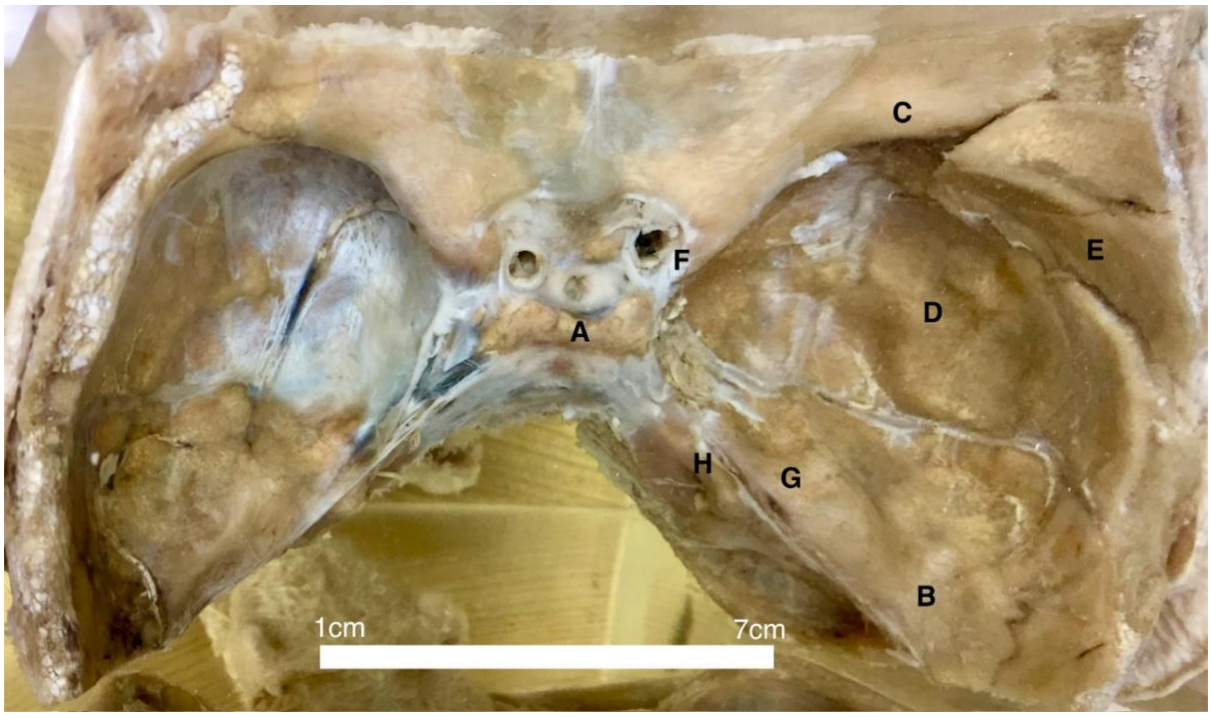

Figure 2.2.4-1. *A close-up image from the superior angle of a human cadaver head showing the middle cranial fossae where A) Sellae* turcica*; B) petrous bone; C) lesser wings of the sphenoid; D) the greater wings of the sphenoid; E) temporal bone; F) optic canal; G) carotid foramen; H) internal carotid and a nerve root. Specimen from Melbourne University Anatomy Lab. Image © Alannah Pearson.*

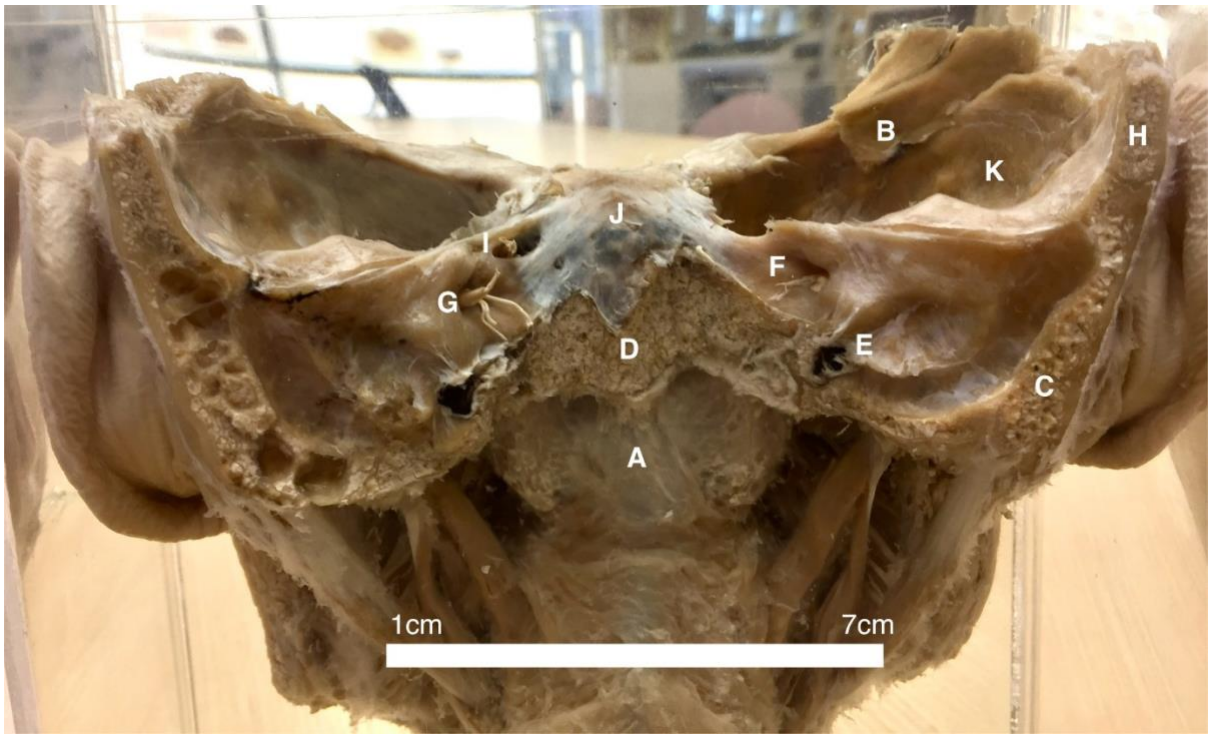

Figure 2.2.4-0-2 A midline section of a human cadaver head showing the middle cranial fossae, where A) spinal column; B) lesser wing of the sphenoid; C) squamous part of the petrous bone; D) basilar part of the basioccipital bone; F) foramen lacerum; G) carotid canal and deep petrosal nerve; H) temporal bone; I) Foramen ovalae; J) sellae turcica with dural tissue. Specimen from Melbourne University Anatomy Lab. Image © Alannah Pearson.

The interaction between the MCF and temporal lobe are potentially affected by structural changes to cranial morphology. For example, differences in angle of the cranial base nonhuman primates are associated with shifts in facial block angle (Lieberman et al., 2000b; McCarthy, 2001; 2004), while a further reduction in facial angle occurs in modern humans (Bastir et al., 2010; Bastir & Rosas, 2016; Lieberman, 2000a) combined with associated changes to mandibular form (Bastir et al., 2004).

Without a systematic examination the suitability of MCF measurements as a proxy for temporal lobe size, the accuracy of inferences in fossil species remains uncertain. The undertaking such an assessment is essential to understand whether the relative lengthening of the MCF in fossil *Homo* as suggested by Bastir et al. (2011) and Bastir et al. (2008) did not occur in fossil *Homo* but enlarged temporal lobes were present only in extant *Homo sapiens.*

Furthermore, the MCF has also been used to infer temporal lobe morphology in *Homo neanderthalensis* through comparisons between El Sidron fossil specimens and extant *Homo sapiens* (Rosas et al., 2014). There is a further complication by an absence of delimiting boundaries on the external surface of the temporal lobe of the brain and in endocasts (Kobayashi et al.2018). Thus, this makes understanding temporal lobe evolution difficult for palaeoneurologists and a comparative study of the evolution in temporal lobe size based on fossil endocasts has been unattainable.

2.2.5. Temporal Lobe Anatomy

The brain is divided into left and right hemispheres with the temporal lobe difficult to define in the superoposterior regions requiring either dissection or imaging techniques to delineate the borders with no distinguishable external boundaries on the lateral surface of the brain (Nolte, 2013; Rilling & Seligman, 2002; Borden et al., 2016). The temporal lobe and associated anatomy indicates the position of the temporal lobe in situ within the cranium (Figure 2.2.5.1).

The temporal lobe is separated from the frontal and parietal lobes by the lateral sulcus- a deep fissure within which Heschl's gyrus serves to define the posterior border on the inner or medial surface of the temporal lobe (Petrides, 2012). The superior temporal sulcus is very long and continues antero-superiorly from the temporal pole to terminate at the inferior parietal lobule and provide a definition for the borders of different subregions of the cerebral hemisphere (Borden et al., 2016; Petrides, 2012)

Superiorly, the temporal lobe is bound by the temporal pole where most anterior part of the superior temporal sulcus runs ventrally to meet at a parallel position to the lateral fissure.

The superior temporal sulcus forms the inferior border of the superior temporal gyrus and the superior border of the middle temporal gyrus.

Inferiorly, the temporal lobe is bound from below the superior temporal sulcus in a series of sulci collectively referred to as the inferior temporal sulcus which these convolutions are often retained on the endocranial surface of the middle cranial fossae (Labra et al., 2023; Bastir et al., 2008; Pearson et al., 2020; Bryant & Preuss, 2018).

Medially, the temporal lobe is defined by the parahippocampal gyrus where the parahippocampal cortex is continuous with the subiculum and the hippocampus. The hippocampal fissure separates the subiculum and from the dentate gyrus. Laterally adjacent inferomedial temporal region are three sulci known as the temporal incisure, the rhinal sulcus, and the collateral sulcus. The temporal lobe is bound by the collateral sulcus at the lateral boundary of the posterior parahippocampal region where this long sulcus continues posteriorly to the occipital region to form the ventral border of the lingual gyrus. Close to the end of the parahippocampal part of the collateral sulcus, a short forward projecting extension cuts through the parahippocampal gyrus known as the parahippocampal extension of the collateral sulcus where the anterior end meets the splenium of the corpus callosum (Petrides, 2012),

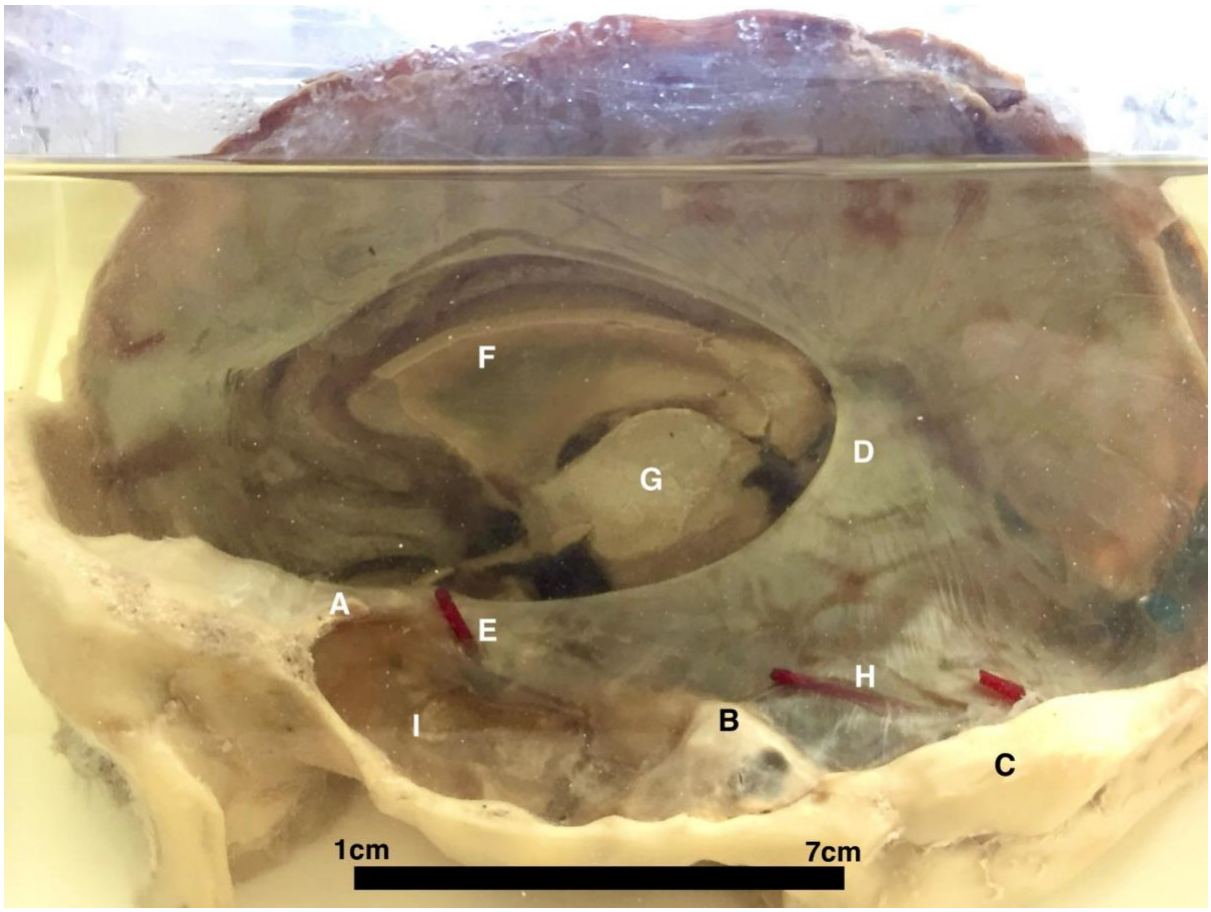

Figure 2.2.5-1 The lateral view of a mid-section of the modern human cadaver skull with the left cerebral hemisphere in-situ depicting the A) lesser wing of the sphenoid bone; B) petrous bone; C) the occipital bone; D) falx cerebri; E) internal carotid artery; F) corpus collosum; G) the limbic lobe; H) internal jugular vein; I) tentorium cerebelli. Specimen from the Melbourne University Anatomy Lab. Image © Alannah Pearson.

2.3. Primate Brain Function and Evolution

Generally, most studies into primate brain evolution have focused on comparisons with modern humans, in particular, the complexity of tasks performed by macaques and chimpanzees. The primary focus of studies has been on absolute and relative brain size comparisons with modern humans which are known to possess the largest brain size of any living primate. The following sections provide a discussion of absolute and relative primate brain studies, the socio-behavioural and ecological implications of nonhuman primate brain evolution and the implications of cerebral reorganisation for anthropoid brain evolution.

The brain is the largest organ in the head and its relative size is an important determinant of skull shape among primates. Relative to body mass primates have the largest brains of any terrestrial mammal except for marine mammals (Manger, 2006). There are differences, of course, between primate species and clades. For example, lemurs, lorises and tarsiers all have relatively smaller brains compared to monkeys and great apes with the largest absolute brain size in modern humans (Strier, 2017; Grabowski 2016; Grabowski et al., 2023). The primate brain is a complex organ with many regions relatively smaller or larger compared to each other (Semendeferi & Damasio, 2000; Rilling et al., 2006; Gonzales et al., 2015). Cerebral reorganisation of these brain regions includes the brainstem, cerebellum, and cerebrum and differs among primate species, which is associated with different neurofunctional, dietary and socio-behavioural adaptations (Strier, 2017; Grabowski et al., 2023; Pearson & Polly 2023b; 2024).

2.3.1. Cerebral Anatomy

The external surface of the brain and anatomy discussed here is provided in Figure 2.3.1.1 The frontal lobe of the brain has the most anterior point at the frontal pole and extends the central sulcus. The lateral sulcus separates the frontal from the temporal lobe where this extends laterally to the cingulate sulcus. Inferiorly, the frontal lobe continues as the orbital part of the frontal lobe and is associated with the orbits (Nolte, 2009; Nolte, 2013; Borden et al. 2016).

The parietal lobe extends posteriorly from the central sulcus to the upper most extent of the parieto-occipital sulcus and the lowermost extent at the pre-occipital notch. Inferiorly, the parietal lobe is bound by the lateral sulcus while medially it is bound by the sub parietal

and calcarine sulci where anteriorly it is delimited by the frontal lobe and posteriorly by the parieto-occipital sulcus (Nolte, 2009; Nolte 2013; Borden et al. 2016).

The temporal lobe of the brain is bound superiorly by the lateral sulcus and the inferior boundary of the parietal lobe. The posterior limit of the temporal lobe is bound by the parieto-occipital sulcus and on the inferior limit by the pre-occipital notch. The medial surface has no true limit but is bound by an 'hypothetical line' that extends from the pre-occipital notch to the splenium of the corpus collosum where the superior boundary ends at the collateral sulcus (Nolte, 2009; Nolte, 2013; Borden et al. 2016).

The occipital lobe of the brain is delimited anteriorly by the parietal and temporal lobes in terms of both the lateral and medial surfaces. The limbic lobe is thin cortex encircling the telencephalon-cephalon junction. The limbic lobe is located between the corpus collosum, frontal, parietal and occipital lobes, and curves medially into the surface of the temporal lobe (Nolte, 2009; Nolte, 2013; Borden et al. 2016).

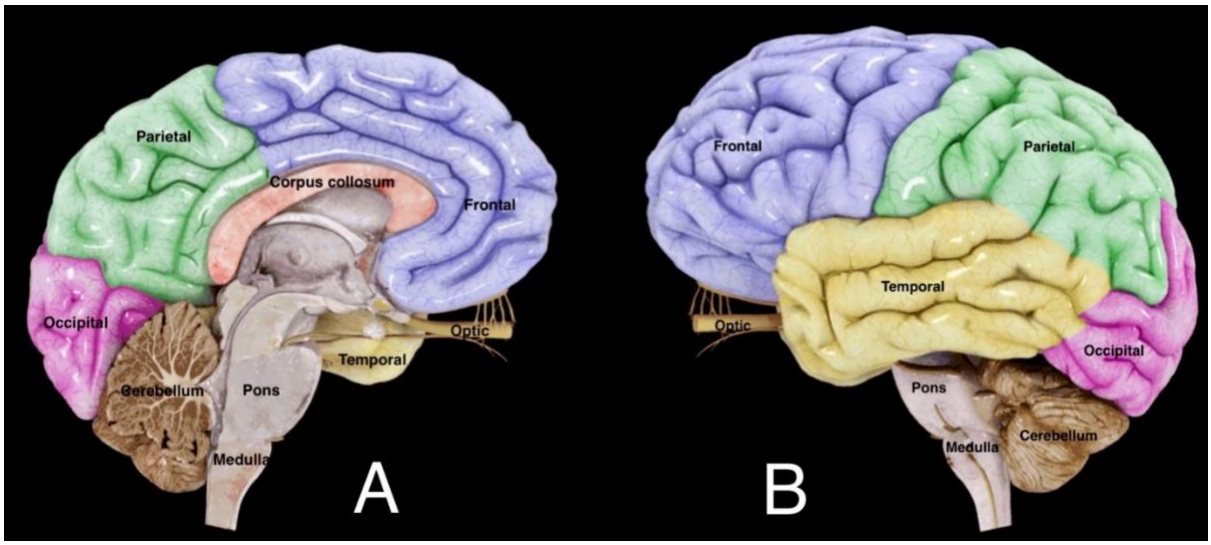

Figure 2.3.1-1 The anatomy of the human brain from a virtual model A) medial internal aspect and B) lateral aspect depicting the divisions of the brain with the temporal lobe (yellow); occipital lobe (pink), parietal lobe (green), frontal lobe (purple) and cerebellum (brown); corpus collosum (orange), the optic nerve, medulla and pons as labelled. Image modified from Essential Anatomy 5 IOS App. Image © Alannah Pearson.

2.3.2. Cerebral vascular systems

A comparison of the cerebral vascular systems in primates is important to define the endocranial shared morphologies and variations where there are implications for differences in cerebral blood supply. In turn, variation in cerebral vascular supply has relevance to potential differences cerebral regions to expand at different rates during cerebral development and growth between primate species in an evolutionary context. For paleoneurology, where inferences of brain evolution are reliant on endocranial form, differences in positioning of vascular foramina can relate to changes to relative cerebral structures (Falk, 1990). For example, the pattern and branches of the middle meningeal arteries are particularly variable and play a significant role in cerebral vasculature as well as brain drainage (Falk, 2008).

In primates, there are different adaptations for blood supply to the brain that reflect evolutionary relationships. Generally, the external carotid artery is responsible for supplying blood flow to structures of the neck and face, while the internal carotid and the vertebral artery supplies blood flow to the brain (Romanes, 2009; Borden et al., 2016). The internal carotid enters the cranial cavity as two distinct arterial branches: the stapedial passes through the stapes bone in the inner ear, and the promontory artery which crosses the promontorium, a raised surface in the middle ear, to the enter the cranial cavity (Fleagle, 2013; White & Folkens, 2011; Lieberman, 2011). However, there are distinct variations among primates as noted by Boyer et al. (2016) and Fleagle (2013) where the Lemuridae possess a relatively larger stapedial artery compared to lorises, galagos and cheirogaleids which are argued to rely on unique branch of the external carotid known as the ascending pharyngeal to provide the major blood supply to the front of the brain while the stapedial artery supplies the remainder of the brain (Fleagle, 2013 but see Boyer et al, 2016). In contrast, in haplorrhine primates,

including tarsiers, neotropical and old-world monkeys, all great apes including humans, the stapedial artery is absent in adults and the promontory artery provides the main blood supply for the brain (Fleagle, 2013).

2.3.3. Olfactory systems

The sensation of smell is carried by the olfactory nerves which end in paired projections called the olfactory bulbs which are located beneath the frontal lobes in most primates. The olfactory nerves receive input from sensory membranes within the turbinate of the internal nasal cavity (Nolte, 2009; Romanes, 2009).

The evolution of the olfactory system and the relative position to the orbits is morphologically variable among primates. For example, in primates and most other mammals, the nasal cavity has many turbinates attached to several different bones that derive from the ethmoid located in the sphenoid recess with the olfactory nerve passing between the orbits from the internal cranial cavity to the cerebrum (Fleagle, 2013).

In the strepsirrhines, there is a greater reliance on olfactory senses compared to haplorrhines with a retention of the vomeronasal organ located anteriorly on the palate as in many other mammals and is associated with the presence of a rhinarium and a longer snout and the detection of chemical and scent-based signals (Gould & Sauther, 2009; Fleagle, 2013). In contrast, haplorrhines including tarsiers, monkeys and all apes have a simplified nasal structure with a reduction in the reliance on smell which is similarly associated with a reduction in the absolute and relative size of the olfactory bulbs in anthropoids (excluding tarsiers) with a general trend for reduced olfactory reliance in favour of enhanced visual acuity (Gonzales et al., 2015; Sherwood & Gomez-Robles, 2017; Dominy & Lucas, 2001; Kawamura et al., 2012; Kirk & Kay, 2004; Villeux & Kirk, 2014).

2.3.4. Visual systems

The brain is functional organ and as such does not exist in isolation but in comparative anatomy where the brain and functional aspects of association systems including the visual system are important to discuss how changes to visual structures in the cranium may have associated changes to the visual systems of the brain. All primates rely extensively on the visual system to navigate their surroundings. There are considerable differences among primate visual systems, both in terms of the bony structure of the orbits and the soft tissue structures of the brain and eyeball. Generally, there is a correlation between eye size and ecology in all mammals including primates (Veilleux & Kirk, 2014).

Generally, primates have a greater visual reliance than other mammals, but visual acuity is variable. For example, nocturnal primates have relatively larger eyes and bony orbits than diurnal species (Kirk, 2006; Ross and Kirk, 2007). There are distinct differences among primates, were nocturnal primates generally have monochromatic vision except for *Daubentonia madagascariensis* where the blue visual wavelength is retained to allow cathemeral and nocturnal foraging (Melin et al., 2012). In contrast, diurnal neotropical monkeys are highly variable and generally have sex-linked trichromatic vision with both sexes of howler monkeys (*Alouatta*) possessing trichromatic vision (Kawamura et al., 2012). In contrast, most old-world monkeys and all apes have trichromatic vision in both sexes and relatively greater visual acuity than observed in neotropical monkeys and strepsirrhines (Kirk & Kay, 2000; Dominy & Lucus, 2001; Dominy, 2004).

In the cranium in extant strepsirrhines and most mammals, the lateral side of the orbit contains the zygomatic bone and frontal bone to join together to form the post orbital-bar or surrounded by a complete bony ring to allow protection from the masticatory muscles ((Moore,

2009). In contrast to strepsirrhines, haplorrhines including tarsiers, possess a bony orbit which is further contained by a postorbital closure which functions to further protect the eye from the increased effects of the masticatory muscles (White & Folkens, 2011; Lieberman 2011; Fleagle, 2013).

The overall structure of the eyeball is similar among all primates with the main difference in the structure of the retina where the light sensitive cells line the back of the eye (Rodieck, 1988; Melin et al., 2013). In general, the primate retina contains two types of cell types referred to as rods which are very sensitive to light but do not distinguish colour and cones which are sensitive to colour reception. In many nocturnal primates, the retina is composed almost predominantly of rods associated with the monochromatic vision.

In strepsirrhines and many nocturnal mammals, the retina contains an extra layer the *tapetum lucidum* which reduces diurnal visual acuity but enhances nocturnal acuity by reflecting incoming light back from the retina and preventing light-blindness (Fleagle, 2013). In contrast, haplorrhines do not possess a *tapetum lucidum* but instead possess a fovea in the eye where light-sensitive cones which are densely packed together enabling higher visual acuity with an increased number of cones in old-world monkeys and apes (Kirk & Kay, 2000). Inferences of fossil primate visual acuity is correlated with the relative size of the optic foramen which transmits the optic nerve from the eye to the brain and comparisons with extant taxa can provide an estimate visual acuity in extinct primates (Kirk & Kay, 2000).

The majority of diurnal primates have trichromatic colour vision, but there is species-specific diversity, but the majority of old-world monkeys and nonhuman apes possess trichromatic vision similar to that found in modern humans (Nolte, 2013). For extensive

discussion on the variation among strepsirrhine and haplorrhine primates where opsin and cone genes have been studied by Melin et al. (2013) and Perry et al. (2007).

2.3.5. Auditory and vestibular systems

The auditory senses play an important role for primates. In nocturnal primates where hearing is used to locate prey such as in Tarsiidae (Rosenberger, 2010; Gursky, 2015, 2019; Gursky & Nekaris, 2019) and in *Duabentonia madgascariensis* (Sterling & McCreless, 2006). The sensitivity of hearing apparatus and senses is also relevant to warn of approaching predators and is essential for receiving and recognising vocal signals emitted by both non-group and group members (Coleman & Colbert, 2010).

In terms of gross anatomy, the primate auditory system is divided into three parts or the outer, middle, and inner ear. The outer ear comprises the external ear lobe and a tube leading from the structure of the eardrum to the tympanic membrane (Romanes, 2012). The soft outer ear lobe of primates is extremely variable in size, shape, and mobility. For example, in strepsirrhines and tarsiers the ear lobe is large and membranous and highly mobile with a distinct set of muscles to enable precise movements used extensively to locate prey and also avoid predators (Coleman, & Colbert, 2010). In contrast, monkeys and all apes possess a relatively smaller ear lobe which is not mobile, but the outer ear is still responsible for receiving sound input, localising the information in terms of direction before transferring the information to the auditory canal where the tympanic membrane of the inner ear is activated (Nolte, 2009).

In all primates, the middle ear is covered by a thin sheet of bone called the auditory bulla. The tympanic membrane is a very thin connective tissue spread across the outside of the auditory meatus and tympanic membrane is highly sensitive with the input of sound waves transmitted as mechanical movements along the three ossicles of the middle ear and to the last

of these, the stapes bone, which then transfers sound waves into the fluid filled inner ear (Romanes, 2012).

The inner ear contains three functionally different parts contained within the petrous portion of the temporal bone. The first of these, the cochlea, is a fluid-filled pressure sensitive organ responsible for registering the movement of fluid and sending impulses to the brain through the acoustic nerve (Nolte, 2009). The semicircular canals are three fluid-filled chambers with the vestibule containing the saccule and utricle, all of which are associated with the sensation and processing of movement and orientation in space relative to gravity. This maintenance of equilibrium is highly associated with locomotion and maintaining balance (Nolte, 2009; Fleagle, 2013).

In all primate taxa, tympanic bone surrounds the eardrum and the relative position to the middle ear cavity varies considerably. The association between the semicircular canals and locomotion varies across primates. Faster moving and more specialised arboreal taxa compared to slower-moving arboreal and terrestrial quadrupeds including the families Lorisidae and Hominidae which have smaller relative semicircular canals compared to vertical clinging and leaping Lemuriformes and Tarsiiformes and specialised brachiators such as the Hylobatidae (small apes) with relatively larger semicircular canals (Spoor et al., 2007).

The physiological reasons for the differences in the configuration of the auditory bullae remains unclear. However, an inflated auditory bulla is found in many small nocturnal primates and may be associated with an increased registration of low frequency sounds and a potential adaptation for nocturnal predation of flying insects (Zimmerman, 2016). For example, in lemurs, the tympanic ring is suspended within the auditory bulla cavity while in lorises, the tympanic ring is connected to the wall of the bullae (Fleagle, 2013). In contrast, neotropical

monkeys possess a tympanic ring that is fused to the lateral wall of the bullae, while in tarsiers and catarrhines including all apes, the tympanic ring is attached to the lateral wall of the bullae and extends to form the bony ectotympanic tube (Fleagle, 2013).

2.3.6. Cerebral Functional Areas

The functional aspects of the brain and associated cerebral fibres and nerves are necessary for any discussion on comparative neuroanatomy and inferences from endocrania for extinct taxa where differences in the size and position of foramina that transmit nerves have relevance for the associated cerebral regions and functional attributes. Traditionally, the brain is divided into functional areas based on the original divisions in 1909 by Brodmann which has since been extended with the availability of further cytoarchitectural investigations (Amunts & Zilles, 2015). In this thesis, the following details of the major Broadman areas is intended as a generalised description only (see Figure 2.3.6.1).

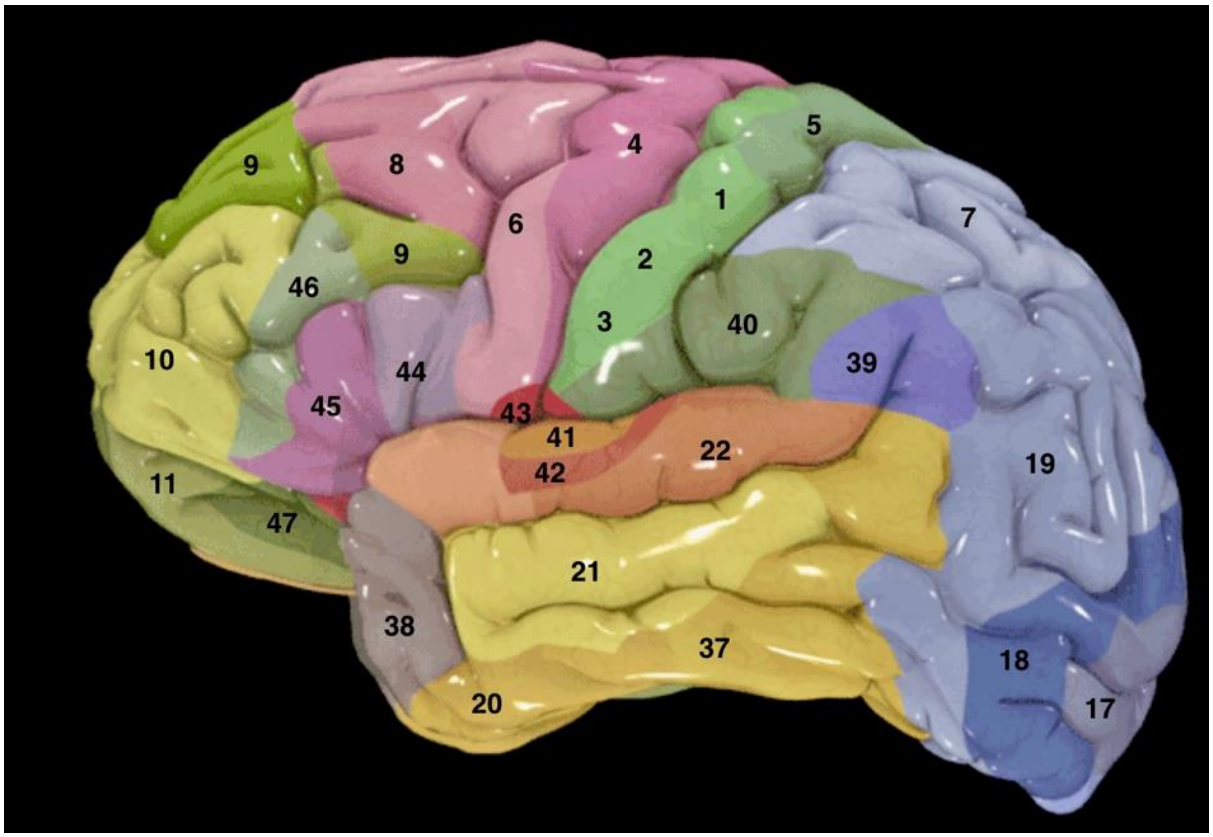

Figure 2.3.6-1 An image of a virtual brain in lateral aspect with Broadman's Areas labelled as discussed in the text. Image developed using Virtual Essentials Anatomy 5 IOS App. Image © Alannah Pearson

On the lateral surface of the frontal lobe, Area 4 corresponds to the precentral gyrus and is the primary function of discrete voluntary movements with the Area 6 positioned anteriorly and corresponding to the premotor cortex with stimulation of Area 6 passing signal to Area 4 where more generalised movement is then signalled. Positioned anteriorly to Area 6 is Area 8 which controls voluntary bilateral eye-movements (Nolte, 2009). Positioned further anteriorly, Areas 9, 10, 11 and 46 comprise the majority of the prefrontal cortex and are responsible for higher executive functions and do not appear to have any motor functions (Nolte, 2009). Located inferiorly and corresponding to the opercular and triangular gyri are Areas 44, 45 and 47 respectively which is associated with the left hemisphere and the motor speech area (Broca's Speech Area).

Located on the lateral surface of the parietal lobe, Areas 3, 1 and 2 correspond to the postcentral gyrus and are associated with the primary sensory area of the brain where signals are received as general sensations from throughout the body. Located at inferior-most base of the postcentral gyrus at the junction of the lateral sulcus is a secondary sensory area associated with the sensation of pain (Nolte, 2009). Area 40 is located near the supramarginal gyrus and Area 39 corresponds to the angular gyrus which are involved in imaging of the body and language processing.

On the lateral surface of the occipital lobe, Area 17 is the primary visual area and located on the medial surface of the occipital lobe where extends laterally across the occipital pole. The visual image from the eye that was dissected from the retina for transmission to the brain is re-assembled in Area 17 which is the posterior-most region of the occipital lobe, before imaging processing continues anteriorly in the adjacent Areas 18 and 19 and in the inferior temporal cortex with Areas 20, 21 and 37, respectively (Nolte, 2009).

On the lateral surface of the temporal lobe and adjacent to the lateral sulcus, is the primary auditory area of the brain where Areas 41 and 42 are located. The posterior portion of Area 22 referred to as Wernicke's area is associated with the interpretation of language (Nolte, 2009). Trauma received to this region of the brain results in the inability to comprehend spoken words (Romanes, 2012).

The limbic lobe is defined by cingulate and colossal sulci which delimit the superior and inferior boundaries of the cingulate gyrus which is a prominent part of the limbic lobe with cingulate gyrus associated with sexual and other behavioural aspects (Nolte, 2013).

2.3.7. Cerebral Fibres and Cranial Nerves

The discussion of the cerebral fibres and pathways is relevant to comparative neuroanatomy and for paleoneurology where inferences for extinct taxa must rely on the endocranial surface. The passage of cranial nerves through foramina in the skull has a clear association with the musculature, functional regions of the brain and sensory structures that these nerves innervate. The divisions and pathways of nerve fibres and the capacity for cerebral plasticity is directly related to the axonal and nerve fibre densities and neuronal pathway transmission speeds which do not show and apparent association with absolute brain size but rather the variation in modern humans and nonhuman primates shows a potential link between neuronal density and functional capacity and efficiency (Nolte, 2013).

The central nervous system comprises short association fibres that connect adjacent gyri and are often called U-fibres and long association tracts that consist of three major bundles: the *cingulum*, *uncinate fasciculus* (the Uncus) and the *arcuate fasciculus*.

The *cingulum* lies within the white matter of the cingulate gyrus and connects the frontal and parietal lobes and the ipsilateral parahippocampal gyrus, and to other parts of the temporal lobe and is considered a part of the limbic lobe (Nolte, 2013). The curved *uncinate fasciculus* forms of connection between the orbital gyrus of the frontal lobe, and the parts of the middle and inferior frontal gyri with the anterior region of the temporal lobe (Romanes, 2009). The deeper fibres of this bundle (*inferior occipitofrontal fasciculus*) extend into the occipital lobe and the *arcuate fasciculus* connects to the superior and middle frontal gyri with parts of the temporal lobe where the uppermost fibres constitute the *superior longitudinal fasciculus* (Nolte, 2013).

There are two primary fibre connections between the cerebral hemispheres known as the *corpus callosum* and the *anterior commissure*. The *corpus callosum* is a broad band of myelinated fibres that connects the cortical regions of one lobe with similarly placed regions in the opposing lobe (Nolte, 2013). At the most anterior point of the corpus collosum, the colossal fibres curve anteriorly to form the *anterior forceps* which is responsible for connecting regions of the frontal lobes while posteriorly, while fibres of the colossal *body* connect regions of parietal to the frontal lobes (Nolte, 2013; Borden et al., 2016). At the posterior-most extent of the *corpus callosum*, the colossal fibres of the *splenium* radiate posteriorly as the *posterior forceps* (Nolte, 2013). The cerebral commissures are associated with short-term memory and the transference of learned tasks from one hemisphere of the brain to the other (Nolte, 2009).

Nerve fibre projection tracts include the radiating masses of subcortical white fibres called the *corona radiata*. Posteriorly, the *corona radiata* condense to form the internal capsule where V-shaped bands of fibres descend between the *lentricular nucleus* laterally and the *caudate nucleus* and thalamus medially before continuing into the midbrain as the *crus cerebri* (Romanes, 2009).

The internal capsule is divided into five main components. The anterior limb is located between the *caudate* and the *lentiform nucleus* with the fronto-pontine fibres and other fibres connecting the thalamus with the frontal cortex (Nolte, 2009). Located between the posterior limbs of the internal capsule are the corticobulbar fibres where the largest of these, the posterior limb consists of the corticospinal and parieto-occipital-temporo-pontine fibres (Nolte, 2013). The retro lenticular fibres originate mostly from the lateral geniculate and pass behind the lentiform nucleus to form part of the *corona radiata* (Nolte, 2009). These sublenticular fibres are responsible for the auditory areas in the temporal lobe (Nolte, 2013).

There are twelve cranial nerves which are responsible for conducting and innervating sensory systems of the brain.

The olfactory nerve (I) consists of short, fine fibres that passes across the mucus membrane on the roof of the nasal cavity to receive scent signal before this is passed through the perforated bony plate to enter the olfactory bulb. The olfactory bulb and the continuous olfactory nerve tract are extended parts of the telencephalon and are not strictly considered nerves (Nolte, 2009). However, the optic nerve (II) originates in the retina posteriorly in the eyeball. The nerve fibres leave the eyeball and surrounding orbit to enter the middle cranial fossa of the skull where they merge with the contralateral fibres of the optic chiasm. Similar to the olfactory bulb, the optic chiasma and continuous tracts are considered extended parts of the diencephalon (Nolte, 2009).

The oculomotor nerve (III) projects from the midbrain to enters the orbit and innervate four of the six extrinsic eye muscles and the intrinsic eye muscles as well as the upper eyelid. The trochlea nerve (IV) projects from the midbrain where it originates from the posterior surface to enter the orbit near the oculomotor nerve and innervates the superior oblique extrinsic eye muscle. The trigeminal nerve (V) arises from the pons of the brain in three branches with each passing through different foramina of the skull to provide sensory fibres to the face, nose, and mouth (Nolte, 2009). The third branch of the trigeminal nerve contains a motor component for the muscles of mastication and the *tensor tympani* muscle for the middle ear.

The abducens nerve (VI) arises at the pontine-medullary junction and enters the orbit with the oculomotor and trochlea nerve to innervate the lateral rectus extrinsic eye muscle (Romanes, 2009). The facial nerve (VII) consists of two branches that originate at cerebello-

pontine and divide complexly. For example, the facial nerve supplies the innervation to the muscles of facial expression, the stapedius in the middle ear, two pairs of salivary glands, the soft palate of the mouth and lastly, the taste buds at the anterior-most part of the tongue (Nolte, 2009).

The vestibulocochlear nerve (VIII) originates in the medulla oblongata at the cerebello-pontine and enters the inner ear as two sections where the cochlea nerve responsible for hearing and the vestibular nerve is responsible for maintaining balance (Nolte, 2013). The glossopharyngeal nerve (IX) exists in the medulla oblongata to supply the taste buds of the posterior-most part of the tongue as well as the parotid salivary glands and to innervate the muscles of the pharynx. The vagus nerve (X) originates in the medulla oblongata to supply the sensory innervation to the pharynx, larynx, thoracic and abdominal viscera as well as part of the ear being responsible for maintaining aspects of balance equilibrium related to the ears.

The accessory nerve (XI) has both a spinal and cranial component where the cranial component is considered an accessory to the vagus nerve, while the spinal component (the root) innervates the large neck muscles, the sternocleidomastoid muscles, and the trapezius muscles (Nolte, 2013). The final cranial nerve, the hypoglossal nerve (XII) originates in the medulla oblongata to enter the skull and supply innervation to the muscles of the tongue.

2.3.8. Comparative Cerebrocranial Anatomy in Anthropoid Primates

The interconnected structures of the temporal cerebrocranial system comprise the temporal lobe of the brain and the middle cranial fossa of the skull. The morphogenesis of the cerebrocranial temporal regions is complex and driven by complex cell to cell signalling networks which are specific to the cellular type and occurring throughout the embryonic stages of development. During embryonic development, the basicranium is derived from

endochondral ossification and cartilage precursors (Thorgood, 1993), while the temporal lobe is derived from neural crest cells and the meninges of the brain derived from the cephalic mesoderm (Richtsmeier & Flaherty, 2013). This morphogenesis is responsible for the close spatial correspondence between the temporal lobe of the brain and the middle cranial fossa and is consistent across all mammalian taxa including anthropoid primates.

2.3.9. Absolute and Relative Primate Brain Size

The absolute and relative-to-body-mass, brain size in *Homo sapiens* is largest of all mammals except for marine mammals (Manger, 2006).

While most studies have focused on absolute brain size in nonhuman primates (Isler, 2008; Navarrete et. al, 2018) others have focused on human evolution and language development (Falk, 1992; Holloway, 1980). There are many enlarged specialised regions in the human brain including Broca's Cap which is located only the left hemisphere and is relevant for speech production (Amunts & Zilles, 2012).

Cerebral reorganisation in terms of temporal lobe has generated conflicting conclusions about whether or not *Homo sapiens* fit the generalised trend of relative brain size to temporal lobe size compared to other anthropoids (Semendeferi & Damasio, 2000; Rilling & Insel 1996; 2002; Pearson et al., 2023). However, the nonhuman primate brain does not appear to be an allometrically 'scaled-up' version of the modern human brain but is species-specific (Rilling 2006; Pearson et al, 2023).

Absolute and relative brain size increase has been the core focus in human evolution and especially regarding language development (Falk, 1992, 2012; Holloway, 2012; Beaudet, 2017). The have been several recent studies of nonhuman primate brain size and shape from endocasts (Sansalone et al., 2019; Beaudet et al., 2016) but these do not show the complexity

of brain evolution but rather a generalised trend of size increase and generalised changes to brain shape (Labra et al., 2023). The relevance of cerebral reorganisation is discussed extensively by Bruner et al. (2014) where the functional craniology hypothesis is considered in terms of reciprocal changes between skull and brain form and where a change in one is necessary to change the other. This is highly relevant for paleoneurology to better understand where and when cerebral reorganisation occurred in extinct taxa and the implications of different brain regions changing relative to other which has both neurofunctional and socio-behavioural implications.

The specialisations and unique brain evolution trajectories of nonhuman primates are necessary to understand the evolutionary changes that occurred in cerebral reorganisation and the anatomical and functional differences between nonhuman primate species and tour own species.

2.3.10. Implications of Cerebral Reorganisation

The application of studying cerebral reorganisation, or the relative change of one brain region to another, can provide far more meaningful investigation of potential functional changes in primate brain evolution than the generalised study of overall brain size and form. For example, *Victoriapithecus macinesi*, a 15-million-year-old fossil cercopithecine possessed olfactory bulbs that were relatively larger than expected for brain size in a Middle Miocene cercopithecine and indicated the potential retention of an ancestral trait in this species (Gonzales et al., 2015). Additionally, relative size changes to the precuneus of the parietal lobe in some extant anthropoids is different to that observed in modern humans (Bruner et al., 2014)

There is also evidence for the reorganisation of white matter tracts between chimpanzees and macaques with humans showing further specialisation (Roumazeilles et al.,

2020). However, there is no clear evidence of the homology of these gross anatomical changes between human and nonhuman primates and the application to extinct taxa is only an estimation in terms of neurofunctional aspects (Bruner, 2021). A more recent examination of absolute, relative temporal lobe size to brain size in Hominidae and fossil hominins by Pearson and Polly (2024) did not find an increase in relative temporal lobe size in later fossil hominins which suggests that other regions of the cerebrum potential are relatively larger with greater reliance possible on the frontal and prefrontal cortices in later fossil *Homo* associated with higher functioning tasks (Sherwood et al., 2017; Rilling 2006).

2.4. Virtual Anatomy and Analysis Methods

In this thesis, all virtual 3D crania were aligned in the Frankfurt horizontal plane before digitally sectioned along the transverse (coronal) plane to remove the neurocranial vault and access the middle cranial fossa (MCF) of the endocranium. The virtual segmentation process from the brain within the skull, the meningeal layers, vascular systems and the cerebral cortex is represented in Figure 2.4.1.

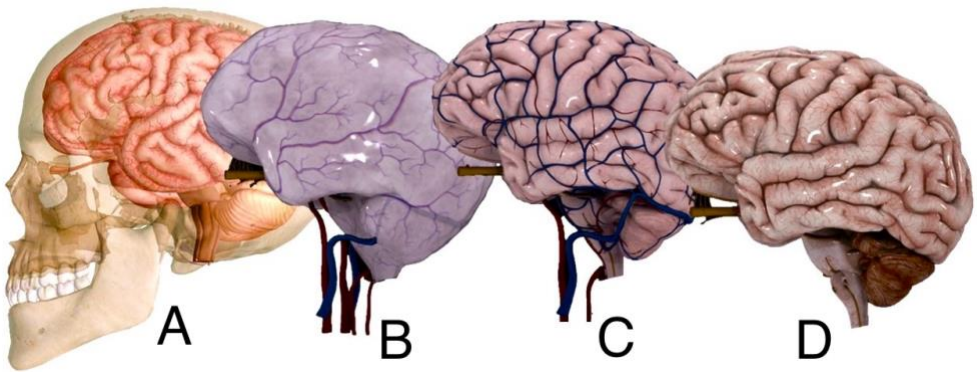

Figure 2.4-1 An image in lateral angle depicting the cerebrocranial anatomy of a modern human where A) in-situ skull brain (cerebrocranium); B) the brain when covered by meninges; C) the brain with vascular system and the meninges removed; D) the brain without the meninges or vascular systems. Image developed using Essential Anatomy 5 IOS App. Image © Alannah Pearson.

2.4.1. Computed Tomography

Computed Tomography (CT) is now a widespread imaging technique which uses radiation and refraction methods while moving around the object in question. Ponce de Leon and Zollikofer (2005) describe CT imaging processes where a planar beam of parallel X-rays sent through the subject and received by a one-dimensional detector array on the opposite side to the beams. Unlike in traditional X-radiography (X-Ray) where the source detector is stationary, in CT it rotates around the subject to obtain projections from different points of view.

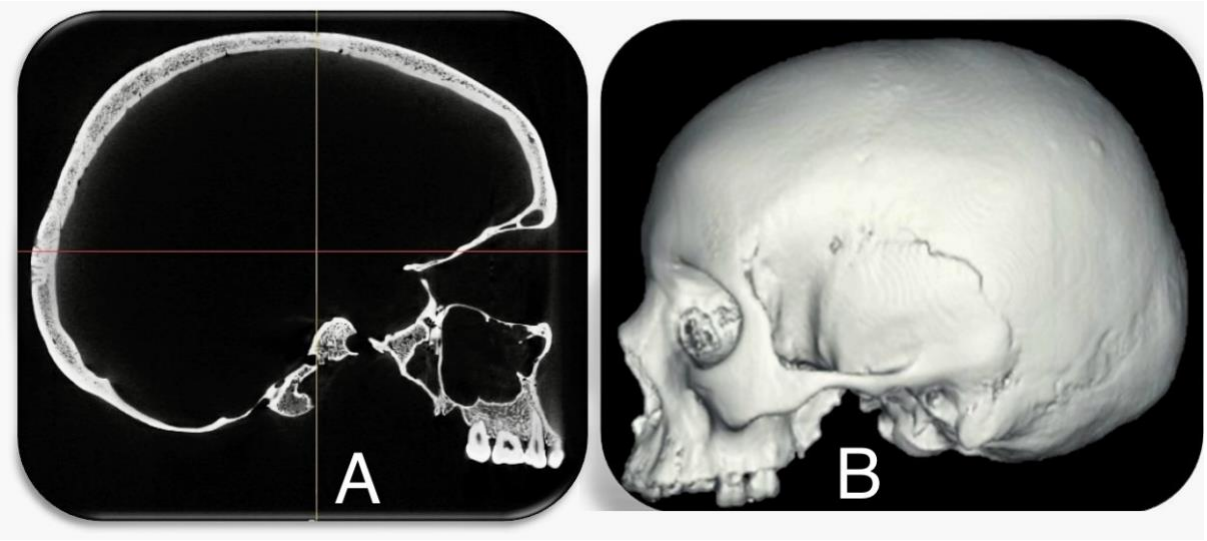

Figure 2.4.1-1 A depiction of A) A mid-section image from a CT stack of images of a modern human cranium and B) the lateral aspect of a virtual 3D skull generated from CT scans. Image © Alannah Pearson.

Each voxel (x, y, z) of the scanned subject contributes to various projections. This process is a standard method from many CT types, be they helical, multi-slice or slice-by-slice functions (Goldman 2008). Once these images are recorded by the processes described above, back-projection inversely reconstructs the acquired CT slices to form an image stack. From here these image slices can be converted into a three-dimensional mesh (a 3D virtual model). This is a semi-automated segmentation step where the image projections are spread in the

reverse order to their acquisition along the x-ray-path and then superimposed on a cross-sectional plane to enable the generation of a 3D virtual mesh (Ponce de Leon & Zollikofer, 2005). In this thesis, virtual segmentation of all raw CT and µCT data and post-processing was carried out in 3DSlicer (Fedrov et al. 2014) (see Figure 2.4.1.1).

In this thesis, I did not request any CT scanning on subjects nor scan any subjects myself but rather relied on various international researchers and institutions who had already undertaken CT scanning of subjects. All researchers and institutions who provided specimen and imaging access are in the Digital Acknowledgments at the end of the thesis.

2.4.2. Magnetic Resonance Imaging

In this thesis, Magnetic resonance imaging (MRI) was used to collect volumetric data from *in-vivo* brain MRI to produce 3D virtual models (see Figure 2.4.2.1). MRI is a stereoscopic technique similar to computed tomography (CT), where for each voxel of an object the MRI signal must be received and decoded with any given voxel conveying information about its relative location, and as with CT, image reconstruction is via back-projection and voxels superimposed.

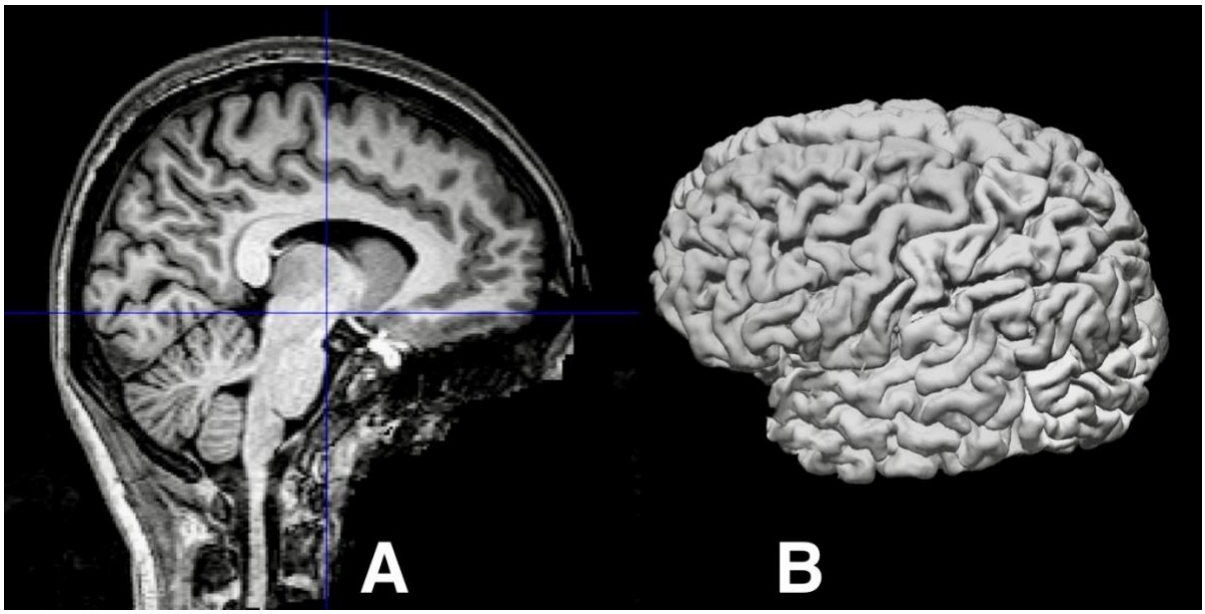

Figure 2.4.2-1. A depiction of the A) a mid-section angle of MRI scan of a modern human B) a lateral angle of a virtual 3D brain of the left hemisphere generated from the MRI scans. Image © Alannah Pearson

Compared to CT, MRI is more technically demanding but also less invasive (the energy of radio signals is about one millionth of the energy of x-rays and does not damage tissues). However, strong magnetic fields are required. A radio frequency signal is sent with a current through superconducting coils cooled to near zero temperatures. These fields are in a tesla range that is 30,000 times stronger than a magnetic field of earth and thus, extreme caution is needed to avoid potentially harmful displacement of metal objects, either outside or inside the human body. However, the benefit of MRI is the absence harmful ionising radiation in CT imaging and the higher definition and the ability to differentiate between various soft tissues.

In MRI, the signal emitted by each voxel contains information about the density H-atoms and the chemical composition within the body. The relationship of H-atoms and surrounding electrons creates tissue-specific values of T1 and T2 MR imaging with different tissues emitting signals at different intensities (Zollikofer & Ponce de Leon, 2005).

2.4.3. 3D Laser Surface Scanning

In this thesis, I also used a third imaging modality to acquire 3D virtual models using laser surface scanning (see Figure 2.4.3.1.) Three-dimensional laser surface scanners capture light reflected from a subject by using an independent light source of "known" values onto the subject so that depth cues can be returned from the reflected light signal (Ponce de Leon & Zollikofer 2005). Devices like the NextEngine scanner used in this thesis, involve a narrow set of laser beams scanning the surface of the subject along virtual gridlines (Ponce de Leon & Zollikofer, 2005). Virtual gridlines are set by the scanner has the laser beams follow a 'known' trajectory which varies depending on the distance between the object and the scanner or whether the macro, wide or extended modes of operation are used. There are advantages and disadvantages in precision and accuracy to each mode but for a small object like a tarsier skull or human carpal bone the macro setting is best suited but to scan a larger object such as a modern human skull the extended mode is best suited. In this thesis, I have used the wide mode to scan research quality casts.

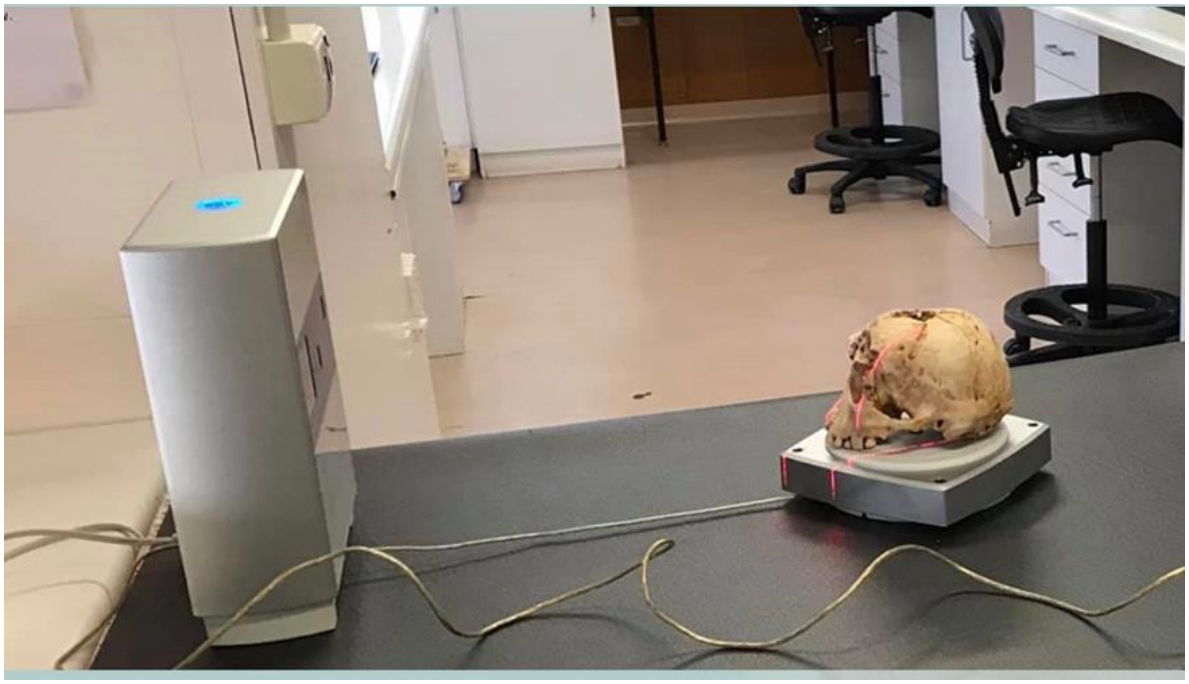

Figure 2.4.3-1 The setup for 3D Laser surface scanning of a research quality cast held at ANU Biological Anthropology department. Image © Alannah Pearson.

The increased use of 3D laser surface scanning in biological anthropology and subdisciplines has highlighted several known issues with accuracy of 3D laser surface scanners which are largely based on purchase cost with cheaper scanners like the NextEngine scanner often having lower precision compared to more expensive scanners like the Breuckmann scanners (Friess, 2012). Generally, a laser surface scanner "wraps" a 2D image of the object using the lasers and cameras to create a series of surfaces images of the 3D object with only the surfaces facing the scanner able to be recorded (Ponce de Leon & Zollikofer, 2005).

This can be partially overcome using a 3D laser surface scanner like the NextEngine scanner which rotates the object around a known path using the turntable set to a constant 3D rotation around a 'known' trajectory. This has somewhat alleviated the problem of "holes" or missing surface information during scanning. I have further improved this 360° rotation method by using the 360° rotation scanning followed by scanning each surface of the object independently and then using the Scan Soft software to connect the 360° rotation to each the

single surface scans. This creates smaller “holes” common in 3D laser surface scanning and allows a more reliable estimation of the surfaces. In addition, ‘hole filling’ was conducted using Poisson surface reconstruction algorithm (Kazhdan et al., 2006) in the software MeshLab to generate higher precision estimation of the missing sections of the surfaces. The Poisson surface reconstruction creates a complete 3D virtual model which is then suitable for data analysis. Although the scanning process I have outlined is more time-consuming, the 3D virtual models have an improved accuracy of 0.0508mm.

2.4.4. Close Range 3D Photogrammetry

In this thesis, I used a fourth imaging modality referred to as Close-Range 3D Photogrammetry to acquire 3D virtual models where CT and µCT imaging was unavailable and the endocranial surface inaccessible using a 3D laser-surface scanner. Three-dimensional Close-Range Photogrammetry was employed to generate 3D virtual models from research quality casts following the protocols and techniques outlined in Mallison & Wings (2014) and Luhmann et al. (2014) (see Figure 2.4.4.1.).

Figure 2.4.4-1 The 3D Close-Range Photogrammetry of a research quality cast held at ANU Biological Anthropology department. Image © Alannah Pearson

3D Close Range Photogrammetry is an extension of the 2D photogrammetry technique where two-dimensional (2D) images are acquired using a digital SLR camera. Scaling markers with identifiers which are automatically noted by the post-processing software *Agisoft PhotoScan* version 1.2.6 (Agisoft, 2016) allow for correct scaling of the object with image acquisition acquired by taking extensive overlapping photographs in clockwise rotation around the stationary object. Thus, multiple overlapping 2D images of the front, left, back, right, and top ensured the best coverage of the object and aided in reducing post-processing time with each image providing a location relative to each other (Luhmann et al., 2014). To acquire images of the underside of the object while it remained stationary, a contrasting-coloured background ensured that the post-processing software recognises the underside as a different region to the top (Mallison & Wings, 2014).

The endocranial surface of a research quality cast was obtained using the same protocols outlined above for the exterior surface of a skull. To capture the endocranial surface, multiple 2D overlapping photographs while the object was stationary with 2D images of the

endocranial surface acquired through large and small gaps corresponding to the missing sections in the original fossil specimens.

In post-processing, all the 2D images were loaded into *Agisoft PhotoScan* version 1.2.6 (Agisoft, 2016) with scaling dimensions of the research quality cast recorded by the software from the scaling bars used when capturing images of the exterior surface of the cast. The exterior and interior 3D virtual surfaces were then merged into the single 3D virtual cranium and endocranium of the research quality cast. Quantification of the scaling of the 3D virtual specimen were compared to the original measurements recorded on the research quality cast and the published measurements from the original fossil specimens. There was no deviation between scaling 3D virtual specimen and research quality cast or the original fossil specimen.

2.4.5. Virtual Endocasts

In this thesis, the Computed Tomography scans were used to generate virtual 3D endocasts in extant taxa. The generation of 3D virtual endocasts followed the protocols outlined in Zollikofer & Ponce de Leon (2005) with modification following Fedorov et al. (2012) and processed in the software *3D Slicer* (Fedorov et al., 2012).

All CT and µCT scans were first segmented using a semi-automated process to separate out all bony tissue from 'noise' before a semi-automated segmentation process to apply an additional number of pixels to the cranium with this process closing any naturally occurring foramina, auditory and orbital regions. A 3D virtual line was generated and manually positioned using the CT scans to close the foramen magnum and create a 'water-tight' cranium. The internal cranial cavity was then virtually 'filled' to generate a 3D virtual endocast.

The initial pixels added to the cranial tissue during segmentation process were then removed from the skull and the precise number added to the virtual endocast. This process

ensured that the 3D virtual endocast filled the entire endocranial cavity and the number of pixels calculated was species-specific. For example, the number of pixels calculated to close all bony orbits and foramina was dependent on the bony cranial tissue and thinner and more fragile cranial bones in extant *Homo sapiens* required more pixels to close the cranium than thicker cranial bones in extant *Gorilla gorilla*. This process allowed the generation of both on a 3D virtual endocasts and crania (Figure 2.4.5.1). The volume of the endocast was calculated directly in cubic centimetres within the software *3D Slicer* (Fedorov et al., 2012).

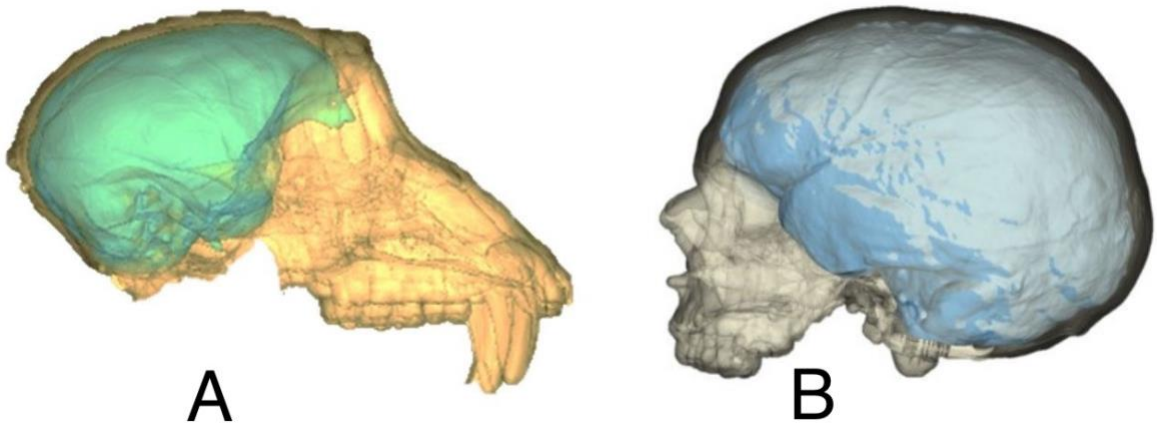

Figure 2.4.5-1 Virtual endocast generated from CT scans in lateral view of A) right later view of a mangabey and B) left lateral view of a modern human. Image © Alannah Pearson.

2.4.6. Data collection and Phylogenetic Comparative Methods

Data collection included linear 2D measurements from the virtual 3D crania which were aligned in the Frankfurt horizontal plane before digitally sectioned along the transverse (coronal) plane to remove the cranial vault and access the endocranium including the middle cranial fossa. The 3D virtual crania were generated using three different imaging methods noted above including CT segmentation in *Mimics 17* (Materialise, 2018), laser surface scanning using NextEngine *ScanSoft* and 3D Photogrammetry using *Agisoft PhotoScan* version 1.2.6 (Agisoft, 2016), and virtual endocast generation using *3D Slicer* (Federov et al., 2012).

Measurements of the middle cranial fossa were recorded using in *CheckPoint* (Stratovan, 2018) then converted to linear metrics using interlandmark distances (in mm) in the *R* package Geomorph 3.0.6 (Adams et al., 2013). All volumetric data for the brain and temporal lobes were acquired directly from the MRI in cubic centimetres using the software Brainsuite *17a* (Shattuck & Leahy, 2002).

In this thesis, the evolutionary context of anthropoid taxa was necessary to maintain and investigate changes between extant and fossil taxa. The average was calculated for each species before analysis and all data natural log-transformed (base e) to preserve linear scaling relationships following Simpson, Roe, & Lewontin (2003) to examine relative and absolute changes in the cerebrocranial temporal regions. Phylogenetic comparative methods were used to examine the differences in anthropoid evolution (Cornwall & Nakagawa, 2017).

Generally, tree topology, branch lengths, and models of phenotypic change consider the nonindependence between species in statistical analysis where species that share an evolutionary history may be similar in cerebrocranial traits. However, these methods assume that phylogenetic trees are known, and that the models are without error. This includes an assumption that specific distributions of character states across a tree result from ancestral state reconstructions, but these are, of course, uncertain.

The influence of phylogeny was examined using phylogenetic generalised least-squares (PGLS) regression and a consensus anthropoid tree modified from 10 K Trees Version 3 (Arnold, Matthews, & Nunn, 2010). Trait Mapping was also conducted to examine the relative and proportional changes to the temporal lobe in anthropoid evolution to examine the congruence between traits and the anthropoid phylogeny following Martins and Hansen (1997) with Blomberg's K (kappa) statistic used to examine statistical significance (Blomberg,

Garland, & Ives, 2003). The specific details of these analyses are provided in Chapter 1, Chapter 6 and Chapter 7 published as Pearson et al. (2020), Pearson & Polly (2023b) and Pearson & Polly (2024).

In this thesis, all data were tested for correlations using ordinary least-squares regression and multiple regressions for prediction of temporal lobe size, reduced major axis regression to examine allometric trends, and phylogenetic generalised least-squares regression to accommodate anthropoid phylogeny and all statistical analyses conducted using the package 'Phylogenetics for Mathematica' Version 6.5 (Polly, 2019) in the software *Mathematica 20* (Wolfram, 2023).

2.5. Overview of Extant and Extinct Anthropoids Studied

In this thesis, I have adopted the classification system for extant anthropoid primates following Groves (2001) and Fleagle (2013) where the Infraorder Anthropoidea excludes the Tarsiiformes and Lemuriforms. For extinct anthropoid primates, the classification system adopted follows Fleagle (2013) and Hartwig (2002). A thorough and detailed morphological, ecological and socio-behavioural description for the extant anthropoid taxa studied is provided Appendix A, while a detailed description of the fossil specimens, estimated dating, geological sites and endocranial descriptions of the extinct taxa studied are presented in Appendix B. A list of specimen identifications, imaging modalities and source information for the specimens studied is provided in Appendix C.

The following sections will provide an overview of brief morphological, classification and evolutionary details of the extant and extinct taxa studied to indicate the shared evolutionary affinities between the extant and extinct anthropoids studied.

2.5.1. Extant Anthropoid Primates Studied

The following sections provide a summary of the extant taxa studied to describe the shared and evolutionary morphological, environmental, and socio-behavioural traits of the extant species to provide context for the extinct taxa studied but see Appendix A and B for more in-depth descriptions.

2.5.1.1. Infraorder Platyrrhini

The infraorder Platyrrhini classification follows Groves (2001) and Fleagle (2013) where the Order Primates is divided into Semiorders Strepsirrhini and Haplorrhini, the suborder Anthropoidea with the infraorder Platyrrhini including the neotropical monkeys inhabiting South and Central America with the taxonomic classification below discussed at the family rank with the species studied indicated in bold. A general description at family rank is provided below with a more extensive account in Appendix A.

Order Primates (Linnaeus, 1758)

Suborder Haplorrhini (Pocock, 1918)

Infraorder Platyrrhini (Saint-Hilarie, 1812)

Family Cebidae (Bonaparte, 1831)

Subfamily Saimiriinae (Miller, 1924)

Genus *Saimiri* (Voigit, 1831)

***Saimiri sciureus* (Linnaeus, 1758)**

Subfamily Cebinae (Bonaparte, 1831)

Genus *Sapajus* (Kerr, 1792)

***Sapajus apella (*Silva, 2001)**

2.5.1.1. Family Cebidae

In general, neotropical monkeys of the Infraorder Platyrrhini are more arboreal than the Infraorder Catarrhini and possess a more ancestral dental formula of 2:1:3:3 (there are exceptions) which is shared by extinct stem-anthropoids (see section 2.5.2). The Family Cebidae includes the neotropical monkeys *Saimiri sciureus* (squirrel monkeys) and *Sapajus apella* (robust capuchins) which consist of three genera and 29 species (Mittermier, Rylands & Wilson, 2013). A brief description of the morphological, environmental and sociobehavioural traits is provided below from my own observations unless indicated otherwise.

Both *Saimiri sciureus* and *Sapajus apella* are small- to medium-sized neotropical monkeys which both possess hind-limbs that are longer than forelimbs as is consistent with postcranial traits in arboreal monkeys (Fleagle, 2013). In general, morphologically, *Saimiri sciureus* has a head which is slightly more oval compared to the rounded head in Sapajus apella with both possessing a relatively larger brain size for body size and higher social complexity than other neotropical monkeys (Rylands & Mittermeir,2013). Both species share a relatively shorter face and broad premolars with sexually dimorphic canines and smaller third molars (Mittermier, Rylands & Wilson, 2013).

The adaptation of prehensile tails in neotropical monkeys is frequently observed but here only the taxa studied in this thesis will be discussed. The use of prehensile tails in neotropical monkeys is often argued as a capacity to provide extra support during forging on the terminal branches in the forest canopy and arboreal quadrupedal locomotion (Mittermier, Rylands & Wilson, 2013).

Sapajus apella do not have a prehensile tail which is more commonly used to support for foraging and in arboreal locomotion, but only juvenile robust capuchins seem capable to support their body weight using the prehensile tail by assuming a tripod posture to hang by the tail (personal observation). In contrast, *Saimiri sciureus* is an adept arboreal quadruped but possesses a prehensile tail and uses the long tail as an extra support to grasp during locomotion along terminal branches of the forest canopy and during climbing or leaping (personal observation). There appears to be a slight difference in the forelimb to hindlimb length compared to *Sapajus apella*, with *Saimiri sciureus* having slightly longer hindlimbs than forelimbs which are used more frequently in climbing and leaping with more time spent on arboreal supports than *Sapajus apella* (personal observation).

Both genera share a similar environmental zone in the neotropics where habits include moist tropical and subtropical, lowland, and submontane regions and extending into dry deciduous and semi-deciduous forests, scrub and farmland-forest mosaics (Mittermier, Rylands & Wilson, 2013).The broad similarities in extensive environmental adaptations allow both genera to be more generalised in diet and habitat usage but both differ during dry and wet seasons in food preferences with fallback foods including palm nuts with thick husks consumed by *Sapajus apella* with the adaptation of a stone-and-anvil technique to crack open the thick seed husks which requires both learning by juveniles and may be related to the more opposable thumbs in *Sapajus apella* compared to *Saimiri sciureus* which does not have the adaptation of stone tool usage nor the need for more robust hindlimbs to allow the bipedal stance of lifting stones as seen in *Sapajus apella* (Mittermier, Rylands & Wilson, 2013).

2.5.2. Infraorder Catarrhini

The infraorder Catarrhini classification follows Groves (2001) and Fleagle (2013) where the Order Primates is divided into Semiorders Strepsirrhini and Haplorrhini, the suborder Anthropoidea with the infraorder Catarrhini including the Afro-Eurasian monkeys and apes inhabiting some part of Europe, the Africa continent, throughout parts of mainland Asia and island southeast Asia with the taxonomic classification below including the species studied here indicated in bold. A general description at family rank is provided below with a more extensive account in Appendix A.

Order Primates (Linnaeus, 1758)

Suborder Haplorrhini (Pocock, 1918)

Infraorder Catarrhini (Saint-Hilarie, 1812)

Superfamily Cercopithecoidea (Gray, 1821)

Family Cercopithediae (Gray, 1821)

Subfamily Cercopithecinae (Gray, 1821)

Tribe Papioini (Burnett, 1828)

Genus *Macaca* (Lacepede, 1799)

***Macaca mulatta* (Zimmerman, 1780)**

Genus *Papio* (Erxleben, 1777)

***Papio anubis* (Lesson, 1827)**

Genus *Cercocebus* (Saint-Hilarie, 1812)

***Cercocebus atys* (Audebert, 1797)**

Superfamily Hominoidea (Gray, 1825)

Family Hylobtaidae (Gray, 1870)

Genus *Hylobates* (Illiger, 1811)

***Hylobates lar* (Linnaeus, 1771)**

Family Hominidae (Gray, 1825)

Subfamily Ponginae (Elliot, 1912)

Genus *Pongo* (Lacepede, 1799)

***Pongo pygmaeus* (Linnaeus, 1760)**

Pongo abelii (Lesson, 1827)

Subfamily Homininae (Gray, 1825)

Genus *Gorilla* (Saint-Hilaire, 1853)

***Gorilla gorilla* (Savage, 1847)**

Genus *Pan* (Oken, 1816)

***Pan troglodytes* (Blumenbach, 1799)**

***Pan paniscus* (Schwarz, 1929)**

Genus *Homo* (Linnaeus, 1758)

***Homo sapiens* (Linnaeus, 1758)**

2.5.2.2. Family Cercopithediae

In contrast to the Infraorder Platyrrhini, members of the Infraorder Catarrhini have a much broader distribution and are located across Africa, Arabia, Asia and southern parts of Europe. In general, catarrhines are semi-terrestrial with some taxa more arboreal than others and with a more derived dental formulae of 2:1:2:3 compared to stem-anthropoids and extinct and extant platyrrhines (Fleagle, 2013).

In this thesis, the extant old-world monkeys studied were from the family Cercopithecidae includes the subfamily Cercopithecine or more commonly known as 'cheek-pouch' monkeys and the subfamily Colobinae which include the colobine monkeys and are found almost exclusively on the Asian and African continents with the exception a few species of *Macaca* and *Papio* which are located in northern African, southern Europe and southern northern and southern regions of Arabia (Fleagle, 2013). There are 42 species in the Cercopithecinae which includes macaques, mangabeys, baboons, and geladas.

In this thesis, the extant taxa studied included the Tribe Papionini including the *Macaca mulatta* known commonly as the rhesus macaques, *Cercocebus atys* or the capped mangabeys, and *Papio anubis* or the olive baboons (Zinner, Fickenscher & Roos, 2013).

In an evolutionary context of the papionins, the genus *Macaca* diverged at approximately 10- 6 million years ago followed by the more robust *Papio* baboons and then the genus *Cercocebus* comprising the slenderer mangabeys (Jablonski, 2002; Kay et al., 1997; Gilbert et al., 2018). There are shared environmental, morphological and evolutionary traits in extant and extinct papionions including *Papio angusticeps* (McKee & Keyser, 1994) stem-catarrhines including *Aegyptopithecus* (Jablonski, 2002) and stem-cercopithecoids such as *Victoriapithecus* (Benefit & McCrossin, 2002).

Morphologically, papionins share the catarrhine traits of a tubular tympanic bone rather than an auditory bulla as more commonly found in extant and extinct platyrrhines and some extinct stem-anthropoids, the reduction from three to two pre-molars, higher visual acuity, trichromatic vision and more sociobehavioural complexity (Pearson and Polly, 2023b). The majority of species in the tribe Papionini are more terrestrial or semi-terrestrial with some

arboreal taxa but sexual dimorphism is more pronounced in terrestrial taxa compared to arboreal taxa (Fleagle, 2013).

In general, species in the genus *Macaca* including *Macaca mulatta* studied here are medium-sized old-world monkeys with minimal sexual dimorphism and females often more socially dominant than observed in other papioninins and a variable diet and habitat (Zinner, Fickenscher & Roos, 2013).

In contrast to *Macaca mulatta*, *Cerecocebus atys*, have a slenderer body with longer hind limbs and longer tails with and some sexual dimorphism present. The canines are often larger and interorbital breadth is wider and a longer tympanic tube than observed in other papionins or the crested mangabeys (Zinner, Fickenscher & Roos, 2013). Both *Macaca* and *Cercocebus* are more arboreal or semi-terrestrial quadrupeds with these longer hindlimbs in more arboreal species allowing for leaping and climbing with longer tail aiding in balancing on thin branches in the upper canopy (Zinner, Fickenscher & Roos, 2013).

In contrast to *Macaca* and *Cercocebus*, the genus *Papio* is mostly terrestrial with hindlimbs and forelimbs of approximately the same length and much greater sexually dimorphism (Zinner, Fickenscher & Roos, 2013).

Environmental adaptations in the papioninins are variable to accommodate habitats in a wide environmental zone and from the tropical, flooded rainforests in Uganda and rainforests of the DRC, arid shrublands of northern Kenya and Ethiopia and into mountainous areas of the central Sahara and forested galleries of Asia, farmlands and human inhabited regions (Zinner, Fickenscher & Roos, 2013). Although all these taxa are predominantly frugivorous, florivorous and omnivorous, diet is flexible with environmental changes from dry to wet seasons. Generally, the more arboreal taxa in *Cercocebus* inhabit more densely forested and seasonal

flooded environments and both florivorous and frugivorous while *Macaca* are tend towards more frugivorous and omnivorous inhabiting a wider range of environments and arboreal but also more semi-terrestrial inhabiting forests and woodland environments compared to the more frugivorous and omnivorous and terrestrial species in *Papio* which inhabit more open woodlands and savannas (Zinner, Fickenscher & Roos, 2013).

2.5.2.3. Family Hylobatidae

The family Hylobatidae includes the small apes with the classification system following Groves (2001) and Fleagle (2013). The descriptions of the small apes are discussed at the family rank. A thorough discussion of the morphological, environmental, and socio-behavioural aspects of the species studied provided in Appendix A.

The evolutionary history of the Hylobatidae is complex. Although the small apes share many characteristics in common with the great apes including dental formulae, shape of thorax, absence of a tail, there are also specialized adaptations which are specific the Hylobatidae including extremely elongated upper limbs suited to brachiation, a relatively smaller cranium compared to the great apes and lack of sexual dimorphism (Groves, 2001; Chivers et al, 2013; Fleagle, 2013).

The molecular divergence for the Hylobatidae was first published complete genome sequence by Carbone et al. (2014) indicating a near simultaneous divergence of the four genera with phylogenetic relationships between the genera difficult to definitively separate. Carbone et al., (2014) noted that a molecular LAVA insertion into the Hylobatid genome, which is absent in the great apes, old-world or neotropical monkeys makes the Hylobatidae more unique among extant anthropoid primates.

2.5.2.4. Family Hominidae

The family Hylobatidae includes the great apes with the classification system following Groves (2001) and Fleagle (2013). The descriptions of the great apes are discussed at the family rank with a more thorough discussion of the morphological, environmental, and socio-behavioural aspects of the species studied in Appendix A.

There is an extensive evolutionary record for extinct and extant members of the subfamily Ponginae but only the extant orangutans were studied here due to poor fossil remains for the fossil orangutans and similarly all great ape species with the exception of fossil hominins. In terms of genetic divergence, there are three recognized species of *Pongo* but Steiper (2006) estimating divergence dates between the Bornean-Sumatran orangutans at 5 – 3 mya with a conclusion of greater genetic diversity in the Sumatran orangutan *Pongo abelii* than expected given the smaller range compared to the Bornean orangutan, *Pongo pygmaeus*. More recently, Nater (2017) identified a new species of orangutan, the Tapanuli orangutan (*Pongo tapanuliensis*) using molecular and morphological evidence to indicate that this species was both genetically and geographically distinct from the Sumatran orangutan, *Pongo abelii*.

In the Bornean orangutan *Pongo pygmaeus* there are three recognised subspecies *including Po. Pygmaeus pygameus, Po. p. moroi and Po. p. wurmbii* which have been identified using both morphological and geographical isolation (Groves, 2001). In terms of geographical isolation, Goosens et al. (2009) noted that waterways and major rivers in Borneo acted as barriers between the populations and limiting movement.

The genus *Gorilla* expresses more a high degree of genetic variation within the species and is important to recognize when examining individuals that appropriate consideration of subspecies traits are taken into account. Groves (2003) argued there are two distinct species of

Gorilla both phenotypically and genetically*:* the Eastern Gorilla, *Gorilla beringei* and the Western gorilla, *Gorilla gorilla*. The Eastern Gorilla is now recognised as two subspecies: the Mountain Gorilla (*Gorilla beringei beringei*) and the Eastern Lowland Gorilla (*Gorilla beringei graueri*). The divergence for the Eastern gorilla using D-Loop mitochondrial analyses indicated *Gorilla beringei* separated into two distinct clades with *G. b. beringei* and *G. b. graueri* diverging approximately 380 thousand years ago (Jensen-Seaman and Kidd 2001).

The Western Gorilla has a more complex genomic history. There is evidence that subspecies *Gorilla gorilla gorilla* (the western lowland gorilla) diverged into several sub-clades where various regional populations of *G. g. gorilla* have distinct differences in haplogroup composition which is associated with the Pleistocene "geographical and environmental changes isolated populations resulting in genetic bottlenecks where upon climatic stability. these populations show evidence of reunion (Clifford et al. 2004).

The Cross River Gorilla (*Gorilla gorilla diehli)* is a small isolated population distinct from *G. gorilla gorilla* where gene flow extisted until approximately 320 years ago whereafter this ceased and the subspecies *G. g. diehli* diverged at approximately 17, 800 years ago with *G. g. diehli* now isolated to a small fragmented sections of range near the Cross River on the Cameroon-Nigerian border (Thalmann et al. 2011).

Within the genus *Pan* there are two recognised species, the bonobo *Pan paniscus* and the common chimpanzee *Pan troglodytes*. There are no subspsecies recognised for Pan paniscus which has populations that express higher genetic diversity than noted in *Homo sapiens* but lower than found in *Pan troglodytes* (Eriksson et al. 2004). The genetic distances between *Pan paniscus* and *Pan troglodytes* are correlated with the geographical population barriers served by rivers and other waterways with *Pan paniscus* isolated to a region in the

larger bend in the Congo River (Groves, 2001; (Eriksson et al. 2004). In contrast, there are four recognised subspecies in *Pan troglodytes* including which is divided *P. t. troglodytes* (the Central Chimpanzee*), P. t. schweinfurthii* (Eastern Chimpanzee*), P. t. verus* (Western Chimpanzee) and *P. t. ellioti* (Nigerian-Cameroon chimpanzee). The evolutionary divergences of chimpanzee subspecies are noted by Becquet et al. (2007) to follow the divergence of the Western Chimpanzee first, followed by the Eastern and then the Central chimpanzee subspecies.

2.5.2. Extinct Anthropoid Primates Studied

In this thesis, I have adopted the classification system for anthropoid primates following Groves (2001) and Fleagle (2013) where the Infraorder Anthropoidea excludes the Tarsiiformes and Lemuriforms. For the extinct anthropoid primates, the classification system adopted follows Fleagle (2013) and Hartwig (2002). A thorough description of the fossil specimens, estimated dating, geological sites and endocranial descriptions of the extinct taxa studied are provided in Appendix B.

Extinct anthropoid taxa include wide variety of species and those studied are indicated in bold. Stem-anthropoids dated to approximately 36 million years ago and recovered from the Fayum sites in Egypt; extinct platyrrhines dated to approximately 20 million years ago recovered from the neotropical sites in Brazil and Argentina; stem-catarrhines recovered Fayum site in Egypt dated to approximately 25 million years ago; fossil cercopithecines recovered from East Africa dated to approximately 15 million years ago and Plio-Pleistocene fossil papionins from South Africa dated to approximately 5 to 1 million years. The extinct taxa from the subfamily Hominini include fossil hominin species from the Pliocene in South and East Africa dated to approximately 3 million years ago; early *Homo* from East Africa dated

to approximately 2 million and 1.8 million years ago recovered from Java dated to approximately 1.5 million years ago; Middle Pleistocene fossil *Homo* recovered from South Africa, Europe and Flores dated between 700,000 to 500, 0000 years ago; Late Pleistocene fossil *Homo* recovered from Africa and Europe dated to approximately 100,000 to 10, 000 years ago.

2.5.2.1. Stem-Anthropoids

The stem-anthropoids are classified under the Suborder Haplorrhini and Infraorder Anthropoidea and includes extinct taxa from the Late Eocene to Late Oligocene from Africa. The taxonomic classification system used for stem-anthropoids this thesis follows Beard (2002) with taxa studied detailed below and species studied indicated in bold. A general description at family rank is provided below with a more extensive account in Appendix B.

Order Primates (Linnaeus, 1758)

Suborder Haplorrihini (Pocock, 1918)

Infraorder Anthropoidea (Mivart, 1864)

Family Parapithecidae, (Schlosser, 1918)

Genus *Apidium* (Osborn, 1908)

***Apidium phiomense* (Osborn, 1908)**

Genus *Parapithecus* (Schlosser, 1910)

***Parapithecus grangeri* (Simons, 1974)**

Family Proteopithecidae (Simons, 1997)

Genus *Proteopithecus*, (Simons, 1989)

***Proteopithecus sylviae* (Simons, 1989)**

2.5.2.1.1. Family Proteopithecidae

The Family Proteopithecidae includes the genus *Proteopithecus* is represented by one extinct species. Fossil specimens attributed to *Proteopithecus sylviae* have been recovered from the Fayum Depression, Egypt from Quarry L-41 and the lower part of the Jebel Qatrani Formation and dated to the Late Eocene. Generally, the morphology of *Proteopithecus sylviae* indicates a relatively small anthropoid primate with postcranial anatomy most similar to small platyrrhines (Beard, 2002; Simons & Seiffert, 1999). Craniodentally the dental formula is 2:1:3:3 similar to other stem-anthropoids with relatively larger canines suggesting sexual dimorphism (Beard, 2002).

2.5.2.1.2. Family Parapithecidae

The Family Parapithecidae includes the genus *Apidium* is represented by three extinct species and the genus *Parapithecus* represented by two extinct species. Both *Apidium* and *Parapithecus* have been recovered from the Fayum Depression, Egypt in the upper part of the Jebel Qatrani Formation and dated to the Early Oligocene.

Fossil specimens attributed to the genus *Apidium* consist of partial crania, cranial fragments, and mandibular and dental remains and like to many stem-anthropoids, the dental formulae are 2.1.3.3 but in *Apidium*, the P2 is smaller relative to P3-4 compared to *Parapithecus* while cranial material indicates a complete postorbital closure and relatively large olfactory bulbs relative to cranial size (Beard, 2002). Fossil specimens attributed to the genus *Parapithecus* consist of mandibular, postcranial, dental, and fragmentary cranial remains with a relatively shorter facial skeleton and snout compared to *Apidium* which may relate to the reduced upper incisors and uniquely in *Parapithecus grangeri*, the complete absence of

lower incisors (Beard, 2002). In both *Apidium* and *Parapithecus* the molars are of similar size but there are relatively larger P_2 in *Parapithecus* than *Apidium* (Beard, 2002).

2.5.2.2. Stem-Platyrrhines

The stem-platyrrhines are classified under the Suborder Haplorrhini and Infraorder Platyrrhini which includes extinct taxa from the Early to Middle Miocene from South America. The taxonomic classification system follows Fleagle & Tejedor (2002) with the species studied indicated in bold. A general description at family rank is provided below with a more extensive account in Appendix B.

Order Primates (Linnaeus, 1758)

Suborder Haplorrhini (Pocock, 1918)

Infraorder Platyrrhini (Saint-Hilarie, 1812)

Family Atelidae (Gray, 1925)

Subfamily Pitheciinae (Mivart, 1865)

Tribe Homunculini (Ameghino, 1894)

Genus *Homunculus* (Ameghino, 1894)

***Homunculus patagonicus* (Ameghino, 1894)**

Family Cebidae (Bonaparte, 1831)

Subfamily Cebinae (Bonaparte, 1831)

Subfamily Saimiriinae (Miller, 1924)

Genus *Dolichocebus* (Kraglievich, 1951)

***Dolichocebus gaimanensis* (Kraglievich, 1951)**

Subfamily Aotinae (Elliot, 1931)

Genus *Tremacebus* (Hershkovitz, 1974)

***Tremacebus harringtoni* (Rusconi, 1933)**

2.5.2.2.1. Family Atelidae

The extinct stem-platyrrhines attributed to the Family Atelidae include the genus *Homunculus* which is represented by one extinct species.

Fossil remains for *Homunculus patagonicus* have been recovered Rio Gallegos site from the Santa Cruz Formation from southernmost Santa Cruz Province, Argentina and dated to the Early to Middle Miocene. Generally, the morphology of *Homunculus patagonicus* includes mandibular, postcranial, and cranial material with relatively small lower canines and incisors and series of substantial shearing crests. The facial skeleton has a prominent snout and relatively deep face with moderately sized orbits and narrow interorbital space, while the cranium is globular (Fleagle & Tejedor, 2002).

2.5.2.2.2. Family Cebidae

Stem-platyrrhines attributed to the Family Cebidae include the genus *Dolichocebus* which is represented by only one extinct species and the genus *Tremacebus* which is also represented by only one extinct species. Fossil remains for *Dolichocebus gaimanensis* have been recovered from Caiman, Chubut Province, Argentina and dated to the Early Miocene. Morphologically, the cranium of *Dolicliocchus gaimanensis* suggests a medium-sized stem-platyrrhine with moderately large orbits and a narrow interorbital region and a relatively narrow braincase. The fossil remains for *Tremacebus harringtoni* have been recovered from Sacanana, Chubut Province, Argentina and dated to the Early Miocene. Morphologically, the cranium of *Tremacebus harringtoni* has a broad snout with relatively large orbits with a wide interorbital

region and considered dissimilar to the extant nocturnal platyrrhine, *Aotus* and may indicate a similar nocturnal ecology (Fleagle & Tejedor, 2002).

2.5.2.3. Stem-Catarrhines

Stem-catarrhines are classified under the Suborder Haplorrhini and Infraorder Catarrhini and include extinct taxa from the Early to Late Oligocene from Africa. The taxonomic classification system follows Rasmussen (2002) with the species studied indicated in bold. A general description at family rank is provided below with a more extensive account in Appendix B.

Order Primates (Linnaeus, 1758)

Suborder Haplorrhini (Pocock, 1918)

Infraorder Catarrhini (Saint-Hilaire, 1812)

Family Propliopithecidae (Strauss, 1961)

Genus *Aegyptopithecus* (Simons, 1965)

***Aegyptopithecus zeuxis* (Simons, 1965)**

Family Oligopithecidae (Kay and Williams, 1994)

Genus *Catopithecus* (Simons, 1989)

***Catopithecus browni* (Simons, 1989)**

2.5.2.3.1. Family Propliopithecidae

Stem-catarrhines attributed to the Family Propliopithecidae include the genus *Aegyptopithecus* consists of two extinct species.

Fossil remains attributed to the genus *Aegyptopithecus* have been recovered from the Fayum Depression in the upper sequence of the Jebel Qatrani Formation and date to the early

Oligocene. Morphologically, *Aegyptopithecus zeuxis* was a large and robust stem-catarrhine with an estimated body size similar to extant gibbons and howler monkeys (Simons, 1965; Kay et al., 1981; Simons & Rasmussen, 1991). There are several cranial specimens of *Aegyptopithecus* indicating a robust facial skeleton with broad interorbital space and the temporal lines converge above the orbits in males forming a prominent sagittal crest. There is evidence of an auditory bullae which is positioned fairly posteriorly similar to in extant *Alouatta* and there is a large promontory canal and relatively larger olfactory bulbs (Radinsky, 1975; Simons, 1993).

2.5.3.2.2. Family Oligopithecidae

The Family Oligopithecidae is represented by fossil specimens attributed to the genus *Catopithecus* which is represented by only one extinct species.

Fossil remains for *Catopithecus browni* have been recovered from the Fayum Depression, Egypt in the lower sequence of the Jebel Qatrani Formation, Quarry L-41 and dated to Late Eocene. Morphologically, *Catopithecus browni* is a small-bodied stem-catarrhine but possess many ancestral traits including an unfused mandibular symphysis and postcranially, Seiffert et al. (2000) compares the humerus of *Catopithecus* and propliopithecines where *Catopithecus* is more similar to a generalised arboreal quadruped. Cranially, the facial skeleton is projecting with a broader snout than any extant anthropoid or strepsirrhine, but the orbits are relatively small. The cranial vault appears relatively small similar to strepsirrhines with the braincase that is relatively smaller than more recent extinct and extant anthropoids (Pearson and Polly, 2023b). There is suggestion of sagittal and nuchal

crests and yet the ectotympanic is more platyrrhine-like with an angular form rather than a tubular one observed in extant catarrhines (Simons, 1989).

2.5.2.4. Extinct Cercopithecoids

Early extinct cercopithecoids are classified under the Suborder Haplorrhini and Infraorder Catarrhini and include extinct taxa from the Middle Miocene from Africa. The taxonomic classification system follows Benefit & McCrossin Fleagle (2002) with the species studied indicated in bold. The taxonomic classification is detailed below with species studied indicated in bold. A general description at family rank is provided below with a more extensive account in Appendix B.

Order Primates (Linnaeus, 1758)

Suborder Haplorrhini (Pocock, 1918)

Infraorder Catarrhini (Saint-Hilaire, 1812)

Superfamily Cercopithecoidea (Gray, 1821)

Family Victoriapithecidae (von Koenigswald, 1969)

Genus *Victoriapithecus* (von Koenigswald, 1969)

***Victoriapithecus macinnesi* (von Koenigswald, 1969)**

2.5.2.4.1. Family Victoriapithecidae

The Family Victoriapithecidae is represented by the genus *Victoriapithecus* which is represented by one extinct species.

The fossil remains attributed to *Victoriapithecus macinnesi* have been recovered from Napak, Uganda; Maboko Formation, Kenya, Tugen Hills Sequence, Kenya and are dated to the Middle Miocene. Morphologically, *Victoriapithecus macinnesi* has less flexed cranial base

with longer a mid-cranial region and there is evidence of temporal lines convergence, and the orbits are taller than wide in in this case, the cranial morphology *Victoriapithecus* closely resembles the stem-catarrhine *Aegyptopithecus* (Simons, 1987). The cranium is small with a relatively large olfactory bulb for a mid- Miocene stem-cercopithecoid and the postcranially, *Victoriapithecus macinnesi* is indicative of a quadrupedal semi-terrestrial monkey (Benefit, 1999; Benefit & McCrossin 2002; Gonzles et al., 2015).

2.5.2.5. Extinct Cercopithecines

The extinct cercopithecines are classified under the Suborder Haplorrhini and Infraorder Catarrhini and Superfamily Cercopithecoidea and include extinct taxa from the Early Pliocene to the Late Pleistocene in Africa. A consolidation into *Papio izoldi* which includes all a small species of *Papio* recognised from South Africa (*P. izodi, P. wellsi and P. angusticeps*) was advocated by Szalay & Delson (1979) and is followed here. The taxonomic classification follows Jablonski (2002) with species studied indicated in bold. A general description at family rank is provided below with a more extensive account in Appendix B.

Order Primates (Linnaeus, 1758)

Suborder Haplorrhini (Pocock, 1918)

Infraorder Catarrhini (Saint-Hilaire, 1812)

Superfamily Cercopithecoidea (Gray, 1821)

Family Cercopithecidae (Gray, 1821)

Subfamily Cercopithecinae (Gray, 1821)

Tribe Papionini (Burnett, 1828)

Subtribe Papionina (Burnett, 1828)

Genus *Papio* (Erxleben, 1777)

***Papio angusticeps (izodi)* (Gear, 1926)**

Genus *Dinopithecus* (Broom, 1937)

***Dinopithecus ingens* (Broom, 1937)**

2.5.2.5.1. Family Cercopithecidae

The fossil species attributed to the Family Cercopithecidae include genus *Papio* which consists of three recognised extinct species and the genus *Dinopithecus* is represented by one extinct species.

Fossil remains attributed to *Papio angusticeps (izodi)* have been recovered from Taung, Sterkfontein, Kromdraai, Cooper's Cave, and Haasgat Cave, South Africa and all are dated to the Late Pleistocene. Morphologically, *Papio angusticeps (izodi)* has a well-developed supraorbital torus and dentally this species is indistinguishable from species attributed to the genus *Parapapio* except for a cranially distinct trait in the concavity and steep orbital profile (Gilbert et al., 2018; McKee & Keyser 1994).

Fossil remains attributed to the *Dinopithecus ingens* have been recovered from Swartkrans, South Africa and are dated to the mid-Pliocene. Morphologically, *Dinopithecus ingens* is one of the largest cercopithecoids and only *Theopithecus oswaldi* from the Late Pleistocene is larger. *Dinopithecus ingens* possess a very large and sexually dimorphic cranium with indications of strong masticatory and nuchal muscles and the temporal lines converge in both sexes where in males form sagittal and nuchal crests. The supraorbital torus is robust while the interorbital region is relatively broad and minimal cranial base flexion is consistent with a large, terrestrial quadrupedal cercopithecine (Jablonski, 2002).

2.5.2.6. Extinct Hominins

Extinct hominins are classified under the Suborder Haplorrhini and Infraorder Catarrhini and Family Hominidae and the Subfamily Homininae and include extinct taxa from the Early Pliocene to the Late Pleistocene in Africa, Asia, Middle East, and Europe. The taxonomic classification follows White (2002) and Dunsworth & Walker (2002) with species studied indicated in bold. A general description at family rank is provided below with a more extensive account in Appendix B.

Order Primates (Linnaeus, 1758)

Suborder Haplorrhini (Pocock, 1918)

Infraorder Catarrhini (Saint-Hilaire, 1812)

Superfamily Hominoidea (Gray, 1825)

Family Hominidae (Gray, 1825)

Subfamily Homininae (Gray, 1825)

Genus *Australopithecus* (Dart, 1925)

***Australopithecus africanus* (Dart, 1925)**

Genus *Paranthropus* (Broom, 1938)

***Paranthropus aethiopicus* (Arambourg & Coppens, 1968)**

***Parapanthropus boiesi* (Leakey, 1959)**

Genus *Homo* (Linnaeus, 1758)

***Homo habilis* (Leakey, 1964)**

***Homo erectus* (Dubois, 1892)**

***Homo ergaster* (Groves & Mazak, 1975)**

***Homo floresiensis* (Brown, 2004)**

***Homo heidelbergensis* (Schoetensack, 1908)**

***Homo neanderthalensis* (King, 1864)**

***Homo sapiens* (Linnaeus, 1758)**

2.5.2.6.1. Family Hominidae

The fossil hominins attributed to the Family Hominidae include at least three recognised genera, *Australopithecus* consisting of at least six extinct species, the genus *Paranthropus* consisting of at least three extinct species and the genus *Homo* comprising at least ten extinct species. All extinct taxa attributed to the subfamily Homininae utilise terrestrial bipedalism with larger absolute brain size to body size (Grabowski, 2006) and an association with stone tool use or manufacture and complex soicio-behavioural traits (Gowlett, 2012; Lieberman, 2011Lieberman et al., 2000a, 2000b; McArthy 2001, 2004).

Fossil remains attributed to *Australopithecus africanus* have been recovered from Taung, Makapansgat and Sterkfontein, South Africa and dated to approximately 3 – 2 million years ago. Morphologically, *Au. africanus* crania are more globular with less neurocranial cresting than observed in other species of *Australopithecus* or in *Paranthropus*. The face is relatively prognathic with bony pillars framing the nasal aperture. The dental remains indicate that the post-canine teeth are relatively larger than in *Au. afarensis* but not as disproportionally large as observed specimens attributed to the genus *Paranthropus* (White, 2002).

Fossil specimens attributed the *Paranthropus aethiopicus* have been recovered from West Turkana, Kenya and Omo Shungura, Ethiopia and dated to 2.7 – 2.3 million years ago. Morphologically, the cranial base is unflexed and the face is ‘dished’ with laterally flaring zygomatic arches. The dentition has large anterior teeth relative to post-canine teeth when compared to the hyper-condition observed in *P. robustus* and *P. boisei* (White, 2002).

Fossil specimens attributed to *Paranthropus boiesi* have been recovered from Olduvai Gorge, Koobi Fora, West Turkana, Kenya; Omo, Shungura, Ethiopia and dated to 2.3 – 1.4 million years ago. Morphologically, the crania are noted to have a 'dished' face with high and anteriorly flared zygomata and sagittal and nuchal crests. Dentally, there is extreme post canine megodontia and highly moralised premolars (White, 2002).

Fossil specimens attributed to *Homo habilis* have been recovered from the sites of Omo and Hadar, Ethiopia; Olduvai Gorge, Tanzania; East Lake Turkana, Kenya; and Sterkfontein, South Africa and dated to approximately 2.33 - 1.6 million years ago. On average, the absolute endocranial capacity is larger than that observed in *Australopithecus* specimens but smaller than *Homo ergaster* (Pearson & Polly, 20024). There is the presence of a supraorbital torus, and the upper face is wider than the midface breadth. Dentally, the premolars are smaller than *Australopithecus* and *Paranthropus* and more consistent with species of the genus *Homo* (Dunsworth & Walker, 2002; Cartmill & Smith, 2009)

Fossil remains attributed to *Homo ergaster* have been recovered from Koobi Fora and West Turkana, Kenya; Olduvai Gorge, Tanzania; Swartkrans, South Africa and Dmanisi, Republic of Georgia and dated to approximately 1.8 – 1.6 million years ago. Morphologically, African *Homo ergaster* has smaller cheek teeth compared to *Australopithecus* or *Homo habilis* and a more gracile mandible. The cranial capacity is larger than in earlier hominins and characterised by thinner bones than in Asian *Homo erectus* and s cranium that is long and low with sagittal keeling, projecting brow ridges and a prominent occipital torus and a broad facial skeleton (Dunsworth & Walker, 2002; Cartmill & Smith, 2009).

Fossil remains attributed to *Homo erects* have been recovered from Narmada, India; Hexian, Gongwangling (Lantian), Zhoukoudtan, Jianshi and Yunxian, China;

Sambungmachavn, Solo, Trinil, Ngandong, Modjokcrto and Sangiran, Indonesia and dated between 1.6 million years ago 50 thousand years ago. Morphologically, the cranium is long and low with greatest cranial breadth toward base. The frontal bone has a pronounced supraorbital torus, supratoral sulcus and a frontal keel. There is a significant degree of postorbital constriction compared to *Homo sapiens* (Dunsworth & Walker, 2002; Cartmill & Smith, 2009).

Fossil remains attributed to *Homo floresiensis* have been recovered from Laing Bua cave, Flores, Indonesia and dated between 100,000 to 50, 000 years ago (Brown, 2004). Morphologically, *Homo floresiensis* has unique dental, cranial, and postcranial morphology that is most similar to early *Homo* from East Africa rather than *Homo sapiens* or Asian *Homo erectus* (Aiello, 2010; Jungers, 2013). The estimated cranial capacity is small and resembles *Australopithecus* or early *Homo* and postcranial elements suggest a small stature of one metre in height with an estimated body mass of only 29kg (Fleagle, 2013) and may represent aspects of the Island Rule dwarfing (Diniz-Filho & Raia, 2017) but the taxonomic position remains unclear (Argue et al., 2009).

Fossil remains attributed to *Homo heidelbergensis* have been recovered from Heidelberg, Germany; Kabwe, Southern Africa; Bodo in Eastern Africa; Petralona in Greece and potentially Dali, China and dated to 700 000–130 000 years ago. Morphologically, cranial similarities between the African and European fossils are noticeable. The cranium is characterised by a larger cranial capacity, divided brow ridges and compared to *Homo erectus*, *Homo heidelbergensis* has smaller teeth and a mandible with a broader ramus and a deeper corpus but lacking a chin (Smith, 2002; Cartmill & Smith, 2009).

Fossil remains attributed to *Homo neanderthalensis* have been recovered from Mount Carmel, Israel; and throughout Europe and dated to 300,000 and 35,000 years ago. Morphologically, *Homo neanderthalensis* has a prognathic face with an unusually large nasal region and large arching brow ridges over the orbits. The cranium is rounded with a prominent 'bun' posteriorly and flattened parietal bones. The brain is absolutely and relatively large. Postcranially, the limbs are robust with shortened distal elements (Cartmill & Smith, 2009).

Fossil remains attributed to extinct *Homo sapiens* have been recovered from Jebel Irhoud, Morocco; Omo Kibish Formation, Ethiopia; Herto in the Middle Awash region, Ethiopia; Mount Carmel, Israel; Cro-Mignon, France, and dated to 300,000 years ago to 10, 000 years coinciding with the last glacial maximum. Morphologically, *Homo sapiens* possess relatively and absolutely smaller dentition, a vertical mandibular ramus and a chin, a shortened and retracted face that is positioned beneath reduced brow ridges and high vertical forehead. Postcranially, the skeleton tends towards more gracile limbs (Cartmill & Smith, 2009).

2.6. Conclusion

In conclusion, the evolution of the cerebrocranial temporal regions in anthropoid primates has been provided within the context of comparative cerebrocranial anatomy and the shared evolutionary lineages between extant and extinct anthropoids. The four of virtual anatomical techniques and phylogenetic comparative methods have been discussed within the context of the extensive extant and extinct anthropoid sample. Further detailed description of the extant and extinct primates is provided in Appendix A and B with the specimen identifications and museum source details in Appendix C.

2.7. References

Adams, D. C., Otárola-Castillo, E., & Paradis, E. (2013). Geomorph: An r package for the collection and analysis of geometric morphometric shape data. *Methods in Ecology and Evolution*, 4:4, 393–399.

Adams, D.C., Cardini, A., Monterio, L.R., O'Higgins, P., & Rohlf, F.J. (2011) Morphometrics and phylogenetics: principal components of shape from cranial modules are neither appropriate nor effective cladistic characters, *Journal of Human Evolution*, 60:2, 240-243.

Amunts, K., & Zilles, K. (2015) Architectonic Mapping of the Human Brain beyond Brodmann, *Neuron*, 88:6, 1086-1107.

Arnold, C, Matthews, L. J., Nunn, C. L. (2010). The 10kTrees website: A new online resource for primate phylogeny. *Evolutionary Anthropolgy*,19: 114–118.

Argue, D., Morwood, M. J., Sutikna, T., & Saptomo, E. W. (2009). *Homo floresiensis*: A cladistic analysis. *Journal of Human Evolution*, *57*, 623–639.

Balzeau, A., Grimaud-Hervé, D., Détroit, F., Holloway, R.L., Combès, B., Prima, S., (2013) First description of the Cro-Magnon 1 endocast and study of brain variation and evolution in anatomically modern *Homo sapiens*, *Bull. Mém. Soc. Anthropol*. Paris, 25, 1-18.

Barton, R.A., (2006) Primate Brain Evolution: Integrating Comparative, Neurophysiological, and Ethological Data, *Evolutionary Anthropolgy*,15:224 –236.

Barrickman, N.L., (2017) 'Energetics, Life History, and Human Brain Evolution' In: *Evolution of Nervous Systems* (2nd Edition), (ed.) Kass, J.H., Academic Press, pp.

Bastir, M., & Rosas, A. (2006). Correlated variation between the lateral basicranium and the face: A geometric morphometric study in different human groups. *Archives of Oral Biology*, 51(9), 814–824.

Bastir, M., & Rosas, A. (2016). Cranial base topology and basic trends in the facial evolution of *Homo*. *Journal of Human Evolution*, 91, 26–35.

Bastir, M., Rosas, A., Gunz, P., Pena-Melian, A., Manzi, G., Harvati, K., Hublin, J. J. (2011). Evolution of the base of the brain in highly encephalized human species. *Nature Communications*, 2, 588.

Bastir, M., Rosas, A., & Kuroe, K. (2004). Petrosal orientation and mandibular ramus breadth: Evidence for an integrated petroso-mandibular developmental unit. *American Journal of Physical Anthropology*, 123(4), 340–350.

Bastir, M., Rosas, A., Lieberman, D. E., & O'Higgins, P. (2008). Middle cranial fossa anatomy and the origin of modern humans. *The Anatomical Record*, 291(2), 130–140.

Bastir, M., Rosas, A., Stringer, C., Cuetara, J. M., Kruszynski, R., Weber, G. W., et al. (2010). Effects of brain and facial size on basicranial form in human and primate evolution. *Journal of Human Evolution*, 58:5, 424–431.

Beard (2002) Basal anthropoids. In: Hartwig WC (ed) *The Primate Fossil Record*. Cambridge University Press, Cambridge, UK, pp 133–149.

Benefit BR (1999) *Victoriapithecus*: The key to Old World monkey and catarrhine origins. *Evol Anthropol* 155–174

Benefit BR, McCrossin M (2002) The Victoriapithecidae: Cercopithecoidea. In: Hartwig WC (ed) *The Primate Fossil Record*. Cambridge University Press, Cambridge, UK, pp 241–253.

Bequet, C., Patterson, N., Stone, A.C., Przeworksi, M., & Rich, D. (2007) Genetic structure of chimpanzee populations, *Plos Genetics*, 3:4, 617-626.

Blomberg, S. P., Garland, T. J., & Ives, A. R. (2003). Testing for phylogenetic signal in comparative data: Behavioral traits are more labile. *Evolution*, 57(4), 717–745.

Brodmann, K., (2005). *Brodmann's Localisation in the Cerebral Cortex*, 3rd edition, (trans.) Garey, L., Springer New York, NY., USA. https://doi.org/10.1007/b138298

Boesch, C., Uehara, S., Ihobe, H., Marchant L. (2002) Variations in chimpanzee–red colobus interactions, In: *Behavioural Diversity in Chimpanzees and Bonobos*. (eds.) Boesch, C., Hohmann, G., Cambridge: Cambridge University Press, pp 221-230.

Borden, N. M., Forseen, S. E., & Stefan, C. (2016). *Imaging anatomy of the human brain a comprehensive atlas including adjacent structure*s. New York: Demos Medical Publishing.

Boyer, D. M., Kirk, E. C., Silcox, M. T., Gunnell, G. F., Gilbert, C. C., Yapuncich, G.S., Allen, K. L., Welch, E., Bloch, JI., Gonzales, L. A., Kay, R. F. & Seiffert, E. R. (2016) Internal carotid arterial canal size and scaling in Euarchonta: Re-assessing implications for arterial patency and phylogenetic relationships in early fossil primates, J Hum Evol., 97: 123-144.

Braunsdorf, M., Blazquez-Freches, G., Roumazeilles, L., Eichert, N., Schurzad, M., Uithol, S., Bryant, K.L., Rogier B., Mars, R.B. (2021) Does the temporal cortex make us human? A review of structural and functional diversity of the primate temporal lobe, *Neuroscience & Biobehavioral Reviews*.

Bruner, E. (2015) Functional craniology and brain evolution, In: *Human Paleoneurology*, (ed.) Bruner E., Springer, Switzerland. pp 57-94.

Bruner, E. (2017). The fossil evidence of human brain evolution. In: *Evolution of Nervous Systems Volume 4: The evolution of the human brain: Apes and other ancestors.* Kaas, J. H. (ed.), Academic Press, Boston, USA, pp. 63–92.

Bruner, E. (2017b) Language, paleoneurology, and the frontoparietal system. F*rontiers in Human Neuroscience,* 11(349): 1-5.

Bryant, K. L., & Preuss, T. M. (2018). A comparative perspective on the human temporal lobe, In: *Digital Endocasts: From skulls to brains*, (eds.) Bruner, E., Ogihara, N., & Tanabe, H.C, Tokyo: Springer, Japan KK, pp. 239–258.

Bush EC, Simons EL, Allman JM (2004) High-resolution computed tomography study of the cranium of a fossil anthropoid primate, *Parapithecus grangeri*: new insights into the evolutionary history of primate sensory systems. Anat Record 281:1083–1087.

Carbone, L., Harris, A., Gnerre, S. et al. (2014) Gibbon genome and the fast karyotype evolution of small apes. *Nature* 513, 195–201.

Cardini, A., Polly, P.D., Dawson, R., Milne, N. (2015) Why the long face? Kangaroos and wallabies follow the same 'rule' of cranial evolutionary allometry (CREA) as placentals. *Evolutionary Biology*, 42: 169-176.

Cardini, A., Polly, P.D. (2013). Larger mammals have longer faces because of size-related constraints on skull form. *Nature Communications*, 4: 2458: 1-7.

Conroy, G.C. (1990). *Primate Evolution.* W.W. Norton and Co.: New York.

Cope, E.D (1884) *The Vertebrata of the Tertiary formations of the West*. Report of the United States Geological Survey of the Territories vol. 3

Cornwell, W., Nakagawa, S. (2017) Phylogenetic comparative methods, *Current Biology*, 27:9, R333-R336.

Cartmill, M., & Smith, F. H. (2009*) The Human Lineage*, Hoboken, New Jersey: Wiley.

Chivers, D.J. (2013) Family Hylobtidae (Gibbons), In: *Handbook of the Mammals of the World. Vol. 3. Primates.* (eds.) Mittermeir, R.A., Rylands, A.B, & Wilson, D.E., Lynx Edicons, Barcelona, pp.

Clifford, S.L., Anothony, N.M., Bawe-Johnson, M., Abernathy, K.A., Tutin, E.G, White, J.T., Bermingo, M., Golsmith, M.L., McFarland, K., Jeffery, K.J. et al., (2004) Mitochondrial DNA, phylogeography of the western lowland gorillas (Gorilla gorilla gorilla). *Molecular Ecology*. 13, 1551-1556.

Coleman, M.N. & Colbert, M.W. (2010) Correlations between auditory structures and hearing sensitivity in non-human primates. *Journal of Morphology*, 271:5, 511-532.

Dart, R.A., (1925) *Australopithecus africanus*: the man-ape of South Africa, *Nature*.

Dart, R.A. (1926) Taung and its significance, *Nat. Hist.*

Diniz-Filho, J. A. F., & Raia, P. (2017). Island rule, quantitative genetics and brain–body size evolution in *Homo floresiensis*. *Proceedings of the Royal Society B: Biological Sciences*, *284*(1857), 20171065. https://doi.org/ 10.1098/rspb.2017.1065

Dominy, N. J. & Lucas, P. W. (2001) Ecological importance of trichromatic vision to primates, *Nature* 410 (6:826): 363–366.

Dominy, N.J. (2004) Color as an indicator of food quality to anthropoid primates: ecological evidence and an evolutionary scenario, In: *Anthropoid Origins: New Visions*, (eds.) Ross C.F & Kay R.E, Kluwer, Academic/Plenum Publishers, New York, pp 615–644.

Dunbar, R.I.M., (1998) The social brain hypothesis. *Evolutionary Anthropology*, 6 (5): 178–190.

Dunbar, R.I.M., (2009) The social brain hypothesis and its implications for social evolution, *Annals of Human Biology*, 36:5, 562-572.

Dunsworth, H. & Walker, A (2002) Early genus Homo, In: Hartwig WC (ed) *The Primate Fossil Record*. Cambridge University Press, Cambridge, UK, pp 419–435.

Enlow, D.H., & Hans, M.G. (2008) *Essentials of Facial Growth*, 2nd edition, Needham Press, Ann Arbor.

Eriksson, J., Hohmann, G., Boesch, C., & Vigliant, L. (2004) Rivers influence genetic population structure of bonobos (*Pan paniscus*). *Molecular Ecology*, 13, 3425-3435.

Falk, D., (2014) Interpreting sulci on hominin endocasts: old hypotheses and new findings, *Frontiers in Human Neuroscience*, 8:134.

Falk, D., (2008) 'Enlarged Occipital/Marginal Sinuses and Emissary Foramina: Their significance in hominid evolution', In: *Evolutionary History of the 'Robust' Australopithecines*, (ed.) Grine, F. E., New Brunswick, New Jersey: Transaction Publishers, pp. 85-96.

Falk, D., Redmond, J.C. Jr., Guyer, J., Conroy, G.C., Recheis, W., Weber, G.W., & Seidler, H., (2000) Early hominid brain evolution: a new look at old endocasts, *Journal of Human Evolution*, 38, 695–717.

Falk, D. (1990) Brain evolution in *Homo*: The "radiator" theory, Behavioural and Brain Sciences, 13, 333-381.

Falk, D. (1980a) A reanalysis of the South African australopithecine natural endocasts, *Am. J. Phys. Anthropol.*

Falk, D., (1980b) Hominid brain evolution: The approach from paleoneurology, *Yearbook of Physical Anthropology*, 23:93-107.

Falk D (1978) Brain evolution in Old World monkeys. Am J Phys Anthrop 48:315–320.

Fedorov, A. et al., (2012) 3D Slicer as an Image Computing Platform for the Quantitative Imaging Network. *Magnetic Resonance Imaging*, 30(9):1323-41.

Fleagle, J.G., (2013) *Primate Adaptation and Evolution*, 3rd Edition, Academic Press.

Jablonski, NG (2002) Fossil Old World monkeys: The late Neogene radiation. In: Hartwig WC (ed) *The Primate Fossil Record*. Cambridge University Press, Cambridge, UK, pp 255–299.

Jensen-Seaman, M.I., & Kidd, K.K. (2001) Mitochondrial DNA variation and biogeography of eastern gorillas. *Molecular Ecology*. 10, 2241-2247.

Klingenberg, C.P. (2013) Cranial integration and modularity: insights into the evolution and development from morphometric data. *Hystrix*, 1-16.

Kay RF, Ross C, Blythe, WA (1997) Anthropoid origins. Science 275(5301):797–804

Kirk C, Kay RF (2004) Evolution of high visual acuity in the Anthropoidea. In: Ross CF, Kay R (eds) Anthropoid Origins: New Visions. Kluwer Academic/Plenum Publishers, New York, pp 539–602.

Kobayashi, Y., Matsui, T., & Ogihara, N. (2018). Inferring cortical subdivisions based on skull morphology. In: *Digital Endocasts*, (eds.) Bruner, E., Ogihara, N., & Tanabe, H.C.., Springer KK. Tokyo, Japan, pp. 33-46.

Kochiyama, T., Ogihara, N., Tanabe, H. C., Kondo, O., Amano, H., Hasegawa, K., Akazawa, T. (2018). Reconstructing the Neanderthal brain using computational anatomy. *Scientific Reports*, 8(1), 6296.

Gilbert CC, Frost SR, Kelsey D, Pugh KD, Anderson M, Delson E (2018) Evolution of the modern baboon (Papio hamadryas): A reassessment of the African Plio-Pleistocene record. J Hum Evol 122: 38–69

Gomez-Robles, A., Smaers, J.B., Holloway, R.L., Polly, P.D., & Wood, B.A., (2017) Brain enlargement and dental reduction were not linked in hominin evolution, *PNAS*, 114:3, 468–473.

Gonzales, L.A, Benefit, B.R, McCrossin, M.L, Spoor, F. (2015) Cerebral complexity preceded enlarged brain size and reduced olfactory bulbs in old world monkeys. *Nature Communications*, 6:75–80.

Gonzalez, P.N., Vallejo-Azar, M.· Aristide, L., Lopes, R., dos Reis, S.F., Perez, S.I. (2022) Endocranial asymmetry in New World monkeys: a comparative phylogenetic analysis of morphometric data, Brain Structure and Function, 227:469–477.

Goosens, B., Chikhi, L., Jali, M.F., James, S., Lackerman-Ancrenaz, M & Burford, M.W. (2009) Taxonomy, geographical variation and population genetics of Bornean and Sumatran orangutans. In: *Orangutans: Geographic Variation in Behavioural Ecology and Conservation*, (eds.) Wich, SA., Atmoko, S.S.U.S, Seita, T.M., & van Schaik, C.P. Oxford University Press, Oxford, UK.

Gould. L., Sauther, M. (2009) *Lemurs, Ecology and Adaptation*, Springer, New York,

Gowlett, A.J.J. (2012) Shared intention in early artefacts: an exploration of deep structure and implications for communication and language, In: *African Genesis: perspectives on hominin evolution*, (eds.) Reynolds, S.C. and Gallagher A., Cambridge, UK. Cambridge University Press, pp-506-530.

Grabowski, M. (2016) Bigger brains led to bigger bodies? The correlated evolution of human

brain and body size. *Curr. Anthropol* 57(2):174-196.

Grabowski, M., Kopperud, B.T., Tsuboi, M., Hansen, T.F. (2023) Both Diet and Sociality Affect Primate Brain-Size Evolution, *Systematic Biology*, 72: 2, 404–418.

Groves, C.P. (2003) A History of Gorilla taxonomy, In: *Gorilla Biology: A Multidisciplinary Perspective*, (eds.) Taylor, A.B., Goldsmith, M.L, Cambridge University Press, Cambridge, UK.

Groves, C.P. (2001) *Primate Taxonomy*, Smithsonian Institution Press, Washington, USA.

Gurche JA (1982) Early Primate Brain Evolution. In: Armstrong E, Falk D (eds) *Primate brain evolution: methods and concepts.* Springer US, Boston, pp 227–246.

Gursky, S. (2019) Echolocation in a Nocturnal Primate? Folia Primatol, 90:379–391.

Gursky, S., Nekaris, K.A.I. (2019) Nocturnal Primate Communication: Ecology, Evolution and Conservation, Folia Primatol, 90:273–278.

Gursky, S. (2015) Ultrasonic Vocalizations by the Spectral Tarsier, Tarsius spectrum, Folia Primatol, 86:153–163.

Harirngton A, Silcox MT, Yapuncich GS, Boyer DM, Bloch JI (2016) First virtual endocasts of adapiform primates. J Hum Evol 99:52–78.

Jablonski, NG (2002) Fossil Old World monkeys: The late Neogene radiation. In: Hartwig WC (ed) The Primate Fossil Record. Cambridge University Press, Cambridge, UK, pp 255–300

Hohmann, G., & Fruth., B. (2002) Dynamics in social organization of bonobos (*Pan paniscus*) In: *Behavioural Diversity in Chimpanzees and Bonobos*, (eds.) Boesch, C., Hohmann, G., Cambridge: Cambridge University Press; pp 138-150.

Holloway, R. L. (2018). On the making of endocasts: The new and the old in paleoneurology. In *Digital Endocasts*, (eds.) Bruner, E., Ogihara, N., & Tanabe, H.C., Tokyo: Springer Japan KK, pp 1-8.

Holloway, R.L., Broadfield, D.C., & Yuan, M.S., (2004) *The Human Fossil Record, Volume Three, Brain Endocasts: The Paleoneurological Evidence*, Hoboken, New Jersey: Wiley.

Kawamura, S., Hiramatsu, C., Melin, A.D, Schaffner, C.M., Aureli, F., Fedigan., L.M. (2012) Polymorphic Color Vision in Primates: Evolutionary Considerations. In: *Post-Genome Biology of Primates*, (eds) Irai, H., H. Imai,H., Y. Go, Y., Tokyo: Springer, pp. 93-120.

Kay, R.F., & Kirk, E.C. (2000) Osteological evidence for the evolution of activity pattern and visual acuity in primates. *American Journal of Physical Anthropology*. 113:235-262.

Kirk, E. C., & Kay, R.F (2004) Evolution of high visual acuity in the Anthropoidea, In: *Anthropoid Origins: New Visions*, (eds.) Ross C.F, Kay, R.F., Kluwer Academic/Plenum Publishers, New York, pp 539–602.

Labra, N., Mounier, A., Leprince, Y., Rivière, D., Didier, M., Bardinet, E. et al. (2023) What do brain endocasts tell us? A comparative analysis of the accuracy of sulcal identification by experts and perspectives in palaeoanthropology. *Journal of Anatomy*, 1–23.

Lieberman, D. E. (2011). *The Evolution of the Human Head*. Cambridge, Massachusetts. London, England: The Belknap Press of Harvard University Press.

Lieberman, D. E., Pearson, O. M., & Mowbray, K. M. (2000a). Basicranial influence on overall cranial shape. *Journal of Human Evolution*, 38(2), 291–315.

Lieberman, D. E., Ross, C. F., & Ravosa, M. J. (2000b). The primate cranial base: Ontogeny, function, and integration. *American Journal of Physical Anthropology*, 31, 117–169.

Maddison, W. P., & Maddison, D.R. (2021). Mesquite: a modular system for evolutionary analysis. (Version 3.70), Retrieved from http://www.mesquiteproject.org

Martins, E. P., & Hansen, T. F. (1997). Phylogenies and the comparative method: A general approach to incorporating phylogenetic information into the analysis of interspecific data. *American Naturalist*, 149: 646–667.

Materialise. (2018). Mimics 17 (version 17). Leuven, Belgium: Materialise Corporation.

Melin, AD, Matsushita Y, Moritz GL, Dominy NJ, Kawamura S. (2013) Inferred L/M cone opsin polymorphism of ancestral tarsiers sheds dim light on the origin of anthropoid primates. Proc R Soc B 280: 20130189. http://dx.doi.org/10.1098/rspb.2013.0189

Melin, AD, Moritz, G.L., Fosbury, RE., Kawamura S., Dominy, NJ. (2012) Why aye-ayes see blue, Am. J. Primatol., 74: 185-192.

McCarthy, R. C. (2001). Anthropoid cranial base architecture and scaling relationships. *Journal of Human Evolution*, 40(1), 41–66.

McCarthy, R. C. (2004*). Constraints on Primate Craniofacial Growth and Architecture*. (Doctor of Philosophy). The George Washington University.

McKee JK, Keyser AW (1994) Craniodental remains of *Papio angusticeps* from the Haasgat Cave site, South Africa. Int J Primatol, 15:823–841.

Moore, W.J. (2009) *The Mammalian Skull*, Cambridge University Press, Cambridge, UK.

Moss, M.L., & Young, R.W., (1960). A functional approach to craniology. *Am J Phys Anthrop* 18:281-292.

Murray, EA, Bussey TJ, Saksida, L.M., (2007) Visual perception and memory: a new view of the medial temporal lobe function in primates and rodents. *Ann Rev Neurosci* 30:99–122.

Nater, A., Greminger, M.P., Nurcahyo, A., Nowak, M.G., de Manuel Montero, M., Desai, T., Groves, C.P., Pybus, M., Sonay, T.B., Roos, C., Lameira, A.R., Wich, S.A., Askew, J., Davila-Ross, M., Fredriksson, G.M., de Valles, G., Casals, F., Prado-Martinez, J., Goossens, B., Verschoor, E.J., Warren, K.S., Singleton, I., Marques, D.A., Pamungkas, J., Perwitasari-Farajallah, D., Rianti, P., Tuuga, A., Gut, I.G., Gut, M., Orozco-Wengel, P., van Schaik, C.P., Bertranpetit, J., Anisimova, M., Scally, A., Marques-Bonet, T., Meijaard, E. and Krützen, M. (2017). Morphometric, behavioural, and genomic evidence for a new orangutan species. *Current Biology*, 27.

Neubauer, S., Gunz, P., Weber, G.W., Hublin, J-J. (2012) Endocranial volume of *Australopithecus africanus*: New CT-based estimates and the effects of missing data and small sample size, *Journal of Human Evolution*, 62:4:

Neumayer L (1906) Über das Gehirn von Adapis parisiensis Cuv. Neues Jahrb Min Geol Palaont 2:100–104.

Nolte, J. (2009) *The Human Brain: An Introduction to its Functional Anatomy*, 6th edition, Mosby Elsevier, Philadelphia, Pennsylvania, USA.

Nolte, J. (2013) *The Human Brain in Photographs and Diagrams*, 4th edition, Saunders Elsevier, Philadelphia, Pennsylvania, USA.

O'Meara, B., Ané, C., Sanderson, M.J., Wainwright, P.C., (2006) Testing for different rates of continuous trait evolution using likelihood. *Evolution*, 60:922-933.

Pearson A., Polly P.D., Bruner E., (2020) Is the middle cranial fossa a reliable predictor of temporal lobe volume in extant and fossil anthropoids? *Am J Phys Anthropol*, 172: 698–713.

Pearson, A., Polly, P.D., Bruner, E., (2021) Temporal lobe evolution in Javanese *Homo erectus* and African *Homo ergaster*: inferences from the cranial base, *Quaternary International*, 603:5-21.

Pearson, A., Bruner, E., & Polly, P.D. (2023a) Updated imaging and phylogenetic comparative methods reassess relative temporal lobe size in anthropoids and modern humans, *Am J Biol Anthropol*. 1–9.

Pearson, A., & Polly, P. D. (2023b). Temporal lobe evolution in extant and extinct Cercopithecoidea. *Journal of Mammalian Evolution*, 30, 683–694. https://doi.org/10.1007/s10914-023-09664-6

Pearson, A., & Polly, P. D. (2024) Temporal lobe evolution in Hominidae and the origin of human lobe proportions, *Am J Biol Anthropol.*

Petrides, M. (2012) *The Human Cerebral Cortex: An MRI Atlas of the Sulci and Gyri in MNI Stereotaxic Space*, Academic Press, London, UK., Waltham, San Diego, USA.

Perry, G H., Martin, R D., Verrelli, B. C. (2007) Signatures of Functional Constraint at Aye-aye Opsin Genes: The Potential of Adaptive Color Vision in a Nocturnal Primate, Molecular Biology and Evolution, 24:9, 1963-1970.

Polly, P. D. (2022). Phylogenetics for Mathematica (Version 6.5). Bloomington, Indiana: Department of Earth and Atmospheric Sciences, Indiana University. Retrieved from http://pollylab.indiana.edu/software.html.

Radinsky L (1974) The fossil evidence of anthropoid brain evolution, Am J Phys Anthrop 41:15–28.

Richtsmeier, J. T., & Flaherty, K. (2013). Hand in glove: Brain and skull in development and dysmorphogenesis. *Acta Neuropathologica*, 125(4), 469–489.

Rilling, J.K., Glasser, M.F., Jbabadi, S., Andersson, J., & Preuss, T.M., (2012) Continuity, divergence, and the evolution of brain language pathways, *Frontiers in Evolutionary Neuroscience*, 3:11.

Rilling, J.K. (2014) Comparative primate neurobiology and the evolution of brain language systems, *Current Opinion in Neurobiology*, 28:10–14.

Rilling, J. K, & Seligman, R. A. (2002). A quantitative morphometric comparative analysis of the primate temporal lobe. *J Hum Evol*, 42(5), 505-533.

Rilling, J. K. (2006). Human and nonhuman primate brains: Are they allometrically scaled versions of the same design? *Evolutionary Anthropology*, 15, 65–77.

Rodieck, R.W. (1988) The Primate Retina, In: Comparative Primate Biology, Volume 4: Neurosciences, (eds) Steklis, H.D., & Erwin, J., Alan R. Liss, New York, NY. pp. 203-278.

Rylands, A.B., & Mittermeir, R.A. (2013) Family Cebidae (Squirrel monkeys and capuchins), In*: Handbook of the Mammals of the World. Vol. 3. Primates.* (eds.) Mittermeir, R.A., Rylands, A.B, & Wilson, D.E., Lynx Edicons, Barcelona, pp.

Sansalone, G., Allen, K., Ledogar, J., Ledogar, S., Mitchell, D.R., Profico, A., Castiglione, S., Melchionna, M., Serio, C., Mondanaro, A., Raia, P., & Wroe, S., (2020) Variation in the strength of allometry drives rates of evolution in primate brain shape, *Proc. R. Soc. B*, 287: 20200807.

Semendeferi, K., Damasio, H. (2000). The brain and its main anatomical subdivisions in living hominoids using magnetic resonance imaging. *J. Hum. Evol*., 38:317-332.

Shattuck, D. W., & Leahy, R. M. (2002). BrainSuite: An automated cortical surface identification tool. *Medical Image Analysis*, 6(2), 129–142.

Sherwood, CC., Bauernfeind, AA. L. V., Raghanti, M. A & Hof, P. R. (2017) Evolutionary Specializations of Human Brain Microstructure, In: Evolution Of Nervous Systems Volume 4: The Evolution Of The Human Brain: Apes And Other Ancestors, (ed) J. H. Kaas, 2nd edution, Elsevier Inc.

Silcox, M.T., Bertrand, O.C., Harrington, A.R., Lang, M.M., San Martin-Flores, G.A., López-Torres, S. (2023). Early Evolution of the Brain in Primates and Their Close Kin. In: Dozo, M.T., Paulina-Carabajal, A., Macrini, T.E., Walsh, S. (eds) *Paleoneurology of Amniotes* . Springer, Cham. https://doi.org/10.1007/978-3-031-13983-3_12.

Simon, EL (1995a) Crania of *Apidium*: primitive anthropoidean (Primates, Parapithecidae) from the Egyptian Oligocene. *American Museum Noviates*, 3124, 1-10.

Simons EL (1995b) Egyptian Oligocene primates: a review. Yearb Phys Anthropol 38:199–238.

Simons, EL., Rasmussen, DT. (1996) Skull of *Catopithecus browni,* an early Tertiary catarrhine, *American Journal of Physical Anthropology,* 100: 261-292.

Simons EL (1997) Preliminary description of the cranium of *Proteopithecus sylviae*, an Egyptian late Eocene anthropoidean primate. Proc Natl Acad Sci U S A 94:14970–14975.

Simons EL (2001) The cranium of *Parapithecus grangeri*, an Egyptian Oligocene anthropoidean primate. *Proc Natl Acad Sci U S A,* 98(14):7892–7897

Simons EL, Seiffert ER, Ryan TM, Attia Y (2007) A remarkable female cranium of the early Oligocene anthropoid *Aegyptopithecus zeuxis* (Catarrhini, Propliopithecidae). Proc Natl Acad Sci U S A ,104(21):8731–8736.Simpson, G. G., Roe, A., & Lewontin, R. C. (2003). *Quantitative Zoology*, (Revised ed.), Dover Publications, New York, NY, USA.

Smith, F.H. (2002) Migrations, radiations and continuity: patterns in the evolution of Middle and Late Pleistiocene humans, In: Hartwig WC (ed) The Primate Fossil Record. Cambridge University Press, Cambridge, UK, pp 437–456.

Stratovan. (2021). Stratovan Checkpoint, UC, Davis, California: Stratovan Corporation.

Sterling EJ, McCreless EE (2006) Adaptations in the aye-aye: a review. In: Gould L, Sauther ML (Eds), *Lemurs: Ecology and Adaptation*. New York: Springer. pp 159–184.

Strier, K. B. (2017) *Primate Behavioural Ecology*, 5th edition, Routledge, New York, NY, USA.

Thalmann, O., Wegmann, D., Spitzner, M., Arandjelovic, M., Guschanski, K., Leuenberger, C., Bergal., R.A, & Viglant, L. (2011) Historical sampling reveals dramatic demographic changes in western lowland gorilla populations. *Evolutionary Biology*. 11:85, 85.

Thorgood, P. (1993) Differentiation and morphogenesis of cranial skeletal tissues, In: *The Skull, Volume 1,* (eds.) Hanken, J., & Hall, B.K., The University of Chicago Press, Chicago, USA, pp. 112-152.

Veilleux, C.C., & Kirk, C.E. (2014) Visual acuity in mammals: effects of eye size and ecology. *Brain, Behavior Evolution*, 83(1):43–53

White, T. D., & Folkens, P. A. (2011). *Human Osteology* (3rd ed.). Burlington, San Diego, Oxford: Academic Press.

White T.D. (2002) Earliest Hominids, In: Hartwig WC (ed) *The Primate Fossil Record.* Cambridge University Press, Cambridge, UK, pp 407–417.

Wolfram (2021). Wolfram Mathematica (Version 13.0). Champaign, Illinois: Wolfram Research, Inc.

Wich, S.A., Singleton, I., Nowak, M.G., Utami Atmoko, S.S., Nisam, G., Arif, S.M., Putra, R.H., Ardi, R., Fredriksson, G., Usher, G., Gaveau, D.L.A and Kühl, H.S. (2016). Land-cover changes predict steep declines for the Sumatran orangutan (*Pongo abelii*). *Science Advances* 2(3): e1500789.

Williamson, E.A., Maisels, F.G. & Groves, C.P. (2013) Family Hominidae (Great Apes), In: *Handbook of the Mammals of the World. Vol. 3. Primates*. (eds.) Mittermeir, R.A., Rylands, A.B, & Wilson, D.E., Lynx Edicons, Barcelona, pp.

Zinner, D., Fickenscher, G.H., Roos, C. (2013) Family Cercopithecidae (Old World Monkeys), In: *Handbook of the Mammals of the World. Vol. 3. Primates*. (eds.) Mittermeir, R.A., Rylands, A.B, & Wilson, D.E., Lynx Edicons, Barcelona, pp.

Zimmerman, E. (2016) Acoustic divergence and communication of cheirogaleids with special emphasis to mouse lemurs, In: *The Dwarf and Mouse Lemurs of Madagascar*, (eds.) Lehman, S.M., Radespiel, U., Zimmerman, E., Cambridge University Press, Cambridge, UK, pp. 405-421.

Zollikofer, C.P.E., Ponce de Leon, M.S. (2005) *Virtual Reconstruction: A Primer in Computer-Assisted Paleontology and Biomedicine.* Wiley-Liss, New York; Chichester.

Pearson, A., Polly, P. D., & Bruner, E. (2020). Is the middle cranial fossa a reliable predictor of temporal lobe volume in extant and fossil anthropoids? *American Journal of Physical Anthropology*.172(4),698-713.

In this chapter, I provide quantification of the first aim of this thesis by confirming the association between temporal lobe volume of the brain and middle cranial fossa size in anthropoids and providing a reliable prediction of temporal lobe size in fossil anthropoids with application for examining cerebral reorganisation.

Chapter 3: Is the middle cranial fossa a reliable predictor of temporal lobe volume in extant and fossil anthropoids?

3.1 Abstract

We investigate the suitability of middle cranial fossa (MCF) size as a proxy for temporal lobe volume (TLV), examining the strength of the association between TLV and MCF metrics and assess the reliability predicting TLV in fossil anthropoids. The temporal lobe of the primate brain is a multimodal association cortex involved in long-term memory, auditory, and visual processing with unique specialisations in modern humans for language comprehension. The MCF is the bony counterpart for the temporal lobe providing inferences for fossil hominin temporal lobe evolution. We now investigate whether the MCF is a suitable proxy for the temporal lobe. A sample of 23 anthropoid species (n = 232, including 13 fossil species) from computed tomography (CT) scans of ex vivo crania and magnetic resonance imaging (MRI) of the in vivo brain were generated into three-dimensional (3D) virtual models. Seven linear metrics were digitally measured on the right MCF with right TLV calculated from in vivo MRI.

Regression analyses produced statistically significant correlations between TLV and all MCF metrics ($r \geq 0.85$; $p \leq 0.0009$) with TLV predictions within ±1 standard error and three MCF metrics (posterior-width, mid-length, and mid-width) the most reliable predictors of TLV with only one metric weakly associated with TLV. These findings indicate a strong association between the MCF and TLV, provide reliable predictors of fossil TLV that were previously unattainable, allow the inclusion of fragmentary fossil material, and enable inferences into the emergence of modern human temporal lobe morphology.

3.2 Introduction

The primate brain has a well-defined Sylvian fissure, dividing the temporal lobe from the remaining cerebral cortex, while function-ally, it is a multimodal association cortex where long-term memory, auditory, and visual processing in primates has further neurobiological specializations in modern humans, specific to language processing and comprehension (Bryant & Preuss, 2018). Compared with other anthropoids, the modern human temporal lobe is considered disproportionately large (Rilling, 2006; Rilling & Seligman, 2002); however, see Semendeferi and Damasio (2000) for alternate interpretations. For palaeoneurologists, inferences from fossil hominins may indicate when modern human temporal lobe morphology emerged.

The middle cranial fossa (MCF) has a potential structural interaction between the brain and cranium, where morphological changes to the temporal lobe are likely affected by brain and cranial morphology. For example, changes to cranial base angle in nonhuman primates is associated with shifts in facial block angle (Lieberman, Ross, & Ravosa, 2000; McCarthy, 2001), while further reduction in facial angle is evident in modern humans (Bastir et al., 2010;

Bastir & Rosas, 2016; Lieberman, Pearson, & Mowbray, 2000) combined with associated changes to mandibular form (Bastir, Rosas, & Kuroe, 2004).

In the fossil record, the soft-tissue brain does not preserve, and brain morphology must be indirectly inferred from endocasts, physical or virtual molds of the endocranial cavity (Holloway, 2018). Further-more, the close spatial correspondence between the brain and endocranium is noticeable on the surface of the MCF, where some sulcal imprints of the temporal lobe are retained on the lateral, anterior, and inferior endocranial surface (Falk, 1978, 1980, 2014; Falk et al., 2018; Gonzales, Benefit, McCrossin, & Spoor, 2015; Rosas, Pena-Melian, Garcia-Tabernero, Bastir, & De La Rasilla, 2014). It is reasonable to extend the "functional craniology" hypotheses by Moss and Young (1960) into an evolutionary context with reciprocal inter-action between the brain and cranium (Bruner, 2017).

Without systematically examining the suitability of MCF measurements as a proxy for temporal lobe, the accuracy of fossil inferences remains uncertain. Such an assessment is important because the relative lengthening of the MCF in fossil Homo has been implicated in the emergence of enlarged temporal lobes in extant *Homo sapiens* (Bastir et al., 2011; Bastir, Rosas, Lieberman, & O'Higgins, 2008) and the MCF used to infer temporal lobe morphology in *Homo neanderthalensis* through comparisons between El Sidron and extant *Homo sapiens* (Rosas et al., 2014). Moreover, the lack of delimiting boundaries on the external surface of the temporal lobe or on endocasts (Kobayashi, Matsui, & Ogihara, 2018) makes comparing data from previous studies difficult and so, for palaeoneurologists, a comparative study of the evolution in temporal lobe size based on fossil endocasts has remained unattainable.

Here, we examine whether MCF size is a suitable proxy for TLV by evaluating a set of standardised metrics that can be measured even in fragmentary fossils to determine which

metrics are more strongly or weakly associated with TLV and to assess their reliability for predicting TLV. We apply the resulting prediction equations to a series of key anthropoid fossils to determine the degree of uncertainty that arises from the choice of which MCF metrics are used.

3.3 Materials and Methods

3.3.1. Sample composition

The total sample (N = 232) consisted of 23 anthropoid species, including 13 fossil species (Table 1), from ex vivo cranial CT (n = 154) and T1-weighted structural in vivo brain MRI (n = 78). The in vivo human MRI sample in this study was accessed from the Open Access Series of Imaging Studies (OASIS) with appropriate human ethics protocol approvals (see Marcus et al., 2007), while nonhuman primate in vivo MRI was accessed from National Chimpanzee Brain Resource with the necessary animal ethics protocol approvals (see Rilling & Insel, 1999).

Table 1- Anthropoid sample (N = 232) detailing digital modality type of the 11 extant anthropoid species and 13 fossil anthropoid species (in bold).

Species	**CT**	**MRI**	**n**
Homo sapiens	44	40[a]	84
Homo sapiens (Cro-Magnon 1; Singa 1; Skhul 5; Mladecˇ 1)	4		4
Homo neanderthalensis (Gibraltar 1)	1		1
Homo heidelbergensis (Bodo; Kabwe)	2		2
Homo ergaster (KNM-ER-3883; KNM-ER-3733; OH9)	3		3
Homo habilis (ER-1805)	1		1
Australopithecus africanus (STS-5)	1		1
Paranthropus boisei (KNM-ER-406)	1		1
Pan troglodytes	10	6[b]	16
Pan paniscus	14	4[b]	18
Gorilla gorilla	10	2[b]	12
Pongo pygmaeus	13	4[b]	17
Hylobates lar	14	4[b]	18
Papio sp.	4	2[b]	6
Papio angusticeps (DNMHN-CO100)	1		1
Dinopithecus ingens (DNMHN-SK544)	1		1
Macaca mulatta	12	4[b]	16
Cercocebus atys	4	4[b]	8
Aegyptopithecus zeuxis (CGM-40237)	1		1
Parapithecus grangeri (DPC-18651)	1		1
Sapajus apella	6	4[b]	10
Saimiri sciureus	4	4[b]	8
Homunculus patagonicus (MPV-3501)	1		1
Tremacebus harringtoni (FML-619)	1		1

[a] Human in vivo MRI from Open Access Series of Imaging Studies (OASIS).

[b] Nonhuman primate in vivo MRI from National Chimpanzee Brain Resource.

The sample comprised two different imaging modalities with in vivo MRI preferred for soft-tissue imaging and ex vivo high-resolution CT for hard-tissue imaging. This meant samples were not from the same individuals; however, species classification was confirmed in both datasets following the protocol in Pearson, Groves, and Cardini (2015). In *Papio*, the MRI sample contained *Papio cynocephalus*, but in the CT sample, it was necessary to substitute with *Papio anubis* to maintain sample size. Although substitution was not ideal, we do not anticipate any issue considering high hybridisation rates between *P. anubis* and *P. cynocephalus* (Ackermann, Rogers, & Cheverud, 2006; Rogers et al., 2019; Zinner, Wertheimer, Liedigk,

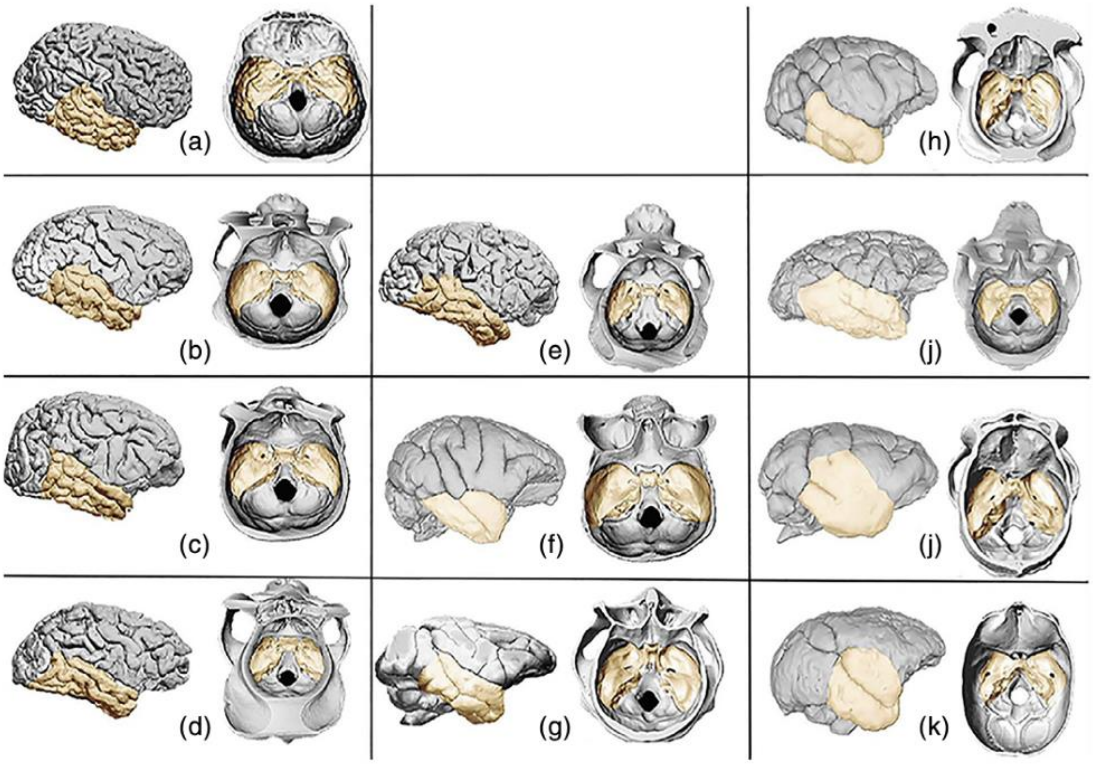

Figure 1 Depiction of the right temporal lobe and middle cranial fossa boundaries (in gold) on virtual models of the brain and endocranium in the 11 extant anthropoid species included in this study. Note: Cerebellum not always depicted and figures not to scale *a) Homo sapiens; b) Pan troglodytes; c) Pan paniscus; d) Gorilla gorilla; e) Pongo pygmaeus; f) Hylobates lar; g) Cercocebus atys; h) Macaca mulatta; i) Papio sp.; j) Sapajus apella; k) Saimiri sciureus.*

Groeneveld, & Roos, 2013), cranial similarity (Frost, Marcus, Bookstein, Reddy, & Delson,

2003; Gilbert, 2011; Gilbert, Frost, Pugh, Anderson, & Delson, 2018) and hybrid-clinal geographical zones such as southeastern Kenya and Tanzania (Kingdon, Butynski, & De Jong, 2008; Kingdon, Butynski, & De Jong, 2016) all contribute to taxonomic complexity and continuing uncertainty (Groves, 2001). Specific locale details for all but one of the specimens in *Papio* CT sample enabled confirmation that more than half of our sample originated in the present hybridisation zone in southeastern Kenya. Moreover, any statistical uncertainty arising from substituting one species for another in this combined sample has additionally been accommodated into our regression and prediction analysis. We followed Groves (2001) and Fleagle (2013) for classifications of extant and fossil anthropoid taxonomy.

3.3.2. Comparative anatomy

The interconnected structures of the temporal cerebrocranial system include the temporal lobe of the brain and the middle cranial fossa of the skull. The morphogenesis of the brain and the skull are initiated and driven by complex cell–cell signalling networks specific to cellular type and involved throughout embryonic stages with the basicranium derived from endochondral ossification and cartilage precursors, while temporal lobe morphology is affected by neural-crest cells and meninges derived from cephalic mesoderm (Richtsmeier & Flaherty, 2013). This complex morphogenesis is responsible for the close spatial correspondence between the temporal lobe of the brain and the cranial base consistent in mammalian taxa, including anthropoid primates.

The endocranium comprises the anterior cranial fossa associated with the frontal lobe of the brain, the posterior cranial fossa (PCF) associated with the cerebellum and occipital lobes, while the MCF is associated with the temporal lobes of the brain (Borden, Forseen, & Stefan, 2016). The MCF consists of the squamous and petrous parts of the temporal bone and

the greater wings of the sphenoid, bound anteriorly by the lesser wings of the sphenoid; laterally by the squamous part of the temporal bone and posteriorly by the petrous part of the temporal bone (White, Black, & Folkens, 2011). We define the boundaries for the right anthropoid MCF (Figure 1) following Lieberman, Pearson, and Mowbray (2000), McCarthy (2001) and White et al. (2011).

Table 2. The anatomical descriptions and measurement points used to define the right anthropoid middle cranial fossa (MCF) and corresponding points used for metrics in Figure 2.

Point	Description
Carotid sulcus (CS)	Medial margin of the internal carotid sulcus on the tuberculum sellae, inferior to the middle clinoid process, posteromedial to the superior orbital fissure.
Foramen lacerum (FL)	Anteromedial margin of the foramen lacerum, medial to the carotid canal, and on the lateral border of the sellae turcica.
Petrous apex (PA)	Point on the apex of petrous portion, slightly superior to the depression of the semilunar ganglion.
Posterior petrous (PP)	Point on the petrous portion, located on the margin of transverse sinus and petrosquasomal suture.
Anterior temporal pole (AP)	Point of deepest indentation on sphenoidal surface, corresponding to the anterior temporal pole of the cerebrum and the most anterior boundary of middle cranial fossa.
Sphenosquamosal (SQ)	Point on the sphenosquamosal suture of the lesser wing of the sphenoid, inferior to the sphenoid ridge at the junction of frontal branch of the middle meningeal artery, corresponding to pterion on the ectocranial surface.

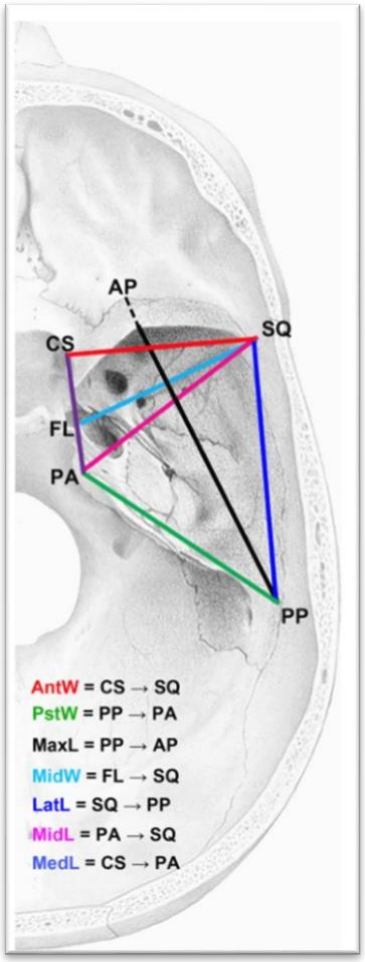

Figure 2. An illustration of a modern human middle cranial fossa with the seven measurements used in this study shown on the right MCF (not to scale) with associated MCF anatomy and descriptions in Table 2. Original illustration courtesy of Eduardo Saiz.

The brain is divided into left and right hemispheres with the temporal lobe separated by the Sylvian fissure (Nolte, 2009). The temporal lobe is delineated superiorly by the ascending

and descending rami of the Sylvian fissure, superoposteriorly by the fusiform gyrus, inferoposteriorly by the preoccipital notch and inferomedially by the parahippocampal gyrus and terminating medially at the margins of the medulla and pons (Borden et al., 2016; Mai, Paxinos, & Voss, 2008). We define the boundaries for the right anthropoid temporal lobe (Figure 1; Table 2), following Aldridge (2011), Rilling and Seligman (2002) and Semendeferi and Damasio (2000).

3.3.3. Data collection and measurement error

All data collection, digital imaging processing and measurements were conducted by a single operator (AP) to reduce interobserver error. All MCF metrics and TLV were calculated using the right side of the specimen; however, in some fossil species, the left side of the MCF was between replicates relative to the total between-group variation (Bailey & Byrnes, 1990). A single specimen from each extant species (n = 11) was measured on two separate occasions and measurement error calculated as % ME = 100 × MS (within)/(MS (within) + MS (among)). For the seven MCF metrics, measurement error ranged from ≤1% to 4%, while the right TLV measurement error was ≤1% (results not shown). Therefore, we considered intraobserver error had a minimal effect on this study and was unlikely to affect further analyses.

3.3.4. Statistical Analyses anatomy

3.3.4.1. Anthropoid MCF variation

The extent of variation in the seven MCF metrics among extant and fossil anthropoids was investigated using correlation principal component analysis (PCA) in PAST 3.19 (Hammer, Harper, & Ryan, 2001).

3.3.4.2. MCF-TLV association

Bivariate ordinary least-squares (OLS) regression was used to deter-mine the strength of association between each of the seven MCF metrics and TLV in extant anthropoids. All analyses were conducted using the species-average for the MCF variables and TLV. To linearise scaling relationships (see Simpson, Roe, & Lewontin, 2003), MCF variables were converted (from mm) into natural logarithmic units (base e), while the cube-root of TLV was calculated then converted into a natural logarithmic unit (base e) and a 95% confidence interval fitted to the log–log regressions. The potential influence of phylogeny was also examined using phylogenetic generalised least-squares (PGLS) regression and a consensus anthropoid tree modified from Version 3 of 10 K Trees (Arnold, Matthews, & Nunn, 2010). Trait Mapping followed Martins and Hansen (1997) to test the correlation between TLV, MCF variables and the anthropoid phylogeny using Blomberg's K (kappa) statistic for significance, where K is closer to 1 when traits show a higher-than-expected correlation with phylogeny (Blomberg, Garland, & Ives, 2003). The OLS, PGLS and K calculations were per-formed with Phylogenetics for Mathematica Version 6.5 (Polly, 2019).

3.3.4.3. Predicting TLV

The bivariate OLS regressions provided prediction equations for estimating TLV from each MCF variable, calculated as TLV = (a* log[x]+ b). The reliability of the predictions for extant anthropoid species was calculated as the percentage of prediction errors (PPE) where PPE = (predicted – observed)/predicted × 100). PPE reports how much uncertainty there is in an estimate relative its size, and is there-fore, arguably more important for evaluating prediction

equations than correlation coefficients, coefficients of determination and p-values from regressions (Smith, 1984).

Fossil predicted TLV was calculated from each MCF variable using prediction equations provided by the bivariate OLS regression models where TLV = (a × log[x]+b). The reliability of fossil predictions was determined by applying a bracket of uncertainty using the standard error (s.e.) from the bivariate OLS regression models to calculate the upper and lower estimates for predicted TLV in each specimen where predicted TLV = (a × log[x]+ b ± s.e). This allowed the inherent differences of each MCF variable to be accommodated, where slight changes in the range of uncertainty in each MCF variable are associated with differences in the standard error and accommodated into the prediction reliability. Thus, the linear scaling relationship of brain size is also accommodated into the TLV predictions where the range of uncertainty is proportion-ate to absolute size, hence, larger predicted TLV have a greater uncertainty bracket (in cm^3) compared to smaller predicted TLV and narrow uncertainty bracket (in cm3) as per conversion from natural log units (base e) into volumetric units (cm^3). All TLV pre-dictions were conducted using Phylogenetics for Mathematica version 6.5 (Polly, 2019).

3.4. Results

3.4.1. Anthropoid MCF variation

PCA evaluated anthropoid MCF variation, where the majority of MCF variation was due to absolute size, with longer and wider MCF contra-sting with narrower and shorter MCF (Figure 3a, b; Table 4). An initial PCA compared extant and fossil anthropoids (Figure 3a; Table 4), with PC1 explaining 89% of variance associated with absolute size in six MCF

variables, where longer and wider MCF separated extant *Homo sapiens* and fossil hominins from other anthropoids. Although PC2 explained a much smaller amount of total variance (6%) it was associated with a single MCF variable, with a longer or shorter medial-length separating some extant and fossil anthropoids. Subsequent PCs explained less than 3% each and will not be considered here. A second PCA compared extant *Homo sapiens* with fossil hominins (Figure 3b; Table 4), with PC1 explaining 53% of total variance. associated with six MCF variables, where a long and wide MCF separated extant *Homo sapiens* from most fossil hominins, whereas PC2 explained 22% of total variance associated with three MCF variables, with an MCF that was long, narrow (anteriorly), but wide (posteriorly) versus a long, wide (anteriorly) but narrow (posteriorly) MCF. Despite PC3 explaining 14% of total variance it was associated with only one MCF variable, separating most fossil hominins from modern humans according to a long versus short medial-length (Table 4). The subsequent PCs explained less than 5% each and will not be considered further.

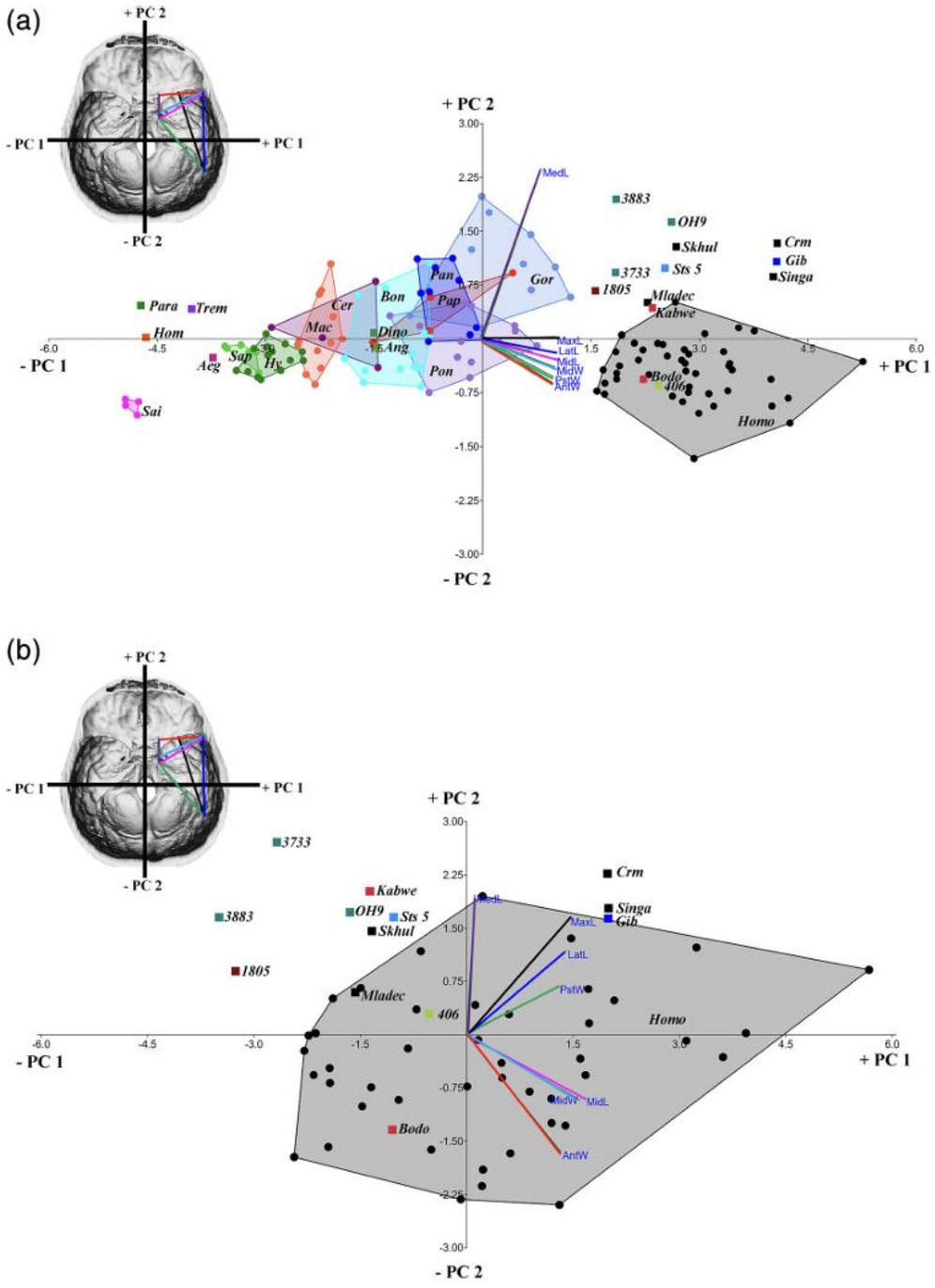

Figure 3 a-b. Principal component analysis (PCA) of seven MCF variables with biplot illustratingMCF variable and corresponding positive or negative PC loadings for A) PCA of extant and fossil anthropoids with MCF variance of PC1 (89%) versus PC2 (6%) associated with long/wide MCF or short/narrow MCF and B) PCA of extant *Homo sapiens* and fossil hominins with MCF variance of PC1 (53%) versus PC2 (22%) corresponding to a long, posteriorly wide MCF versus long, anteriorly wide MCF. Abbreviations: Homo = extant *Homo sapiens*; Crm = fossil *Homo sapiens* (Cro-Magnon 1); Singa = fossil *Homo sapiens* (Singa 1); Mladecˇ = fossil *Homo sapiens* (Mladecˇ 1); Skhul = fossil *Homo sapiens* (Skhul 5); Gib = *Homo neanderthalensis* (Gibraltar 1); Kabwe = *Homo heidelbergensis* (Kabwe 1); Bodo = *Homo heidelbergensis* (Bodo); 3883 = *Homo ergaster* (ER-3883); 3733 = *Homo ergaster* (ER-3733); OH9 = *Homo ergaster* (OH 9); 1805 = *Homo habilis* (ER-1805); 406 = *Paranthropus bosiei* (ER-406); Sts-5 = *Australopithecus africanus* (STS-5); Pan = *Pan troglodytes*; Bon = *Pan*

paniscus; Gor = *Gorilla gorilla*; Pon = *Pongo pygmaeus*; Hy = Hylobates *lar*; Mac = *Macaca mulatta*; Cer = *Cercocebus atys*; Pap = *Papio anubis*; Ang = *Papio angusticeps* (CO-100); Dino = *Dinopithecus ingens* (SK-554); Aeg = *Aegyptopithecus zeuxis* (CGM-402327); Para = Parapithecus *grangeri* (DPC-18651); Sap = *Sapajus apella*; Sai = *Saimiri sciureus*; Hom = *Homunculus patagonicus* (MPV-3501); Trem = *Tremacebus harringtoni* (FML-619).

Table 4- Principal component analysis (PCA) for the anthropoid MCF variance listing PCs, percentage of variance, eigenvalues, MCF variables, and PC loadings for (a) extant and fossil anthropoids, where only the first two PCs had substantial effect on MCF variance and (b) extant *Homo sapiens* and fossil hominins, where the first two PCs had substantial effect on MCF variance and, despite PC3 having a lower contribution to total variance, it remains important for medial-length variation. Statistically significant results are reported in bold.

Extant and fossil anthropoid PCA							
PC		**Eigenvalue**			**% variance**		
1		6.24906			89.27		
2		0.430447			6.15		
3		0.194312			2.77		
4		0.0653414			0.93		
5		0.0340782			0.48		
6		0.0188937			0.27		
7		0.00786499			0.11		
PC loadings							
MCF	**PC 1**	**PC 2**	**PC 3**	**PC 4**	**PC 5**	**PC 6**	**PC 7**
AntW	0.3792	−0.23974	0.57126	−0.10182	0.52592	0.39202	0.31812
PstW	0.38215	−0.20603	−0.37675	0.79077	0.025401	0.16875	0.21567
MaxL	0.39292	0.012634	−0.32015	−0.19052	0.48286	−0.32818	−0.57658
MidW	0.3906	−0.15285	0.3437	0.062592	−0.23939	−0.75675	0.13505
LatL	0.38463	−0.074964	−0.50788	−0.55187	−0.14878	0.15713	0.47613
MidL	0.39372	−0.10281	0.20444	−0.08898	−0.64032	0.32893	−0.46822
MedL	0.31663	0.92756	0.10658	0.10777	0.012546	0.067726	0.23594
Fossil hominin PCA							
PC		**Eigenvalue**			**% variance**		
1		3.74172			53.45		
2		1.55385			22.19		
3		1.01057			14.43		
4		0.379008			5.41		
5		0.14209			2.03		
6		0.112582			1.60		
7		0.0601772			0.85		
PC loadings							
MCF	**PC 1**	**PC 2**	**PC 3**	**PC 4**	**PC 5**	**PC 6**	
AntW	0.37038	−0.46066	0.28757	0.14789	−0.55028	0.37688	
PstW	0.36112	0.19242	−0.51859	0.67218	0.21297	0.14114	
MaxL	0.40347	0.45861	0.046429	0.068465	−0.51209	−0.15924	
MidW	0.44575	−0.25715	0.27577	0.086387	0.24125	−0.75844	
LatL	0.39251	0.3304	−0.27433	−0.65752	−0.04794	0.01356	
MidL	0.46463	−0.2501	0.053382	−0.23789	0.50901	0.42872	
MedL	0.031338	0.55009	0.70147	0.15879	0.26461	0.23123	

Abbreviations: MCF metrics= AntW, anterior-width; PstW, posterior-width; MidW, mid-width; MaxL, maximum-length; LatL, lateral-length; MidL, midl-ength; MedL,medial-length.

3.5.2. MCF-TLV association

OLS regression produced statistically significant correlations ($r \geq 0.85$; $p \leq 0.0009$) between the seven MCF variables and anthropoid TLV (Figure 4a–g, Table 5).

Table 5. Parameters for ordinary least-squares regression and phylogenetic generalised least-squares regression detailing the regression statistics for the seven MCF metrics and temporal lobe volume. Statistically significant results reported in bold.

Regression Statistics									
	OLS				**PGLS**				
MCF Metrics	*a*	*b*	*r*	*p*	*a*	*b*	r^2	*p*	*k*
AntW	0.944	−1.906	0.95	0.0001	0.845	−1.626	0.88	<0.0001	0.66
PstW	1.020	−2.438	0.98	0.0001	0.950	−2.223	0.96	<0.0001	0.76
MidW	0.951	−2.088	0.98	0.0001	0.924	−2.003	0.96	<0.0001	0.62
MaxL	0.983	−2.678	0.92	0.0001	0.853	−2.227	0.82	0.0001	0.77
LatL	1.088	−2.975	0.93	0.0001	0.903	−2.339	0.81	0.0002	0.57
MidL	0.908	−1.972	0.98	0.0001	0.937	−2.056	0.96	<0.0001	0.89
MedL	0.601	−0.623	0.85	0.0009	0.450	−0.271	0.63	0.0033	0.90
AntW	0.944	−1.906	0.95	0.0001	0.845	−1.626	0.88	<0.0001	0.66

Abbreviations: OLS, ordinary least-squares regression: a = slope; *b* = intercept; *r* = correlation coefficient; *p* = permutated p-value. PGLS, phylogenetic generalized least-squares regression: *a* = slope; *b* = intercept; r = correlation coefficient; p = permutated p-value; r^2 = coefficient of determination; k = Blomberg's Kappa; MCF metrics = AntW, anterior-width; PstW, posterior-width; MidW, mid-width; MaxL, maximum-length; LatL, lateral-length; MidL, mid-length; MedL, medial-length.

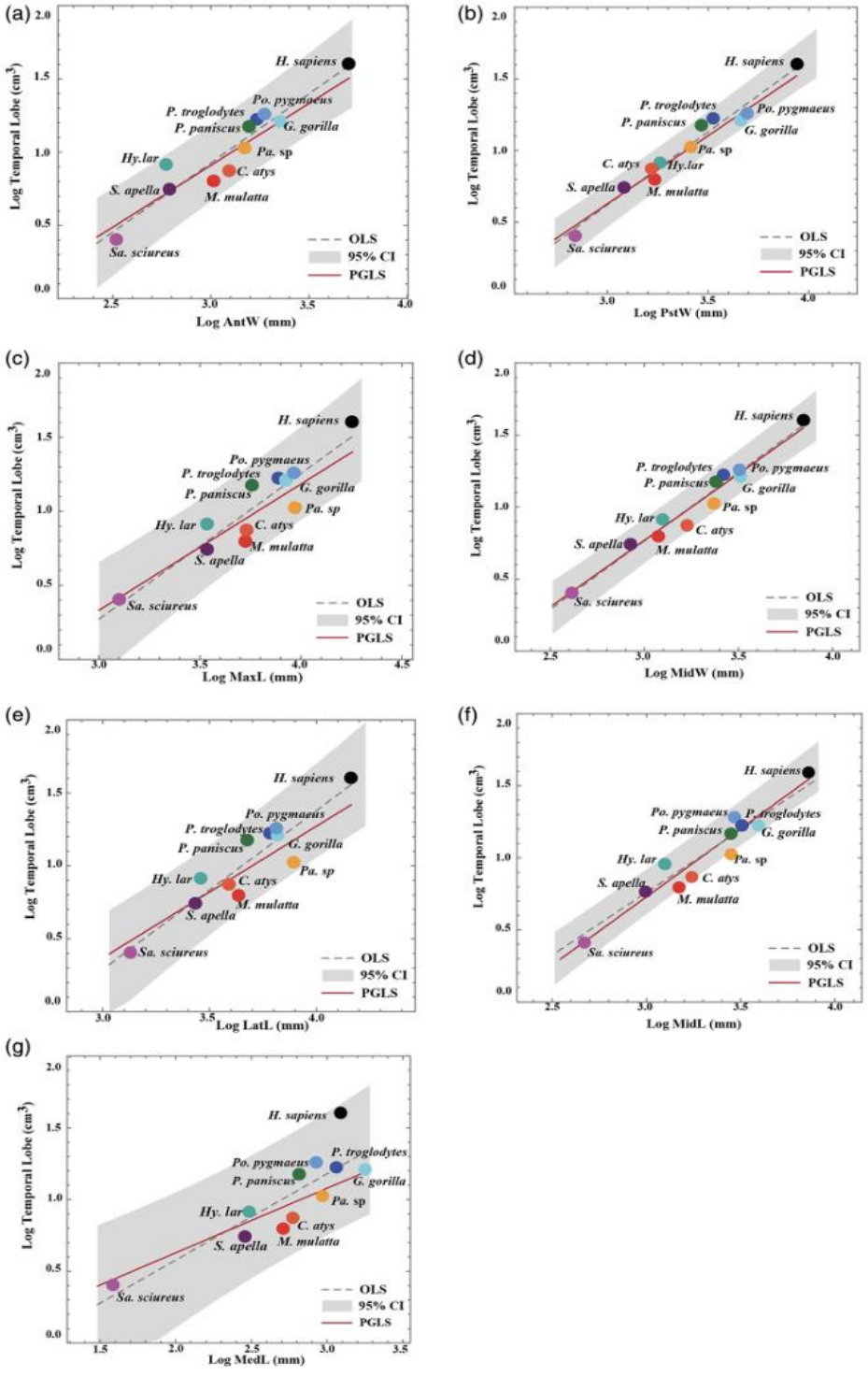

Figure -4-g. Bivariate OLS and PGLS log–log regressions showing the correlation between seven MCF variables and TLV in extant anthropoids. All taxa fall within the 95%confidence interval (grey shaded section) with black-dashed line indicating the OLS regression line and the solid red line representing the PGLS regression line. The corresponding regression parameters are provided in Table 5.

Of the seven MCF variables, the strongest correlations with TLV occurred equally in posterior-width, mid-length, and mid-width ($r = 0.98$), while medial-length had the weakest correlation with TLV ($r = 0.85$). PGLS regression was also conducted; however, results did not differ substantially from the OLS regression and will not be discussed further. Trait mapping indicated no statistically significant correlation between TLV, five MCF variables and phylogeny ($k = 0.57$ to 0.77), however, mid-length ($k = 0.89$) and medial-length ($k = 0.90$) did show a stronger correlation with phylogeny (Figure 5a–h; Table 5). Although the PGLS regressions did not differ substantially from OLS regressions, we report both analyses for comparative purposes only, and unless otherwise indicated, results relate to OLS regressions.

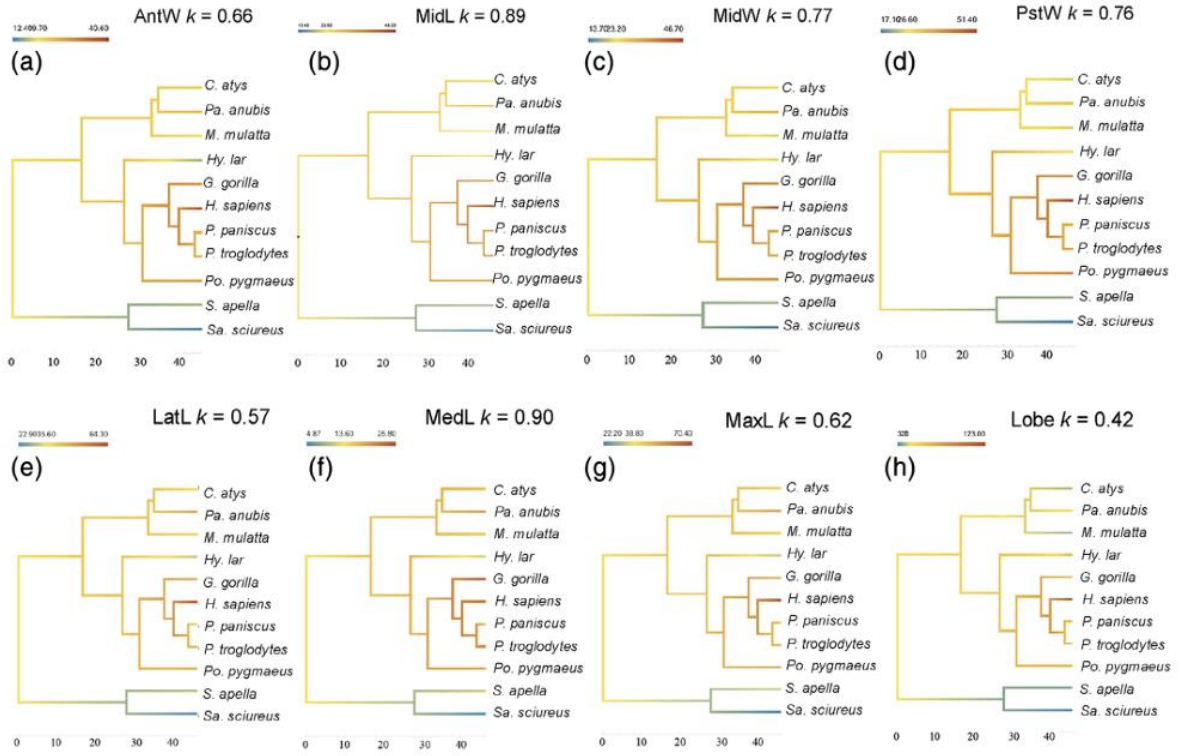

Figure 5 a-h. Trait-Mapping showing the correlation between the seven MCF variables, TLV, and the extant anthropoid phylogeny using Blomberg's K for statistical significance with values closer to 1 representing higher phylogenetic correlation. Heat-map colouring refers to absolute size of a variable with red equivalent to larger and blue, smaller values.

3.4.2. Predicting TLV

Predicted TLV was calculated from the seven MCF variables using the OLS regression equations with a prediction uncertainty bracket of ±1 s.e where the strongest MCF predictors of TLV (posterior-with, mid-length, and mid-width) were capable of predicting TLV to within±11 cm3, ± 19 cm3, and ± 12 cm3, respectively. Only one MCF variable (medial-length) was weakly associated with TLV and a poor predictor of anthropoid TLV with PPE also indicating medial-length underestimated TLV in extant *Homo sapiens* and *Saimiri sciureus* by 30% and 24%, respectively, but overestimated TLV in *Macaca mulatta* by 20% (Table 6).

Table 6. Percentage of prediction errors (PPE) for seven MCF metrics in extant anthropoids calculated as the difference between observed and predicted temporal lobe volumes and percentage of prediction reliability calculated as difference between observed and predicted TLV (in cm^3) divided by observed TLV. Negative and positive values indicate an increase or decrease respectively in the predicted value from the observed.

Percentage prediction errors							
Species	**AntW**	**PstW**	**MidW**	**MaxL**	**LatL**	**MidL**	**MedL**
Homo sapiens	−1%	−2%	−2%	−6%	−3%	−4%	−30%
Pan troglodytes	−7%	−6%	−5%	−7%	−7%	−2%	−1%
Pan paniscus	−6%	−8%	−4%	−16%	−15%	−1%	−10%
Gorilla gorilla	4%	7%	3%	−2%	−3%	4%	9%
Pongo pygmaeus	−7%	5%	−1%	−3%	−7%	−6%	−11%
Hylobates lar	−29%	−3%	−7%	−15%	−16%	−9%	−5%
Macaca mulatta	15%	7%	4%	19%	19%	10%	20%
Papio sp.	6%	2%	8%	16%	19%	9%	12%
Cercocebus atys	14%	−4%	11%	12%	6%	7%	16%
Sapajus apella	−2%	−6%	−7%	7%	2%	−6%	13%
Saimiri sciureus	14%	11%	−2%	−9%	6%	−5%	−24%
Percentage prediction reliability							
Species	**AntW**	**PstW**	**MidW**	**MaxL**	**LatL**	**MidL**	**MedL**
Homo sapiens	−4%	+7%	+10%	−25%	−13%	+16%	+67%
Pan troglodytes	−21%	+19%	+17%	−22%	−22%	+6%	−3%
Pan paniscus	−18%	+22%	+14%	−38%	−36%	+3%	+28%
Gorilla gorilla	+16%	−29%	−14%	−7%	−9%	−17%	−43%
Pongo pygmaeus	−21%	−23%	+5%	−11%	−22%	+20%	+31%
Hylobates lar	−46%	+8%	+16%	−30%	−32%	+21%	+13%
Macaca mulatta	+52%	−19%	−12%	+75%	+73%	−30%	−84%
Papio sp.	+21%	−5%	−31%	+82%	+103%	−34%	−50%
Cercocebus atys	+51%	+9%	−38%	+43%	+18%	−23%	−67%
Sapajus apella	−5%	+11%	+13%	+18%	+6%	+12%	−37%
Saimiri sciureus	+22%	−16%	+2%	−10%	+8%	+6%	+21%

Abbreviations: MCF metrics=AntW, anterior-width; PstW,posterior-width;MidW,mid-width;MaxL,maximum-length;LatL,lateral-length;MidL,midlength;MedL,medial-length

The predicted TLV for extant and fossil anthropoids were within an uncertainty bracket of ±1 s.e, with the predicted TLV obtained from PGLS regression models consistently lower than those from OLS regressions (Table 7), except for mid-length which had marginally higher

PGLS predicted TLV but as many taxa share very similar OLS and PGLS predicted TLV this result is not considered substantially different (Figure 6a–g).

Table 7. Extant and fossil anthropoid predicted temporal lobe volume (cm^3) listed with the corresponding MCF variable calculated from the bivariate ordinary least-squares regression equations.

Anthropoid predicted temporal lobe volumes							
Taxa	**MCF metrics**						
ID	**AntW**	**PstW**	**MaxL**	**MidW**	**LatL**	**MidL**	**MedL**
H. sapiens	118.1	113.8	91.4	110.1	106.6	103.5	40.2
CRM 1	116.4	109.1	151.5	154.2	141.0	97.2	88.1
Singa 1	124.3	178.6	134.7	138.8	113.9	100.8	78.2
Mladecˇ 1	88.9	95.6	98.3	81.0	63.3	79.0	55.5
Skhul 5	113.2	71.4	106.3	82.4	90.2	67.3	76.4
Gibraltar	114.6	162.1	111.4	145.2	137.2	112.1	84.2
Kabwe	50.9	143.5	96.6	67.5	111.7	73.1	52.8
Bodo	96.3	142.4	67.4	111.4	50.8	97.8	36.4
KNM-ER 3883	66.3	42.0	83.0	65.1	69.1	58.9	85.1
KNM-ER 3733	34.5	87.9	100.8	46.9	115.4	65.3	57.4
OH9	84.6	106.9	106.4	82.8	52.0	72.0	85.6
KNM-ER 1805	54.1	70.9	78.9	67.8	67.9	60.8	52.7
KNM-ER 406	76.4	194.9	94.2	91.0	75.1	84.8	34.6
STS 5	52.5	76.6	103.9	88.0	106.5	96.6	64.9
P. troglodytes	31.1	32.2	30.9	32.7	30.8	37.0	38.3
P. paniscus	28.0	26.6	21.1	29.6	21.9	33.2	24.7
G. gorilla	43.9	48.5	34.9	42.8	34.5	44.0	54.0
Po. pygmaeus	34.7	53.9	39.2	41.8	34.1	35.2	30.2
Hy. lar	8.5	14.4	10.9	13.1	10.7	12.3	13.7
Pa. sp	26.3	23.0	39.6	28.5	44.3	29.3	32.8
CO-100	29.4	14.9	23.1	32.9	18.6	24.7	22.1
SK 554	25.7	28.6	26.4	15.8	25.1	16.2	24.8
M. mulatta	16.8	13.1	19.3	12.3	19.0	14.3	20.3
C. atys	20.9	12.5	19.7	19.1	16.3	16.9	23.0
CGM-40327	3.2	8.6	8.7	5.2	11.8	6.5	10.2
DPC-18651	2.4	1.5	3.7	2.3	3.0	2.9	15.2
S. apella	8.9	8.3	11.0	8.1	9.9	8.2	12.9
Sa. sciureus	4.1	3.9	3.0	3.3	3.7	3.2	2.7
MPV-3501	4.0	1.3	2.8	3.7	2.8	5.4	10.8
FML-619	3.0	2.3	6.0	6.2	6.1	6.3	17.1

Abbreviations: MCF metrics=AntW, anterior-width;PstW, posterior-width; MidW, mid-width;MaxL, maximum-length; LatL, lateral-length; MidL, midlength; MedL, medial-length.

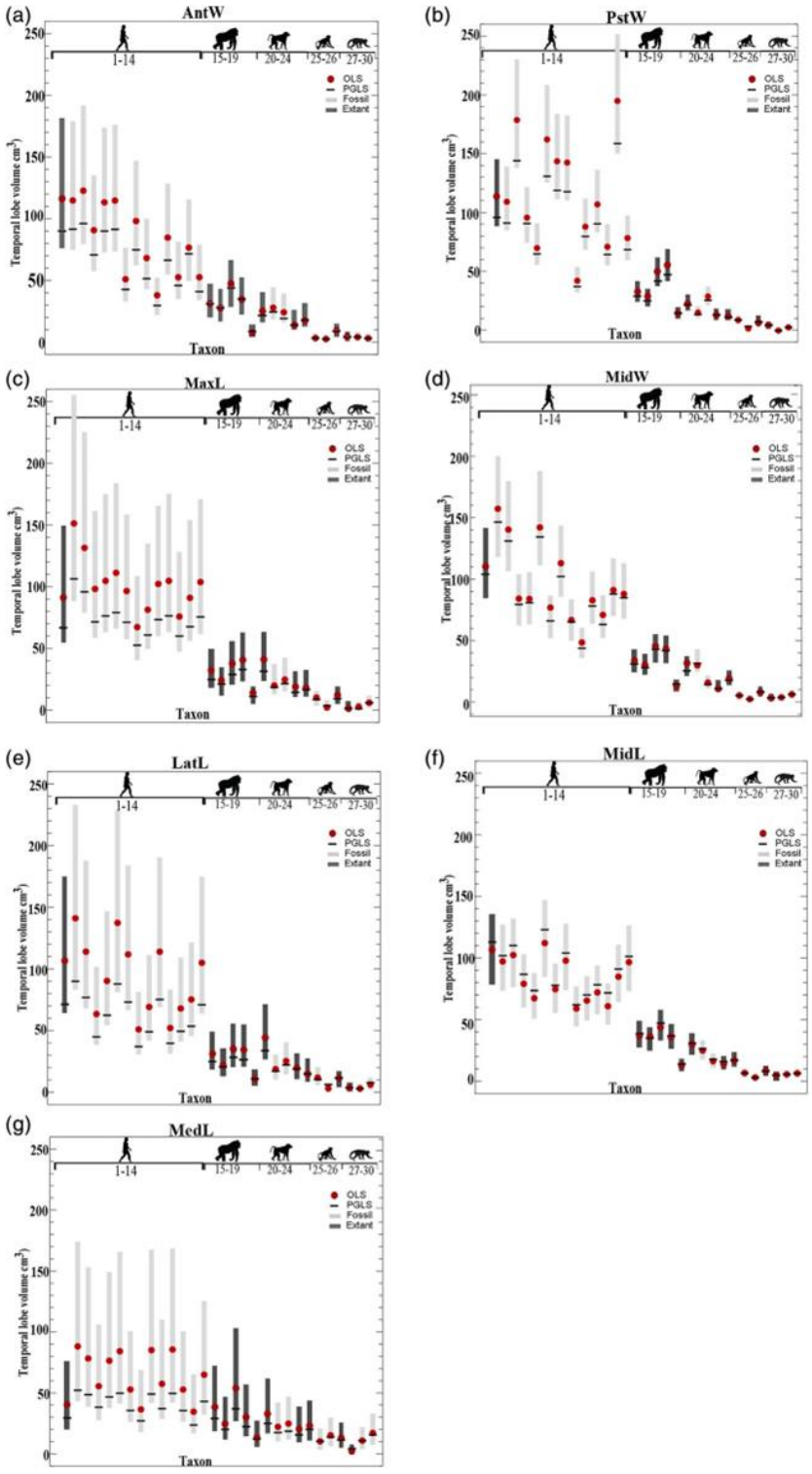

Figure 7 a-g. Predictions of TLV from the seven MCF variables in extant and fossil anthropoids. Taxa numbering corresponds to groups: extant humans and fossil hominins (**1–14**), great and small apes (**15–19**), extant and fossil old world monkeys (**20–24**), fossil anthropoids (**25–26),** extant and fossil new world monkeys (**27–30**). Light-grey bars indicate the ±1 s.e. uncertainty for predicted TLV in fossil specimens, dark-grey bars indicate the ±1 s.e. uncertainty for predicted TLV in extant species. *1 = extant Homo sapiens; 2 = fossil Homo sapiens (Cro-Magnon 1);3= fossil Homo sapiens (Singa 1);4= fossil Homo sapiens (Mladecˇ 1); 5 = fossil Homo sapiens (Skhul 5);6 = Homo neanderthalensis (Gibraltar1);7=Homo heidelbergensis (Kabwe 1); 8 = Homo heidelbergensis (Bodo); 9 = Homo ergaster (ER-3883); 10 = Homo ergaster (ER-3733);11 = Homo ergaster (OH 9);12= Homo habilis (ER-1805);13 = Paranthropus boisei (ER-406);14 =Australopithecus africanus (STS-5);15=Pan troglodytes ;16=Pan paniscus; 17=Gorilla gorilla;18 = Pongo pygmaeus; 19=Hylobates lar; 20 = Papio sp.;21=Papio angusticeps (CO100);22= Dinopithecus ingens(SK-554);23=Macaca mulatta;24=Cercocebus atys; 25 = Aegyptopithecus zeuxis (CGM-402327);26=Parapithecus grangeri(DPC-18651);27= Sapajusapella;28=Saimiri sciureus;29=Homunculus patagonicus (MPV-3501);30= Tremacebus harringtoni (FML-619)*.Dark-grey bar = Extant species ±1 s.e. uncertainty of predicted TLV, Light-grey bar = Fossil species ±1 s.e. uncertainty of predicted TLV; OLS, solid red

3.5. Discussion

This study aimed to investigate the suitability of the anthropoid MCF as a proxy for temporal lobe volume (TLV) and determine the reliability of predicting TLV in fossil anthropoids.

Predictions of fossil anthropoid TLV were based on extant anthropoid in vivo MRI to calculate TLV and ex vivo cranial CT to register seven MCF metrics approximating temporal lobe location. The separate comparative studies of extant anthropoid temporal lobe allometry (Rilling, 2006; Rilling & Seligman, 2002) and anthropoid basicranial angle (Lieberman, Pearson, & Mowbray, 2000; Lieberman, Ross, & Ravosa, 2000; McCarthy, 2001) provided the foundations for our study. We investigated the correlation in extant anthropoids between TLV and MCF size using OLS and PGLS regressions with our results confirming a strong correlation between extant anthropoid TLV and MCF size ($r \geq 0.85$; $p \leq 0.0009$). Although a close spatial correspondence exists between the temporal lobe and the MCF, interpretations are not straightforward with such a close spatial association likely causing temporal lobe morphology to be dependent on both brain and cranial form. For inferences of fossil brain evolution, our results enable future researchers to determine the confidence of predictions from fossils when using the MCF as a proxy for the temporal lobe in anthropoids.

3.5.1. Importance of quantifying MCF- TLV association

This present study provides a quantification for the strength of the association between the MCF and TLV in anthropoids and the suitability of the MCF as a proxy for the temporal lobe.

Modern humans have disproportionately large temporal lobes compared to other anthropoids (Rilling, 2006; Rilling & Seligman, 2002) with differing basicranial angles also separating mod-ern humans and some fossil hominins from other primates (Lieberman, Pearson, & Mowbray, 2000) and henceforth hypotheses suggested the emergence of larger temporal lobes in extant *Homo sapiens* could be inferred from changes in MCF morphology of fossil Homo (Bastir et al., 2008; Bastir et al., 2011). This present study provides support that the MCF is suitable for inferring fossil brain morphology, where our results apply both ordinary and phylogenetically controlled statis-tical methods to provide reliable predictions of TLV with well-defined brackets of prediction uncertainty for fossil specimens.

Considering the close anatomical correspondence between cerebrocranial systems, the assumption that a strong correlation should exist between cerebral volumes and basicranial elements is not unreasonable. For example, Kubo et al. (2014) found a statistically significant correlation between cerebellar volume and PCF in a small sample of extant *Homo sapiens* where despite no regression models, cerebellum volume was predicted for fossil Homo. The inclusion of more anthropoid species could enable robust statistical investigations to establish if all PCF metrics correlate strongly with cerebellar volume and, if, like we have shown with the MCF and TLV, the PCF is a suitable proxy for cerebellar volume.

Although Lieberman (2011) refers to McCarthy (2004) describing an apparent isometric scaling trend between temporal lobe size and the middle cranial fossa in primates, no specific methodological details were provided. Unfortunately, McCarthy (2004) compiled brain volumes from an extremely small sample from the ex vivo brain published in Stephan, Frahm, and Baron (1981) and MRI volumes from the in vivo brain published in Rilling and Insel (1999) and Semendeferi and Damasio (2000) among others, incorporating different

sampling conditions, protocols, unknown species identification procedures, imaging parameters and neuroanatomists introducing contrary findings such as occurred between Rilling (2006); Rilling and Seligman (2002), and Semendeferi and Damasio (2000). As such, it is not possible to com-pare the significance of these findings by McCarthy (2004) with our study considering those issues outlined above. Nonetheless, this does strongly indicate the need for research like this present study to pro-vide a rigorous methodological investigation of the MCF-TLV association.

Our results indicated there was a strong correlation between all MCF metrics and TLV but this was not without exception, with medial-length not conforming to the same pattern observed in the other MCF metrics. For example, very low predictions of TLV were observed in extant *Homo sapiens* (40cm^3), fossil *Homo sapiens* Mladecˇ 1 (55 cm^3), *Homo heidelbergensis* Bodo (36 cm^3) and *Paranthropus boisei* ER-406 (35 cm^3) potentially associated with similarly short medial-length observed also in PCA (Figure 3a,b; Table 4). Further-more, the stem-platyrrhine, *Tremacebus harringtoni* (FML-619) had an improbably large predicted TLV (17cm^3) but shared similar medial-length to extant catarrhines where TLV was overestimated by 20% in *Macaca mulatta*.

It may not be unsurprising that medial-length has a weaker correlation with TLV than the other metrics for several reasons. Firstly, only an anteromedial region of the temporal lobe was approximated by our metric for medial-length. We note, the temporal lobe does not spatially correspond to the midline of the MCF (for example, the sella turcica) but is instead laterally off-set slightly, following anteroposteriorly from the orbital fissure, tracing the underlying carotid sulcus to the junction of the petrous apex and terminating near the basioccipital region of the skull and is potentially confounded by many “nonbrain” structures

such as meningeal, nervous and vascular systems. Secondly, while our medial-length metric does not incorporate the basicranial midline, posterior or anterior cranial fossae, nor the facial block, it does share similarities with aspects of the cranial base previously argued to be involved in major changes in anthropoid and specifically, human cranial evolution (Lieberman, 2011; Lieberman, Pearson, & Mowbray, 2000; Lieberman, Ross, & Ravosa, 2000; McCarthy, 2001). It should be noted that the basicranial rotational model influencing the facial block proposed by Lieberman, Pearson, and Mowbray (2000); Lieberman, Ross, and Ravosa (2000); and McCarthy (2001) is opposed by Bastir (2018) and Bastir and Rosas (2006, 2016) as oversimplified, arguing that the size and positioning of the MCF do not strongly relate to the variation in the mid-line cranial base angle in *Homo*. Therefore, considering these cerebrocranial interactions, we recommend against using medial-length as a proxy for the temporal lobe even though our study indicates it is still statistically significant as a predictor for fossil TLV. However, the stronger correlation with TLV and greater prediction reliability for posterior-width, mid-width and mid-length emphasize the suitability of these three MCF metrics for predicting TLV in fossil specimens.

3.5.2. Implications of the MCF as a proxy for TLV

In extant anthropoids, the cerebral structures commonly referred to as "lobes," which include the temporal lobe, do not have a true micro-anatomical or cytoarchitectural existence but are generalized or arbitrary divisions with major and minor sulci often used to define the generalized boundaries separating the "lobes" for macroanatomical purposes (Sherwood, Bauernfeind, Raghanti, & Hof, 2017). Externally, the temporal lobe does have a natural superior boundary formed by the Sylvian fissure, but the ascending rami are externally continuous with the parietal lobe, a similar situation also occurs for the superior temporal gyrus,

while the preoccipital notch forms a natural posterior boundary but again, both the superior and inferior temporal gyri are continuous with the parietal and occipital lobes on the external surface of the brain (Mai et al., 2008). The lack of discernible neuroanatomical structures to define the superior and posterior limits of the temporal lobe does not allow for a reliable approximation of temporal lobe boundaries. Instead, internal neuroanatomy is necessary to more reliably define the temporal lobe boundaries and to accommodate the absence of a midsagittal line associated with the somewhat "concave" form of the temporal lobe curving around the mesencephalon and the pons (Borden et al., 2016).

For paleoneurologists, there are clear limitations when the external surface of the brain cannot be used to reliably estimate temporal lobe boundaries. In endocasts, the preservation of sulcal imprints is imperfect with information either not clearly visible or completely absent (Van Minh & Hamada, 2017), which is also often the case in fossil *Homo* (Kobayashi et al., 2018). Our study provides reliable predictors of fossil anthropoid TLV and uncertainty brackets to allow evolutionary comparisons of fossil temporal lobe size, which has not been possible, with paleoneurologists previously limited to generalized inferences of fossil temporal lobe morphology.

The fragile sphenoid bone forms the anterior boundary of the MCF and is often partially, or completely, destroyed in many fossil species. The absence of the lesser or greater wings of the sphenoid exclude inferences of temporal lobe length or width with estimations acquired from close phylogenetically related species as with *Homo erectus* and *Homo ergaster* (Bruner, Grimaud-Hervé, Wu, de la Cuétara, & Holloway, 2015) or complete species substitution as with *Homo sapiens* and *Homo neanderthalensis* (Kochiyama et al., 2018; Rosas et al., 2014). Regardless, the differences between species are evolutionary relevant and our

findings indicate that only few as two or three MCF metrics are required to reliably predict TLV from fragmentary fossil material.

In conclusion, this study provides quantification that anthropoid MCF size is a suitable proxy for TLV, with seven MCF metrics strongly associated with TLV. Three MCF metrics were the most reliable predictors of TLV with the range of predictions in small and large brained species for MCF metrics posterior-width reliable ±11 cm3 (±24%), mid-length ± 19 cm3 (±31%), and mid-width ± 12 cm3 (±38%); how-ever, medial-length was the least reliable predictor of TLV in anthropoids. These findings are relevant for studying fragmentary fossil material, inferring temporal lobe morphology in fossil endocasts with implications for potentially tracing the emergence of modern human temporal lobe morphology and cognitive specializations.

3.6. Acknowledgments

We dedicate this work to the late Emeritus Professor Colin Groves (The Australian National University) in appreciation of the early support, consultation, and stimulating discussions on primate evolution. Grants supporting this work: A.P. was funded by the Australian Government Research Training Program Scholarship (2016-Present) and E.B. funded by the Spanish Government (#PGC2018-093925-B-C31). We thank the following institutions and people for digital data access: The Smithsonian National Museum of Natural History care of K. Helgen and M. Tocheri (funded by Smithsonian 2.0 Fund and the Smithsonian's Collections Care and Preservation Fund); Museum National d'Historie Naturelle, Paris (MNHN) care of P. Mennecier and A. Froment; National Museums of Kenya (NMK) care of F. Spoor; The Natural History Museum, London (NHM) care of R. Kruszynki and C.

Stringer; Digital Morphology Museum (DMM) care of the Primate Research Institute, Kyoto University (KUPRI); NESPOS Society e.V. and care of J.J. Hublin and the Anatomisches Institut, Universität Leipzig; University of Pennsylvania Museum of Archeology and Anthropology and the Open Research Scan Archive (ORSA) care of J. Monge and P. T. Schoenemann (NSF proposal # 0447271); The National Chimpanzee Brain Resource care of J. Rilling; OASIS: Cross-Sectional: Principal Investigators: D. Marcus, R, Buckner, J, Csernansky J. Morris (#P50 AG05681, #P01 AG03991, #P01 AG026276, #R01 AG021910, #P20 MH071616, #U24 RR021382). The following digital access acknowledged from Morphosource (www.MorphoSource.org), Duke University: Tremacebus data M7939-FML-619 care of R. Kay (#EAR 1349741); Homunculus data M7940-MPM-PV-3501 care of R. Kay; Aegyptopithecus data M2376-CGM-40327 care of Alan Walker (funded by Pennsylvania State University); fossil Papio data M6305-DNMNH-CO-100 care of The Plio-Pleistocene Section of the Ditsong National Museum of Nat-ural History and J. Adams (funded by Department of Anatomy and Developmental Biology, Monash University); extant primates from the Museum of Comparative Zoology, Harvard University care of the "Lucas and Copes MCZ scans" (funded by the Wenner Gren Founda-tion and NSF DDIG #0925793), M10756-AMNH-M-51380 care of the AMNH Department of Mammalogy and E. Delson (funded by AMNH and NYCEP).

3.7. Author contributions

Alannah Pearson contributed to the concept design, conducted data acquisition, contributed to data analysis and interpretation, drafted the initial manuscript and revisions, P.

David Polly contributed to data analysis and interpretation, and manuscript revisions; Emiliano Bruner contributed to the concept design, data interpretation and manuscript revisions.

3.8. Data availability statement

The data that supports the findings of this study are available in the supplementary material of this article.

3.9. References

Ackermann, R. R., Rogers, J., & Cheverud, J. M. (2006). Identifying the mor- phological signatures of hybridization in primate and human evolution. *Journal of Human Evolution, 51*(6), 632–645. https://doi.org/10.1016/ j.jhevol.2006.07.009

Adams, D. C., Otárola-Castillo, E., & Paradis, E. (2013). Geomorph: An r package for the collection and analysis of geometric morphometric shape data. *Methods in Ecology and Evolution, 4*(4), 393–399. https:// doi.org/10.1111/2041-210x.12035

Aldridge, K. (2011). Patterns of differences in brain morphology in humans as compared to extant apes. *Journal of Human Evolution, 60*(1), 94–105. https://doi.org/10.1016/j.jhevol.2010.09.007

Arnold, C., Matthews, L. J., & Nunn, C. L. (2010). The 10kTrees website: A new online resource for primate phylogeny. *Evolutionary Anthropology, 19*, 114–118.

Bailey, R. C., & Byrnes, J. (1990). A new, old method for assessing mea- surement error in both univariate and multivariate morphometric stud- ies. *Systematic Zoology, 39*(2), 124–130.

Bastir, M. (2018). Back to basics: Morphological analysis in Paleoanthro- pology. In J. Schwartz (Ed.), *Biological Theory* (pp. 205–227). Boston: MIT-Press.

Bastir, M., & Rosas, A. (2006). Correlated variation between the lateral basicranium and the face: A geometric morphometric study in differ- ent human groups. *Archives of Oral Biology*, *51*(9), 814–824. https:// doi.org/10.1016/j.archoralbio.2006.03.009

Bastir, M., & Rosas, A. (2016). Cranial base topology and basic trends in the facial evolution of *Homo*. *Journal of Human Evolution*, *91*, 26–35. https://doi.org/10.1016/j.jhevol.2015.11.001

Bastir, M., Rosas, A., Gunz, P., Pena-Melian, A., Manzi, G., Harvati, K., … Hublin, J. J. (2011). Evolution of the base of the brain in highly encephalized human species. *Nature Communications*, *2*, 588. https:// doi.org/10.1038/ncomms1593

Bastir, M., Rosas, A., & Kuroe, K. (2004). Petrosal orientation and mandibu- lar ramus breadth: Evidence for an integrated petroso-mandibular developmental unit. *American Journal of Physical Anthropology*, *123*(4), 340–350. https://doi.org/10.1002/ajpa.10313

Bastir, M., Rosas, A., Lieberman, D. E., & O'Higgins, P. (2008). Middle cra- nial fossa anatomy and the origin of modern humans. *The Anatomical Record*, *291*(2), 130–140. https://doi.org/10.1002/ar.20636

Bastir, M., Rosas, A., Stringer, C., Cuetara, J. M., Kruszynski, R., Weber, G. W., … Ravosa, M. J. (2010). Effects of brain and facial size on basicranial form in human and primate evolution. *Journal of Human Evolution*, *58*(5), 424–431. https://doi.org/10.1016/j.jhevol.2010.03.001

Blomberg, S. P., Garland, T. J., & Ives, A. R. (2003). Testing for phylogenetic signal in comparative data: Behavioral traits are more labile. *Evolution*, *57*(4), 717–745.

Borden, N. M., Forseen, S. E., & Stefan, C. (2016). *Imaging anatomy of the human brain a comprehensive atlas including adjacent structures*. New York: Demos Medical Publishing.

Bruner, E. (2017). The fossil evidence of human brain evolution. In: J. H. Kaas (Ed.), *Evolution of nervous systems volume 4: The evolution of the human brain: Apes and other ancestors* (Vol. 4, pp. 63–92). Amster- dam, Boston: Elsevier Inc.

Bruner, E., Grimaud-Hervé, D., Wu, X., de la Cuétara, J. M., & Holloway, R. (2015). A paleoneurological survey of *Homo erectus* endocranial met- rics. *Quaternary International*, *368*, 80–87. https://doi.org/10.1016/j. quaint.2014.10.007

Bryant, K. L., & Preuss, T. M. (2018). A comparative perspective on the human temporal lobe. In E. Bruner, N. Ogihara, & H. C. Tanabe (Eds.), *Digital Endocasts: From skulls to brains* (pp. 239–258). Tokyo: Springer Japan KK.

Cardini, A. (2017). Left, right or both? Estimating and improving accuracy of one-side-only geometric morphometric analyses of cranial variation. *Journal of Zoological Systematics and Evolutionary Research*, *55*(1), 1–10. https://doi.org/10.1111/jzs.12144

Damasio, H. (2005). *Human brain anatomy in computerized images* (2nd ed.). New York: Oxford University Press.

Falk, D. (1978). Brain evolution in Old World monkeys. *American Journal of Physical Anthropology*, *48*(3), 315–319. https://doi.org/10.1002/ajpa. 1330480307

Falk, D. (1980). Hominid brain evolution: The approach from paleoneurology. *American Journal of Physical Anthropology*, *23*, 93–107.

Falk, D. (2014). Interpreting sulci on hominin endocasts: Old hypotheses and new findings. *Frontiers in Human Neuroscience*, *8*, 134. https://doi. org/10.3389/fnhum.2014.00134

Falk, D., Zollikofer, C. P. E., Ponce de Leon, M., Semendeferi, K., Alatorre Warren, J. L., & Hopkins, W. D. (2018). Identification of in vivo sulci on the external surface of eight adult chimpanzee brains: Implications for interpreting early hominin Endocasts. *Brain, Behavior and Evolution*, *91* (1), 45–58. https://doi.org/10.1159/000487248

Fleagle, J. G. (2013). *Primate adaptation and evolution* (3rd ed.). San Diego, Waltham, London: Academic Press.

Frost, S. R., Marcus, L. F., Bookstein, F. L., Reddy, D. P., & Delson, E. (2003). Cranial allometry, phylogeography, and systematics of large- bodied papionins (primates: Cercopithecinae) inferred from geometric morphometric analysis of landmark data. *The Anatomical Record Part A, 275*(2), 1048–1072. https://doi.org/10.1002/ar.a.10112

Gilbert, C. C. (2011). Phylogenetic analysis of the African papionin bas- icranium using 3-D geometric morphometrics: The need for improved methods to account for allometric effects. *American Journal of Physical Anthropology*, *144*(1), 60–71. https://doi.org/10.1002/ajpa.21370

Gilbert, C. C., Frost, S. R., Pugh, K. D., Anderson, M., & Delson, E. (2018). Evolution of the modern baboon (*Papio hamadryas*): A reassessment of the African Plio-Pleistocene record. *Journal of Human Evolution*, *122*, 38–69. https://doi.org/10.1016/j.jhevol.2018.04.012

Gonzales, L. A., Benefit, B. R., McCrossin, M. L., & Spoor, F. (2015). Cere- bral complexity preceded enlarged brain size and reduced olfactory bulbs in Old World monkeys. *Nature Communications*, *6*, 7580. https:// doi.org/10.1038/ncomms8580

Groves, C. P. (2001). *Primate taxonomy*. Washington DC: Smithsonian Institution Press.

Hammer, Ø., Harper, D. A. T., & Ryan, P. D. (2001). Past: Paleontological statistics software package for education and data analysis. *Palaeontologia Electronica*, *4*(1), 1–9.

Holloway, R. L. (2018). On the making of endocasts: The new and the old in paleoneurology. In E. O. Bruner, N. Ogihara, & H. C. Tanabe (Eds.), *Digital Endocasts* (pp. 1–8). Tokyo: Springer Japan KK.

Kingdon, J., Butynski, T. M., & De Jong, Y. (2008). *Papio anubis*. *The IUCN Red List of Threatened Species*, *2008*, e.T40647A10348950. https://doi.org/10.2305/IUCN.UK.2008.RLTS.T40647A10348950.en

Kingdon, J., Butynski, T. M., & De Jong, Y. (2016). *Papio cynocephalus*. *The IUCN Red List of Threatened Species*, *2016*, e. T15933A129038584. https://doi.org/10.2305/IUCN.UK.20161.RLTS. T92250442A92250811.en

Kobayashi, Y., Matsui, T., & Ogihara, N. (2018). Inferring cortical subdivi- sions based on skull morphology. In E. Bruner, N. Ogihara, & H. C. Tanabe (Eds.), *Digital Endocasts* (pp. 33–46). Tokyo: Springer KK. Kochiyama, T., Ogihara, N., Tanabe, H. C., Kondo, O., Amano, H., Hasegawa, K., … Akazawa, T. (2018). Reconstructing the Neanderthal brain using computational anatomy. *Scientific Reports*, *8*(1), 6296. https://doi.org/10.1038/s41598-018-24331-0

Kubo, D., Tanabe, H. C., Kondo, O., Ogihara, N., Yogi, A., Murayama, S., & Ishida, H. (2014). Cerebellar size estimation from endocranial measure- ments: an evaluation based on MRI data. In T. Akazawa, N. Ogihara,

H. C. Tanabe, & H. Terashima (Eds.), *Dynamics of learning in Neander- thals and modern humans* (Vol. 2, pp. 209–215). Tokyo: Springer.

Lieberman, D. E. (2011). The evolution of the human head. Cambridge, Massachusetts. London, England: The Belknap Press of Harvard Uni- versity Press.

Lieberman, D. E., Pearson, O. M., & Mowbray, K. M. (2000). Basicranial influence on overall cranial shape. *Journal of Human Evolution*, *38*(2), 291–315. https://doi.org/10.1006/jhev.1999.0335

Lieberman, D. E., Ross, C. F., & Ravosa, M. J. (2000). The primate cranial base: Ontogeny, function, and integration. *American Journal of Physical Anthropology*, *31*, 117–169

Mai, J. K., Paxinos, G., & Voss, T. (2008). *Atlas of the human brain* (3rd ed.). New York, London, Burlington, San Diego: Academic Press.

Marcus, D. S., Wang, T. H., Parker, J., Csernansky, J. G., Morris, J. C., & Buckner, R. L. (2007). Open access series of imaging studies (OASIS): Cross-sectional MRI data in young, middle aged, nondemented, and demented older adults. *Journal of Cognitive Neuroscience*, *19*(9), 1498–1507. https://doi.org/10.1162/jocn.2007.19.9.1498

Martins, E. P., & Hansen, T. F. (1997). Phylogenies and the comparative method: A general approach to incorporating phylogenetic information into the analysis of interspecific data. *American Naturalist*, *149*, 646–667.

Materialise. (2018). *Mimics 17 (version 17)*. Leuven, Belgium: Materialise Corporation.

McCarthy, R. C. (2001). Anthropoid cranial base architecture and scaling relationships. *Journal of Human Evolution*, *40*(1), 41–66. https://doi. org/10.1006/jhev.2000.0446

McCarthy, R. C. (2004). *Constraints on Primate Craniofacial Growth and Archi- tecture*. (Doctor of Philosophy). The George Washington University,

Moss, M. L., & Young, R. W. (1960). A functional approach to craniology. *American Journal of Physical Anthropology*, *18*(4), 281–292.

Nolte, J. (2009). *The human brain: An introduction to its functional anatomy* (6th ed.). Philadelphia: Mosby Elsevier.

Pearson, A., Groves, C., & Cardini, A. (2015). The 'temporal effect' in homi- nids: Reinvestigating the nature of support for a chimp-human clade in bone morphology. *Journal of Human Evolution, 88*, 146–159. https:// doi.org/10.1016/j.jhevol.2015.06.012

Polly, P. D. (2019). Phylogenetics for Mathematica (Version 6.5). Bloom- ington, Indiana: Department of Earth and Atmospheric Sciences, Indiana University. Retrieved from http://pollylab.indiana.edu/ software.html

Richtsmeier, J. T., & Flaherty, K. (2013). Hand in glove: Brain and skull in development and dysmorphogenesis. *Acta Neuropathologica*, *125*(4), 469–489. https://doi.org/10.1007/s00401-013-1104-y

Rilling, J. K. (2006). Human and nonhuman primate brains: Are they allo- metrically scaled versions of the same design? *Evolutionary Anthropol- ogy*, *15*, 65–77. https://doi.org/10.1002/evan.00000

Rilling, J. K., & Insel, T. R. (1999). The primate neocortex in comparative perspective using magnetic resonance imaging. *Journal of Human Evo- lution*, *37*, 191–223.

Rilling, J. K., & Seligman, R. A. (2002). A quantitative morphometric com- parative analysis of the primate temporal lobe. *Journal of Human Evolu- tion*, *42*(5), 505–533. https://doi.org/10.1006/jhev.2001.0537

Rogers, J., Raveendran, M., Harris, R. A., Mailund, T., Leppälä, K., Athanasiadis, G., … Consortium, B. G. A. (2019). The comparative genomics and complex population history of *Papio* baboons. *Science Advances*, *5*, eaau6947.

Rosas, A., Pena-Melian, A., Garcia-Tabernero, A., Bastir, M., & De La Rasilla, M. (2014). Temporal lobe sulcal pattern and the bony impres- sions in the middle cranial fossa: The case of the el Sidron (Spain) neandertal sample. *The Anatomical Record*, *297*(12), 2331–2341. https://doi.org/10.1002/ar.22957

Semendeferi, K., & Damasio, H. (2000). The brain and its main anatomical subdivisions in living hominoids using magnetic resonance imaging. *Journal of Human Evolution*, *38*(2), 317–332. https://doi.org/10.1006/ jhev.1999.0381

Shattuck, D. W., & Leahy, R. M. (2002). BrainSuite: An automated cortical surface identification tool. *Medical Image Analysis*, *6*(2), 129–142. Sherwood, C. C., Bauernfeind, A. L. V., Raghanti, M. A., & Hof, P. R. (2017). Evolutionary specializations of human brain microstructure. In J. H. Kaas (Ed.), *Evolution of nervous systems volume 4: The evolution of the human brain: Apes and other ancestors* (2nd, 4, pp. 121–139). Amsterdam, Boston: Elsevier Inc.

Simpson, G. G., Roe, A., & Lewontin, R. C. (2003). *Quantitative zoology* (Revised ed.). New York: Dover Publications.

Smith, R. J. (1984). Allometric scaling in comparative biology: Problems of concept and method. *American Journal of Physiology*, *246*(2 Pt 2), R152–R160. https://doi.org/10.1152/ajpregu.1984.246.2.R152

Stephan, H., Frahm, H., & Baron, G. (1981). New and revised data on vol- umes of brain structures in insectivores and primates. *Folia Primatologica*, *35*, 1–29.

Stratovan. (2018). *Stratovan Checkpoint (version December 20, 2018)*. UC, Davis, California: Stratovan Corporation.

Van Minh, N., & Hamada, Y. (2017). Age-related changes of sulcal imprints on the endocranium in the Japanese macaque (*Macaca fuscata*). *Ameri- can Journal of Physical Anthropology*, *163*(2), 285–294. https://doi.org/ 10.1002/ajpa.23205

White, T. D., Black, M. T., & Folkens, P. A. (2011). *Human Osteology* (3rd ed.). Burlington, San Diego, Oxford: Academic Press.

Zinner, D., Wertheimer, J., Liedigk, R., Groeneveld, L. F., & Roos, C. (2013). Baboon phylogeny as inferred from complete mitochondrial genomes. *American Journal of Physical Anthropology*, *150*, 133–140. https://doi. org/10.1002/ajpa.22185.

Pearson, A., Polly, P.D. & Bruner, E. (2021) Temporal lobe evolution in Javanese *Homo erectus* and African *Homo ergaster*: Inferences from the cranial base. *Quaternary International*, 603:5-21.

In this chapter, I assess the second aim of this thesis to apply of a limited number of middle cranial fossa metrics to predict temporal lobe size in fragmentary fossil skulls.

Chapter 4: Temporal lobe evolution in Javanese Homo erectus and African Homo ergaster: Inferences from the cranial base

4.1. Abstract

Increased brain size is a characteristic of the *Homo erectus* hypodigm compared to early fossil hominins with changes in cerebral reorganisation of evolutionary importance for the genus Homo. The close spatial proximity of the temporal lobes of the brain to the cranial base, specifically, the middle cranial fossa (MCF), provides inference of temporal lobe evolution. To date, differences in MCF proportions and relative scaling in the *H. erectus* hypodigm compared to extant *Homo sapiens* is unknown. A total sample (n = 51) of cranial Computed Tomography scans (CT) from extant *H. sapiens* and fossil specimens attributed to African *Homo ergaster* and Javanese *H. erectus* were generated into three-dimensional (3D) virtual models with three linear metrics digitally measured on the MCF and two metrics to approximate cranial size. Reduced Major Axis (RMA) log-log regressions and resampling with permutations determined if relative MCF scaling in the fossil sample was greater than observed among extant *H. sapiens*.

An increase or decrease in MCF proportions in the fossil sample compared to extant *H. sapiens* was used to determine potential changes in temporal lobe size. There were no differences in the allometric trend of relative MCF scaling with no statistically significant differences suggesting that the fossil sample were beyond the range observed for extant *H. sapiens*, but the effects of the small fossil sample size could not be excluded. However, relative MCF proportions showed extant *H. sapiens* had a larger MCF to relative to cranial size, while specimens attributed to Javanese *H. erectus* which had a relatively longer and wider MCF compared to African *H. ergaster*. These findings indicate that despite sampling limitations, the fossil sample did not show differences in allometric scaling compared to extant *H. sapiens*, but these specimens attributed to Javanese *H. erectus* and African *H. ergaster* share the same total cranial size but had different MCF proportions relative to cranial size. The paleoneurological implications are that these specimens attributed to Javanese *H. erectus* had longer and wider temporal lobes relative to total brain size compared to African *H. ergaster* suggesting different patterns of cerebrocranial organisation within the *Homo erectus* hypodigm.

4.2. Introduction

Initial descriptions of fossil specimens attributed to the *Homo erectus* hypodigm span more than a century and several continents with continued debate among palaeoanthropologists as to whether the extent of morphological variation is representative of single or multiple species. There are two opposing viewpoints of the broad morphological variation observed within the hypodigm, where those favouring a single species concept, consider the broad variation in *Homo erectus sensu lato* representative of chronospatially differentiated ‘morphs’ (Anton, 2003), which may include informally recognised paleodemes such as the potential

European ‘morph’ from the Republic of Georgia (Lordkipanidze et al., 2013). Conversely, the morphological variation to those favouring multiple species define *Homo erectus sensu stricto* as restricted to continental and island Asia (Wood, 1994), while *Homo ergaster* (Groves and Mazak, 1975) is restricted to African and European specimens. Unfortunately, the taxonomic debate concerning single or multiple species within the *Homo erectus* hypodigm has reached no resolved consensus. For palaeoneurologists investigating hominin brain evolution, the uncertainty of unresolved taxonomy is compounded by incomplete cranial material from Asia where endocast reconstruction often relies on estimation from African specimens (Bruner et al., 2015), where if multiple species do exist, species-specific variation could be obscured.

The Asian paleoanthropological record is further complicated by dating uncertainties in Java and China. However, in Java, several sites now have revised dating with a new chronology indicating a continuous occupation of *H. erectus* throughout Java from earliest site of Sangiran (1.51–0.93 My) based on 40Ar/39Ar dating (Larick et al., 2001; Zaim et al., 2011), to Trinil as an intermediate occupation (540- 430 Ky) until the most recent site of Ngnadong (117-108 Ky) suggesting potential coexistence with other fossil Homo species (Rizal et al., 2020). Unfortunately, dates for site of Sambungmacan remain unresolved with an uncertain timespan bracket from 70 to 40 Ky (Yokoyama et al., 2008) to 546 -143 Ky using combined Ar/Ar and ESR/U-series dating (Indriati et al., 2011). Revised dating of several *H. erectus* sites in China is ongoing (Norton et al., 2010).

Regardless of the unresolved archaeological and taxonomic context, the importance of specimens attributed to the *H. erectus* hypodigm is recognised. Since initial descriptions, palaeoanthropologists have noted the increase in endocranial capacity in the *H. erectus* hypodigm compared to earlier fossil hominins and implications for human evolution (Von

Koenigswald, 1956; Weidenreich, 1947). Although *Homo erectus s. l.* is associated with emergence of increased brain size, some researchers have questioned whether there is a the continued increase in brain size over time present in Asian *H. erectus* compared to African specimens (Rightmire, 1986) while others suggested an increase of 160 cc per million years (Anton and Swisher, 2001). Currently, the earliest date attributed to African *Homo ergaster* is a juvenile specimen from Drimolen, South Africa dated to 2.04–1.95 My using uranium-series electron spin resonance (US-ESR) and palaeomagnetism with adult brain size and shape already similar to *Homo erectus s. l.* and beyond the range of early hominin species (Herries et al., 2020).

A single definitive paleoneurological study of the *H. erectus* hypodigm was not broadly available until Bruner et al. (2015) examined endocranial metrics in African, Chinese and Javanese specimens of *Homo erectus s. l.*, finding no clear distinguishing metric between taxa except for absolute size differences, arguing small sample sizes and large individual variation within *H. erectus s. l.* restricted clearer inferences with individual variation in *H. erectus s. l.* suggested to be as great as the magnitude observed in extant *Homo sapiens* (Bruner, 2018).

Early comparisons of external cranial morphology between Javanese *H. erectus* and extant *H. sapiens* noted the greater basicranial width nearer the cranial base in Javanese *H. erectus* compared to the upper cranial vault in extant *H. sapiens* (Weidenreich, 1941, 1947). Greater basicranial width relative to neurocranial width also influenced endocast morphology with relatively wider temporal areas but flatter parietals associated with neurocranial 'keeling' in *H. erectus s. l* (Bruner et al., 2015). Furthermore, wider basicrania have been associated with flatter basicranial flexion in *H. erectus s. l.* compared to extant *H. sapiens* and later fossil Homo (Baba et al., 2003; Bruner et al., 2015, 2016). Basicranial morphology in *H. erectus s. l.*

includes the middle cranial fossa (MCF) which is potentially associated with variation in hominin facial prognathism (Bastir, 2018; Bastir and Rosas, 2016; Bastir et al., 2010; Lieberman et al., 2000a), relative lengthening of the temporal lobes in fossil Homo (Bastir et al., 2008, 2011; Lieberman, 2011) and the emergence of disproportionately enlarged temporal lobes in extant *H. sapiens* compared to other extant anthropoids (Rilling and Seligman, 2002). Recently, Pearson et al. (2020) have shown the suitability of predicting temporal lobe volume from the MCF in extant and fossil anthropoids, providing statistical support for the anatomical association between the temporal lobes of the brain and the MCF, the bony counterpart of the skull.

4.2.1. Objectives

Here we examine the middle cranial fossa (MCF) to infer lobe evolution using a comparative sample of extant *H. sapiens* and fossil specimens attributed to African *H. ergaster* and Javanese *H. erectus*. We asked if relative MCF scaling and MCF proportions in the fossil sample were greater than observed in extant *H. sapiens* using log-transformed RMA regressions and a resampling RMA bootstrap procedure. The presence of increases or decreases in the relative MCF proportions in the fossil sample compared to extant *H. sapiens* could be infer changes to the temporal lobes relative to total cranial size. This approach could determine variation in temporal lobe morphology in fossil specimens attributed to African *H. ergaster*, Javanese *H. erectus* and other fossil hominins compared to extant *Homo sapiens*.

4.3. Materials and Methods

4.3.1. Sample composition

A total sample (n = 51) of Computed Tomography (CT) scans were generated into three-dimensional (3D) virtual cranial models (Table 1). A sample of adult extant *Homo sapiens* crania (n = 44) were compared three specimens attributed to African *H. ergaster* (KNM-ER 3883, KNM- ER 3733, OH 9) and four specimens attributed to Javanese *H. erectus* (Sangiran 2, Sangiran 4, Sambungmacan 3 and a cast of Sangiran 17). All cranial CT scans were sourced from original specimens except Sangiran 17 where a research quality cast was used due to accessibility issues to CT of the original fossil material. All individual specimen IDs and associated institutional details are provided (Suppl. Tab. 1). We note the fossil specimens included in this study do not reflect the temporal range for *Homo erectus s. l.* which spans 2 million to 50 thousand years ago, and to this end, the individual fossil specimens are considered comparative to extant *H. sapiens* and not representative of a species.

4.3.2. Data Collection

All digital imaging processing, data collection and measurements were conducted by one operator (AP) to remove inter-observer bias.

The virtual 3D crania aligned in the Frankfurt horizontal plane before digitally sectioned along the transverse (coronal) plane, digitally removing the neurocranial vault to access the middle cranial fossa (MCF) of the endocranium (Figure. 1). The generation of virtual crania and CT segmentation procedures followed the common protocols described in Zollikofer and Ponce de Leon (2005). Sangiran 17 specimen was not the original fossil but sourced from a research quality cast of the reconstruction by Aziz et al. (1996) which included the

endocranial surface. The partial facial skeleton and mostly complete neurocranial vault meant the endocranial surface was not accessible using a 3D laser surface scanner, however, a 3D virtual mesh of the endocranium and ectocranium was obtained using 3D photogrammetry following protocol and techniques in Mallison and Wings (2014). To confirm the integrity and examine the reliability of the virtual 3D mesh, linear measurements were digitally collected on the 3D virtual cranium, compared to published measurements from the original fossil and those digitally collected on two other 3D virtual crania of Sangiran 17 casts with no substantial differences between the virtual 3D Sangiran 17 cranium produced by one of us (AP) and it was retained in this study. Although the use of cast material instead of the original fossil material is always least preferred, anatomical descriptions of the internal and external cranial anatomy were carefully consulted to ensure the anatomical integrity of the 3D virtual model as well as the geometric integrity. All digital imaging processing techniques were conducted in Mimics 17 (Materialise, 2018) and Agisoft PhotoScan version 1.2.6 (Agisoft, 2016).

Table 1. Sample (N = 51) for extant *Homo sapiens*, fossil *Homo ergaster* and *Homo erectus* specimens with corresponding labels used in this study, geological dates and site localities.

Species	**ID**	**Age (Ma)**	**Site**	**N**
Homo sapiens	*H. Sapiens*	Recent	Global	**44**
Homo ergaster				**3**
	KNM ER-3733	1.78	Koobi Fora, Kenya	
	KNM ER-3883	1.6-1.5	Koobi Fora, Kenya	
	ONH 9	1.47	Olduvai Gorge, Tanzania	
Homo erectus				**4**
	Sm3	0.05-0.01	Sambungmacan, Central Java	
	S2	1.6-1.5	Sangiran, Central Java	
	S4	1.6-1.5	Sangiran, Central Java	
	S17	1.02-1.1	Sangiran, Central Java	

Dates: [a] Anton (2003). [b] Leakey (1971). [c] Zaim et al. (2011). [d] Larick et al. (2001).

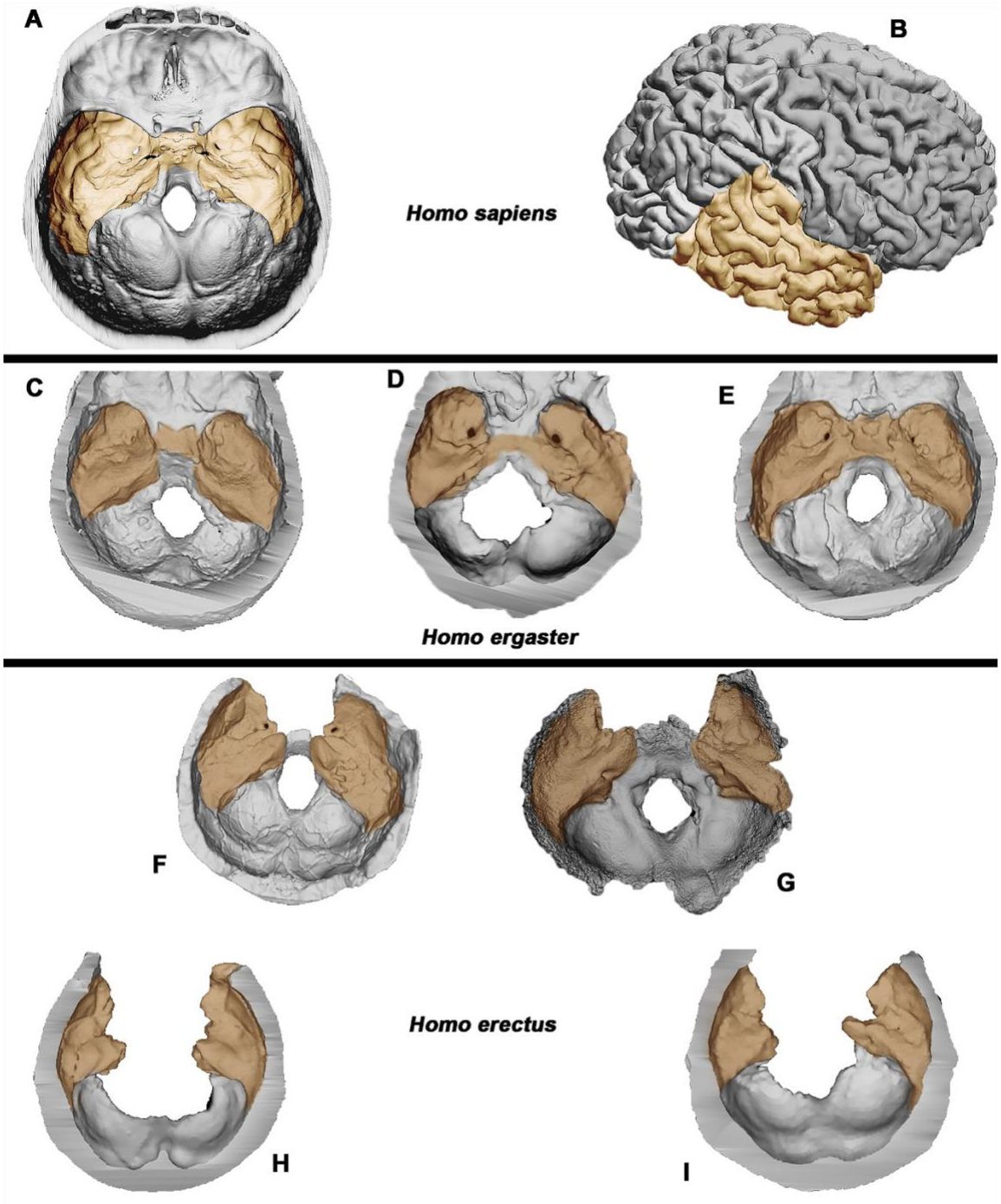

Figure 1. Depiction of endocranial surface of the cranial base from 3D virtual mesh with the middle cranial fossa (MCF) highlighted in gold showing A) Extant *Homo sapiens* MCF and B) extant *Homo sapiens* temporal lobe of the brain generated from MRI (comparative purpose only not included in the study); fossil specimens attributed to African *Homo ergaster* C) KNM-ER3733, D) OH9, E) KNM-ER3883; fossil specimens attributed to Javanese *Homo erectus* F) S4, G) S17, H) S2, I) Sm3. Images are not to scale. (For interpretation of the references to color in this figure legend, the reader is referred to the Web version of this article.)

4.3.3. Anatomical Descriptions

Anatomically, a close spatial correspondence exists between the brain and cranium, where the endocranial floor comprises the anterior cranial fossa (ACF) associated with the frontal lobes of the brain; the posterior cranial fossa (PCF) is associated with the cerebellum and occipital lobes, while the middle cranial fossa (MCF) is associated with the temporal lobes of the brain (Borden et al., 2016). The bony MCF consists of the squamous and petrous parts of the temporal bone and the greater wings of the sphenoid but is bound anteriorly by the lesser wings of the sphenoid and laterally by the squamous part of the temporal bone, while posteriorly, it is bound by the petrous part of the temporal bone (White et al., 2012). This study was conducted on virtual crania and endocrania using published virtual imaging protocols (Zollikofer and Ponce de Leon, 2005) and more recently following approach in Pearson et al. (2020), but we provide brief anatomical descriptions of the extant comparative sample and the fossil material and, unless otherwise stated, original fossil endocast descriptions follow Holloway et al. (2004).

4.3.3.1. Extant *Homo sapiens*

The comparative sample of extant *Homo sapiens* crania comprised adult individuals with all third molars fully erupted, non-pathological and of known sex. Thus, the CT scans of these original specimens were sourced from the original institution collections of the Anatomy Department, University of Liepzig (ULAC) and the ORSA archive, Mor-ton collection at the University of Pennsylvania. All specimens were complete without any signs of fractures or trauma injuries or other noticeable cranial pathologies. Although we did not conduct cranio-metric analyses comparing extant *Homo sapiens* cranial form, all specimen details including

sex and locality information were noted, cross- recorded with cranial morphology with dolichocephalic or brachycephalic cranial forms potentially influenced by evolutionary cerebrocranial trends associated with geographical clines (Holloway, 2002). The endocranial morphology of the sample in this study was consistent with high resolution provided by the CT scans which enabled unobstructed, clear inspection of endocranial surface and cerebral imprints retained on the cranial base, noting the presence of meningeal arteries, specific cerebral convolutions including defined sulci and various endocranial venous pathways, foramina, well-preserved carotid canals and complete preservation of the sellae turcica in all specimens. No specimens with noticeable cranial or endocranial pathologies were retained in the study.

4.3.3.2. African *Homo ergaster*

4.3.3.2.1. KNM-ER 3733.

Fossil specimen KNM-ER 3733 was recovered in 1975 from the site of Koobi Fora, Kenya. Although KNM-ER 3733 is commonly attributed to an adult female determined by less robust cranial morphology no certain sex determination can be made which is a common limitation in paleoanthropology. KNM-ER 3733 is partially complete cranium with minimal distortion to the right MCF, but very slight distortion is present and is possibly associated with the missing regions of the facial skeleton on the right side. When viewed posteriorly, there is a mild anteroposterior deformation affecting the cranial base. The endocranial surface of the cranial base in KNM-ER 3733 appears to have undergone some form of erosion processes which may have affected the appearance and clarity of endocranial imprints. Regardless, the anterior temporal poles of the temporal lobes are present, the right side of the sellae turcica is

distorted mediolaterally on the right portion of the MCF. The temporal poles project anteriorly and appear to rotate inferiorly with a very mild medial rotation toward the center of the facial block. The petrous pyramid appears large and positioned superiorly above the posterior cranial fossae. Unfortunately, the sellae turcica is too distorted to describe whether the angle or position is similar to extant *Homo sapiens*. The endocast is described in Holloway et al. (2004) noting little distortion to the fossil material itself requiring minimal reconstruction to produce a traditional endocast. The estimated endo-cranial volume was 848 ml calculated using the water displacement method (see Holloway, 1981). However, the erosion of the endocranial surface has poorly preserved the imprints of meningeal vessels but from the foramen spinosum, the middle meningeal vessel bifurcates into middle and posterior branches, the latter following the inferior margins of the temporal lobes.

4.3.3.2.2. KNM-ER 3883.

KNM-ER 3883 was recovered in 1976 from excavations at Koobi Fora, Kenya and is attributed to an adult male determined by the robust cranial morphology. The partial cranium is mostly complete, although much of the facial skeleton is not preserved with only a partial zygomatic and orbital region on the right-side retained. The endocranial surface of the cranial base in KNM-ER 3883 displays some distortion affecting the left side of the MCF, which when viewed inferiorly, torsion appears to deform the cranial base toward the left-side of the posterior cranial fossa. The distortion affecting the MCF is noticeable when comparing between the left and right sides with the dorsum sellae distorted, particularly toward the right-side, compressing the right MCF medially but the petrous bone appears only minimally affected and reminiscent of KNM-ER 3733. The endocast of KNM-ER 3883 is described in Holloway et al. (2004) with only minimal reconstruction of the cerebellar lobes required to produce a

traditional endocast with an estimated endocranial volume of 804 ml using the water displacement method. Although the KNM-ER 3883 is a mostly complete cranium, the internal bony surface in a similar condition to KNM-ER 3733 with erosion of the internal table of bone making identification of cerebral convolutions very difficult. The position of the anterior temporal pole suggests the temporal lobe would likely have projected anteriorly with a potential mild medial rotation. Despite the sparse meningeal pattern on the endocast, the bifurcation pattern is similar to KNM-ER 3733.

4.3.3.2.3. OH 9.

The fossil specimen OH 9 was recovered from excavations at Olduvai Gorge, Tanzania in 1960 and is represented by a partial calvarium with the right-side of the neurocranium incomplete. The facial skeleton is not preserved but the fragmentary neurocranial vault indicates a rounded but defined supraorbital torus and a noticeable postorbital constriction. The endocranial surface of the cranial base in OH 9 is well preserved, however, the posterior cranial fossa is incomplete with the lesser wing of the sphenoid and the dorsum sellae on the right side not preserved. There appears a mild distortion to the anterior temporal pole of the right MCF, however, when viewed inferiorly, cranial base deformation, if present, is very mild and is likely associated with the broken occipital and surrounding areas of the foramen mag-num. The endocranial surface of the greater wing of the sphenoid near the left anterior temporal pole appears to enlarged compared to the right, with possible rotation and inferior torsion to the temporal lobe. A partial traditional endocast for OH 9 required minimal reconstruction with an estimated endocranial volume of 1067 ml recorded using the water displacement method (Holloway et al., 2004). Although the endocranial surface is well preserved, sulcal impressions are difficult to discern but the temporal lobes include several unusual features with a unique

folding pattern and impression of an anterior meningeal branch across the temporal lobe (Bruner et al., 2016).

4.3.3.3. Javanese *Homo erectus*

4.3.3.3.1. Sambungmacan 3.

Fossil specimen Sambungmacan 3 is attributed to the archaeological site of Sambungmacan in the Solo River Valley of Central Java, Indonesia, despite not being found in situ but recovered from a curio shop in New York city, United States after being illegally removed from Indonesia without a permit (Delson et al., 2001; Marquez et al., 2001). Sambungmacan 3 is represented by a calotte with articulated fragments of the cranial base but none of the facial skeleton preserved. The neurocranial vault is intact and well-rounded and the supraorbital torus is thick and not rounded or arching as observed in African *H. ergaster*. The endocranial surface of the cranial base is well preserved but very incomplete with the greater and lesser wings of the sphenoid not complete and no region of anterior temporal pole. Fortunately, the right petrous bone is completely preserved while the left petrous bone is partially complete. When viewed superiorly, the endo-cranial surface appears to show a potential but slight distortion to the left petrous bone, but this cannot be confirmed here. The endocast of Sambungmacan 3 is described in Broadfield et al. (2001) with a traditional endocast reconstructed and endocranial volume estimated at 917 ml using the water displacement method (Holloway, 1981). The endo-cast displays prominent meningeal vessels with the left middle meningeal bifurcating into three distinct branches.

4.3.3.3.2. Sangiran 2.

Sangiran 2 is represented by a calotte discovered in 1937 attributed to the Sangiran site in the Solo River Valley of Central Java, Indonesia. Although the facial skeleton is not preserved, a small section of the arched supraorbital torus is retained and displays a well-defined postorbital constriction. The cranial base is only partially pre-served with no remnants of the sphenoid preserved but the supramastoid region of the temporal bone appears robust and broad when viewed posteriorly. The endocranial surface of the cranial base is incomplete with poorly preserved greater and lesser wings of the sphenoid with the left and right petrous bones of the MCF are partially preserved and the squamous and mastoid portions of the temporal bone. The right petrous bone is incomplete and undistorted with a small part of the greater wing of the sphenoid articulated. The left petrous bone appears to be distorted and inferiorly rotated toward dorsum sellae and foramen magnum which are missing. The endocast of Sangiran 2 has required moderate reconstruction to produce a traditional endocast with an estimated endocranial volume of 813 ml using the water displacement method and morphological details on the endocast are listed as similar to other Javanese specimens including well-defined imprints of the meningeal vessels (Holloway, 1981; Holloway et al., 2004).

4.3.3.3.3. Sangiran 4.

Fossil specimen Sangiran 4 is represented by a partial calvarium and maxilla fragment discovered in 1939 and associated with the Sangiran site in the Solo River Valley of Central Java, Indonesia. The calvarium is large with the partial neurocranium revealing very thick cranial bones and the facial skeleton represented only by the associated maxilla fragment. The cranium appears robust and the temporal bones appear to display very prominent mastoid processes and sharp, defined nuchal planes. The endocranial surface of the cranial base in Sangiran 4 is well-preserved but highly cracked however, the foramen magnum, posterior

cranial fossa and dorsum sellae are complete. Unfortunately, most of the greater and lesser wings of the sphenoid are not preserved, the anterior margin of the greater wing of the sphenoid is retained but the cerebral anterior temporal pole could not reliably be identified. The endocast of Sangiran 4 has been described in Holloway (1981) requiring moderate reconstruction to produce a traditional endocast with an estimated endocranial volume of 908 ml using the water displacement method. Although no definite cerebral convolutions are retained on the endocranial surface, the isolated neurocranial fragment associated with Sangiran 4 preserves a large middle branch of the middle meningeal artery.

4.2.3.3.4. Sangiran 17.

The fossil specimen Sangiran 17 was discovered in 1969 and attributed to the Sangiran site in the Solo River Valley of Central Java, Indonesia. Sangiran 17 is the most complete specimen attributed to Javanese *H. erectus* and is large cranium, a partial but very prognathic facial skeleton with a robust supraorbital torus, well-defined nuchal region and prominent mastoid processes (Aziz et al., 1996). The endocranial surface of the cranial base is well preserved and without apparent distortion. The posterior cranial fossa is complete and the MCF is mostly preserved with complete squamous and petrous bones, dorsum sellae, a partial sellae turcica and articulated anterior margin of the greater wings of the sphenoid. The endocast of Sangiran 17 has been described in Holloway (1981) as requiring minimal reconstruction to produce a traditional endocast with an estimated endocranial volume of 1004 ml using the water displacement method. The endocast has well-defined meningeal vessels on the temporal lobe with clear bifurcation of the posterior and anterior branches, however, the right sylvian fissure is partially damaged. Sangiran 17 is represented in this study by a research quality cast

(Australian National University) with endocranial surface digitally reproduced using 3D photogrammetry and associated virtual techniques (Section 4.3.2).

4.3.2. Measurements

Three endocranial metrics were digitally measured on the endo-cranial surface of the right MCF while two cranial metrics were digitally measured on the exterior surface of the cranium (Fig. 2; Table 2).

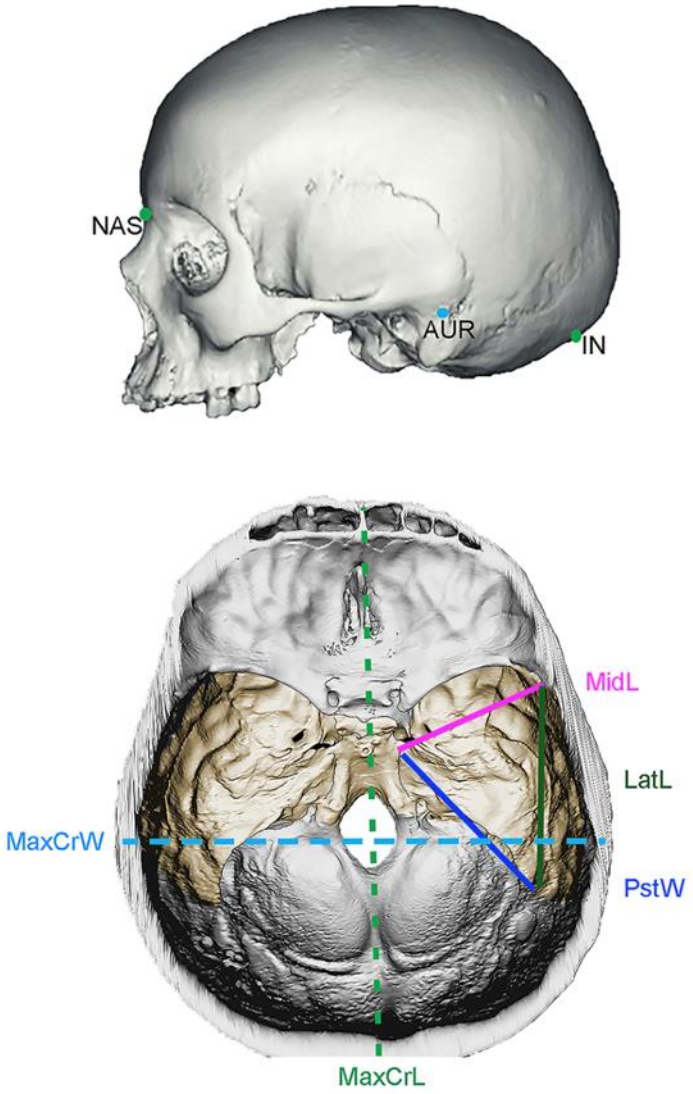

Figure 0-1 Illustration of the measurements on the ectocranial surface and middle cranial fossa metrics from a virtual 3D mesh in extant *Homo sapiens*. Abbreviations: MaxCrW = Maximum cranial width; MaxCrL =

Maximum cranial length; MidL = Mid-length, PstW= Posterior-width, LatL = Lateral length. Corresponding anatomical descriptions in Table 2.

In a single fossil specimen (OH 9) the left-side MCF was measured instead of the right to avoid potential issues associated with possible mild taphonomic deformation (Section 4.3.2). Although side-substitution is not preferred, we anticipate minimal effect from left-right substitution in a single specimen where interspecific variation is often higher than intraspecific when using size measurements (Cardini, 2017).

Table -2 Anatomical descriptions and points on the endocranium to measure the right middle cranial fossa (MCF) and measurement points on the ectocranium to measure cranial size square-root (maximum cranial length x maximum cranial width) in Figure. 2.

Cranial and Endocranial Measurements	
ID	**Description**
PA (petrous apex)	Point on the apex of petrous portion, slightly superior to the depression of the semilunar ganglion.
PP (posterior petrous)	Point on the petrous portion, located at the junction of the transverse sinus margin and petrosquamosal suture.
SQ (sphenosquamosal)	Point on the sphenosquamosal suture of the lesser wing of the sphenoid, inferior to the sphenoid ridge at the junction of frontal branch of the middle meningeal artery (when present), corresponding to pterion on the ectocranial surface.
N (Nasion)	Intersection on the midsagittal plane of the nasofrontal sutures
I (Inion)	Intersection on midsagittal plane of superior nuchal lines
AU (Auriculare)	Point above external auditory meatus at the intersection of the root for the zygomatic process

The implications for the temporal lobe inferences of potential MCF asymmetry introduced from side-substitution are considered to have minimal effect with the greatest brain asymmetry (lateralisation variation) occurring in extant *Homo sapiens* but also common in other great ape species (Neubauer et al., 2020). We do not anticipate issues considering our use of size-based measurements, the anticipated presence of endocranial asymmetry and the statistical regression methods we employ compare extant *H. sapiens* to the fossil sample and not between individual specimens.

The greatest cranial width in *H. erectus s. l.* occurs at the temporomastoid region and not in the upper parietal bones as observed in other Mid-Late Pleistocene Homo and extant *H.*

sapiens. To accommodate this, we used biauriculare to measure maximum cranial width (MaxCrW) instead of the standard metric for cranial breadth, bi-euryon, which is considered unsuitable in early fossil Homo and *H. erectus s. l.* (Cartmill and Smith, 2009). We also define maximum cranial length (MaxCrL) as nasion-inion rather than the more standard measurement (glabella-opisthocranion), where glabella and opisthocranion are metrically determined measurements without the anatomical foundations of suture junctions or defined rugose muscle attachment zones (Bookstein, 1997) thereby contributing to highly subjective identification and measurement errors (Cartmill and Smith, 2009).

We acknowledge glabella requires accommodating the supraorbital torus which is a highly variable in thickness among *Homo erectus s. l.* specimens with an unknown functional purpose but does not appear to be involved in cerebrocranial development and is absent in extant *H. sapiens*. Nasion is a bony region in direct articulation with the neurocranial and facial skeletons and is both highly reliable as a measurement and structurally relevant to cranial base angle and morphology. Although nasion is incomplete in Sangiran 2, an edge of the inferior margin on the mid-line appears present allowing maximum cranial length to be measured. In Sangiran 4, nasion is not present and the average was calculated for this specimen using the values from the other Javanese *H. erectus* This ensured that Sangiran 4 was included in further analyses and with the other fossil specimens from Sangiran site occupying the upper and lower specimens. This ensured that Sangiran 4 was included in further analyses and with the other fossil specimens from Sangiran site occupying the upper and lower limits of this variable (161.6 mm–196.7 mm), Sangiran 4 was not outside the range of other Sangiran specimens in our study. We do not anticipate issues arising from calculating the average for a single metric in one fossil

specimen. We calculated a proxy for total cranial size as the square-root of maximum cranial length multiplied by maximum cranial width or Sqrt (MaxCrL x MaxCrW).

All metrics were digitally collected as three-dimensional (3D) landmarks in CheckPoint (Stratovan, 2018), converted to linear measurements (in mm) using inter-landmark distances in the R package Geomorph 3.0.6 (Adams et al., 2013) for further statistical analyses.

4.3.3. Statistical analyses

All statistical analyses including Principal Components Analysis (PCA) and bivariate Reduced Major Axis (RMA) linear regressions were conducted in Past version 4.0 (Hammer et al., 2001) unless otherwise stated, however, calculations for 'bootstrap' RMA regressions were performed by one of us (PDP) using Mathematica version 12.0 (Wolfram, 2019).

4.3.4. Cranial base and MCF variation

Three MCF and two cranial variables were analysed using a correlation matrix with Principal Component Analysis (PCA) to investigate the extent of variation among the MCF and cranial variables in extant *H. sapiens* and fossil specimens attributed to Javanese *H. erectus* and African *H. ergaster*. PCA is a standard in the morphometric 'toolkit' used to investigate morphological variation and will not be explained further. Commonly, PCs explaining less than 5% of total variance would be excluded from further consideration (Jolliffe, 2002), however, morphological similarity may be high in intraspecific studies and variation spread broadly spread among PCs, while interspecific studies such as this one might not be as amendable to such rigid cut-offs where differences in sample sizes between extant and fossil taxa are relevant to interpreting the significance of variation.

4.3.5. MCF allometric scaling

The potential for the all or part of the MCF to have an allometric association with total cranial size was examined using bivariate Reduced Major Axis (RMA) linear regression models to accommodate the tendency for MCF length or width metrics, as an anatomical region of the cranial base to be naturally associated with maximum cranial length or width, total cranial size was calculated as the square-root of maximum cranial length (MaxCrL) multiplied by maximum cranial width (MaxCrW) following Sokal and Rohlf (1995) and Simpson et al. (2003). In this way, correlations between measurements of MCF length or width were not directly analyzed against maximum cranial length or width where a potential bias could be introduced. Each MCF variable and the variable of total cranial size was log-transformed (base 10) as common in allometric studies (Jungers, 1985).

Bivariate RMA linear regressions were used to investigate the presence of allometric scaling between MCF variables and cranial size where prediction uncertainty errors in RMA are associated with both X and Y variables applying the "best-fit" line of regression using the sum of the products of residuals across both X and Y variables (LaBarbera, 1989; Martin and Barbour, 1989). An allometric slope was present when the value did not equal 1.0, indicating the absence of isometric fit when using log-transformed variables (Wharton et al., 2006; Jungers et al., 1995).

Log-log bivariate RMA regressions were first used to investigate the presence of allometric scaling between the MCF measurements and cranial size in the total sample of extant *H. sapiens* and the fossil sample, however the potential for the total sample to include as many as three putative species of the genus Homo was a concern where species-specific scaling could influence outcomes by the presence of a 'grade-shift'. Where the possibility of several distinct

evolutionary taxa would ordinarily be addressed by using much larger sample sizes to permit more sophisticated statistical approaches (Fuentes et al., 2020; Polly, 2001; Smaers and Rohlf, 2016; Mitteroecker et al., 2004, 2005), we did investigate whether extant *H. sapiens* and the fossil sample shared similar allometric trajectories by comparing slope and intercept values between regressions. Our small fossil sample size prevented the use of sample-means or "species averages" with the adequate statistical robusticity required in such allometric studies (Mitteroecker et al., 2004, 2005; Scott et al., 2018).

We employed an alternate but similar approach to Mitteroecker et al. (2004) and Gilbert and Jungers (2017) by indirectly comparing regression slopes of both the fossil sample and extant *H. sapiens* by excluding extant *H. sapiens* to determine whether slope values differed when only the fossil sample included in analysis. We extended this approach following morphometric principles similar to Mitteroecker et al. (2004, 2005) and Sokal and Rohlf (1995) to examine whether the fossil sample departed from the range observed in extant *H. sapiens* more than was expected by chance. To examine if the fossil sample was beyond the range of extant *H. sapiens*, the probability of achieving a difference as large or larger than observed in extant *H. sapiens* was calculated using RMA regressions with random sampling and permutations (10, 000 times) with a statistical significance ($p \leq 0.05$) between regression slope and intercept values. The 'bootstrap' randomisations were calculated in Mathematica.

4.3.6. Relative MCF proportions

The tendency for MCF measurements as a region of the cranial base, to be associated with cranial size and scale with cranial size would not be unexpected. To examine if MCF measurements scaled relative to cranial size or any deviation from scaling principles, we calculated relative MCF proportions as a ratio using size-standardised variables where each

MCF variable was divided by total cranial size, determined as PstW/Cranial Size [Sqrt(MaxCrL x MaxCrW)] following common morphometric principles (Sokal and Rohlf, 1995; Jungers, 1985; Jungers et al., 1995).

Bivariate Reduced Major Axis (RMA) linear regression models were used to investigate the scaling associations between MCF measurements and cranial size. Similar to the approaches outlined (Section 2.5.2), we again accommodated the potential for species-specific MCF associations and the effects of a 'grade-shift' on outcomes, nothing the limitations of our small fossil sample size.

We first examined the relative scaling of the MCF to cranial size in bivariate RMA regressions using the total sample which included extant *H. sapiens* and the fossil sample. Following the approach outlined above (Section 2.5.2) using similar methodological principles to Mitteroecker et al. (2004) and Gilbert and Jungers (2017), we indirectly compared the regression slopes for extant *H. sapiens* and the fossil sample by excluding extant *H. sapiens* to ask whether the slope values differed when only the fossil sample was included. Comparison and calculation of RMA regression models using the size-standardised MCF variables were performed in Mathematica.

The potential importance of any departure in relative MCF scaling to cranial size could also indicate changes to MCF proportions relative to cranial size with implications for changes to the temporal lobes relative to brain size and cerebral reorganisation. The small fossil sample size did not permit robust statistical interspecific comparison of changes to MCF proportions, but a preliminary comparison was possible. Size- standardised variables of the MCF and cranial size were grouped by putative species and the mean calculated for each MCF proportion, providing a "species average" to directly compare MCF proportions among the three species.

We then asked whether there was any relative increase or decrease in the MCF proportions between taxa thereby providing an estimation for change in relative MCF proportions between species.

4.4. Results

4.4.1. Cranial base and MCF variation

Principal Component Analysis (PCA) was used to examine the variation between the three MCF and two cranial variables in the sample of extant *H. sapiens* and fossil specimens attributed to African *H. ergaster* and Javanese *H. erectus* (Figure. 3; Table 3). The first principal component (PC1) accounted for 56% of total variance and was mostly associated with absolute size as indicated by the direction of the MCF and cranial variables vectors illustrated in the biplot (Figure. 3a), while PC2 accounted for less total variance (20%) associated with maximum cranial width (MaxCrW) and maximum cranial length (MaxCrL) in Javanese *H. erectus* and African *H. ergaster* with most fossil specimens lying outside the range of extant *H. sapiens*.

Although PC3 accounted for less total variance (13%), inspection of the PC loadings confirmed the association with absolute cranial size in all taxa but a longer MCF mid-length (MidL) in extant *H. sapiens* from extant *H. sapiens* where these groups are separated along an oblique line defined by the three MCF variables (Figure. 3a), however, PC 3 indicates a negative correlation between cranial size and MCF variables LatL and PstW, while MidL shows an opposing trend suggesting that MidL is distinctive between *H. sapiens* and the fossil sample (Fig. 3b). However, it is worth nothing the small fossil sample does lower the potential

for these specimens to exert an effect on overall MCF variation, but there does appear to be a distinct difference between fossil sample and *H. sapiens*.

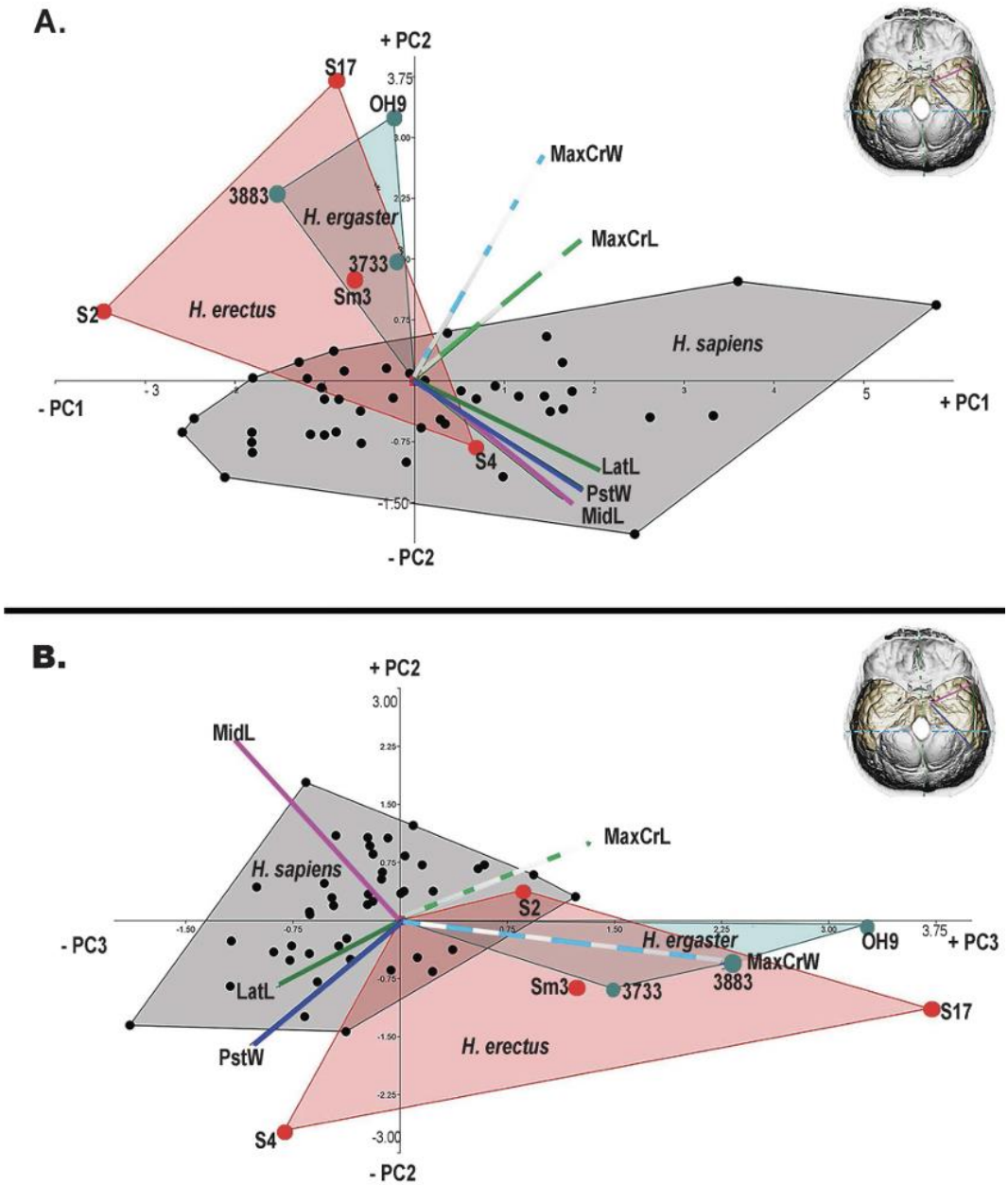

Figure 3 Principal Component Analysis (PCA) of the three MCF variables and 2 cranial variables with biplot illustrating variables and corresponding angle the negative or positive axis among extant *Homo sapiens* and fossil specimens attributed to African *Homo ergaster* and Javanese *Homo erectus* where A) variance accounted for PC1 (56%) associated with absolute size variation across all variables while variance in PC2 (20%) associated with narrow/wide maximum cranial width (MaxCrW) and shorter/long maximum cranial length (MaxCrL) in all taxa, B) Variance accounted for by PC3 (13%) associated only with MCF variables and a long/short MCF mid- length (MidL) evident between extant *Homo sapiens*, African *Homo ergaster* and Javanese *Homo erectus.*

Table 3. Principal Component Analysis (PCA) listing significant PCs, percentage of variance and PC loadings corresponding to MCF and cranial variables. Significant results reported in bold.

PCA Variance					
PC	Eigenvalue	% Variance			
1	2.78523	**56**			
2	0.977263	**20**			
3	0.642525	**13**			
4	0.371748	7			
5	0.223235	4			
PC Loadings					
ID	PC 1	PC 2	PC 3	PC 4	PC 5
LatL	**0.5164**	-0.27499	-0.27437	-0.1831	-0.74088
PstW	**0.47698**	-0.33349	-0.51084	0.064836	0.62938
MidL	**0.40863**	-0.36471	**0.73195**	0.40222	0.049724
MaxCrL	**0.45435**	**0.42424**	**0.31922**	-0.6838	0.21
MaxCrW	**0.36388**	**0.70723**	-0.16159	0.57698	-0.091626

4.4.2. MCF allometric scaling

Bivariate Reduced Major Axis (RMA) regression was conducted using the log-log transformed (base 10) MCF variables against total cranial size variable (Figure. 4a–c; Table 4). There was no indication of an isometric association between the MCF variables and total cranial size, instead an allometric scaling association was observed (a =1.6918 to 2.0166) with a moderate correlation ($r \leq 0.46$; $r2 \leq 0.21$; $p \leq 0.0515$). We investigated whether the fossil sample departed the scaling association observed in extant *H. sapiens* by excluding the fossil sample to compare regressions (Figure.4d-f; Table 4) with consistently stronger correlation between the MCF variables and cranial size now observed ($r \leq 0.78$ $r2 \leq 0.60$, $p \leq 0.0001$).

Table 4 Reduced Major Axis (RMA) regression parameters for log-log transformed (base 10) MCF and cranial size variables and RMA regression parameters for extant *Homo sapiens* examining effect of fossil specimens on correlations. Statistically significant results reported in bold ($p \leq 0.05$).

All specimens log-log RMA Regression Parameters					
Metric	a	b	r^2	r	p
PstW	**2.0166**	**-2.664**	**0.14**	**0.38**	***0.0081***
LatL	**1.6918**	-1.8612	**0.21**	**0.46**	***0.0008***
MidL	**1.7955**	-2.2180	0.08	0.28	**0.0515**
***Homo sapiens* log-log RMA Regression Parameters**					
Metric	a	b	r^2	r	p
PstW	1.75352	-2.08376	0.58	0.34	***<0.0001***
LatL	**1.68967**	**-1.84832**	**0.74**	**0.54**	***<0.0001***
MidL	**1.36738**	**-1.27531**	**0.78**	**0.60**	***<0.0001***

To test the statistical significance of this difference, we compared the and slope and intercept between RMA regression models for extant *H. sapiens* and the fossil sample using a bootstrap procedure with random sampling and permutations (10, 000 times) to estimate the probability that the difference in slopes was as large or larger than the observed value by chance (Figure. 5; Table 5). There was no indication of statistically significant differences in the slopes or intercepts (a =$p \geq 0.36$; b =$p \geq 0.24$), however, the MCF variable PstW had a slope and intercept that was more different between the fossil sample and extant *H. sapiens* than the other MCF variables, but this was not statistically significant. We acknowledge the small fossil sample and potentially high variation within extant *H. sapiens* was a known limitation of these approaches.

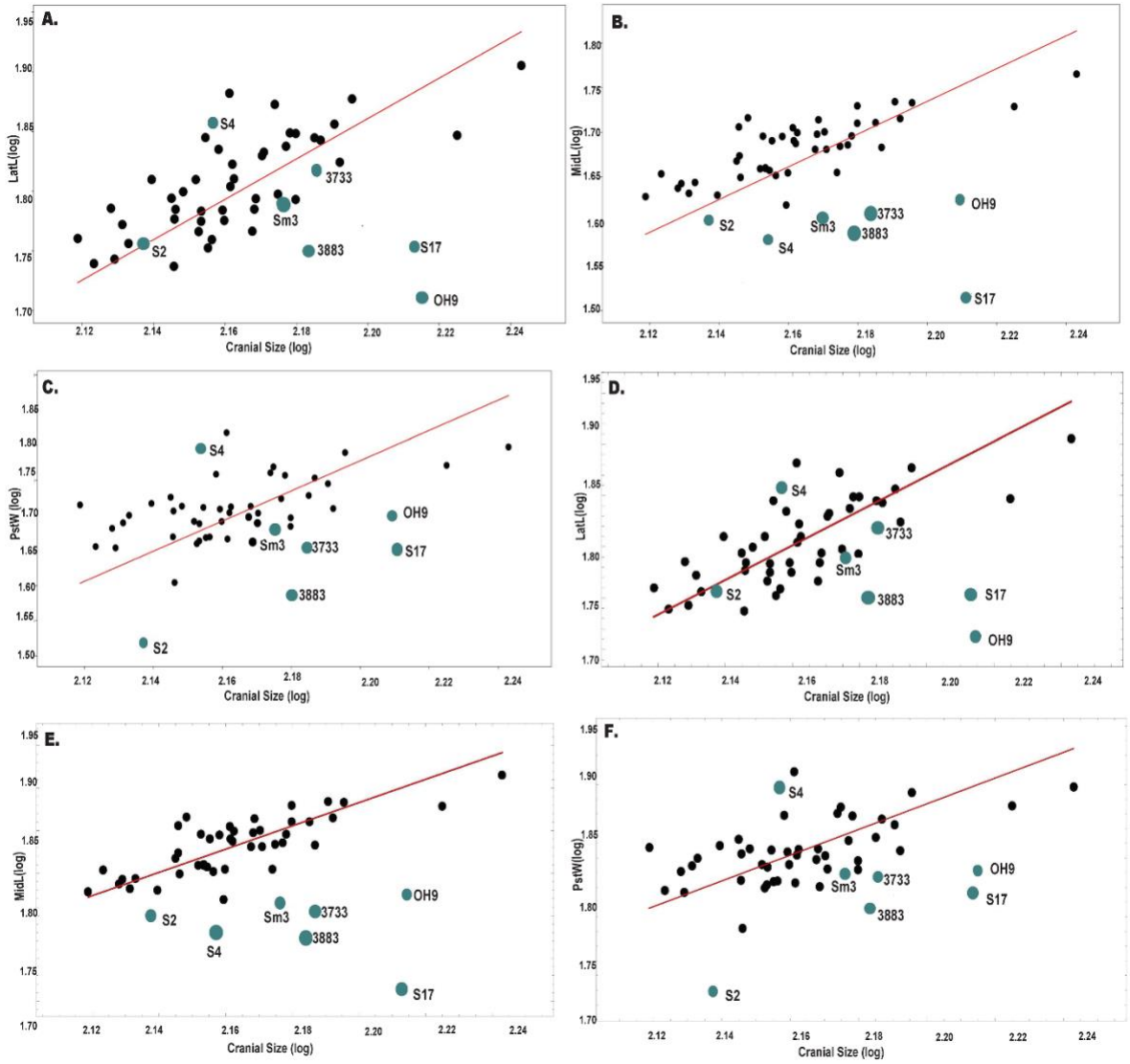

Figure 4- Bivariate linear Reduced Major Axis (RMA) regressions for log-log transformed (base 10) MCF variables and cranial size illustrating A-C) the combined sample regressions and D-F) regression line fit to extant *Homo sapiens* and excluding fossil specimens. Abbreviations: Cranial Size =Sqrt(MaxCrW =Maximum cranial width/MaxCrL =Maximum cranial length), MidL =Mid-length, PstW =Posterior-width, LatL =Lateral length. Black dot =extant *Homo sapiens*; Blue dot =fossil specimens *Homo erectus/Homo ergaster*. Corresponding regression parameters in Table 4.

Table -6 Reduced Major Axis (RMA) regression parameters for log-log transformed (base 10) MCF and cranial size variables comparing the differences between slope and intercept in extant *Homo sapiens* and fossil specimens using bootstrap random sampling and permutations (10,000 times). Differences between slopes are measured in degrees with statistically significant results reported in bold ($p \leq 0.05$).

Log-log RMA Regression Parameters						
Homo sapiens				Fossil Specimens		
Metrics	**a**	**b**	**p**	**a**	**b**	**p**
LatL	**1.68967**	**-1.84832**	**<0.0001**	1.74177	-2.02131	0.2052
PstW	**1.75352**	**-2.08376**	**<0.0001**	2.91791	-4.70052	0.0939
MidL	**1.36738**	**-1.27531**	**<0.0001**	1.28973	-1.22051	0.1720
Comparison of Slope and Intercept						
Metrics	**Slope (degrees)**	**p**		**Intercept**		**p**
LatL	0.76	0.9333		0.17		0.8826
PstW	10.78	0.3578		2.62		0.2386
MidL	1.61	0.8766		0.05		0.7066

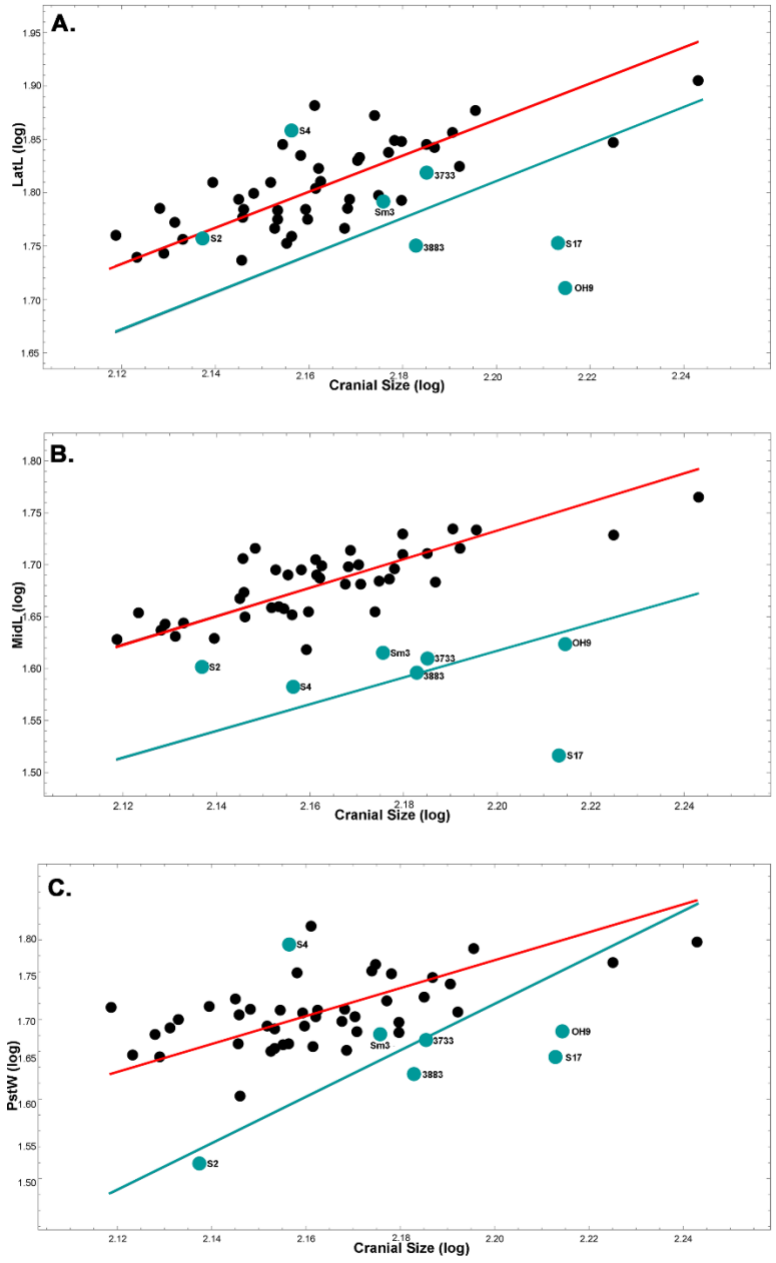

Figure 5- Bivariate linear Reduced Major Axis (RMA) regressions for size-standardised MCF variables illustrating A-C) the combined sample regressions and D-F) regression line fit to extant *Homo sapiens* and excluding fossil specimens. Abbreviations: MidL (Standardised) =Mid-length/Cranial Size, PstW (Standardised) = Posterior-width/Cranial Size, LatL (Standardised) =Lateral length/Cranial Size. Black dot =extant *Homo sapiens*; Blue dot =fossil specimens *Homo erectus/Homo ergaster*. Corresponding regression parameters in Table 6.

4.4.3. Relative MCF Proportions

Bivariate Reduced Major Axis (RMA) linear regressions were conducted using size-standardised MCF variables against total cranial size (Figure. 6a–c; Table 6). There was no indication of an isometric association between variables suggesting an allometric trend existed (a =0.80233 to 1.2612) and there was a moderate to high correlation between all size-standardised MCF variables ($r \leq 0.71$; $r^2 \leq 0.50$; $p \leq 0.001$). The lowest correlation was observed between PstW and MidL proportions (r =0.33, r^2 =0.11, p =0.0192), while much stronger correlations occurred between PstW and LatL proportions (r ≤0.71; r2 ≤0.50; p ≤ 0.001). We examined if the fossil sample departed from the scaling trend observed in extant *H. sapiens* by excluding the fossil sample from RMA regressions to compare the outcome (Figure 6 d–f; Table 6) with consistently weaker correlations observed between LatL and MidL proportions and PstW and MidL proportions (r <0.02; r^2 <0.00; p <0.9436), however, PstW and LatL proportion remained strong (r <0.62; r^2 < 0.38; p <0.001).

Table 6 Relative MCF proportions using size-standardised variables with Reduced Major Axis (RMA) regression parameters and RMA regression parameters for extant *Homo sapiens* examining effect of fossil specimens on correlations. Statistically significant results reported in bold (p ≤0.05).

All specimens MCF Proportions RMA Parameters					
Metric	***a***	***b***	***r*²**	***r***	***p***
PstW/MidL (Standardized)	0.8023	0.042604	0.11	0.33	***0.0192***
LatL/MidL (Standardized)	1.2612	0.031166	**0.16**	**0.40**	***0.0041***
PstW/LatL (Standardized)	**1.0119**	0.084899	**0.50**	**0.71**	***0.0001***
***Homo sapiens* MCF Proportions RMA Parameters**					
Metric	***a***	***b***	***r*²**	***r***	***p***
PstW/MidL (Standardized)	0.55307	0.135905	0.00	0.02	**<*0.0001***
LatL/MidL (Standardized)	**1.83107**	**-0.165226**	0.00	0.01	**<*0.0001***
PstW/LatL (Standardized)	**1.01271**	**0.083626**	**0.38**	**0.62**	**<*0.0001***

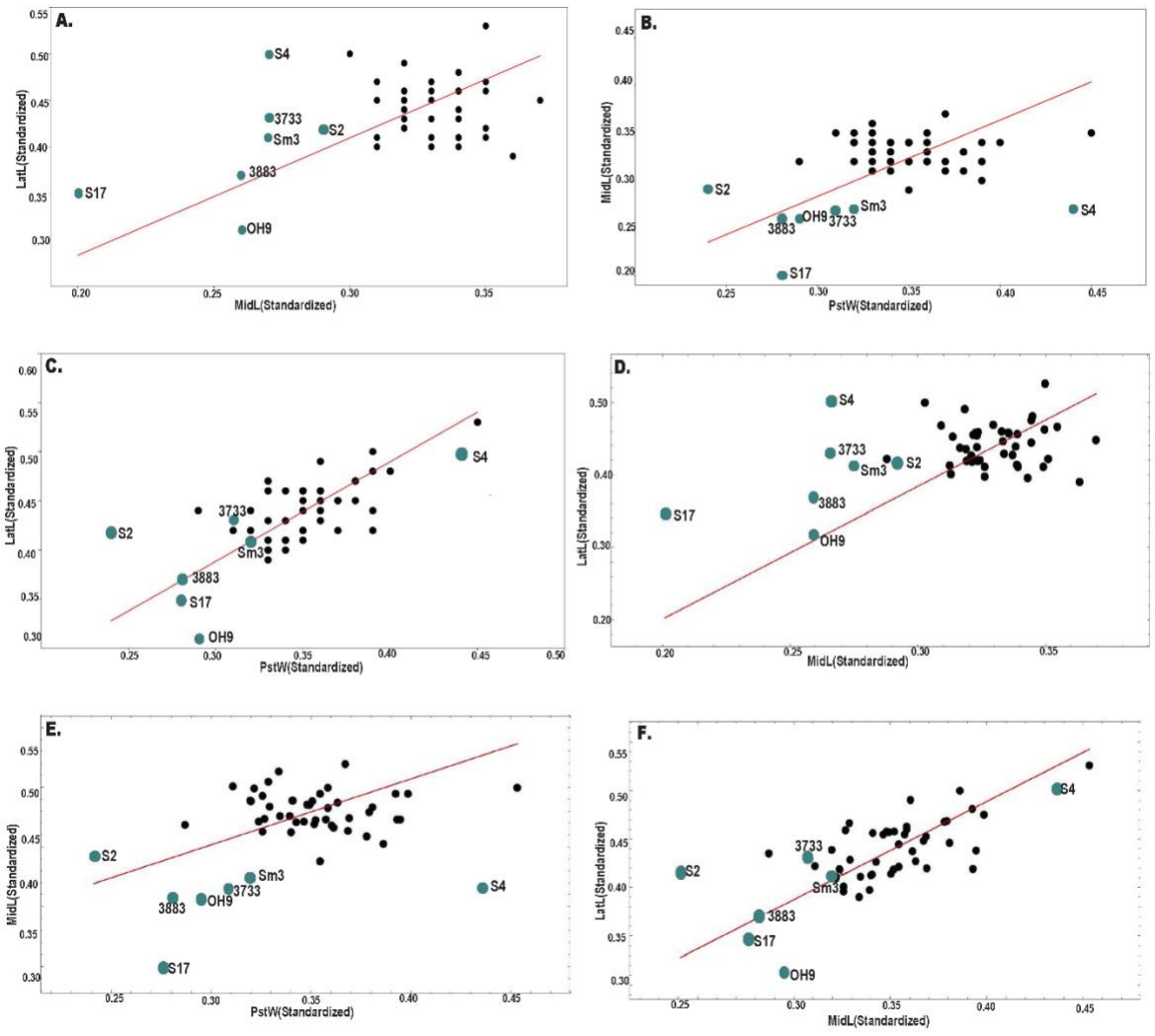

Figure 6. Bivariate linear Reduced Major Axis (RMA) regressions for size-standardized MCF variables illustrating A-C) the combined sample regressions and D-F) regression line fit to extant Homo sapiens and excluding fossil specimens. Abbreviations: MidL (Standardized) = Mid-length/Cranial Size, PstW (Standardized) = Posterior-width/Cranial Size, LatL (Standardized) = Lateral length/Cranial Size. Black dot = extant Homo sapiens; Blue dot = fossil specimens Homo erectus/Homo ergaster. Corresponding regression parameters in Table 6. (For interpretation of the references to color in this figure legend, the reader is referred to the Web version of this article.)

The outcome of the bootstrap procedure using the log- log variables suggested little gain would be attained with such small sample sizes and a similar procedure was not repeated with the- standardised variables. However, stability in PstW and LatL proportions suggest some similarity with previous findings for PstW to cranial size scaling in the fossil sample

(Section 4.3.2). Interspecific differences were also examined when grouping specimens by species to calculate the "species average" for MCF proportions (Figure. 7; Table 7).

Table 7. The size-standardised MCF proportions and the differences (as percentages) between *Homo erectus*, *Homo ergaster* and extant *Homo sapiens*. Negative values indicate lower proportions, positive values indicate larger proportions. Significant results reported in bold.

Relative MCF Proportions			
ID	**PstW (Standardised)**	**LatL (Standardised)**	**MidL (Standardised)**
H. sapiens	0.35	**0.44**	**0.33**
H. ergaster	**0.29**	0.37	0.26
H. erectus	0.32	0.42	0.26
Interspecific Relative MCF Proportions			
ID	**PstW (Standardised)**	**LatL (Standardised)**	**MidL (Standardised)**
H. sapiens : H. erectus	**+ 3%**	**+2%**	**+8%**
H. sapiens : H. ergaster	**+ 6%**	**+7%**	**+7%**
H. erectus : H. ergaster	**+3%**	**+5%**	0%

Figure 7. Depiction of 3D axis plot comparing relative MCF proportions using size-standardised MCF variables coloured to show individual variation in the total sample and "species averages" for extant *Homo sapiens* (black square), African *Homo ergaster* (blue square) and Javanese *Homo erectus*. Abbreviations: MidL (Standardised) =Mid-length/Cranial Size,PstW (Standardised) =Posterior-width/Cranial Size, LatL(Standardised)=Lateral length/Cranial Size. Black dot =extant *Homo sapien*s, Black square =average extant *Homo sapiens*, Blue dot =fossil specimens for *Homo erectus/Homo ergaster*, Blue square =average *Homo ergaster*, Red square =average Javanese *Homo erectus*. Corresponding regression parameters are in Table 8.

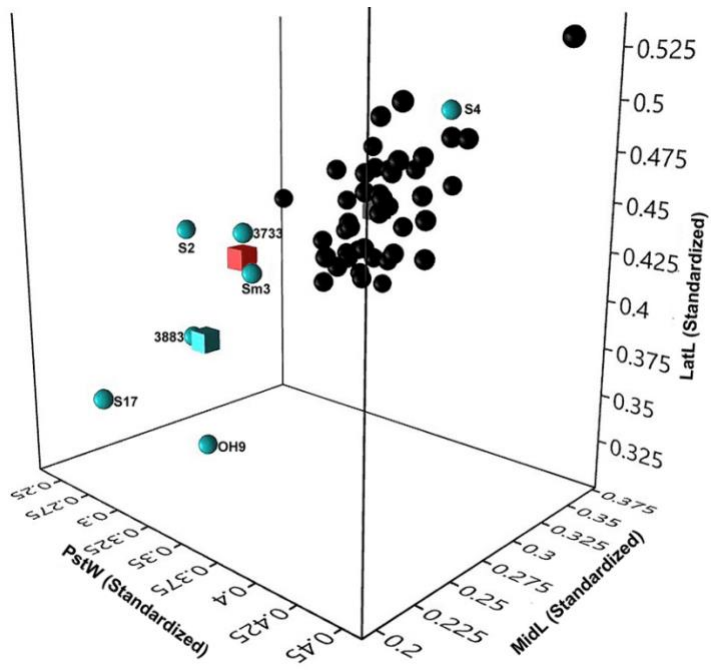

We determined any increase or decrease in MCF proportions to provide an estimate of relative change between species. Extant *H. sapiens* had a larger relative PstW and LatL proportions compared to Javanese *H. erectus* and African *H. ergaster* (2–3% and 6–7% respectively), however, relative MidL proportion was much larger in extant *H. sapiens* than Javanese *H. erectus* and African *H. ergaster* (8% and 7% respectively). Javanese *H. erectus* had a relatively larger PstW proportion compared to African *H. ergaster* (3%) and a relatively larger LatL proportion compared to African *H. ergaster* (5%), however, no difference was observed in the relative MidL proportion in both fossil species. To reiterate, small sample size is a confounding factor in many paleoanthropology studies and the average species value compared to the high individual variation in Javanese *H. erectus* is noticeable compared to African H. *ergaster* and extant *H. sapiens* (Figure. 7, Table 8).

Table 8. Descriptive statistics for the three MCF metrics and two external cranial metrics in extant *Homo sapiens*, *Homo ergaster* and *Homo erectus.*

Descriptive Statistics					
H. sapiens	**LatL**	**PstW**	**MidL**	**MaxCrL**	**MaxCrW**
Min	54.58	40.18	41.54	155.88	107.11
Max	80.41	65.69	58.24	213.93	143.12
Mean	64.27	51.38	48.23	177.10	119.97
Stand. dev	6.23	5.20	3.74	11.61	7.81
Median	62.88	50.69	48.43	176.69	118.00
25 percentile	59.56	48.09	45.15	169.38	115.43
75 percentile	69.41	53.41	50.79	182.46	124.99
Coefficient. var	9.70	10.13	7.76	6.55	6.51
H. ergaster	**LatL**	**PstW**	**MidL**	**MaxCrL**	**MaxCrW**
Min	51.5	42.85	39.43	173.01	130.54
Max	65.85	48.33	42.16	189.74	141.66
Mean	57.87	46.13	40.77	180.87	135.51
Stand. dev	7.31	2.90	1.37	8.41	5.65
Median	56.27	47.22	40.73	179.87	134.32
25 percentile	51.50	42.85	39.43	173.01	130.54
75 percentile	65.85	48.33	42.16	189.74	141.66
Coefficient. var	12.63	6.28	3.55	4.65	4.17
H. erectus	**LatL**	**PstW**	**MidL**	**MaxCrL**	**MaxCrW**
Min	56.7	33.09	32.84	161.59	116.00
Max	72.08	62.59	41.22	196.71	135.63
Mean	61.94	47.16	38.04	177.28	124.37
Stand. dev	7.14	12.12	3.69	14.58	9.76
Median	59.49	46.48	39.05	175.42	122.93
25 percentile	56.82	36.09	34.17	164.58	116.11
75 percentile	69.51	58.91	40.90	191.85	134.08
Coefficient. var	11.53	25.71	9.70	8.22	7.85

4.5 Discussion

This study sought to investigate the variation of the middle cranial fossa (MCF) in extant *H. sapiens* and fossil specimens attributed to African *H. ergaster* and Javanese *H. erectus* to determine effects of allometry and relative MCF proportions with implication for inferring temporal lobe evolution. Linear measurements on the endocranial surface of the right MCF were compared to cranial measurements approximating total cranial size. Previous research of *H. erectus s. l.* endocast morphology (Bruner et al., 2015), nonhuman primate and fossil hominin basicranial variation (Lieberman, 2011; Lieberman et al., 2000b; McCarthy, 2001), MCF morphology and relative lengthening of the temporal lobes in fossil *Homo* (Bastir

et al., 2008, 2011), disproportionately large temporal lobes in extant *H. sapiens* (Rilling and Seligman, 2002) and a strong association between temporal lobe volume and MCF metrics (Pearson et al., 2020) form the foundations of this present study.

4.5.1. Comparative cranial and endocranial variation

Individual variation in *H. erectus s. l.* is often considered as high as in that observed in extant *H. sapiens* (Bruner, 2018) or potentially higher as revealed by previous investigations by Terhune et al. (2007) and Baab (2008) using geometric morphometrics to compare the extent of cranial shape variation observed in *H. erectus s.l.* against the observed variation in extant comparative taxa. Compared to cranial variation in extant and fossil hominids and old-world monkeys, multiple species were supported only when using the entire cranial shape dataset, distinguishing between specimens attributed to Asian *H. erectus* and African *H. ergaster* Baab (2008). Similar findings by Terhune et al. (2007) excluding old-world monkeys but used only the temporal bone which has shown previously to retain high phylogenetic signal and phylogenetic information (Lockwood et al., 2004; Pearson et al., 2015). Although our study did not use geometric morphometrics, the particularly, the temporal bone and the neurocranium has been indicated to retain neutral genetic distances rather than the associated climatic signatures in the facial skeleton (Harvati and Weaver, 2006). Linear measurements of the cranium have been suggested to be less successful at distinguishing between single or multiple species within *H. erectus s.l.*, however, inherent methodological differences have a significant contribution to the outcome with potential allometric changes to cranial form more likely to influence geometric morphometric findings where isometric size differences are removed during Procrustes superimposition, while linear measurements retain this factor but are limited in the determination of more subtle allometric changes. This might explain why specimens

from Zhoukoudian, and Java are more distinguishable by linear measurements (Durband et al., 2005; Kidder and Durband, 2004) than those attributed to Asian *H. erectus* and African/European *H. ergaster* where more subtle allometric changes might influence cranial morphology. The potential differences inherent to the methodological approach where allometric or more subtle morphological variation could influence the outcome warrant consideration.

Although cranial variation within *H. erectus s.l.* appears to be largely influenced by absolute size variation between specimens from Javan and Zhoukoudian, or potentially influenced by allometric shape changes between specimens attributed to Asian *H. erectus* and African *H. ergaster*, endocranial variation is not so straight-forward. Bruner et al. (2016) and Bruner et al. (2015) examined endocranial variation in Asian *H. erectus* and African *H. ergaster* using virtual endocasts but did not find a singular definitive trait to clearly distinguish African *H. ergaster* from Asian *H. erectus*.

We also compared African *H. ergaster* from Asian *H. erectus* using measurements from the endocranium, specifically the middle cranial fossa (MCF), initially finding similar to Bruner et al. (2015) that no singular trait, specifically, no definitive MCF metric distinguished specimens attributed to Javanese *H. erectus* from African *H. ergaster*. Our findings suggested that the cranial measurements were more associated with greater variance among specimens than the endocranial, specifically, the MCF measurements.

However, we note an important caveat regarding the small fossil sample size where these specimens had a potentially reduced ability to exert influence on cranial and MCF variation without the inclusion of influence from the much larger sample of extant *H. sapiens*. This is relevant for consideration of sample limitations and interpretations of morphological

variation. In fact, previous research (Bruner et al., 2015) notes the limitations of sample size with power analysis suggesting a minimum of 37 individuals per group required to reach statistical significance. However, it is very unlikely such numbers are achievable in a paleoanthropology, but small sample sizes are a real issue for potential misinterpretation. It is possible endocranial variation in *H. erectus s.l.* is larger than observed in this present study whereby our findings on the differences in relative MCF proportions might be more relevant considering influence of total cranial size was reduced enabling more subtle differences in proportions to be investigated.

4.5.2. Relative MCF scaling and sampling

In the context of brain evolution and relative scaling, previous studies examining changes in the total brain size or endocranial volume relied on allometric scaling principles of brain to body mass common to all mammalian taxa (Barton, 2006) or the application of complex phylogenetic regression models approximating primate scaling relationships (Grabowski et al., 2016), although whether primates, and more specifically hominins, depart from the other mammalian brain-body mass scaling association remains controversial (Barton and Montgomery, 2019). Our study avoids some contentious issues involving the use encephalization quotients (EQ) in fossil taxa to determine the expected brain-body size range for fossil species in which as Gilbert and Jungers (2017) note association with unnecessary errors where fossil body mass calculation often relies on the uncertain phylogenetic position of many fossil species. Although the small fossil sample size in our study is smaller than ideal, we sought to avoid compounding errors common in other studies where published datasets are compiled to increase sample size which introduces uncontrollable interobserver errors and protocols producing uncertain results (Smith and Jungers, 1997).

We sought to address the scaling relationships between the MCF metrics and total cranial size following similar principles outlined in Gilbert and Jungers (2017) applying log-transformed allometric regressions to examine strength of associations and potential departures associated with the inclusion or exclusion of fossil specimens. Our findings of the scaling relationships between MCF metrics and total cranial size suggested an allometric trend but the potential for fossil specimens to lie beyond the range of extant *H. sapiens* and influence the regressions models could indicate an isometric scaling in extant *H. sapiens*, thereby combining to generate an allometric trend across taxa which was partially supported by an increase in correlation strength once fossil specimens were excluded. However, the closer inspection using randomizations and permutations indicated there were no statistically significant difference between slopes or intercepts among extant *H. sapiens* and fossil sample despite the previous indication of increase in correlation strength.

The MCF of the basicranium and the temporal lobe of the brain are closely associated spatially and functionally with the role of functional craniology on the effects of brain and "non-brain" forces on the morphology of the basicranium and neurocranium involving complex interactions during development and evolution (Bruner, 2017, 2018; Bruner et al., 2019). Although the application of linear measurements to determine patterns of variation between specimens attributed to African *H. ergaster* and Javanese *H. erectus* has been consistent, our findings on MCF scaling relative to cranial size have been complicated by sampling issues. However, our findings on relative MCF proportions did appear to determine relative changes and differences between extant *H. sapiens* and the fossil sample, particularly, MCF posterior-width and lateral-length maintained a strong association including and excluding fossil specimens. Although sample size is small and bootstrap procedure is unlikely to produce

further gains, these differences in relative MCF proportions could suggest the fossil sample is beyond the range for extant *H. sapiens* in these MCF proportions. This possibility was further indicated using species-averages extant *H. sapiens* had relatively larger MCF proportions than both fossil species with but Javanese *H. erectus* was relatively longer and wider posteriorly than African *H. ergaster* (3–5% respectively) while no difference was observed in MCF mid-length between the fossil species.

4.5.3. Temporal lobe evolution in *Homo erectus* and *Homo ergaster*

The involvement of the middle cranial fossa in the variation of hominin facial prognathism (Bastir, 2018; Bastir and Rosas, 2016; Bastir et al., 2010; Lieberman et al., 2000a) and potential influence in the relative lengthening of the temporal lobes in fossil *Homo* (Bastir et al., 2008, 2011) has also been linked to the evolution of enlarged temporal lobes in extant *H. sapiens* compared to other extant anthropoids (Rilling and Seligman, 2002). Recently, Pearson et al. (2020) provided support anatomical association between the temporal lobes of the brain and the MCF, bony counterpart of the skull in extant and fossil anthropoids. Our present study indicates fossil specimens attributed to Javanese *H. erectus* and African *H. ergaster* have different MCF proportions to extant *H. sapiens*. Although Rightmire (1986) and Anton and Swisher (2001) have suggested contrary arguments for total brain size evolution in *H. erectus s. l.*, the endocranial capacities for these specimens (Section 2.3.) is comparable. Therefore, the implications of differences in MCF proportions for temporal lobe evolution following recent research by Pearson and Bruner (2018) and Pearson et al. (2020) indicates that differences in MCF proportions without different total cranial size would have required cerebral reorganization alongside these cranial changes. The implications are that the temporal lobes in Javanese *H. erectus* would have been relatively longer and wider posteriorly than African *H.*

ergaster but were still constrained anteriorly toward the orbits as in African *H. ergaster* where the two species did not differ in relative MCF proportions. To thoroughly investigate MCF size and shape variation, a detailed 3D geometric morphometrics analysis using a larger extant comparative sample and more fossil hominin species is necessary.

The role of the MCF in craniofacial evolution remains complex with the basicranial rotational model influencing facial prognathism and craniofacial evolution (Lieberman, 2011; Lieberman et al., 2000a, 2000b; McCarthy, 2001) but opposed by Bastir (2018) and Bastir and Rosas (2016); Bastir et al. (2006) arguing MCF size and position does not strongly relate to midline basicranial angle in *Homo*. *H. erectus s. l.* has been suggested to possess lower basicranial flexion compared to later fossil *Homo* and extant *H. sapiens* (Baba et al., 2003; Bruner et al., 2015), however, our results suggesting a potential difference in relative MCF width posteriorly but not anteriorly constrained by the same total brain size. Alongside changes to facial block, the MCF is uniquely positioned in the cranium where the temporal lobes of the brain are potentially affected by brain changes such as observed in the relative expansion of the parietal regions in *H. sapiens* (Bruner, 2004; Bruner et al., 2011, 2017; Neubauer et al., 2018) but potentially constrained by non-brain influences including relative orbit size (Pereira-Pedro et al., 2017) and positioning of the MCF relative to the mandibular ramus (Bastir and Rosas, 2005). The influence of the temporomandibular joint (TMJ) in relation to our findings deserves further consideration.

The TMJ is often studied in relation to the functional and phylogenetic principles of biomechanics in living primates and often extrapolated into the fossil record. Our findings indicated there was no difference observed in the relative proportion of MCF mid-length between African *H. ergaster* and Javanese *H. erectus*. The MCF mid-length likely corresponds

more closely to the anterior aspects of the MCF which are influenced more substantially by basicranial flexion and facial block changes (Bastir and Rosas, 2005), however, we observed differences in relative MCF posterior-width are also potentially due to the placement of the glenoid fossa directly below the MCF in modern humans (Sherwood et al., 2002). Terhune (2017) has suggested that anthropoids show a positive allometric trend toward greater facial prognathism and larger glenoid fossae associated with greater mandibular length and larger body mass. The mandibles for Javanese *H. erectus* are observed as being larger and more robust than extant *H. sapiens* (Kaifu et al., 2005) but comparison with mandibles from African *H. ergaster* is inconclusive (Tattersall, 2007). The influence of shifts from mandibular robusticity to gracility over the timespan that *H. erectus s. l.* evolved is important when considering mandibular corpus size and shape are thought to reflect dental size with Kupczik et al. (2009) noting interspecifically, a disproportionate increase in tooth root surface area and tooth crown surface area in anthropoids. However, Javanese *H. erectus* has previously been suggested to possess reduced postcanine crown size relative to African *H. ergaster* (Kaifu et al., 2005).

Although the functional significance of changes to glenoid fossa size and shape remain unknown (Terhune, 2017), it appears increasingly relevant that changes to the masticatory system has important implications for the evolution of the temporal cerebrocranial regions. Investigations of craniodental and brain evolution has been conducted but Gomez-Robles et al. (2017) did not find any association between total brain enlargement and postcanine dental reduction during hominin evolution, however, modelling did indicate a faster rate of brain enlargement and tooth reduction occurred before *Homo habilis*, and hence *H. erectus s. l.* was influenced by faster brain enlargement than dental size reduced under a constant neutral model of trait evolution. The recent study by Herries et al. (2020) indicated that by 2 million years,

the endocast shape of a juvenile *Homo ergaster* specimen was already consistent with other *Homo erectus s.l.* specimens including those from Java and China with endocranial size in the upper range of adult *Australopithecus* and *Paranthropus* and beyond juvenile *Australopithecus*. The timing and effects of brain size increase deserve further investigation and larger fossil sample sizes to investigation the influence of the masticatory system and cerebrocranial temporal regions would be relevant to our findings on potential differences in the relative MCF proportions in Javanese *H. erectus* and African *H. ergaster*.

4.6 Conclusion

This study assessed the implications for temporal lobe evolution through investigation of relative scaling of the middle cranial fossa (MCF) and changes to relative MCF proportions among extant *H. sapiens* and fossil specimens attributed to African *H. ergaster* and Javanese *H. erectus*. Through a series of bivariate linear RMA regressions, we investigated whether relative MCF scaling and MCF proportions in the l sample were beyond the range of extant *H. sapiens*. Our results indicated g relatively larger MCF proportions in extant *H. sapiens* compared to fossil specimens while Javanese *H. erectus* had relatively longer and wider MCF proportions posteriorly than African *H. ergaster* suggesting changes to relative temporal lobe form between both species. Our findings emphasize the importance of quantifying variation to determine sampling limitations and indicate potential differences in cerebrocranial morphology between African *Homo ergaster* and Javanese *Homo erectus* relevant to temporal lobe evolution in the genus *Homo*.

4.7. Funding

This work was supported by the Australian Government Research Training Program Scholarship and the Spanish Government [#PGC2018-093925-B-C31].

4.8. Data availability

Datasets related to this article can be found in the supplementary material. Declaration of competing interest. The authors declare that they have no known competing financial interests or personal relationships that could have appeared to influence the work reported in this paper. Acknowledgements AP thanks Dr Debbie Argue (Australian National University) for initial discussions, Dr Heinrich Mallison (University of Hamburg) for invaluable advice on 3D Photogrammetry techniques and the Biological Anthropology Department (Australian National University) for access to the research cast of Sangiran 17 donated by P. Brown. We acknowledge these institutions and people for digital data access: Senckenberg Forschungsinstitut und Naturmuseum, Frankfurt am Main care of C. Hemm; NESPOS Society e.V. and care of J.J. Hublin and the Anatomisches Institut, Universit¨at Leipzig; Universit¨at Hamburg care of T.M. Kaiser Sangiran 17 virtual cast; University of Pennsylvania Museum of Archaeology and Anthropology and the Open Research Scan Archive (ORSA) care of J. Monge and P. T. Schoenemann (NSF proposal # 0447271); The National Museums of Kenya (NMK) care of F. Spoor; Morphosource (www.MorphoSource.org), Duke University care of D. Boyer Sangiran 17 cast M5791 (ark:/87602/m4/M5791).

4.9. Appendix A. Supplementary data

Supplementary data to this article can be found online at:https://doi. org/10.1016/j.quaint.2020.07.048

4.10. References

Adams, D.C., Ot´arola-Castillo, E., Paradis, E., 2013. geomorph: an r package for the collection and analysis of geometric morphometric shape data. Methods Ecol. Evol. 4, 393–399.

Agisoft, 2016. Agisoft Photoscan Standard, 1.2.6 Ed. Agisoft LLC, St Petersburg, Russia. Anton, S.C., 2003. Natural history of Homo erectus. Am. J. Phys. Anthropol. Suppl. 37,126–170.

Anton, S.C., Swisher, C.C.I., 2001. Evolution and variation of cranial capacity in Asian Homo erectus. In: Indriati, E. (Ed.), A Scientific Life: Papers in Honor of Professor Dr. Teuku Jacob. Yogyakarta, Indonesia. Bigraf Publishing, Jakata, pp. 25–39.

Aziz, F., Baba, H., Watanabe, N., 1996. Morphological study on the Javanese Homo erectus Sangiran 17 skull based upon a new reconstruction. Geological Res. Develop. Centre Paleontology Series 8, 11–25.

Baab, K.L., 2008. The taxonomic implications of cranial shape variation in Homo erectus. J. Hum. Evol. 54, 827–847.

Baba, H., Aziz, F., Kaifu, Y., Suwa, G., Kono, R.T., Jacob, T., 2003. Homo erectus calvarium from the Pleistocene of Java. Science 299, 1384–1388.

Barton, R.A., 2006. Primate brain evolution: integrating comparative, neurophysiological, and ethological data. Evol. Anthropol. 15, 224–236.

Barton, R.A., Montgomery, S.H., 2019. Proportional versus relative size as metrics in human brain evolution. Proc. Natl. Acad. Sci. U. S. A. 116, 3–4.

Bastir, M., 2018. Back to basics: morphological analysis in paleoanthropology. In: Schwartz, J. (Ed.), Biological Theory. MIT-Press, Boston, pp. 205–227.

Bastir, M., Rosas, A., 2005. Hierarchical nature of morphological integration and modularity in the human posterior face. Am. J. Phys. Anthropol. 128, 26–34.

Bastir, M., Rosas, A., 2016. Cranial base topology and basic trends in the facial evolution of Homo. J. Hum. Evol. 91, 26–35.

Bastir, M., Rosas, A., Gunz, P., Pena-Melian, A., Manzi, G., Harvati, K., Kruszynski, R., Stringer, C., Hublin, J.J., 2011. Evolution of the base of the brain in highly encephalized human species. Nat. Commun. 2, 588.

Bastir, M., Rosas, A., Lieberman, D.E., O'Higgins, P., 2008. Middle cranial fossa anatomy and the origin of modern humans. Anat. Rec. 291, 130–140.

Bastir, M., Rosas, A., O'Higgins, P., 2006. Craniofacial levels and the morphological maturation of the human skull. J. Anat. 209, 637–654.

Bastir, M., Rosas, A., Stringer, C., Cuetara, J.M., Kruszynski, R., Weber, G.W., Ross, C.F., Ravosa, M.J., 2010. Effects of brain and facial size on basicranial form in human and primate evolution. J. Hum. Evol. 58, 424–431.

Bookstein, F.L., 1997. Morphometric Tools for Landmark Data: Geometry and Biology. Cambridge University Press, New York.

Borden, N.M., Forseen, S.E., Stefan, C., 2016. Imaging Anatomy of the Human Brain A Comprehensive Atlas Including Adjacent Structures. Demos Medical Publishing, New York.

Broadfield, D.C., Holloway, R.L., Mowbray, K., Silvers, A., Yuan, M.S., Marquez, S., 2001. Endocast of Sambungmacan 3 (Sm 3): a new Homo erectus from Indonesia. Anat. Rec. 262, 369–379.

Bruner, E., 2004. Geometric morphometrics and paleoneurology: brain shape evolution in the genus Homo. J. Hum. Evol. 47, 279–303.

Bruner, E., 2017. The fossil evidence of human brain evolution. In: Kaas, J.H. (Ed.), Evolution of Nervous Systems Volume 4: the Evolution of the Human Brain: Apes and Other Ancestors. Elsevier Inc., Amsterdam, Boston, pp. 63–92.

Bruner, E., 2018. The brain, the braincase, and the morphospace. In: Bruner, E., Ogihara, N., Tanabe, H.C. (Eds.), Digital Endocasts: from Skulls to Brains. Springer KK Japan, Tokyo, pp. 93–114.

Bruner, E., Bondioli, L., Coppa, A., Frayer, D.W., Holloway, R.L., Libsekal, Y., Medin, T., Rook, L., Macchiarelli, R., 2016. The endocast of the one-million-year-old human cranium from Buia (UA 31), Danakil Eritrea. Am. J. Phys. Anthropol. 160, 458–468.

Bruner, E., De La Cuetara, J.M., Holloway, R., 2011. A bivariate approach to the variation of the parietal curvature in the genus homo. Anat. Rec. 294, 1548–1556.

Bruner, E., Esteve-Altava, B., Rasskin-Gutman, D., 2019. A network approach to brain form, cortical topology and human evolution. Brain Struct. Funct.

Bruner, E., Grimaud-Herv´e, D., Wu, X., de la Cu´etara, J.M., Holloway, R., 2015. A paleoneurological survey of Homo erectus endocranial metrics. Quat. Int. 368, 80–87.

Bruner, E., Pereira-Pedro, A.S., Bastir, M., 2017. Patterns of morphological integration between parietal and temporal areas in the human skull. J. Morphol. 278, 1312–1320.

Cardini, A., 2017. Left, right or both? Estimating and improving accuracy of one-side- only geometric morphometric analyses of cranial variation. J. Zool. Syst. Evol. Res. 55 (1), 1–10.

Cartmill, M., Smith, F.H., 2009. The Human Lineage. Wiley-Blackwell, Hoboken, New Jersey.

Delson, E., Harvati, K., Reddy, D.P., Marcus, L.F., Mowbray, K., Sawyer, G.J., Jacob, T., Marquez, S., 2001. The sambungmacan 3 Homo erectus calvaria: a comparative morphometric and morphological analysis. Anat. Rec. 262, 380–397.

Durband, A.C., Kidder, J.H., Jantz, R.L., 2005. A multivariate examination of the Hexian calvaria. Anthropol. Sci. 113, 147–154.

Fuentes, G.J., Polly, P.D., Martins, E.P., 2020. A Bayesian extension of phylogenetic generalized least squares: incorporating uncertainty in the comparative study of trait relationships and evolutionary rates. Evolution 74, 311–325.

Gilbert, C.C., Jungers, W.L., 2017. Comment on relative brain size in early primates and the use of encephalization quotients in primate evolution. J. Hum. Evol. 109, 79–87.

Gomez-Robles, A., Smaers, J.B., Holloway, R.L., Polly, P.D., Wood, B.A., 2017. Brain enlargement and dental reduction were not linked in hominin evolution. Proc. Natl. Acad. Sci. U. S. A. 114, 468–473.

Grabowski, M., Voje, K.L., Hansen, T.F., 2016. Evolutionary modeling and correcting for observation error support a 3/5 brain-body allometry for primates. J. Hum. Evol. 94, 106–116.

Groves, C.P., Mazak, V., 1975. An approach to the taxonomy of the Hominoidae: gracile Villafranchian hominids of Africa. Caspos. Miner Geol. 20, 225–247.

Hammer, Ø., Harper, D.A.T., Ryan, P.D., 2001. Past: paleontological statistics software package for education and data analysis. Palaeontol. Electron. 4, 1–9.

Harvati, K., Weaver, T.D., 2006. Human cranial anatomy and the differential preservation of population history and climate signatures. Anat. Rec. A Discov. Mol. Cell. Evol. Biol. 288, 1225–1233.

Herries, A.I.R., Martin, J.M., Leece, A.B., Adams, J.W., Boschian, G., Joannes-Boyau, R., Edwards, T.R., Mallett, T., Massey, J., Murszewski, A., Neubauer, S., Pickering, R., Strait, D.S., Armstrong, B.J., Baker, S., Caruana, M.V., Denham, T., Hellstrom, J., Moggi-Cecchi, J., Mokobane, S., Penzo-Kajewski, P., Rovinsky, D.S., Schwartz, G.T., Stammers, R.C., Wilson, C., Woodhead, J., Menter, C., 2020. Contemporaneity of Australopithecus, Paranthropus, and early Homo erectus in South Africa. Science 368 (6486), eaaw7293.

Holloway, R.L., 1981. The Indonesian Homo erectus brain endocasts revisited. Am. J. Phys. Anthropol. 55, 503–521.

Holloway, R.L., 2002. Head to head with Boas: did he err on the plasticity of head form? Proc. Natl. Acad. Sci. U.S.A. 99, 14622–14623.

Holloway, R.L., Broadfield, D.C., Yuan, M.S., 2004. The Human Fossil Record Volume Three: Brain Endocasts- the Paleoneurological Evidence. John Wiley & Sons, Inc., Hoboken,New Jersey.

Indriati, E., Swisher 3rd, C.C., Lepre, C., Quinn, R.L., Suriyanto, R.A., Hascaryo, A.T., Grun, R., Feibel, C.S., Pobiner, B.L., Aubert, M., Lees, W., Anton, S.C., 2011. The age of the 20 meter Solo River terrace, Java, Indonesia and the survival of Homo erectus in Asia. PloS One 6, e21562.

Jolliffe, I.T., 2002. Principal Component Analysis, 2 ed. Springer, Berlin. Jungers, W.L., 1985. Size and Scaling in Primate Biology. Springer, New York.

Jungers, W.L., Falsetti, A.B., Wall, C.E., 1995. Shape, relative size, and size-adjustments in morphometrics. Yearbk. Phys. Anthropol. 38, 137–161.

Kaifu, Y., Baba, H., Aziz, F., Indriati, E., Schrenk, F., Jacob, T., 2005. Taxonomic affinities and evolutionary history of the Early Pleistocene hominids of Java: dentognathic evidence. Am. J. Phys. Anthropol. 128, 709–726.

Kidder, J.H., Durband, A.C., 2004. A re-evaluation of the metric diversity within Homo *erectus. J. Hum. Evol.* 46, 299–315.

Kupczik, K., Olejniczak, A.J., Skinner, M.M., Hublin, J.J., 2009. Molar crown and root size relationship in anthropoid primates. Front Oral Biol. 13, 16–22.

LaBarbera, M., 1989. Analyzing body size as a factor in ecology and evolution. Annu.Rev. Ecol. Systemat. 20, 97–117.

Larick, R., Ciochon, R.L., Zaim, Y., Sudijono, Suminto, Rizal, Y., Aziz, F., Reagan, M., Heizler, M., 2001. Early Pleistocene 40Ar/39Ar ages for bapang formation hominins, central Jawa, Indonesia. Proc. Natl. Acad. Sci. U. S. A. 98, 4866–4871.

Leakey, M.D., 1971. Olduvai Gorge: Volume 3, Excavations in Beds I and II, 1960-1963,3. Cambridge University Press, Cambridge, New York.

Lieberman, D.E., 2011. The Evolution of the Human Head. The Belknap Press of Harvard University Press, Cambridge, Massachusetts; London, England.

Lieberman, D.E., Pearson, O.M., Mowbray, K.M., 2000a. Basicranial influence on overall cranial shape. J. Hum. Evol. 38, 291–315.

Lieberman, D.E., Ross, C.F., Ravosa, M.J., 2000b. The primate cranial base: ontogeny, function, and integration. Am. J. Phys. Anthropol. Suppl. 31, 117–169.

Lockwood, C.A., Kimbel, W.H., Lynch, J.M., 2004. Morphometrics and hominoid phylogeny: support for a chimpanzee-human clade and differentiation among great ape subspecies. Proc. Natl. Acad. Sci. U. S. A. 101, 4356–4360.

Lordkipanidze, D., Ponce de Leon, M.S., Margvelashvili, A., Rak, Y., Rightmire, G.P., Vekua, A., Zollikofer, C.P., 2013. A complete skull from Dmanisi, Georgia, and the evolutionary biology of early Homo. Science 342, 326–331.

Mallison, H., Wings, O., 2014. Photogrammetry in paleontology – a practical guide.J. Paleontol. Tech. 12, 1–31.

Martin, R.D., Barbour, A.D., 1989. Aspects of line-fitting in bivarate allometric analyses. Folia Primatol. 53, 65–81.

Marquez, S., Mowbray, K., Sawyer, G.J., Jacob, T., Silvers, A., 2001. New fossil hominid calvaria from Indonesia—sambungmacan 3. Anat. Rec. 262, 344–368.

Materialise, 2018. Mimics 17, 17 ed. Materialise Corporation, Leuven, Belgium.

McCarthy, R.C., 2001. Anthropoid cranial base architecture and scaling relationships. .

Mitteroecker, P., Gunz, P., Bernhard, M., Schaefer, K., Bookstein, F.L., 2004. Comparison of cranial ontogenetic trajectories among great apes and humans. J. Hum. Evol. 46, 679–698.

Mitteroecker, P., Gunz, P., Bookstein, F.L., 2005. Heterochrony and geometric morphometrics: a comparison of cranial growth in *Pan paniscus* versus *Pan troglodytes*. Evol. Dev. 7 (3), 244–258.

Neubauer, S., Gunz, P., Scott, N.A., Hublin, J.J., Mitteroecker, P., 2020. Evolution of brain lateralization: a shared hominid pattern of endocranial asymmetry is much more variable in humans than in great apes. Sci. Adv. 6, eaax9935.

Neubauer, S., Hublin, J.J., Gunz, P., 2018. The evolution of modern human brain shape.Sci. Adv. 4, eaao5961.

Norton, C.J., Gao, X., Liu, W., Braun, D.R., Wu, X., 2010. Central-East China – a Plio- Pleistocene Dispersal Corridor: the current state of evidence for hominin cccupations. In: Norton, C.J., Braun, D.R. (Eds.), Asian Paleoanthropology: from Africa to China and beyond, Vertebrate Paleobiology and Paleoanthropology Series. Springer Dordrecht, Heidelberg, London, New York, pp. 159–168. https://doi.org/ 10.1007/978-90-481-9094-2_12.

Pearson, A., Bruner, E., 2018. A preliminary survey of temporal lobe and cranial morphometrics in extant Haplorrhines. Folia Primatol. 89, 207.

Pearson, A., Groves, C., Cardini, A., 2015. The 'temporal effect' in hominids: reinvestigating the nature of support for a chimp-human clade in bone morphology. J. Hum. Evol. 88, 146–159.

Pearson, A., Polly, P.D., Bruner, E., 2020. Is the middle cranial fossa a reliable predictor of temporal lobe volume in extant and fossil anthropoids? Am. J. Phys. Anthropol.

Pereira-Pedro, A.S., Masters, M., Bruner, E., 2017. Shape analysis of spatial relationships between orbito-ocular and endocranial structures in modern humans and fossil hominids. J. Anat. 231, 947–960.

Polly, P.D., 2001. Paleontology and the comparative method: ancestral node reconstructions versus observed node values. Am. Nat. 157, 596–609.

Rightmire, G.P., 1986. Stasis in Homo erectus? Stasis in Homo erectus defended. Paleobiology 12, 324–325.

Rilling, J.K., Seligman, R.A., 2002. A quantitative morphometric comparative analysis of the primate temporal lobe. J. Hum. Evol. 42, 505–533.

Rizal, Y., Westaway, K.E., Zaim, Y., van den Bergh, G.D., Bettis 3rd, E.A., Morwood, M.J., Huffman, O.F., Grun, R., Joannes-Boyau, R., Bailey, R.M., Sidarto, Westaway, M.C., Kurniawan, I., Moore, M.W., Storey, M., Aziz, F., Suminto, Zhao, J.X., Aswan, Sipola, M.E., Larick, R., Zonneveld, J.P., Scott, R., Putt, S., Ciochon, R.L., 2020. Last appearance of Homo erectus at Ngandong, Java, 117,000-108,000 years ago. Nature 577, 381–385.

Sherwood, R.J., Rowley, R.B., Ward, S.C., 2002. Relative placement of the mandibular fossa in great apes and humans. J. Hum. Evol. 43, 57–66.

Simpson, G.G., Roe, A., Lewontin, R.C., 2003. Quantitative Zoology. Revised, ed. Dover Publications, New York.

Smaers, J.B., Rohlf, F.J., 2016. Testing species' deviation from allometric predictions using the phylogenetic regression. Evolution 70, 1145–1149.

Smith, R.J., Jungers, W.L., 1997. Body mass in comparative primatology. J. Hum. Evol. 32, 523–559.

Sokal, R.R., Rohlf, F.J., 1995. Biometry: the Princples and Practice of Statistics in Biological Research, 3 ed. W.H. Freeman, New York, London.

Scott, N.A., Strauss, A., Hublin, J.-J., Gunz, P., Neubauer, S., 2018. Covariation of the endocranium and splanchnocranium during great ape ontogeny. PloS One 13 (12), e0208999.

Stratovan, 2018. Stratovan Checkpoint. Stratovan Corporation, UC, Davis, California, 2018.12.20.

Tattersall, I., 2007. Homo *ergaster* and its Contemporaries. In: Henke, W., Tattersall, I., Hardt, T. (Eds.), Handbook of Paleoanthropology. Springer, Berlin, pp. 1633–1654.

Terhune, C.E., 2017. Revisiting size and scaling in the anthropoid temporomandibular joint. Zoology (Jena) 124, 73–94.

Terhune, C.E., Kimbel, W.H., Lockwood, C.A., 2007. Variation and diversity in Homo erectus: a 3D geometric morphometric analysis of the temporal bone. J. Hum. Evol. 53, 41–60.

Von Koenigswald, G.H.R., 1956. Meeting Prehistoric Man. Harper, New York.

Weidenreich, F., 1941. The brain and its role in the phylogenetic transformation of the human skull. Trans. Am. Phil. Soc. 31, 320–442. New Series.

Weidenreich, F., 1947. Some particulars of skull and brain of early hominids and their bearing on the problem of the relationship between man and anthropoids. Am. J. Phys. Anthropol. 5, 387–428.

Wharton, D.I., Wright, I.J., Falster, D.S., Westoby, M., 2006. Bivariate line-fitting methods for allometry. Biol. Rev. 81, 259–291.

White, T.D., Black, M.T., Folkens, P.A., 2012. Human Osteology, 3 ed. Academic Press, California.

Wolfram, 2019. Wolfram Mathematica, 12.0. Wolfram Research, Inc., Champaign, Illinois.

Wood, B.A., 1994. Taxonomy and evolutionary relationships of Homo erectus. Cour.Forschungsinst. Senckenberg 171, 159–165.

Yokoyama, Y., Falgueres, C., Semah, F., Jacob, T., Grun, R., 2008. Gamma-ray spectrometric dating of late Homo erectus skulls from Ngandong and Sambungmacan, Central Java, Indonesia. J. Hum. Evol. 55, 274–277.

Zaim, Y., Ciochon, R.L., Polanski, J.M., Grine, F.E., Bettis 3rd, E.A., Rizal, Y., Franciscus, R.G., Larick, R.R., Heizler, M., Aswan Eaves, K.L., Marsh, H.E., 2011. New 1.5 million-year-old Homo erectus maxilla from sangiran (central Java, Indonesia). J. Hum. Evol. 61, 363–376.

Zollikofer, C.P.E., Ponce de Leon, M.S., 2005. Virtual Reconstruction: A Primer in Computer-Assisted Paleontology and Biomedicine. Wiley-Liss, New York; Chichester.

Pearson, A., Bruner, E., Polly, P.D. (2023a) Updated imaging and phylogenetic comparative methods reassess relative temporal lobe size in anthropoids and modern humans. *American Journal of Biological Anthropology,*180(4) 768-776.

In this chapter, I address the third aim of this thesis by confirming whether modern humans have disproportionately large temporal lobes compared to other anthropoids and using updated imaging and phylogenetic comparative methods.

Chapter 5: Updated imaging and phylogenetic comparative methods reassess relative temporal lobe size in anthropoids and modern humans.

5.1 Abstract

Two decades ago, Rilling and Seligman, hereafter abbreviated to RAS Study, suggested modern humans had relatively larger temporal lobes for brain size compared to other anthropoids. Despite many subsequent studies drawing conclusions about the evolutionary implications for the emergence of unique cerebral specializations in *Homo sapiens*, no re-assessment has occurred using updated methodologies. We reassessed the association between right temporal lobe volume (TLV) and right hemisphere volume (HV) in the anthropoid brain. In a sample compiled de novo by us, T1-weighted in vivo Magnetic Resonance Imaging (MRI) scans of 11 extant anthropoid species were calculated by-voxel from the MRI and the raw data from RAS Study directly compared to our sample. Phylogenetic Generalized Least-Squares (PGLS) regression and trait-mapping using Blomberg's K (kappa) tested the correlation between HV and TLV accounting for anthropoid phylogeny, while bootstrapped PGLS

regressions tested difference in slopes and intercepts between monkey and ape subsamples. PGLS regressions indicated statistically significant correlations ($r2 < 0.99$; $p \leq 0.0001$) between TLV and HV with moderate influence from phylogeny ($K \leq 0.42$). Bootstrapped PGLS regression did not show statistically significant differences in slopes between monkeys and apes but did intercepts. In our sample, human TLV was not larger than expected for anthropoids. Updated imaging, increased sample size and advanced statistical analyses did not find statistically significant results that modern humans possessed a disproportionately large temporal lobe volume compared to the general anthropoid trend. This has important implications for h human and non-human primate brain evolution.

5.2. Introduction

Over two decades ago, Rilling & Seligman (2002) hereafter abbreviated to the RAS study determined modern human temporal lobe volume (TLV) was larger, both absolutely and relatively, compared to other anthropoids and suggested a disproportionately large temporal lobe volume was a uniquely modern human trait. Since the initial RAS study, no further re-examination of these findings has been conducted utilizing more updated magnetic resonance imaging (MRI) software, phylogenetic comparative methods, or robust statistical analyses.

The temporal cortex of the brain is involved in many distinct processes with understanding language development in modern humans the focus for many neurobiological and evolutionary studies. Broca's and Wernicke's areas do not appear to have non-human homologues in great apes (Rilling, 2014), but Broca's cap, thought a proxy for Broca's area in endocasts, is often preserved in fossil hominin endocasts and used to study language evolution (Holloway, 1983). For paleoneurology, brain encephalisation and lateralisation have been a

suggested indicator of increased developmental plasticity (Gomez-Robles et al., 2013), and modern human asymmetry has been found to be much more variable compared to other great apes (Neubauer et al., 2020), stressing the importance of species-specific variation.

The specific neurodevelopmental drivers of encephalisation and folding complexity remain undetermined, but increased brain size seems to have a biomechanical role that to equates to more complex folding patterns (Tallinen et al., 2016). However, a solely isometric brain growth is at odds with the unique neural expansion observed in modern humans (Bryant & Preuss, 2018) particularly in increased white matter of the temporal lobe (Roumazeilles et al., 2020). If the modern human temporal lobe is highly specialized (Ardesch et al., 2019) and disproportionately large as suggested by RAS Study and, if the modern human brain is not an allometrically scaled version of the non-human primate brain (Rilling, 2006), then relative temporal lobe size in modern humans has important implications for neurobiology and paleoneurology.

Since the RAS study, several paleoanthropological studies have inferred temporal lobe size and shape changes by analyzing the middle cranial fossa (MCF) as a proxy for the temporal lobe based on the close spatial proximity of the temporal lobe of the brain to the cranial base (Bokde et al., 2005; Borden et al., 2016; Bruner, 2015; Lieberman et al., 2000). The extrapolation of MCF shape changes in fossil *Homo* were used to infer key evolutionary changes to the temporal lobe shape (Bastir et al., 2008; Bastir et al., 2011) and sulcal pattern evolution (Rosas et al., 2014). However, the temporal lobe and MCF estimates were not statistically assessed until recently when Pearson et al. (2020) proposed a predictive equation for temporal lobe volume (TLV) from the MCF in fossil and living anthropoids including fossil hominins.

Despite the clear importance of the RAS findings, no reassessment has been conducted using independent data, more advanced phylogenetic comparative methods, updated imaging methods or statistically robust analyses in the two decades since the RAS study.

Here we provide a re-assessment of the relative and absolute TLV size in extant anthropoids using the published raw data from RAS study to directly compare to a sample compiled de novo by us, with application of more recent approaches to calculating temporal lobe volume (TLV) and hemisphere volume (HV) directly from the MRI (by-voxel) rather than by slice interpolation as per the RAS study. We use more updated phylogenetic comparative methods including Phylogenetic Generalized Least Squares (PGLS) regression and trait mapping rather than phylogenetic independent contrasts used in RAS study, and we employ a bootstrap sampling method to compare the probability of slope differences between the monkey and ape subsamples.

5.3 Materials and Methods

This study compared data from two independent samples of T1-weighted structural in vivo Magnetic Resonance Imaging (MRI) of the brain using the same 11 extant anthropoid species (Table 1).

Table 1. Comparative anthropoid sample for the right temporal lobe volume (TLV) and hemisphere volume (HV) compiled from in vivo Magnetic Resonance Imaging (MRI) scans.

Pearson sample				**Rilling samples**		
Taxon	**N**	**TLV cm^3**	**HV cm^3**	**N**	**TLV cm^3**	**HV cm^3**
Sapajus apella	4	9.3	41.6	4	6.7	33.3
Saimiri sciureus	4	3.4	14.0	4	3.5	11.6
Macaca mulatta	4	11.0	47.0	4	8.9	39.6
Papio anubis	2	21.8	88.5	2	16.5	71.7
Cercocebus atys	4	13.8	57.4	4	11.3	49.4
Hylobates lar	4	15.6	68.7	4	7.7	41.5
Pongo pygmaeus	4	43.8	222.3	4	33.9	203.5
Gorilla gorilla	2	37.4	216.8	2	26.6	198.7
Pan paniscus	4	34.3	178.5	4	27.4	155.6
Pan troglodytes	6	39.5	190.9	6	26.9	168.7
Homo sapiens	40	122.6	675.7	6	108.1	649.5

[a]Nonhuman primate in vivo MRI in National Chimpanzee Brain Resource & human in vivo MRI from Open Access Series of Imaging Studies (OASIS).
[b]Nonhuman primate in vivo MRI in National Chimpanzee Brain Resource and human in vivo MRI (see Rilling & Insel, 1999).

The first sample from the published data in the RAS Study, hereafter referred to as the RAS Sample (n = 44) while the second sample was compiled de novo by us includes the same nonhuman primate individuals as the RAS study but a different and larger sample of humans, referred to hereafter as the Pearson Sample (n = 78).

In the RAS Sample, the right temporal lobe volume (TLV) and right hemisphere volume (HV) of the brain were estimated (in cm3) by interpolating between seven manually segmented MRI coronal slices through the temporal lobe and hemispheres, with TLV calculated based on interpolations between the segmented areas. This approach involved several methodological assumptions that added to the measurements standard errors in RAS Study.

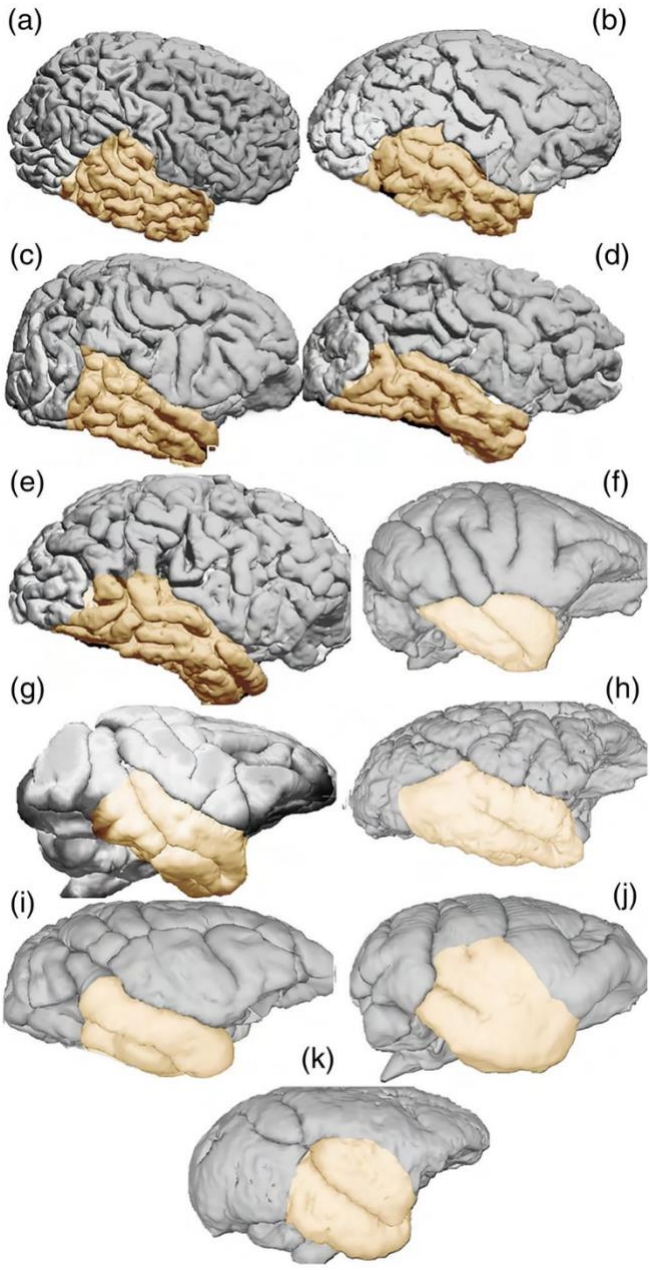

Figure 1. Depiction of 11 taxa of anthropoid right hemisphere three-dimensional (3D) brain generated from in vivo Magnetic Resonance Imaging (MRI) with the temporal lobe in gold. (a) *H. sapiens;* (b) P. *troglodytes*; (c) *P. paniscus;* (d) *G. gorilla;* (e) *P. pygmaeus;* (f) *H. lar;* (g) *C. atys;* (h) *P. anubis;* (i) *M. macaca;* (j) *S. apella;* and (k) *S. saimiri.*

*T*he Pearson Sample used voxel-based volumetric calculation directly from the MRI without interpolation estimation conducted in Brainsuite 17a (Shattuck & Leahy, 2002) following automatic segmentation for *H. sapiens* (Figure 1) and manual segmentation for non-human anthropoids as per Pearson et al. (2020). In the Pearson sample, intraobserver error was

estimated an analysis of variance (ANOVA) as the proportion of the mean-squared differences between replicates relative to the total between-group variation (Bailey & Byrnes, 1990). For the Pearson sample, a single specimen from each extant species (n = 11) was measured on two separate occasions and measurement error calculated as % ME = 100 x MS(within)/(MS (within) + MS (among)). The measurement error for the right TLV was ≤1% (Supplementary Material Table 1). Data collection, image processing and analysis for Pearson sample was conducted by a single operator to reduce inter-observer error.

5.3.1 Statistical analyses

Trait mapping onto the anthropoid phylogeny, Blomberg's K (kappa) and Pagel's λ (lambda) statistic were used to assess the phylogenetic correlations in the traits. K measures the proportion of the tip variance that matches the expectation of Brownian motion relative to the total variance and thus ranges from 0 to 1 (Blomberg et al., 2003). Pagel's λ is a tree scaling factor proportional to how much the internal branch lengths would have to be transformed so that the tip values fit the expectation of a Brownian motion process (Freckleton et al. 2002; Pagel 1993). λ normally ranges from 0 (equivalent to a tree with no internal branch structure and thus no phylogenetic structure in the tip values) to 1 (equivalent to structure that is perfectly consistent with Brownian motion), but higher values up to the proportion between the total tree height and the height minus the length of the shortest branch can occur if the trait has especially strong phylogenetic structure (values higher than this are mathematically impossible because the shortest branch length would become negative).

Phylogenetic Generalized Least-Squares (PGLS) regression (Martins & Hansen, 1997; Revell, 2010) was used to determine the strength of association between TLV and HV in extant anthropoids. To avoid overcorrection for phylogenetic structure, the phylogenetic covariance

matrix used in the PGLS was adjusted by the factor λ that minimized phylogenetic structure in the residuals (Revell, 2010; Symonds & Blomberg, 2014). All analyses were conducted using the species' average for TLV and HV. To linearize scaling relationships (Simpson et al., 2003), the cube-root of TLV and HV were calculated then converted to natural logarithmic units (base e). To accommodate the potential influence of phylogeny, Phylogenetic Generalized Least Squares (PGLS) regression used a consensus anthropoid tree modified from Version 3 of 10 K Trees (Arnold et al., 2010).

We also asked if TLV scales differently to HV in apes and monkeys by testing the difference in their regression slopes and intercepts. We conducted a series of PGLS regressions with a bootstrapping procedure (1000 iterations) to test whether the probability of the differences in slopes or intercepts between monkeys and apes was as large or larger than that observed with a statistical significance ($p \leq 0.05$) between regression slopes and intercepts.

The RAS Study found that human TLV was strongly underpredicted by the regression equation based on all non-human anthropoids. To confirm whether our new data changed this conclusion, we repeated our analyses on their original data to determine whether our methodological changes affected the outcome, then we compared the revised prediction from the RAS to the one derived from our data to determine whether human lobe size was still strongly underpredicted based on scaling in non-human anthropoids (Supplementary Figure 1). All statistical analyses, the PGLS regressions, K and λ calculations and the 'bootstrap' randomizations were performed with Phylogenetics for Mathematica version 6.6 (Polly, 2022) in Mathematica version 13.1 (Wolfram, 2021).

5.4 Results

The RAS study relied on a smaller sample of modern humans (n = 5) and an interpolation method of volumetric calculation, whereas we include an increased sample size of modern humans (n = 40) with volumetric data compiled by-voxel within the neuroanatomy software. The RAS Study tested the differences between the slopes and intercepts of monkeys and apes, examining if modern humans had a larger than expected temporal lobe compared to the monkey and ape regression lines. The RAS Study initially used phylogenetic independent contrasts as a phylogenetic comparative method but did not find any differences between these values and the ordinary variables and then discontinued phylogenetic comparative methods. Here, we examine the RAS Study dataset referred to as the RAS Sample directly compared with our own data, referred to as the Pearson Sample. Unlike RAS Study, we apply phylogenetic comparative methods throughout the analysis.

For the RAS Sample, Phylogenetic Generalized least-squares (PGLS) regression (where optimal $\lambda = 0.795$) produced a statistically significant correlation ($r^2 = 0.98$; $p \leq 0.0001$) between the anthropoid TLV and HV variables (Figure 2, Table 2), while the Pearson Sample produced a similarly strong statistical correlation ($\lambda = 0.925$, $r^2 = 0.97$; $p \leq 0.0001$) between TLV and HV variables (Figure 2, Table 2).

Table 2. Phylogenetic Generalized Least Squares Regression statistics for the correlation between temporal lobe volume (TLV) and hemisphere volume (HV) in the Rilling and Pearson Samples. Abbreviations: a, slope; b, intercept; k, Blomberg's Kappa; p, permutated p-value; PGLS, phylogenetic generalized least-squares regression; r, correlation coefficient; r2, coefficient of determination; SE Regression, Standard error of regression; λ, Pagel's Lambda.

Rilling sample								
Slope	**Intercept**	r^2	**SE**	***p***	**TLV *k***	**TLV λ**	**HV *k***	**HV λ**
0.7949	-0.2751	0.98	0.0127	<0.0001	0.37	0.00	0.40	0.00
Pearson Sample								
Slope	**Intercept**	r^2	**SE**	***p***	**TLV *k***	**TLV λ**	**HV *k***	**HV λ**
0.9101	-0.4011	0.97	0.0285	<0.0001	0.42	0.10	0.42	0.08

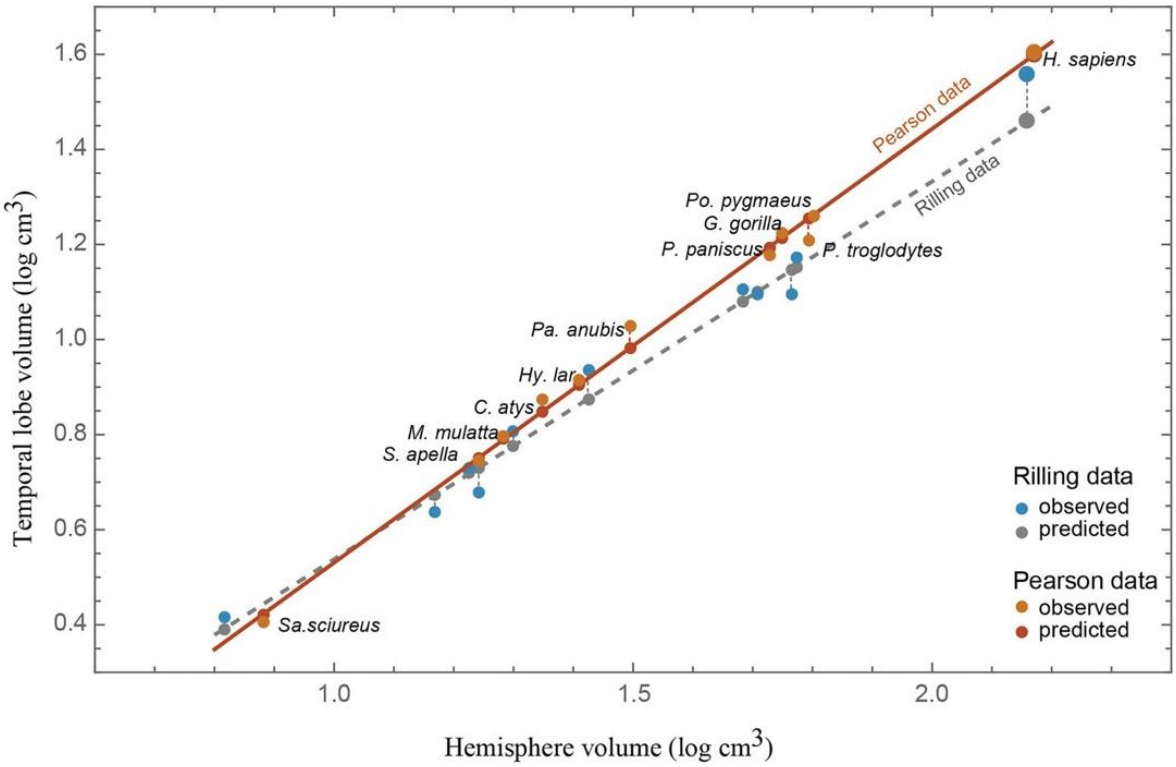

Figure 2-. Comparison of the Phylogenetic Generalized Least- squares regression lines for TLV and HV in anthropoids in the RAS Sample and Pearson Sample.

Trait mapping in the RAS Sample indicated a medium-level influence of phylogeny on HV (k = 0.40, λ = 0.0) or TLV (k = 0.37, λ = 0.0), with similar findings for the Pearson Sample in both HV k = 0.42, λ = 0.1) and TLV (k = 0.42, λ = 0.08) variables respectively, (Figure 3, Table 2). The TLV in humans in both RAS Sample and Pearson Sample is larger than nonhuman primates. To test the difference of the slopes between the monkey and ape

subsamples, PGLS regressions with a bootstrap permutation (1000 iterations) estimated the probability that the difference in slopes was as large or larger than that observed by chance. In the RAS Sample, there was no statistically significant difference in the slopes ($a = p \geq 0.14$). In the Pearson Sample, there was also no statistically significant difference between the slopes ($a = p \geq 0.35$), suggesting that it is suitable to combine monkeys and apes into a single sample because TLV scales the same to HV in both groups (Figure 4, Table 3).

Table 3 -Comparison of slopes and intercepts using Phylogenetic Generalized Least-Squares regression for temporal lobe volume (TLV) and hemisphere volume (HV) in the Rilling and Pearson Samples for monkeys and ape subsamples, bootstrapped with 1000 iterations.

Rilling sample								
Sample	Slope	Intercept	r^2	SE	Difference slope angle	p	Difference intercept angle	p
Monkeys	0.7908	-0.2392	0.97	0.0412	6.1	0.14	0.32	0.04
Apes	0.9801	-0.5635	0.98	0.0402				
Pearson sample								
Sample	Slope	Intercept	r^2	SE	Difference slope angle	p	Difference intercept angle	p
Monkeys	0.9927	-0.4722	0.99	0.0145	1.84	0.37	0.06	0.56
Apes	0.9309	-0.4170	0.99	0.0263				

Abbreviations: a, slope; b, intercept; Difference, absolute angle as the difference between slopes and intercepts; *p*, permutated *p*-value for difference between slopes and intercepts using 1000 iterations; PGLS, phylogenetic generalized least-squares regression; r^2, coefficient of determination; SE, standard error of regression.

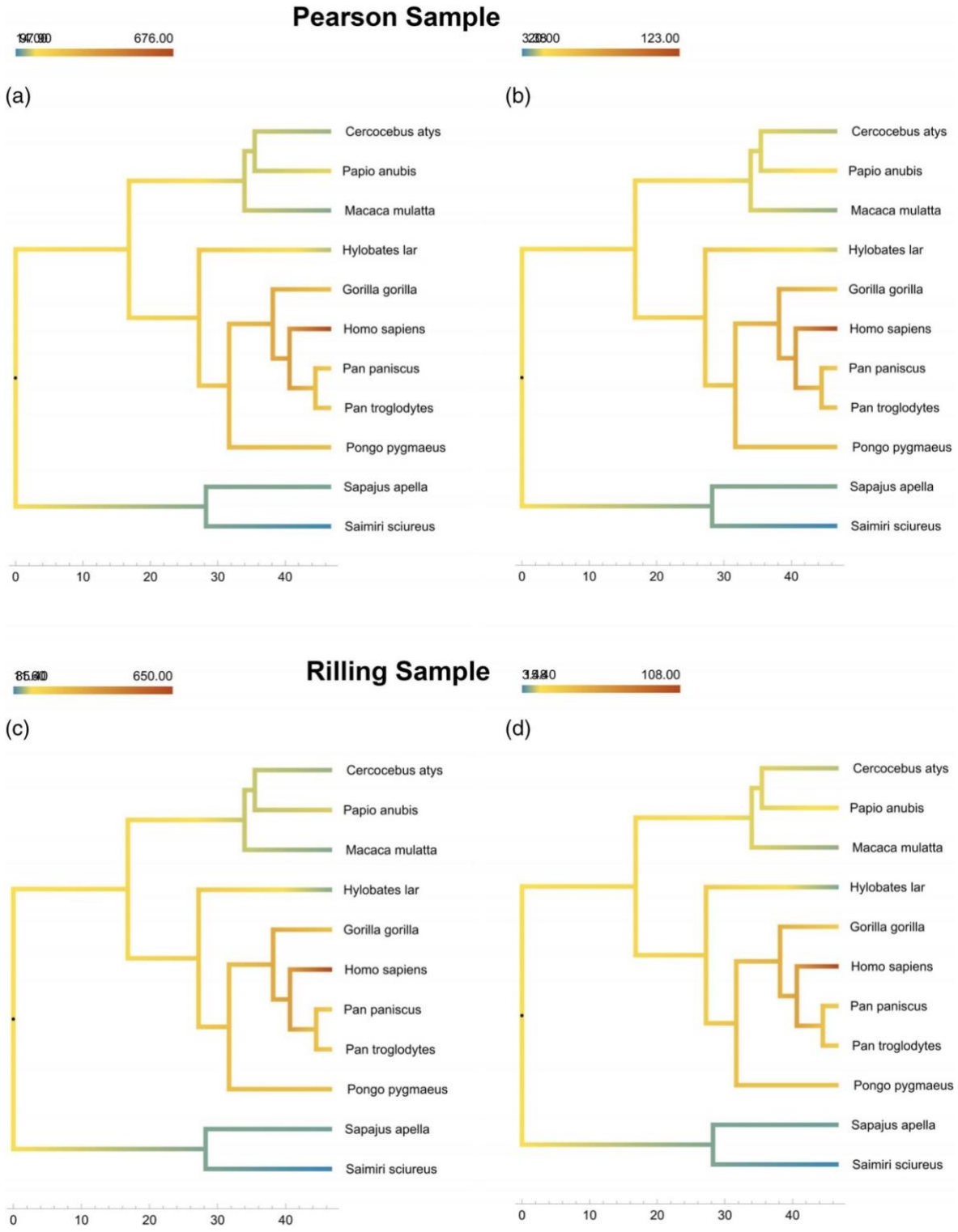

Figure 3- Trait Mapping of TLV and HV of the extant anthropoid phylogeny with Blomberg's K values for the association of the trait with phylogeny (values closer to 1 represent a higher phylogenetic correlation) in Pearson Sample) HV trait mapping and b) TLV trait mapping, and RAS Sample c) HV trait mapping and d) TLV trait mapping. Heat-map coloring refers to absolute size of a variable with red equivalent to larger and blue, smaller values

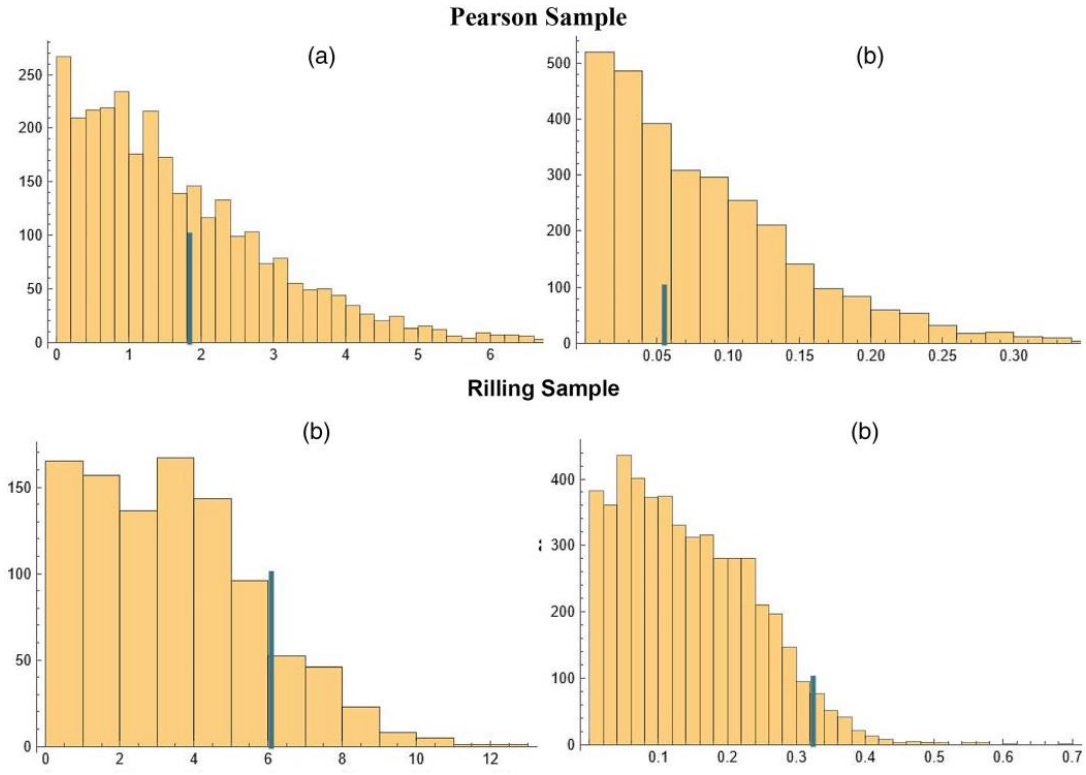

Figure 4. Phylogenetic Generalized Least Squares regression for TLV in monkeys and ape subsamples with bootstrap (1000 iterations) where green line corresponds to the observed value in the Pearson Sample (a) slope and (b) intercept, and RAS Sample (c) slope and (d) intercept.

We also tested the difference of the intercepts between the monkey and ape subsamples using PGLS regressions with bootstrap permutations (1000 iterations) to estimate the probability that the difference in the intercepts was as large or larger than that observed by chance. In the RAS Sample, there was a statistically significant difference in the intercept ($b = p \geq 0.04$), suggesting the conclusions from the RAS study are consistent based on the RAS Sample. In the Pearson Sample, there was no statistically significant difference in the intercept ($b = p > 0.56$). This suggests it is suitable to combine non-human anthropoids into a single sample as both slope and intercept in the Pearson Sample show human TLV is not proportionately larger than other anthropoids compared to the RAS Sample (Figure 1, Table 3). This is further substantiated by the PGLS regressions in both samples which included humans to estimate the regression line.

5.5 Discussion

We compared published data from the RAS study with a sample com- piled de novo by us. In general, our findings are in agreement with those proposed in the RAS study that there is no difference in slope between the monkey and ape regressions. However, our findings showed that modern humans had a temporal lobe volume which was predicted for brain size and the general anthropoid trend. All our results have taken phylogeny into account, whereas RAS discarded phylogenetic methods after they employed phylogenetic independent contrasts and found that the slopes of its regression line was similar to the ordinary non- phylogenetic regression. Considering RAS later remove monkeys from their analysis because the intercepts were different, but the slopes the same, we consider it was premature to discard phylogenetic comparative methods. However, not using a phylogenetic regression allowed RAS to carry out analyses using individuals rather than species-means, which in turn gave them enough data points to estimate a non-human ape regression, while using species-means allows only very few data points. Therefore, we have used a phylogenetic correction in all of our calculations, plus included it in our re-analysis of RAS Study data so that both results are on equal footing. Our regressions on non-human anthropoids show that RAS would still have concluded modern humans had a disproportionately large temporal lobe volume even if they had analyzed their data following our process. However, the results using our new sample do not support their finding that modern humans had a temporal lobe volume that was larger than expected for the general anthropoid trend.

5.1. Updated imaging methods

The RAS study calculated TLV from slice-slice interpolation factored to the number of slices as a proxy for lobe length, which RAS Study admitted could cause some segments of the anterior and posterior of the temporal lobe not to be measured in some individuals. We addressed this issue, though more updated imaging methods available where temporal lobe and hemisphere volumes were calculated within- software program (by-voxel). In using this approach, we avoided the estimation through interpolation techniques in the RAS study and allowed inclusion of a much larger sample size where MRI processing could be calculated faster for *H. sapiens*. It is worthwhile noting, the use of such imaging software capabilities to calculate by-voxel hemisphere and temporal lobe volume was also used by Semendeferi and Damasio (2000) preceding the RAS Study, where those authors noted the large temporal lobe volume in modern humans was not statistically significant compared to other anthropoids.

5.2. Increased sample size

In comparison with the RAS Study, the larger sample compiled de novo by us included the same species, and in many cases, the same individuals as the original RAS study. In their assessment of modern human TLV, the RAS Study concluded *H. sapiens* TLV was disproportionately larger than other anthropoids as determined through calculation of separate regression slopes for apes and monkeys. In assessing if modern humans had larger than expected temporal lobe volumes, RAS Study discarded monkeys from their analysis after finding a difference in the intercepts. We also examined the differences in slopes and intercepts for both monkey and ape subsamples and did not find a statistically significant difference in either slope or intercept. We conclude that temporal lobe volume was not disproportionately

larger in modern humans compared to other anthropoids and follows the general anthropoid trend. It is worth noting our study also includes a much larger *H. sapiens* sample (n = 40) compared to the RAS study (n = 5) allowing better examination of modern human variation, and whether there is a true difference in the relative and absolute TLV compared to other anthropoids.

5.3. Advanced statistical analysis

For comparison with the RAS study, we tested the difference in slopes between the species-averages for monkeys and apes, respectively. We note that despite the smaller sample size when using only five taxa per regression model, we employed PGLS regressions incorporating the monkey and ape phylogenies separately and a bootstrap procedure (1000 permutations) to determine if the probability of the difference in slopes was as large or larger than observed by chance. We did not find statistically significant results, suggesting that the difference in slopes between apes and monkeys is not substantial. Our incorporation of more advanced and robust statistical analyses including the bootstrap permutations attempts to mediate further issues and effects of uncertainty on results.

5.4 Human TLV is not proportionally larger than HV in our data

It is worth noting that our new methods and data are different to RAS Study which changes the result. The important question is how does this occur? We have shown that even using the new phylogenetic comparative methods we employed, the same conclusion would still be reached by RAS Study based on their data. For example, we have shown in our Figure 4, when using their data and our methods, humans have a much larger TLV than predicted by the gray regression line. Whereas our regression line, which is solely derived from non-human

anthropoids, predicts human TLV almost precisely. This indicates that human TLV scales exactly like any other non-human anthropoid.

Firstly, RAS Study did not misrepresent human TLV or HV. As we have shown, the values for both variables are almost identical to those represented here, however, it is worth noting we used a considerably larger human sample size which allowed more variation to be captured. Nevertheless, the values are still similar which does indicate that the TLV and HV values for humans were correct in RAS Study. However, discrepancies arise around the non-human primate species which make the difference between the findings in RAS Study and ours presented here. In nearly every non-human primate species, the estimate of HV was too small in Rilling sample and more importantly, in the great apes, the estimate of TLV was also too small.

The final substantial difference between the RAS Study and our de novo sample was the MRI processing procedures. RAS Study used an area and slice-slice interpolation method which may have missed some sections of the temporal lobe volume. Our approach used 3D voxel calculation with a following checking process of manual adjustment as required using neuroanatomical software. Semendeferi and Damasio (2000) also used neuroanatomical software to define the main lobe divisions of the brain in great apes with their findings suggested similarly to ours: the estimates by RAS Study were too small. In comparison, this indicated our data is likely more accurate because of the 3D volumetric processing for TLV and HV.

In terms of the findings for the regressions, we used by-voxel and 3D volumetric processing which has made our data points more accurate where the slope of the primate regression line brought the apes and monkeys into line with each other on scaling. Thus, the

slopes in apes and monkeys were not statistically significantly different as they were reported by RAS Study. In turn, we also have much smaller scatter around the regression line which is associated with lower prediction error than that found in the RAS Study data.

In general, our data are more comprehensive than that RAS Study, and the changes this makes to the regression slope erases the apparent differences in modern human temporal lobe volume, so that humans now fall exactly on the non-human anthropoid regression line in our study.

5.6 Conclusion

Replication studies are important to confirm robust anatomical and evolutionary foundations. In comparison to RAS Study, our study incorporated different neuroanatomical measurements, technical imaging software, updated phylogenetic comparative methods, larger sample sizes and more robust statistical analyses. We did not find that modern humans possessed a temporal lobe that is larger than expected for the general anthropoid trend which has important evolutionary implications for human and non-human primate neurobiology and paleoneurology.

5.7. Author contributions

Alannah Pearson: Conceptualization (equal); formal analysis (supporting); investigation (lead); methodology (supporting); project administration (lead); resources (lead); validation (supporting); writing – original draft (lead); writing – review and editing (lead). Emiliano Bruner: Conceptualization (equal); supervision (supporting); writing – original draft (supporting). P. David Polly: Conceptualization (equal); formal analysis (lead); investigation

(supporting); methodology (lead); supervision (supporting); validation (supporting); writing – original draft (supporting); writing – review and editing (supporting).

5.8. Acknowledgments

Funding from the Australian Government Research Training Program Scholarship (2016-Present) and the Spanish Government (#PGC2018-093925-B-C31). We appreciate the following: The Smithsonian Division of Mammals (Dr. Kristofer Helgen) and Human Origins Program (Dr. Matt Tocheri) for the scans of USNM specimens used in this research (http://humanorigins.si.edu/evidence/3d-collection/primate).These scans were acquired through the generous support of the Smithsonian 2.0 Fund and the Smithsonian's Collections Care and Preservation Fund; Museum national d'histoire naturelle (MNHN); Digital Morphology Museum (DMM) the Primate Research Institute, Kyoto University (KUPRI); Anatomisches Institut, Universität Leipzig (Germany); University of Pennsylvania Museum of Archeology and Anthropology and the Open Research Scan Archive (ORSA) care of J. Monge and P. T. Schoenemann (NSF proposal # 0447271); The National Chimpanzee Brain Resource care of J. Rilling; OASIS: Cross- Sectional: Principal Investigators: D. Marcus, R, Buckner, J, Csernansky J. Morris (#P50 AG05681, #P01 AG03991, #P01 AG026276, #R01 AG021910, #P20 MH071616, #U24 RR021382). Human in-vivo MRI sourced from open access dataset (see Marcus et al. 2007) Non-human primate in vivo MRI sourced from open access dataset (see Rilling & Insel, 1999). All appropriate ethical permissions were approved at the time of publication. Three anonymous reviewers and the editor provided helpful feedback that improved this manuscript.

5.9. Conflict of interest statement

All authors declare they have no conflict of interest.

5.10. Data availability statement

The data that support the findings of this study are available from https://pollylab.indiana.edu/index.html.

5.11. References

Ackermann, R. R., Rogers, J., & Cheverud, J. M. (2006). Identifying the mor- phological signatures of hybridization in primate and human evolution. *Journal of Human Evolution*, *51*(6), 632–645. https://doi.org/10.1016/ j.jhevol.2006.07.009Adams, D. C., Otárola-Castillo, E., & Paradis, E. (2013). Geomorph: An r package for the collection and analysis of geometric morphometric shape data. *Methods in Ecology and Evolution*, *4*(4), 393–399. https:// doi.org/10.1111/2041-210x.12035

Aldridge, K. (2011). Patterns of differences in brain morphology in humans as compared to extant apes. *Journal of Human Evolution*, *60*(1), 94–105. https://doi.org/10.1016/j.jhevol.2010.09.007

Arnold, C., Matthews, L. J., & Nunn, C. L. (2010). The 10kTrees website: A new online resource for primate phylogeny. *Evolutionary Anthropology*, *19*, 114–118.

Bailey, R. C., & Byrnes, J. (1990). A new, old method for assessing mea- surement error in both univariate and multivariate morphometric stud- ies. *Systematic Zoology*, *39*(2), 124–130.

Bastir, M. (2018). Back to basics: Morphological analysis in Paleoanthro- pology. In J. Schwartz (Ed.), *Biological Theory* (pp. 205–227). Boston: MIT-Press.

Bastir, M., & Rosas, A. (2006). Correlated variation between the lateral basicranium and the face: A geometric morphometric study in differ- ent human groups. *Archives of Oral Biology*, *51*(9), 814–824. https:// doi.org/10.1016/j.archoralbio.2006.03.009

Bastir, M., & Rosas, A. (2016). Cranial base topology and basic trends in the facial evolution of *Homo*. *Journal of Human Evolution*, *91*, 26–35. https://doi.org/10.1016/j.jhevol.2015.11.001

Bastir, M., Rosas, A., Gunz, P., Pena-Melian, A., Manzi, G., Harvati, K., … Hublin, J. J. (2011). Evolution of the base of the brain in highly encephalized human species. *Nature Communications*, *2*, 588. https:// doi.org/10.1038/ncomms1593

Bastir, M., Rosas, A., & Kuroe, K. (2004). Petrosal orientation and mandibu- lar ramus breadth: Evidence for an integrated petroso-mandibular developmental unit. *American Journal of Physical Anthropology*, *123*(4), 340–350. https://doi.org/10.1002/ajpa.10313

Bastir, M., Rosas, A., Lieberman, D. E., & O'Higgins, P. (2008). Middle cra- nial fossa anatomy and the origin of modern humans. *The Anatomical Record*, *291*(2), 130–140. https://doi.org/10.1002/ar.20636

Bastir, M., Rosas, A., Stringer, C., Cuetara, J. M., Kruszynski, R., Weber, G. W., … Ravosa, M. J. (2010). Effects of brain and facial size on basicranial form in human and primate evolution. *Journal of Human Evolution*, *58*(5), 424–431. https://doi.org/10.1016/j.jhevol.2010.03.001

Blomberg, S. P., Garland, T. J., & Ives, A. R. (2003). Testing for phylogenetic signal in comparative data: Behavioral traits are more labile. *Evolution*, *57*(4), 717–745.

Borden, N. M., Forseen, S. E., & Stefan, C. (2016). *Imaging anatomy of the human brain a comprehensive atlas including adjacent structures*. New York: Demos Medical Publishing.

Bruner, E. (2017). The fossil evidence of human brain evolution. In J. H. Kaas (Ed.), *Evolution of nervous systems volume 4: The evolution of the human brain: Apes and other ancestors* (Vol. 4, pp. 63–92). Amster- dam, Boston: Elsevier Inc.

Bruner, E., Grimaud-Hervé, D., Wu, X., de la Cuétara, J. M., & Holloway, R. (2015). A paleoneurological survey of *Homo erectus* endocranial met- rics. *Quaternary International*, *368*, 80–87. https://doi.org/10.1016/j. quaint.2014.10.007

Bryant, K. L., & Preuss, T. M. (2018). A comparative perspective on the human temporal lobe. In E. Bruner, N. Ogihara, & H. C. Tanabe (Eds.), *Digital Endocasts: From skulls to brains* (pp. 239–258). Tokyo: Springer Japan KK.

Cardini, A. (2017). Left, right or both? Estimating and improving accuracy of one-side-only geometric morphometric analyses of cranial variation. *Journal of Zoological Systematics and Evolutionary Research*, *55*(1), 1–10. https://doi.org/10.1111/jzs.12144

Damasio, H. (2005). *Human brain anatomy in computerized images* (2nd ed.). New York: Oxford University Press.

Falk, D. (1978). Brain evolution in Old World monkeys. *American Journal of Physical Anthropology*, *48*(3), 315–319. https://doi.org/10.1002/ajpa.1330480307

Falk, D. (1980). Hominid brain evolution: The approach from paleoneurology. *American Journal of Physical Anthropology*, *23*, 93–107.

Falk, D. (2014). Interpreting sulci on hominin endocasts: Old hypotheses and new findings. *Frontiers in Human Neuroscience*, *8*, 134. https://doi. org/10.3389/fnhum.2014.00134

Falk, D., Zollikofer, C. P. E., Ponce de Leon, M., Semendeferi, K., Alatorre Warren, J. L., & Hopkins, W. D. (2018). Identification of in vivo sulci on the external surface of eight adult chimpanzee brains: Implications for interpreting early hominin Endocasts. *Brain, Behavior and Evolution*, *91* (1), 45–58. https://doi.org/10.1159/000487248

Fleagle, J. G. (2013). *Primate adaptation and evolution* (3rd ed.). San Diego, Waltham, London: Academic Press.

Frost, S. R., Marcus, L. F., Bookstein, F. L., Reddy, D. P., & Delson, E. (2003). Cranial allometry, phylogeography, and systematics of large- bodied papionins (primates: Cercopithecinae) inferred from geometric morphometric analysis of landmark data. *The Anatomical Record Part A, 275*(2), 1048–1072. https://doi.org/10.1002/ar.a.10112

Gilbert, C. C. (2011). Phylogenetic analysis of the African papionin bas- icranium using 3-D geometric morphometrics: The need for improved methods to account for allometric effects. *American Journal of Physical Anthropology*, *144*(1), 60–71. https://doi.org/10.1002/ajpa.21370

Gilbert, C. C., Frost, S. R., Pugh, K. D., Anderson, M., & Delson, E. (2018). Evolution of the modern baboon (*Papio hamadryas*): A reassessment of the African Plio-Pleistocene record. *Journal of Human Evolution*, *122*, 38–69. https://doi.org/10.1016/j.jhevol.2018.04.012

Gonzales, L. A., Benefit, B. R., McCrossin, M. L., & Spoor, F. (2015). Cere- bral complexity preceded enlarged brain size and reduced olfactory bulbs in Old World monkeys. *Nature Communications*, *6*, 7580. https:// doi.org/10.1038/ncomms8580

Groves, C. P. (2001). *Primate taxonomy*. Washington DC: Smithsonian Institution Press.

Hammer, Ø., Harper, D. A. T., & Ryan, P. D. (2001). Past: Paleontological statistics software package for education and data analysis. *Palaeontologia Electronica*, *4*(1), 1–9.

Holloway, R. L. (2018). On the making of endocasts: The new and the old in paleoneurology. In E. O. Bruner, N. Ogihara, & H. C. Tanabe (Eds.), *Digital Endocasts* (pp. 1–8). Tokyo: Springer Japan KK.

Kingdon, J., Butynski, T. M., & De Jong, Y. (2008). *Papio anubis*. *The IUCN Red List of Threatened Species*, *2008*, e.T40647A10348950. https://doi.org/10.2305/IUCN.UK.2008.RLTS.T40647A10348950.en

Kingdon, J., Butynski, T. M., & De Jong, Y. (2016). *Papio cynocephalus*. *The IUCN Red List of Threatened Species*, *2016*, e. T15933A129038584. https://doi.org/10.2305/IUCN.UK.20161.RLTS. T92250442A92250811.en

Kobayashi, Y., Matsui, T., & Ogihara, N. (2018). Inferring cortical subdivi- sions based on skull morphology. In E. Bruner, N. Ogihara, & H. C. Tanabe (Eds.), *Digital Endocasts* (pp. 33–46). Tokyo: Springer KK.

Kochiyama, T., Ogihara, N., Tanabe, H. C., Kondo, O., Amano, H., Hasegawa, K., … Akazawa, T. (2018). Reconstructing the Neanderthal brain using computational anatomy. *Scientific Reports*, *8*(1), 6296. https://doi.org/10.1038/s41598-018-24331-0

Kubo, D., Tanabe, H. C., Kondo, O., Ogihara, N., Yogi, A., Murayama, S., & Ishida, H. (2014). Cerebellar size estimation from endocranial measure- ments: an evaluation based on MRI data. In T. Akazawa, N. Ogihara, H. C. Tanabe, & H. Terashima (Eds.), *Dynamics of learning in Neanderthals and modern humans* (Vol. 2, pp. 209–215). Tokyo: Springer.

Lieberman, D. E. (2011). The evolution of the human head. Cambridge, Massachusetts. London, England: The Belknap Press of Harvard Uni- versity Press.

Lieberman, D. E., Pearson, O. M., & Mowbray, K. M. (2000). Basicranial influence on overall cranial shape. *Journal of Human Evolution*, *38*(2), 291–315. https://doi.org/10.1006/jhev.1999.0335

Lieberman, D. E., Ross, C. F., & Ravosa, M. J. (2000). The primate cranial base: Ontogeny, function, and integration. *American Journal of Physical Anthropology*, *31*, 117–169.

Mai, J. K., Paxinos, G., & Voss, T. (2008). *Atlas of the human brain* (3rd ed.).

New York, London, Burlington, San Diego: Academic Press.

Marcus, D. S., Wang, T. H., Parker, J., Csernansky, J. G., Morris, J. C., & Buckner, R. L. (2007). Open access series of imaging studies (OASIS): Cross-sectional MRI data in young, middle aged, nondemented, and demented older adults. *Journal of Cognitive Neuroscience*, *19*(9), 1498–1507. https://doi.org/10.1162/jocn.2007.19.9.1498

Martins, E. P., & Hansen, T. F. (1997). Phylogenies and the comparative method: A general approach to incorporating phylogenetic information into the analysis of interspecific data. *American Naturalist*, *149*, 646–667.

Materialise. (2018). *Mimics 17 (version 17)*. Leuven, Belgium: Materialise Corporation.

McCarthy, R. C. (2001). Anthropoid cranial base architecture and scaling relationships. *Journal of Human Evolution*, *40*(1), 41–66. https://doi. org/10.1006/jhev.2000.0446

McCarthy, R. C. (2004). *Constraints on Primate Craniofacial Growth and Archi- tecture*. (Doctor of Philosophy). The George Washington University,

Moss, M. L., & Young, R. W. (1960). A functional approach to craniology.*American Journal of Physical Anthropology*, *18*(4), 281–292.

Nolte, J. (2009). *The human brain: An introduction to its functional anatomy*(6th ed.). Philadelphia: Mosby Elsevier.

Pearson, A., Groves, C., & Cardini, A. (2015). The 'temporal effect' in homi- nids: Reinvestigating the nature of support for a chimp-human clade in bone morphology. *Journal of Human Evolution, 88,* 146–159. https:// doi.org/10.1016/j.jhevol.2015.06.012

Polly, P. D. (2019). Phylogenetics for Mathematica (Version 6.5). Bloom- ington, Indiana: Department of Earth and Atmospheric Sciences, Indiana University. Retrieved from http://pollylab.indiana.edu/ software.html

Richtsmeier, J. T., & Flaherty, K. (2013). Hand in glove: Brain and skull in development and dysmorphogenesis. *Acta Neuropathologica*, *125*(4), 469–489. https://doi.org/10.1007/s00401-013-1104-y

Rilling, J. K. (2006). Human and nonhuman primate brains: Are they allo- metrically scaled versions of the same design? *Evolutionary Anthropol-ogy, 15,* 65–77. https://doi.org/10.1002/evan.00000

Rilling, J. K., & Insel, T. R. (1999). The primate neocortex in comparative perspective using magnetic resonance imaging. *Journal of Human Evo lution*, *37*, 191–223.

Rilling, J. K., & Seligman, R. A. (2002). A quantitative morphometric comparative analysis of the primate temporal lobe. *Journal of Human Evolu tion, 42*(5), 505–533. https://doi.org/10.1006/jhev.2001.0537

Rogers, J., Raveendran, M., Harris, R. A., Mailund, T., Leppälä, K., Athanasiadis, G., … Consortium, B. G. A. (2019). The comparative genomics and complex population history of *Papio* baboons. *Science Advances*, *5*, eaau6947.

Rosas, A., Pena-Melian, A., Garcia-Tabernero, A., Bastir, M., & De La Rasilla, M. (2014). Temporal lobe sulcal pattern and the bony impressions in the middle cranial fossa: The

case of the el Sidron (Spain) neandertal sample. *The Anatomical Record*, *297*(12), 2331–2341. https://doi.org/10.1002/ar.22957

Semendeferi, K., & Damasio, H. (2000). The brain and its main anatomical subdivisions in living hominoids using magnetic resonance imaging. *Journal of Human Evolution*, *38*(2), 317–332. https://doi.org/10.1006/ jhev.1999.0381

Shattuck, D. W., & Leahy, R. M. (2002). BrainSuite: An automated cortical surface identification tool. *Medical Image Analysis*, *6*(2), 129–142.

Sherwood, C. C., Bauernfeind, A. L. V., Raghanti, M. A., & Hof, P. R. (2017). Evolutionary specializations of human brain microstructure. In J. H. Kaas (Ed.), *Evolution of nervous systems volume 4: The evolution of the human brain: Apes and other ancestors* (2nd, 4, pp. 121–139). Amsterdam, Boston: Elsevier Inc.

Simpson, G. G., Roe, A., & Lewontin, R. C. (2003). *Quantitative zoology* (Revised ed.). New York: Dover Publications.

Smith, R. J. (1984). Allometric scaling in comparative biology: Problems of concept and method. *American Journal of Physiology*, *246*(2 Pt 2), R152–R160. https://doi.org/10.1152/ajpregu.1984.246.2.R152

Stephan, H., Frahm, H., & Baron, G. (1981). New and revised data on volumes of brain structures in insectivores and primates. *Folia Primatologica*, *35*, 1–29.

Stratovan. (2018). *Stratovan Checkpoint (version December 20, 2018)*. UC, Davis, California: Stratovan Corporation.

Van Minh, N., & Hamada, Y. (2017). Age-related changes of sulcal imprints on the endocranium in the Japanese macaque (*Macaca fuscata*). *Ameri- can Journal of Physical Anthropology*, *163*(2), 285–294. https://doi.org/ 10.1002/ajpa.23205

White, T. D., Black, M. T., & Folkens, P. A. (2011). *Human Osteology* (3rd ed.). Burlington, San Diego, Oxford: Academic Press.

Zinner, D., Wertheimer, J., Liedigk, R., Groeneveld, L. F., & Roos, C. (2013). Baboon phylogeny as inferred from complete mitochondrial genomes. *American Journal of Physical Anthropology, 150*, 133–140. https://doi. org/10.1002/ajpa.22185.

Pearson, A., & Polly, P.D. (2023b) Temporal lobe evolution in extant and extinct Cercopithecoidea, *Journal of Mammalian Evolution*, 30(3), 683-694.

In this chapter, I address the fourth aim of this thesis by determining the relative difference of temporal lobe to brain size in extinct and extant old-world monkeys (Cercopithecoidea) and if potential cerebral reorganisation was associated with socio-behavioural shifts and palaeoenvironmental changes over time.

Chapter 6: Temporal lobe evolution in extant and extinct Cercopithecoidea

6.1. Abstract

Changes to the environmental landscapes from the Eocene to Holocene have influenced the evolution of Cercopithecoidea from arboreal origins in wet, forested regions in the Early Oligocene Fayum to semi-terrestrial lifestyles in drier Neogene landscapes and social systems of larger group living. These eco-behavioural transitions likely accompanied changes in behaviour, brain function, and associated skull morphology. The temporal lobe of the brain, an association cortex, is in close proximity to the middle cranial fossa (MCF) allowing prediction of temporal lobe volume (TLV) and investigation of cerebral reorganisation. We used micro-computed tomography (μCT) cranial scans (n = 135) generated into 3D virtual crania with seven MCF metrics predicting TLV from a multiple regression of 11 extant anthropoid taxa. We studied eight extinct taxa *Proteopithecus sylviae* and *Cateopithecus browni* from the Late Eocene, Early Oligocene *Apidium phiomense*, *Parapithecus grangeri* and *Aegyptopithecus zeuxis*, Middle Miocene *Victoriapithecus macinnesi*, Pliocene *Dinopithecus ingens*,

Pleistocene *Papio angusticeps*, and extant cercopithecines *Cercocebus atys*, *Macaca mulatta* and *Papio anubis*. PGLS regressions examined relative TLV to brain size between extinct and extant taxa. We tested differences in slopes and intercepts between extinct and extant cercopithecoids with statistically significant differences in slopes but not the intercepts with stem-anthropoids having relative smaller TLV for brain size compared to extant cercopithecoids. Potential drivers for temporal lobe evolution include palaeoenvironmental shifts from Eocene tropical rainforests to Plio-Pleistocene savannas. Socio-behavioural implications include change from arboreal to semi-terrestrial lifestyles, higher visual acuity, larger group sizes and greater cognitive complexity.

6.2. Introduction

The diversification of Cercopithecoidea occurred in the context of the climate-driven environmental changes between the Eocene and Holocene. The group's ancestors lived in the wet, forested regions of the Late Eocene to Early Oligocene Fayum, perhaps a similar environment to modern-day Uganda, and postcranial evidence suggests most of them were arboreal quadrupeds inhabiting a swampy, densely vegetated paleolandscape with high rainfall (Simons 1995; Kay et al. 1997). By the Neogene, the paleoenvironment of the Fayum and Northern Africa in general had become drier and more open with forests giving way to sparse open woodlands inhabited by cercopithecoids like *Victoriapithecus* with semi-terrestrial locomotion (Benefit1999). The African paleoenvironment continued a trend towards more open woodland and grassy savanna (DuPont and Leroy 1995), where cercopithecoids like *Dinopithecus* were habitual terrestrial quadrupeds that likely lived in large baboon-like troops during the Plio-Pleistocene and Holocene (Elton 2012).

Adapting to more open landscapes and living in larger troops likely required behavioural adaptations associated with increased inter and intra-group competition and greater social complexity, which has been argued to be associated with larger absolute brain size (Benefit 1999). The relatively large brain in primates functions in reproductive and life history strategies associated with learning and cognitive and memory skills in species with prolonged growth and low reproductive turnover but complex social organisation (Shea 2006; Dunbar2009). For stem-anthropoids inhabiting dense tropical rainforests such as those that existed during the Eocene-Oligocene transition, higher visual acuity and the ability to distinguish between closely spaced visual stimuli, coupled with colour vision that would have allowed the discrimination of red, orange ,and yellow fruits and between those which were ripe and unripe, would likely have been important brain functions (Dominy 2004; Kirk and Kay 2004). This shift away from forest habitats to larger, open-habitat group structures would have changed foraging and anti-predator strategies perhaps in ways that are found in among extant terrestrial primates that form troops the more open landscapes of Africa today (Cheny and Wrangman 1987). Extant cercopithecoids are known to rely extensively on visual communication such as determining colour changes related to sexual communication (Changizi et al. 2006; Moriera et al. 2023) and changes in facial expressions (Peterson et al. 2018), which were all at the expense of auditory and olfactory communication (Strier et al. 2017). The Social Brain Hypothesis posits that the association between increased brain size and larger troop is a causal one, driven by more the complex social behaviours that some cercopithecoids would have started adopting in the Miocene (Barton 2006; Kudo and Dunbar 2009).

Many functions that can logically be linked to these behavioural transitions—memory, object recognition, perception of places and paths—are coordinated through the temporal lobe

of the brain (e.g., Murray et al. 2007; Schuurman and Bruner 2023). The temporal lobe is one of the least studied regions of the primate brain despite its importance in early anthropoid and human evolution, although there are now a few studies in non-human primate outgroups that are relevant to assessing evolution of the temporal lobe in hominin evolution (Rilling 2014; Braunsdorf 2021). Compared to other mammals, primates have greater visual acuity than most other mammals, and anthropoids have greater visual acuity relative to other primates (Kirk and Kay 2004; Veilleux and Kirk 2014). The temporal lobe in anthropoid primates also has an important role in processing visual, auditory and memory-related tasks (Murray et al. 2007). Visual acuity is related to specialised organisation of ganglion cells in the retina and information processed via two pathways, ventral and dorsal, in the middle temporal and inferior temporal cortexes (Pruess 2006). The dorsal pathway neurons are sensitive to object motion, while the ventral pathway neurons are sensitive to object form (Pruess 2006).

Despite the logic that both brain size and proportions of regions like the temporal lobe are likely to have been affected by the environmental transitions of the Cenozoic, examination of absolute or relative brain size in extinct and extant cercopithecoids remains has been pursued by only a few studies (Barton 2006; Grabowski, 2016; Sansalone et. al. 2020). The quantification of cerebral proportions relative to brain size is indicative of cerebral reorganisation, and extinct taxa have the potential to pinpoint when and where in evolution such reorganisation occurred and in what environmental context, allowing a understanding of when behavioural changes may have occurred alongside morphological adaptations. Relative changes to olfactory bulb size and frontal lobe size have been noted alongside increases in absolute brain size during cercopithecoid evolution (Simons 1995; Gonzleas 2015; Harrington 2016). Notably, the identification of cerebral reorganisation in extinct catarrhines have

functional, evolutionary, and phylogenetic significance for the important neuroanatomical changes in the Cercopithecoidea.

Whether the increase in brain size in crown cercopithecoids was associated with the Cenozoic environmental transition and whether it was accompanied by a relative increase or decrease in the temporal lobe remains largely unknown. However, the proposition that the opening of Neogene environmental and concomitant changes in cercopithecoid behaviours was accompanied by temporal lobe reorganization can be tested using both extinct and Recent taxa using the bony middle cranial fossa as a proxy. The Functional Craniology Hypothesis of Moss and Young (1960) suggests that a reciprocal association exists between brain and skull form, where the temporal lobe is in close spatial proximity to the middle cranial fossa (MCF) of the basicranium (Bastir, 2008). This association has allowed MCF metrics to predict temporal lobe volume (TLV) in extant and extinct anthropoids with reasonable accuracy (Rilling and Seligman 2002; Pearson et al. 2020).

The aim of this paper is to determine whether there was an increase in temporal lobe size relative to brain size between extinct and extant cercopithecoids and whether the potential temporal lobe size changes coincided with the paleoenvironmental transitions and whether there is any association with the emergence of anthropoid behavioural ecology. To examine these aims, we studied eight key extinct species from the Cercopithecoidea: *Proteopithecus sylviae* and *Cateopithecus browni* from the Late Eocene of the Fayum in Egypt; *Parapithecus grangeri*, *Apidium phiomense*, and *Aegyptopithecus zeuxis* from the Early Oligocene of the Fayum; East African Middle Miocene *Victoriapithecus macinnesi*; South African Pliocene *Dinopithecus ingens*; and Pleistocene *Papio angusticeps*. We also studied three extant cercopithecines: *Cercocebus atys, Macaca mulatta,* and *Papio anubis*. Evolutionary changes

to relative temporal lobe size among stem anthropoids and extant cercopithecines may pinpoint the timing of cerebral reorganisation in the Cercopithecoidea and the role of phylogenetic and functional drivers in temporal lobe evolution.

6.3. Materials and methods

Two different imaging modalities were used in the initial stages of this study, micro-computed tomography (µCT) scans of ex vivo extinct and extant anthropoid crania (n = 142) and in vivo T1-structural magnetic resonance imaging (MRI) of the human and non-human primate brain (n = 78). The total sample (n = 222) represents 17 anthropoid species including eight extinct catarrhine species (Table 1). Nonhuman primate MRI scans were accessed from the National Chimpanzee Brain Resource with necessary animal ethics protocol approvals (Rilling and Insel 1999) and human MRI scans accessed from the Open Access Series of Imaging Studies (OASIS) with appropriate human ethics protocol approvals (Marcus et al. 2007).

Table 1. The total anthropoid sample (N=222) for the 11 extant and eight extinct anthropoid species (in bold). Digital imaging modality (computed tomography/CT, micro-computed tomography/ µCT, magnetic resonance imaging/MRI) sample sizes with sex distribution in parentheses. The ID column lists the species for extant taxa and the specimen number for extinct taxa (with full identification details in the manuscript). Superscripts: a Human in vivo MRI from the Open Access Series of Imaging Studies (OASIS); b Non-human primate in vivo MRI from the National Chimpanzee Brain Resource.

Taxon	**ID**	**CT/µCT Sample**	**MRI Sample**	**N**
Homo sapiens	*H. sapiens*	44 (25 M/ 19 F)	40a	84
Pan troglodytes	*P. troglodytes*	10 (5 M/5 F)	6b	16
Pan paniscus	*P. paniscus*	14 (6 M/8 F)	4b	18
Gorilla gorilla	*G. gorilla*	10 (6 M/4 F)	2b	10
Pongo pygmaeus	*Po. pygmaeus*	13 (6 M/7 F)	4b	17
Hylobates lar	*H. lar*	14 (7 M/7 F)	4b	18
Papio anubis	*Pa. anubis*	4 (3 M/1 F)	2b	6
Macaca mulatta	*M. mulatta*	12 (6 M/6 F)	4b	16
Cercocebus atys	*C. atys*	4 (3 M/1 F)	4b	8
Sapajus apella	*S. apella*	6 (3 M/3 F)	4b	10
Saimiri sciureus	*S. sciureus*	4 (3 M/1 F)	4b	8
Dinopithecus ingens	SK554	1		1
Papio angusticeps	CO100, CO13	2		2
Aegyptopithecus zeuxis	CGM-40327,CGM-85785,DPC-1208, DPC-5404	4		4
Parapithecus grangeri	DPC-18651	1		1
Victoriapithecus macinnesi	KNM-MB-29100	1		1
Apidium phiomense	DPC-9867	1		1
Cateopithecus browni	DPC-1138	1		1
Proteopithecus sylviae	DPC-14095	1		1

6.3.1. Fossil specimens

In this study, we analysed miro-computed tomography scans of the fossil specimens from collections housed at Duke Lemur Centre Division of Fossil Primates (DPC) DPC- 18651, DPC-9867, DPC-11388, DPC-14095, DPC-1208 and DPC-5401; The Cairo Geological Museum (CGM) CGM-40327, CGM- CGM-85785; The Ditsong National Museum of Natural History (DNMNH) DNMNH:SK:554, CO100, CO135 and SK554 and the National Museums of Kenya (KNM) KNM-MB-29100.

6.3.2. Data collection

To predict the right temporal lobe volume (TLV) in extant and extinct catarrhines, seven linear metrics were digitally measured (in mm) using *Checkpoint* (Stratovan, 2021) on the right middle cranial fossa (MCF) surface in extant anthropoids (Fig. 1). TLV was predicted in the extinct taxa and compared to the predicted TLV in Three extant cercopithecoid species.

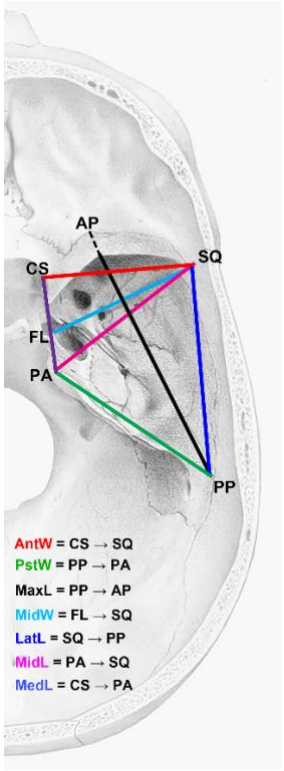

Figure 1. The seven metrics used to predict right temporal lobe volume, shown on the right middle cranial fossa (MCF). See Online Resource 1 for anatomical description of metrics used.

Endocranial volume in extant taxa was calculated (in cm^3) through the generation of virtual endocasts from the µCT scans in *Slicer 4.0* (Fedorov et al. 2012). For extinct taxa, endocranial volumes (in cm^3) were taken from published literature (Online Resource 1, Table 1). For comparison with predicted TLV, the endocranial hemisphere volume (EHV) was calculated as the endocranial volume/2.

6.3.3. Statistical analysis

Preliminary analysis examined whether endocranial volume (EHV) was a suitable proxy for cerebral hemisphere volume. A phylogenetic generalized least-squares (PGLS) regression tested the correlation of extant anthropoid right cerebral hemisphere volume (in cm^3) and right temporal lobe volume (in cm^3) calculated by voxel from the MRI. The temporal lobe data were taken from Pearson et al. (2020), where a more detailed description of how we defined temporal lobe boundaries can be found. Intraobserver error was assessed by an analysis of variance, where measurement error was calculated as the proportion of the mean-squared differences between replicates relative to the total between-group variation (see Bailey and Byrnes 1990). For the seven MCF metrics, measurement error ranged from ≤ 1% to 4%. These were not considered error values of note and analysis proceeded.

A second PGLS regression examined the correlation between endocranial hemisphere volume (EHV) (in cm^3), calculated from the endocasts, and predicted temporal lobe volume (in cm^3), calculated from right MCF metrics. Both PGLS regressions indicated the predicted TLV and endocast EHV were suitable proxies for cerebral volumes (Online Resource,2).

All MCF variables were first converted from linear measurements (in mm) to natural logarithmic units. A multiple regression of MCF variables provided an equation to predict TLV in extant and extinct taxa. The cube-root was taken for TLV and EHV (in cm^3), then converted to natural logarithmic units to linearise the scaling relationships for further analysis (Simpson et al. 2003).

PGLS regressions tested the correlation between TLV and EHV in extant and extinct taxa with PGLS regressions followed Martins and Hansen (1997). A consensus anthropoid tree was downloaded from 10kTrees version 3 (Arnold et al. 2010) containing *Papio anubis*,

Cercocebus atys and *Macaca mulatta* with their molecular divergence dates. We then modified the consensus anthropoid tree in Mesquite version 3.70 (Maddison and Maddison 2021) to include extinct taxa with the generally accepted geological ages and taxonomic affinities used to estimate the phylogeny (Fig. 2).

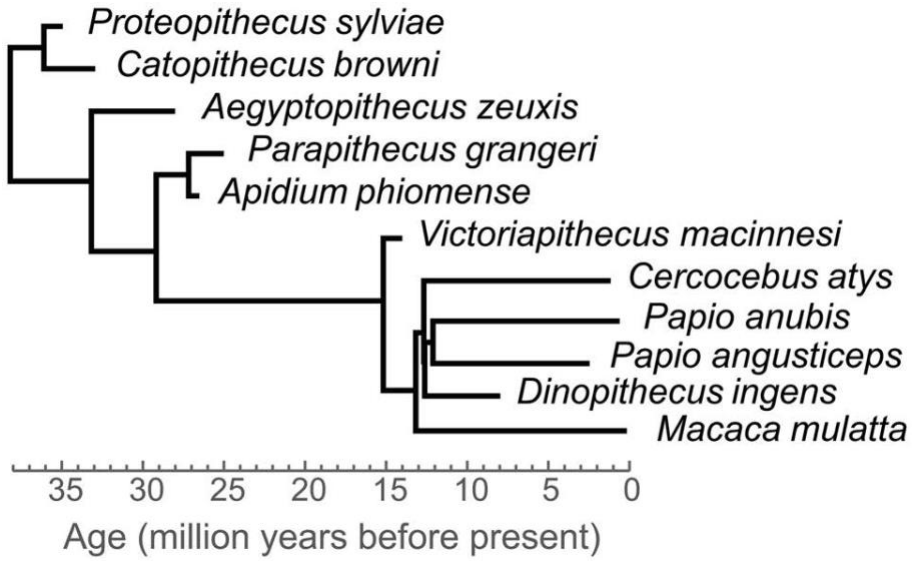

Figure 2. Phylogenetic tree of the cercopithecines used in this study. Scale bar is in millions of years (MYA)

Blomberg's *K* (kappa) statistic was used to assess the phylogenetic correlations of the traits. *K* measures the proportion of the tip variance that matches the expectation of Brownian motion relative to the total variance and thus ranges from 0 to 1 (Blomberg, Garland et al. 2003). Values of *K* close to 0 indicate little congruence between the trait and the phylogenetic tree as expected under Brownian motion, whereas values closer to 1 indicate a strong congruence.

To examine if TLV was relatively larger or smaller than EHV in extinct taxa compared to extant taxa, further PGLS regressions tested whether the values for the slopes and intercepts were as high or higher than those observed by chance using random sampling (5,000 iterations).

All statistical analyses, PGLS regressions, *K* calculations, and trait- mapping were performed using Phylogenetics for Mathematica version 6.5 (Polly 2019) and performed in Mathematica version 13.1 (Wolfram 2019).

6.4. Results

We examined whether there was an increase or decrease in relative TLV to EHV in extinct taxa compared to extant cercopithecoids through trait-mapping, PGLS regressions with random sampling of regression slopes and intercepts between extant cercopithecines and stem-anthropoids.

6.4.1. Predicted temporal lobe volume

A multiple regression of naturally log-transformed TLV and 7 MCF variables provided a statistically significant correlation (adjusted $r^2 = 0.\ 98$, $p < 0.01$) in extant anthropoids (Table 2).

Table 2 Multiple regression statistics for temporal lobe prediction with statistically significant values in bold.

Multiple Regression Statistics							
Multiple R	Multiple r^2	Adjusted r^2	*p*-value	SSE	*b*	SE	p-value
1.00	***0.99***	***0.98***	*0.00*	0.05	-2.17	0.38	***0.01***
Variable		***b***		**SEE b**			***p*-value**
Intercept		-2.16886		0.375522			0.01032
AntW(ln)		-0.42763		0.309932			0.261515
PstW(ln)		0.33318		0.258774			0.288244
MidW(ln)		-0.00491		0.159767			0.977403
MaxL(ln)		0.91834		0.646677			0.250666
LatL(ln)		-1.0303		0.667632			0.220464
MidL(ln)		1.37565		0.422663			0.04732
MedL(ln)		-0.29464		0.145327			0.13568

Abbreviations: b = intercept; r^2 = coefficient of determination; Adjusted r^2 = coefficient of determination adjusted for multiple regression; SE = Standard error of regression; SEE = Standard error of the estimate.

Natural log-transformed variables for TLV and EHV were analysed with a multiple regression with the resultant prediction equation used to predict extant and extinct TLV (Table 3).

Table 3 Natural log-transformed predicted TLV and EHV for Cercopithecoidea with predicted endocranial hemisphere volume (EHV) and temporal lobe volume (TLV).

Taxon	**EHV**	**TLV**
M. mulatta	1.267053013	0.814342
C. atys	1.318656996	0.895762
P. anubis	1.474233539	1.049525
D. ingens	1.480883752	1.001692514
P. angusticeps	1.480883752	1.08482954
V. macinnesi	0.959732819	0.487305224
A. zeuxis	0.717157154	0.481497544
Pa. grangeri	0.580155392	0.180851228
Ap. phiomense	0.555115181	0.041772442
Pr. sylviae	0.100034864	0.375922603
Ca. browni	0.176876084	-0.502391451

6.4.2. Evolution of brain size and temporal lobe size in the Cercopithecoidea

To examine the potential effects of phylogeny on EHV and TLV in the Cercopithecoidea, a PGLS regression of naturally log-transformed TLV and EHV produced a statistically significant correlation ($r^2 = 0.71$, $p \leq 0.00107$) in both extinct and extant taxa (Table 4; Fig. 3).

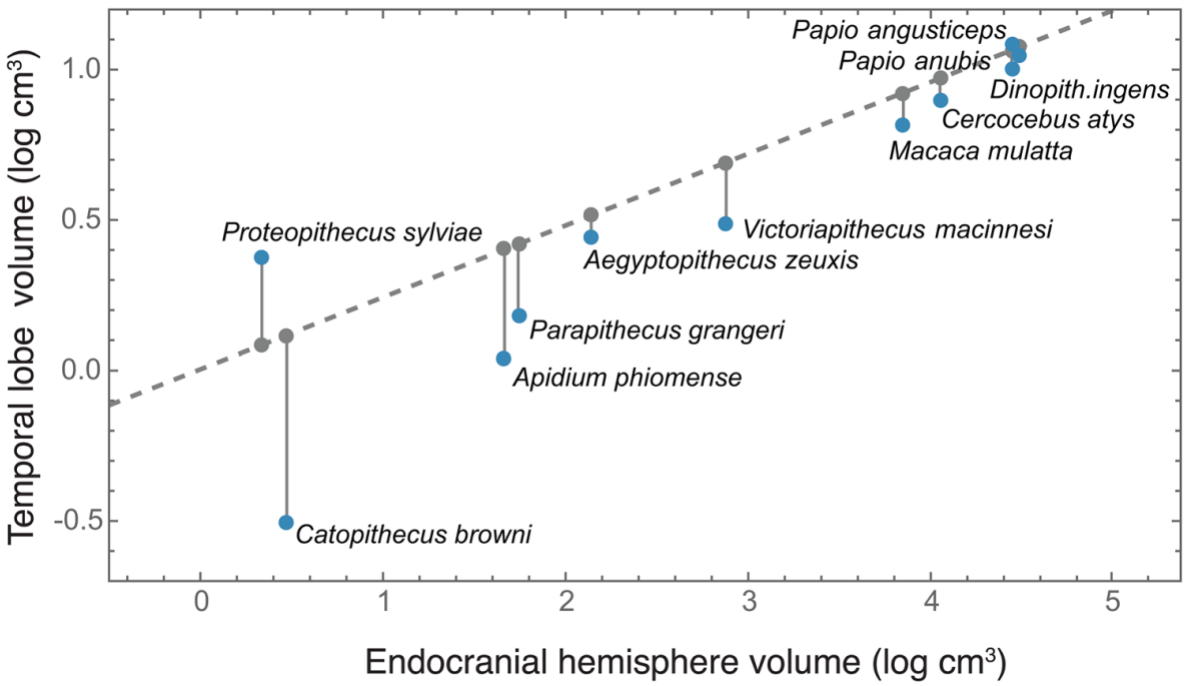

Figure 3 Phylogenetic generalised least-squares regression of temporal lobe volume (TLV) on endocranial hemisphere volume (EHV) in the Cercopithecoidea.

Trait mapping indicated a stronger influence of phylogeny on EHV (k = 3.67) compared to a lesser influence on TLV (k = 0.60) in both extant and extinct taxa (Table 4; Fig. 4).

Table 4 - Phylogenetic generalised least squares regression of temporal lobe volume (TLV) and hemisphere volume (EHV) in the Cercopithecoidea.

PGLS Regression Statistics					
a	*b*	r^2	*p*	EHV *k*	TLV *k*
0.639	0.030	0.71	*0.00107*	3.67	0.60

Abbreviations: PGLS = phylogenetic generalised least-squares regression; a = slope; b = intercept; r^2 = coefficient of determination; p = p-value; k = Blomberg's Kappa.

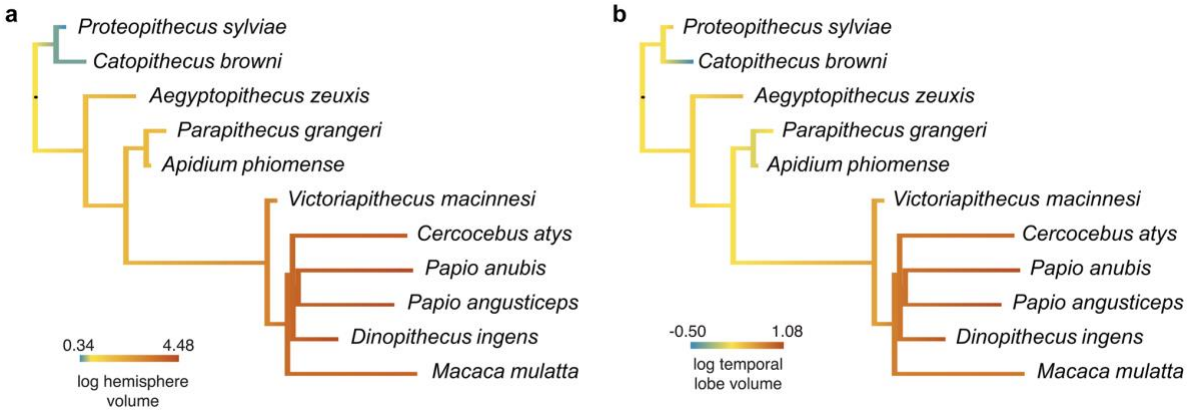

Figure 4. Comparisons of trait-mapping in the Cercopithecoidea. a. EHV; b. TLV.

6.4.3. Relative temporal lobe size to brain size in the Cercopithecoidea

The difference in relative TLV to EHV in the Cercopithecoidea was conducted using two groups of taxa: (1) the clade of Miocene and later taxa, including the 3 extant cercopithecine species and 3 extinct cercopithecoids, and (2) the pre-Miocene stem-group of 5 extinct anthropoid species. PGLS regressions tested whether the slope and intercept values in the two groups were more different than expected by chance using a non-parametric bootstrapping test. The difference in slopes using random sampling with 5,000 iterations was statistically significant (p = 0.0014), while the difference in intercepts using random sampling with 5, 0000 iterations was not statistically significant (p = 0.27) between the two groups (Table 5; Fig. 5).

Table 5. PGLS Regression of temporal lobe volume (TLV) and hemisphere volume (EHV) in stem-anthropoids and extinct and extant cercopithecoids with test for difference in slopes and intercepts and bootstrap (5,000 iterations).

Stem-Anthropoid PGLS Statistics					
a	*b*	r^2	*p*	Slope difference *p*	Intercept difference *p*
-0.086	0.217	-0.09	1.0	0.0014	0.27
Cercopithecoid PGLS Statistics					
a	*b*	r^2	*p*		
1.049	-0.519	0.98	0.00016		

Abbreviations: PGLS = phylogenetic generalised least-squares regression; a = slope; b = intercept; r^2 = coefficient of determination; p = p-value.

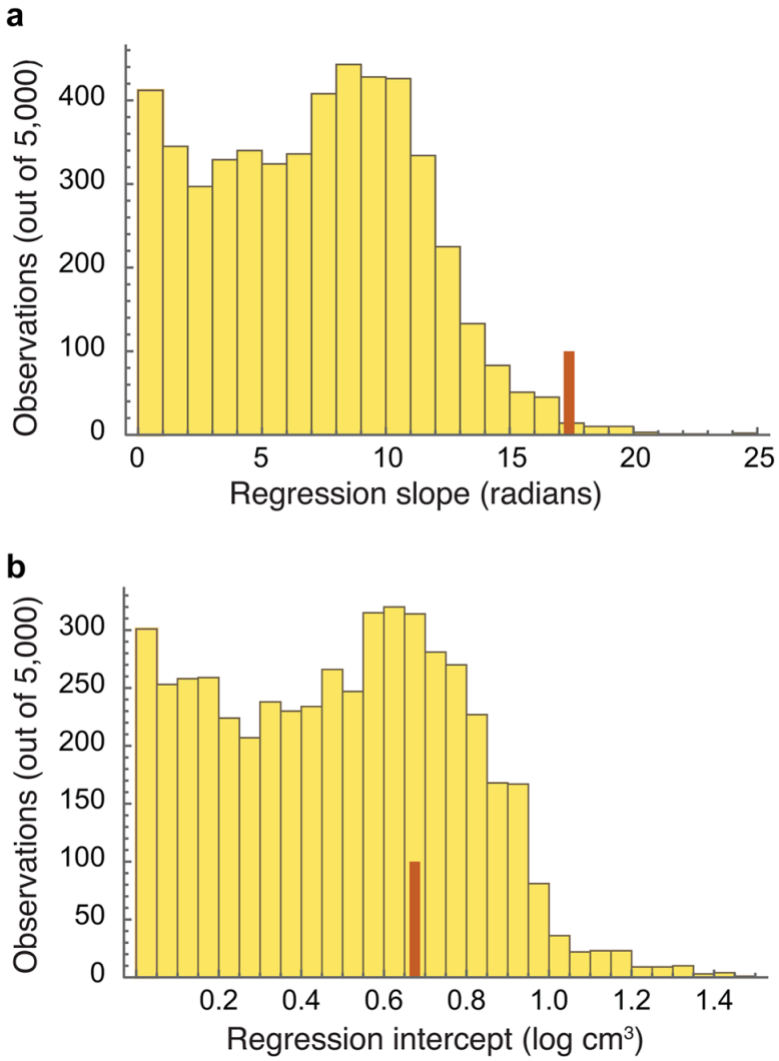

Figure 5. Comparison of random sampling in slopes (**a**) and intercepts (**b**) of stem-anthropoids and extinct and extant cercopithecoids from phylogenetic generalised least squares regression. The red bar represents the slope and intercept values in Table 5.

Ultimately, these findings indicate temporal lobe size was larger relative to brain size in the extant Cercopithecoid clade compared to the stem-anthropoids (Fig. 6).

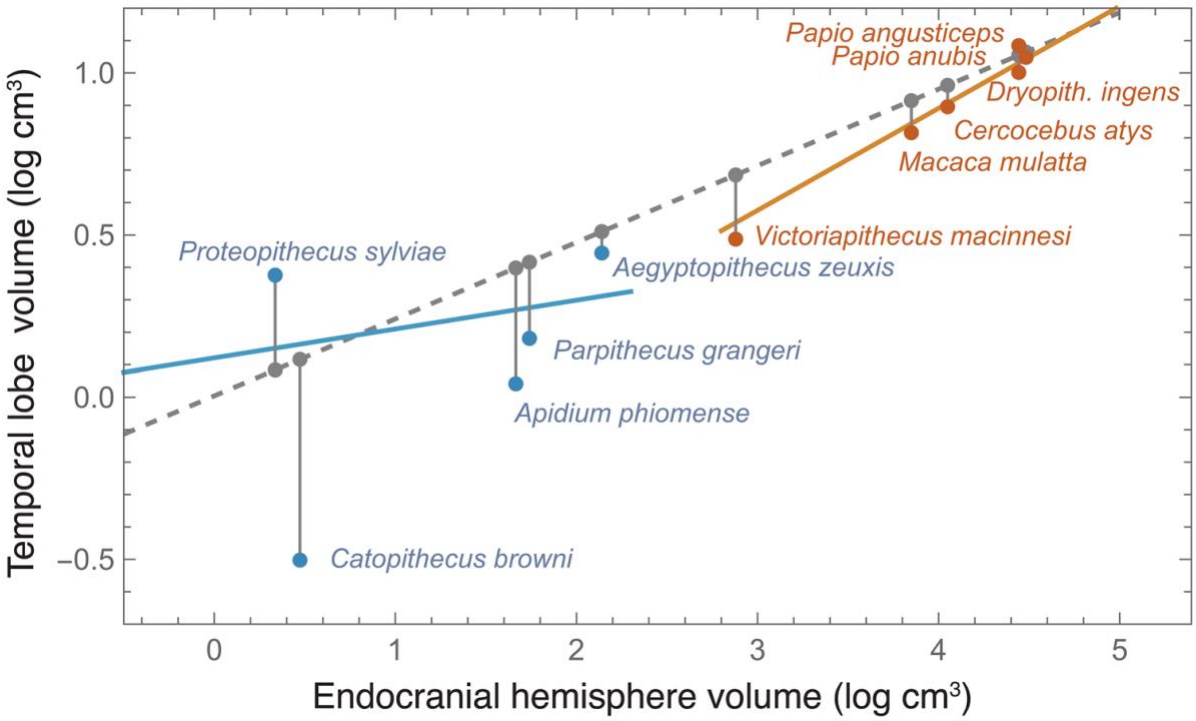

Figure 6. Phylogenetic generalised least squares regression depicting the regression line of TLV on EHV and comparison of slopes between stem-anthropoids (in blue) and crown-clade cercopithecoids (in orange) showing that relative TLV to EHV changed most noticeably between the stem-anthropoids and the crown-clade in the Late Eocene and Early Oligocene.

We note that the Late Eocene taxa *Cateopithecus*, and Early Oligocene taxa *Apidium* and *Parapithecus* lie well below the regression line as fit to the entire catarrhine clade. Differences in the slope for the stem-anthropoids was near zero and slightly negative which suggests that as brain size got larger there was either no relationship to temporal lobe size or that the temporal lobe size became proportionally smaller. In the crown-clade the slope was near 1.0, which suggests isometric scaling with body size: as brain got larger, the temporal lobe scaled 1-to-1 with it.

6.5. Discussion

6.5.1. Brain evolution in the Cercopithecoidea and palaeoenvironmemt

In general, our findings agree with Radinsky (1974) and Falk (1978), who documented an absolute brain size increase in cercopithecoid evolution (Fig. 4b). Our results also suggest a striking shift in the relationship between an increase in temporal lobe size relative to brain size between the stem and crown groups. Because of the links of the temporal lobe to visual acuity, memory, object recognition, and spatial navigation, and the roles that these play in extant cercopithecoid behaviours, it seems plausible that the marked transition between stem and crown scaling of the lobe is related to changes in individual and social behaviours that were associated with the environmental transitions from the Paleogene to the Neogene.

The changes in the palaeoenvironmemt were also likely associated with changes in absolute brain size and body mass. A period of cooling and drying during the Oligocene likely required stem-anthropoids to expand into newer environments, where changes from an arboreal to semi-terrestrial locomotion would likely have been associated with shifts in body mass and diet (Scott 1995; Fleagle 2013) Among extant cercopithecines, species with larger body masses are unable to forage in the thinner upper canopy branches, which is where smaller-bodied cercopithecines have used niche partitioning (Cheney and Wrangham 1987). During the Miocene the continuing drier climate resulted in an expansion of sub-Saharan grassland savannahs and a shift from dense rainforests to more open woodlands favouring semi-terrestrial locomotion rather than obligate arboreal with postcranial and dentition of the extinct cercopithecine *Victoriapithecus* resembling extant taxa which favour semi-terrestrial locomotion also a diet of hard fruit and seeds (Benefit and McCrossin 2002).

Today, terrestrial primate taxa often have larger group sizes and a larger body mass. Studies of *Papio,* with its large body mass and strong sexual dimorphism, show that it has high levels of intragroup aggression and diets that are reliant during the African dry season on poor vegetation consisting of grasses and subterranean foods, supplemented in other seasons with fruit, leaves and occasionally meat consumed by males (Melnick and Pearl 1987). In contrast, *Macaca*, which inhabits tropical rainforest and woodland environments that are dietarily appropriate for a much smaller and absence sexually dimorphic body size and intragroup aggression. The semi-arboreal *Cercocebus* inhabits wetland, tropical woodland forest to open woodlands with smaller body mass and is reliant on the consumption of fruit and leaves (Melnick and Pearl 1987). These comparisons suggest that extinct taxa associated with tropical and rainforest vegetation might have consumed nutrients that would be suitable for larger brain size compared to the lower quality foods of savannas and grasslands. However, we found that extant taxa *Cercocebus* and *Macaca,* which inhabit forests and consume fruit and leaves, had smaller relative brain sizes compared to the savannah taxon *Papio.* Harvey and Brock (1980) argued that diet and intra-family brain size are associated more with diet, where folivores had comparatively smaller brain size than frugivores and a lesser association between range size. In a more recent study by Chambers et al. (2021), diet was a better indicator of brain size than range size or social structure, which is at odds with the expectation of the Social Brain Hypothesis (Chambers et al. 2021). However, both studies suggested that diet variation and consistent access to resources might play a more significant role in primate brain size than social system.

In the Paleocene, early primate and euprimate taxa are thought to have been small-bodied and nocturnal and to have had limited colour perception (Dominy 2004). Their reliance

on prehensile tail or grasping hands and feet to navigate the upper canopies were coupled with keen olfaction to better exploit access to fruit, but in the Eocene, stem anthropoids inhabited forests, exploiting fleshy fruit from palms, figs, and more lipid-rich laurels (Dominy 2004). Extant anthropoid primates are mostly diurnal with a few exceptions such as the nocturnal platyrrhine *Aotus*, but the emergence of colour vision is a staple argument in the divergence of anthropoids from the strepsirrhine-like primates (Fleagle 2013; Strier 2017). Climate cooling in the late Paleogene resulted in increased seasonality in Africa and the loss of the palm forests; this required stem anthropoids to consume of proteinaceous leaves instead of fruit, as observed in the Egyptian Fayum deposits where Early Eocene anthropoids show a shift from fruit and insect diet to Early Oligocene preference for fruit and leaves (Dominy 2004). The the development of trichromatic vision has likely implications for cercopithecoid temporal lobe evolution where the ability to discern young reddish leaves against a background of mature foliage likely selected for those taxa with higher visual acuity which were more able to discern young seasonal leaves with greater nutritional value (Dominy 2004).

6.5.2. Cercopithecine behaviour and implications for temporal lobe size

Our findings indicated an isometric scaling for brain size likely associated with an increase in body size throughout cercopithecoid evolution as previously noted by Radinsky (1974) and Falk (1978). Potential drivers for an increase in brain size in Middle Miocene and Plio-Pleistocene taxa include the emergence of sexual dimorphism in *Aegyptopithecus* (Simons 2007), suggesting increased intragroup social aggression, which is commonly found in extant cercopithecines with larger troop sizes such as savanna baboons (Cheney and Wrangham 1987; Melnick and Pearl 1987; Meguerditchiana et al. 2021).

The temporal lobe in humans is a highly multimodal association cortex associated with language processing, memory tasks, and auditory and visual processing (Rilling 2014). In non-human primates, which are less studied than humans, distinguishing auditory, memory, visual processing has been more difficult (Braunsdorf 2021). A comparison between *Homo sapiens* and *Pan troglodytes* temporal cortex noted homologous language regions hidden beneath a sulcal fold in chimpanzees but visible on the sulcal surface in modern humans (Rilling 2012). Complex vocal communication is not restricted to modern humans, but our species does rely heavily on a language system to the detriment of visual communication. In human and nonhuman primates, visual signalling and the processing of visual communication occurs in the temporal cortex and is associated with facial recognition and memory (Pruess 2006). Thus, in the early emergence of stem anthropoids inhabiting dense tropical rainforest, the ability to distinguish and memorise the faces, facial expressions, and appearance of group members versus other groups would have become increasingly relied upon, especially with the reduction in olfactory reliance for visual senses (Fleagle 2013).

The evolutionary implications for catarrhine reliance on visual communication is related to visual acuity, or the ability to distinguish between closely spaced visual stimuli. Diurnal anthropoids have significantly higher visual acuity than other mammals (Kirk and Kay 2004). In dense tropical rainforests during the Eocene, higher visual acuity combined with colour vision would allow discrimination of red, orange, and yellow fruits (Dominy 2004).

In dense rainforests, low-frequency calls travel further than higher-frequency calls at the same amplitude (Seyfarth 1987; Strier 2017). The use of greater vocal communication to pinpoint other group members may have been traded for greater reliance on visual acuity. For example, Late Eocene *Catopithcus* and *Proteopithecus* had temporal lobes which are

proportionally much larger and smaller, respectively. These differences in relative temporal lobe size could be associated with behavioural attributes, where greater reliance on navigating upper canopies versus lower canopy subsistence could result in a shift towards higher visual acuity, greater memory reliance, and cognitive complexity rather than lower visual acuity but greater auditory reliance. The Late Oligocene stem anthropoid *Parapithecus* was likely diurnal with visual acuity as high as extant primates (Kirk and Kay 2004). Our findings suggest *Parapithecus* had a small temporal lobe relative to brain size, which raises questions about whether increased temporal lobe function and higher cognitive processes were directly related to an increase in cortex size or, more likely, whether *Parapithecus* represents a transitional shift in cerebral reorganisation in the stem group of the Cercopithecoidea.

We found extant *Papio* had a slightly larger relative temporal lobe for brain size. Since baboons are terrestrial quadrupeds that inhabit open grassland and savannah environments, we hypothesize that larger group size, more vocal and visual communication such as the visual pathways processing in the inferior temporal cortex associated with facial recognition (Pruess 2006), behavioural cues including lip-curling and eye-lid flips commonly observed aggression displays among baboons (Strier 2017) likely require greater cognitive demands on the temporal lobe. Our findings imply the presence of interconnections between paleoenvironment and eco-behavioural adaptations in stem anthropoids and throughout extinct cercopithecine evolution.

6.5.3. Relative temporal lobe size in the Cercopithecoidea

Our findings indicate differences in relative temporal lobe size to brain size between extinct and extant cercopithecines and stem anthropoids. The evolution of the stem anthropoid temporal cortex may be influenced by visual and auditory communication. The smaller-bodied Late Eocene taxa were habitually arboreal quadrupeds and leapers inhabiting dense canopies

where the demands of a higher functioning temporal cortex was selected in favour of relatively large olfactory bulbs for brain size (Simons 1995).

We did not find a consistent observable trend in relative temporal lobe size among the stem anthropoids, but Late Eocene *Proteopithecus* had smaller relative temporal lobes to brain size compared to the contemporaneous *Cateopithecus,* which had proportionally much larger temporal lobes for brain size. Early Oligocene *Apidium* and *Parapithecus* both had smaller relative temporal lobes compared to the sexually dimorphic *Aegyptopithecus,* which had temporal lobes proportional to brain size. In the extant and extinct cercopithecines, temporal lobe scaled proportionally with brain size, likely associated with increases in body mass as present in the Middle Miocene extinct cercopithecoid *Victoriapithecus,* Pliocene extinct cercopithecine *Dinopithecus,* Early Pleistocene *Papio,* and extant cercopithecines *Macaca*, *Cercocebus* and *Papio.*

6.6. Conclusion

Our findings about relative temporal lobe size show that the scaling relationship between temporal lobe and brain size changed between the stem cercopithecines of the Late Eocene and Oligocene compared to the crown group in the Late Miocene and Quaternary. The timing of the transition suggests that cerebral reorganisation occurred at several key stages during the evolution of the Cercopithecoidea but was most noticeable in the Late Eocene and Early Oligocene during the initial opening of paleoenvironments.

Through the application of virtual imaging methods and phylogenetic comparative methods, this study expands on previous work conducted on absolute cercopithecoid brain evolution. In general, we found in agreement with previous findings that absolute brain size

increased throughout cercopithecoid evolution. However, we note caution as there is continued debate about the phylogenetic relationships among stem-anthropoid taxa, and because there is a range of phylogenetic, behavioural and neurological differences in the taxa we have studied.

This study provides the first quantification of evolutionary changes to relative brain size and temporal lobe size in the Cercopithecoidea. The inclusion of comparative neuroanatomy and cranial anatomy, phylogenetic comparative methods and robust statistical analyses allow further understanding of relative brain size and temporal lobe evolution in the Cercopithecoidea. Potential drivers for temporal lobe evolution include changes to the processing of visual and communication pathways in response to fluctuating in paleoenvironment and socioecology.

6.7. Data Availability

The data supporting this study are available via Dryad: https://doi.org/10.5061/dryad.xd2547dn3

6.8. Acknowledgements

We thank Colin Groves for his invaluable support in the initial conception of this research and the following museums and researchers for access to digital resources. The Smithsonian Division of Mammals (Dr. Kristofer Helgen) and Human Origins Program (Dr. Matt Tocheri) for the scans of USNM specimens used in this research (http://humanorigins.si.edu/evidence/3d-collection/primate).These scans were acquired through the generous support of the Smithsonian 2.0 Fund and the Smithsonian's Collections Care and Preservation Fund; Museum National d'histoire Naturelle (MNHN); Digital Morphology Museum (DMM) the Primate Research Institute, Kyoto University (KUPRI);

Anatomisches Institut, Universität Leipzig (Germany); University of Pennsylvania Museum of Archeology and Anthropology and the Open Research Scan Archive (ORSA) care of J. Monge and P. T. Schoenemann (NSF proposal # 0447271); The National Chimpanzee Brain Resource care of J. Rilling; OASIS: Cross-Sectional: Principal Investigators: D. Marcus, R, Buckner, J, Csernansky J. Morris (#P50 AG05681, #P01 AG03991, #P01 AG026276, #R01 AG021910, #P20 MH071616, #U24 RR021382). The following digital access is acknowledged from Morphosource (www.MorphoSource.org) for fossil specimens DPC- 18651, DPC-9867, DPC-11388 and DPC-14095, CGM-40327, CGM- CGM-85785, DPC-1208, DPC-5401 care of Alan Walker (funded by Pennsylvania State University); CO100, CO135 and SK554 from the Ditsong National Museums of Natural History; KNM-MB-29100 imaging fossil specimen care of National Musuems of Kenya (Nairobi, Kenya), the Max Planck Institute for Evolutionary Anthropology (Leipzig, Germany), Fred Spoor and Lauren Gonzales.

6.9. References

Arnold C, Matthews LJ, Nunn, CL (2010). The 10kTrees website: A new online resource for primate phylogeny. Evol Anthro19:114–118Bailey RC, Byrnes J (1990) A new, old method for assessing measurement error in both univariate and multivariate morphometric studies. Syst Zool 39(2):124–130

Barton RA (2006) Primate brain evolution: Integrating comparative, neurophysiological, and ethological data. Evol Anthropol 15:224– 236

Bastir M, Rosas A, Lieberman D, O'Higgins P (2008) Middle cranial fossa anatomy and the origin of modern humans. Anat Rec, 291:130–140

Benefit BR (1999) *Victoriapithecus*: The key to Old World monkey and catarrhine origins. Evol Anthropol 155–174

Benefit BR, McCrossin M (2002) The Victoriapithecidae: Cercopithecoidea. In: Hartwig WC (ed) The Primate Fossil Record. Cambridge University Press, Cambridge, UK, pp 241–253

Blomberg SP, Garland, TJ, Ives, AR (2003). Testing for phylogenetic signal in comparative data: Behavioral traits are more labile. Evol 57(4):717–745

Braunsdorf M, Blazquez-Freches G, RoumazeillesL, Eichert N, Schurzad M, Uithol S, Bryant KL, Mars RB (2021) Does the temporal cortex make us human? A review of structural and functional diversity of the primate temporal lobe. Neurosci Biobehav Rev 131:400–410

Bryant KL, Preuss TM (2018) A comparative perspective on the human temporal lobe. In: Bruner E, Ogihara N, Tanabe HC (eds) Digital Endocasts: From Skulls to Brains. Springer, Tokyo, pp 239–258

Bush EC, Simons EL, Allman JM (2004) High-resolution computed tomography study of the cranium of a fossil anthropoid primate, *Parapithecus grangeri*: new insights into the evolutionary history of primate sensory systems. Anat Record 281:1083–1087

Chambers HR, Heldstab SA, OHara SJ (2021) Why big brains? A comparison of models for both primate and carnivore brain size evolution. PLoS One 16(12):e0261185

Changizi MA, Qiong Z, Shinsuke S (2006) Bare skin, blood and the evolution of primate colour vision. Biol Lett 2217–221

Cheney DL, Wrangham RW (1987) Predation. In: Smuts BB, Cheney DL, Seyfarth RM, Wrangham RW, Struhsaker TT (eds) Primate Societies. University of Chicago Press, Chicago, London, pp 227–239

Clutton-Brock TH, Harvey PH (1980) Primates, brains and ecology. J Zool 190:309–323

Dominy NJ (2004) Color as an indicator of food quality to anthropoid primates: ecological evidence and an evolutionary scenario. In: Ross CF, Kay R (eds) Anthropoid Origins: New Visions. Kluwer Academic/Plenum Publishers, New York, pp 615–644

Dunbar RIM (2009) The social brain hypothesis and its implicationsfor social evolution. Ann Hum Biol 36(5):562–572

DuPont LM, Leroy SAG (1995) Steps toward drier climatic conditionsin Northwestern Africa during the Upper Pliocene. In: Vbra ES, Denton GH, Partridge TC, Burckle LH (eds) Paleoclimate and Evolution, with Emphasis on Human Origins. Yale University Press, pp 289 -298

Elton S (2012) Impacts of environmental change and community ecology on the composition and diversity of the southern African monkey fauna from the Plio-Pleistocene to the present. In: Reynolds S, Gallagher A (eds) African Genesis: Perspectives on the Hominin Evolution. Cambridge University Press, Cambridge, UK, pp 471–486

Falk D (1978) Brain evolution in Old World monkeys. Am J Phys Anthrop 48:315–320.

Fedorov A et al (2012) 3D Slicer as an image computing platform for the quantitative imaging network. JMRI 30(9):1323–41

Fleagle JG (2013) Primate Adaptation and Evolution, 3rd Ed. Academic Press, San Diego, Waltham, London

Gilbert CC, Frost SR, Kelsey D, Pugh KD, Anderson M, Delson E (2018) Evolution of the modern baboon (*Papio hamadryas*): A reassessment of the African Plio-Pleistocene record. J Hum Evol 122: 38–69

Gonzales LA, Benefit BR, McCrossin ML, Spoor F (2015) Cerebral complexity preceded enlarged brain size and reduced olfactory bulbs in old world monkeys. Nature Comm 6:75–80

Grabwoksi M (2016) Bigger brains led to bigger bodies? The correlated evolution of human brain and body size. Curr Anthropol, 57(2):174–196

Harirngton A, Silcox MT, Yapuncich GS, Boyer DM, Bloch JI (2016) First virtual endocasts of adapiform primates. J Hum Evol 99:52–78

Jablonski, NG (2002) Fossil Old World monkeys: The late Neogene radiation. In: Hartwig WC (ed) The Primate Fossil Record. Cambridge University Press, Cambridge, UK, pp 255–30

Kay RF, Ross C, Blythe, WA (1997) Anthropoid origins. Science 275(5301):797–804

Kirk C, Kay RF (2004) Evolution of high visual acuity in the Anthropoidea. In: Ross CF, Kay R (eds) Anthropoid Origins: New Visions. Kluwer Academic/Plenum Publishers, New York, pp 539–602

Kudo H, Dunbar RIM (2001) Neocortex size and social network size in primates. Anim Behav 62(4):711–722

Maddison WP, Maddison DR (2021) Mesquite: a modular system for evolutionary analysis Version 3.70. Available at http:// www.mesquiteproject.org

Marcus DS, Wang TH, Parker J, Csernansky JG, Morris JC, & Buckner RL (2007) Open access series of imaging studies (OASIS): Cross-sectional MRI data in young, middle aged, nondemented, and demented older adults. J Cogn Neurosci 19(9):1498–1507

Martins EP, Hansen TF (1997) Phylogenies and the comparative method: A general approach to incorporating phylogenetic information into the analysis of interspecific data. Am Nat 149:646 667

McKee JK, Keyser AW (1994) Craniodental remains of *Papio angusticeps* from the Haasgat Cave site, South Africa. Int J Primatol, 15:823–841

Meguerditchiana A, Marie D, Margiotoudi K, Roth M, Nazarian A J-L, Claidiere N (2002) Baboons (*Papio anubis*) living in larger social groups have bigger brains. Evol Hum Behav 42:30–34

Melnick DJ, Pearl MC (1987) Cercopithecines in multimale groups: genetic diversity and population structure. In: Smuts BB, Cheney DL, Seyfarth RM, Wrangham RW, Struhsaker TT (eds) Primate Societies. University of Chicago Press, Chicago, London, pp 121–134

Moreira LAA, Watsa M, Erkenswick G, Higham JP, Melin AD (2022) Evaluating genital skin color as a putative sexual signal in wild saddleback (*Leontocebus weddelli*) and emperor (*Saguinus imperator*) tamarins. Am J Primatol 85(2):e23456

Moss ML, Young RW (1960) A functional approach to craniology. Am J Phys Anthrop 18:281–292

Murray EA, Bussey TJ, Saksida LM (2007) Visual perception and memory: a new view of the medial temporal lobe function in primates and rodents. Ann Rev Neurosci 30:99–122

Pearson A (2023) Cercopithecoidea Mathematica Notebook PDF. Dryad Dataset https:// doi. org/ 10. 5061/ dryad. xd254 7dn3

Pearson A, Polly PD, Bruner E (2020) Is the middle cranial fossa a reliable predictor of temporal lobe volume in extant and fossil anthropoids? Am J Phys Anthropol 172:698–713

Pearson A, Polly PD, Bruner E (2021) Temporal lobe evolution in Javanese *Homo erectus* and African *Homo ergaster*: Inferences from the cranial base. Quat Int 603:5–21

Peterson A, Abella EF, Grine FE, Teaford MF, Ungar PS (2018) Microwear textures of *Australopithecus africanus* and *Paranthropus robustus* molars in relation to paleoenvironment and diet. J Hum Evol 119:42–63

Polly PD (2019) Phylogenetics for Mathematica Version 6.5. Department of Earth and Atmospheric Sciences, Bloomington, Indiana, Indiana University. Available at http://pollylab.indiana.edu/software. html

Pruess TM (2006) Evolutionary specializations of primate brain systems. In: Ravosa MT, Dagosto M (eds) Primate Origins: Adaptations and Evolution. Springer Science + Business Media, LLC, New York, NY, USA, pp 623–675

Radinsky L (1974) The fossil evidence of anthropoid brain evolution. Am J Phys Anthrop 41:15–28

Rilling JK (2014) Comparative primate neurobiology and the evolution of brain language systems. Curr Opin Neurol 28:10–14

Rilling JK, Insel TR (1999) The primate neocortex in comparative perspective using magnetic resonance imaging. J Hum Evol, 37(2):191–223

Rilling JK, Seligman RA (2002) A quantitative morphometric comparative analysis of the primate temporal lobe. J Hum Evol 42(5):505–533

Rilling JK, Glasser MF, Jbabadi S, Andersson J, Preuss TM (2012) Continuity, divergence, and the evolution of brain language pathways. Front Evol Neurosci

Sansalone G et al (2020) Variation in the strength of allometry drivesrates of evolution in primate brain shape. Proc R Soc B

Schuurman T, Bruner E (2023) A comprehensive anatomical network analysis of human brain topology. J Anatomy

Scott L (1995) Pollen evidence for vegetational and climatic change in southern Africa during the Neogene and Quaternary In: Vbra ES, Denton GH, Partridge TC, Burckle LH (eds) Paleoclimate and Evolution, with Emphasis on Human Origins. Yale University Press, New Haven, CT, pp 65–76

Seyfarth R (1987) Vocal communication and its relation to language. In: Smuts BB, Cheney DL, Seyfarth RM, Wrangham RW, Struhsaker TT (eds) Primate Societies. University of Chicago Press, Chicago,pp 440–451

Shattuck DW, Leahy RM (2002). BrainSuite: An automated cortical surface identification tool. Med. Image Anal 6(2):129–142

Shea, BT (2006) Start small and live slow: Encephalization, body Size, and life history strategies in primate origins and evolution. In: Ravosa MT, Dagosto M (eds) Primate Origins: Adaptations and Evolution. Springer Science + Business Media, LLC, New York,

NY, USA, pp 583–623

Simons E (1995) Egyptian Oligocene primates: a review. Yearb Phys Anthropol 38:199–238

Simons E (1997) Preliminary description of the cranium of *Proteopithecus sylviae*, an Egyptia late Eocene anthropoidean primate, Proc Natl Acad Sci U S A 94:14970–14975

Simons E (2001) The cranium of *Parapithecus grangeri*, an Egyptian Oligocene anthropoidean primate. Proc Natl Acad Sci U S A 98(14):7892–7897

Simons EL, Seiffert ER, Ryan TM, Attia Y (2007) A remarkable female cranium of the early Oligocene anthropoid *Aegyptopithecus zeuxis* (Catarrhini, Propliopithecidae). Proc Natl Acad Sci U S A 104(21):8731–8736

Simpson GG, Roe A, Lewontin RC (2003) Quantitative Zoology(Revised ed.) Dover Publications, New York.

Chapter 8: Discussion Synthesis

8.1. Introduction

In this thesis, I have examined the evolution of the cerebrocranial temporal regions in extant and extinct anthropoids. To address this primary research aim, I examined five key research hypotheses:

1) Confirming the association between temporal lobe volume of the brain and middle cranial fossae size in anthropoids to provide a reliable prediction of temporal lobe size in extinct anthropoids.

2) The application of middle cranial fossa metrics to predict temporal lobe size in fragmentary fossil skulls and examine inter-and intra-specific variation.

3) Re-assess whether modern humans have disproportionately large temporal lobes compared to other anthropoids using a larger sample size, updated imaging techniques and phylogenetic comparative methods.

4) Determine the relative difference of temporal lobe to brain size in extinct and extant old-world monkeys (Cercopithecoidea) and whether cerebral reorganisation was associated with socio-behavioural shifts and palaeoenvironmental changes over time.

5) Examine the evolutionary shifts in temporal lobe size and temporal lobe proportions among extant hominids and fossil hominins.

I will conclude with a synthesis of the implications for each of these research aims and the role of these five key hypotheses for the evolution of the cerebrocranial temporal regions in anthropoid primates and, more broadly, other mammalian taxa.

8.2. Research Aim 1: Predicting temporal lobe volume from the middle cranial fossae: Implications and future directions

In this thesis, the first research aim was to confirm the association between middle cranial fossae and the temporal lobe volume in a comprehensive statistical manner. I developed seven linear measurements of the middle cranial fossae that were carefully selected based on the anatomy and the presence of homologous structures across the 11 extant species anthropoid primates. Virtual segmentation of the temporal lobe followed the definitions outlined in Rilling and Seligman (2002) and neuroanatomical atlases by Borden et al. (2016) and Nolte (2013).

The seven linear measurements of the MCF proved to be highly reliable with ± 1standard error across all extant anthropoid primates and extended into fossil anthropoid primates. The study by Pearson et al. (2020) was the first quantitative investigation of the anatomical correspondence of temporal lobe and middle cranial fossae and provided a predictive set of measurements applicable to anthropoid primates and also suitable for use in fragmentary fossil remains.

The human brain is a complex organ which is responsible for both the autonomic and central nervous system functions. The temporal lobe of the brain is a multimodal association cortex with various functional roles, including auditory and visual processing, memory related tasks, facial recognition, the production of language associated with Broca's Area, speech comprehension and some capacities of spatial awareness (Amunts & Zilles, 2012; Ardesch et al., 2019; Braunsdorf et al., 2021; Binkofski et al., 2000).). Speech comprehension differs from the functional capacity of speech, for example, modern humans suffering from temporal lobe dementia show an inability to distinguish between closely related words as a common neurological diagnostic marker (Crinion et al., 2003).

From an evolutionary perspective, the temporal lobe is of particular interest with an equivalent endocast region to Broca's Area referred to as Broca's Cap where the presence or absence is assumed to be associated with the capacity for speech production in fossil hominins (Falk et al., 2000). In primates, there are many types of complex communication observed and socio-behavioural complexity is not necessarily restricted to the human clade but is present across all extant primates (Holloway, 1983; Rilling 2014).

In terms of gross neuroanatomy, there are no defining boundaries observable on the external lateral surface of the temporal lobe of the brain but rely on the inner structures of the temporal cortex to delimit it from the parietal and occipital lobes (Bokde et al., 2016; Borden, 2005). For neuroanatomists, the study of the temporal lobe is reliant on medical imaging techniques like magnetic resonance imaging (MRI) or dissection of cadaver brains (Stephan et al., 1972). In order to compare the anatomy of the temporal lobe between humans and nonhuman primates and assess the differences, this is only possible through medical imaging or dissection.

For palaeoneurologists, the absence of any defining boundaries visible on the external surface of the temporal lobe has meant investigations have been limited to generalised changes in shape of an endocast (Balzeau et al., 2013; Sansalone et al. 2020). Over time, paleoneurology has advanced the techniques in the study of brain evolution from the early use of physical endocranial moulds (Holloway, 2018) to high-resolution virtual endocasts provided through computed tomography scans and other virtual anatomy visualisation techniques (Bruner, 2017; Zollikofer, & De León, 2013). Fortunately, there is a very good record of temporal lobe sulcal imprints on the anterior, lateral, inferior, and posterior surfaces on the cranial base (Labra et al., 2023; Falk, 2014; Falk et al., 2000; Falk, 1980; van Minh & Hamada; 2017). The inability to anatomically define the limits of the temporal lobe on an endocast has left studies to focus on generalised changes to

endocast form. The endocranial base has been studied by Lieberman et al., (200a; 2000b), McCarthy (2001; 2004) and Bastir et al., (2008; 2010; (2011; 2016). Bastir et al. (2008; 2011) focused investigations into how changes to the middle cranial fossae might reflect temporal lobe form in fossil *Homo*.

Two decades ago, Rilling & Seligman (2002) used a comparative anthropoid in-vivo MRI sample to conclude that modern humans had disproportionately large temporal lobes compared to other living anthropoid primates. Previously, Semendeferi & Damasio (2000) used an MRI sample of the brain in great apes and compared the relative temporal lobe volume to the other lobes in brain and absolute brain size but did not find modern humans had a larger than expected temporal lobe volume for apes. More recent investigations by Pearson et al. (2023a) with a larger dataset compared the Rilling and Seligman (2002) dataset but did not find that the modern human temporal lobe was disproportionately large compared to other living anthropoid primates.

In an extension of comparative cerebrocranial anatomy, Rosas et al. (2014) compared a modern human cadaver temporal lobe and sulcal imprints on the middle cranial fossae with the sulcal imprints preserved on the middle cranial fossae in *Homo neanderthalensis* but no robust statistical analyses were conducted. All research into the middle cranial fossae was assumed based on an anatomical association with the middle cranial fossae and the temporal lobe of the brain and that the MCF was a suitable proxy for the temporal lobe.

In my research presented in Pearson et al. (2020), I confirmed the association of the middle cranial fossae and temporal lobe and developed a statistically robust set of metrics to predict temporal lobe volume from the middle cranial fossae to within ± 1 standard error across a variety of anthropoid primate species including modern humans and squirrel monkeys. The prediction equations for temporal lobe volume from the middle cranial fossae have a substantial value in

providing highly reliable prediction of temporal lobe volume in anthropoid primates from fossil species of extinct *Homo sapiens* to stem-anthropoids.

There are several future directions for research into temporal lobe volume predicted from the middle cranial fossae. Investigations into whether the MCF metrics developed can provide reliable predictions of temporal lobe volume in other mammals would allow an assessment primate temporal lobe evolution within the broader context of mammalian brain evolution and whether similar or different trajectories occurred in other mammals compared to primates.

The second future research direction concerns cerebral reorganisation. The development of a similar set metrics for the anterior cranial fossae and posterior cranial fossae and the association between the frontal lobe and occipital lobe volumes would enable an understanding of cerebral reorganisation in the primate brain. Future research should focus on the relative size the temporal lobes to other brain lobes to enable a robust investigation of how and whether, these different brain regions changed relative to each other. Bruner & Holloway (2010) compared the relative width of the frontal lobes in early *Homo* to brain size but there are currently no predictions for frontal lobe volume from the endocranium. The development of similar endocranial metrics for the cranial vault would also enable a prediction of parietal lobe volume, where Bruner et al. (2017) compared the relative position of the parietal to temporal lobes using linear measurements, but no robust statistical volumetric comparison was conducted.

The implications from my research by Pearson et al. (2020 for palaeoneurology should include the development of predictions for the different cerebral volumes in the brain to allow investigations into cerebral reorganisation with broader application into other mammalian taxa.

8.3. Research Aim 2: Predicting temporal lobe volume in fragmentary fossil skulls and inter-and intra-specific variation: Implications and future directions

In this thesis, the second research aim was to apply the middle cranial fossa metrics and predict temporal lobe volume from fragmentary fossil crania by examining the variation between African and Javanese specimens of *Homo erectus sensu lato*. A subset of the seven middle cranial fossae metrics developed in the first research aim in Pearson et al. (2020) were applied to the African *Homo ergaster* and Javanese *Homo erectus* endocrania (Pearson et al., 2021). It is not uncommon for Javanese fossil specimens and the Chinese Zhoukoudian specimens to be represented only by a cranial vault with the mastoid and nuchal regions preserved and the brow ridges which form a single bony torus but often the facial skeleton is completely missing with the usual exception of Sangiran 17 which is the most complete Javanese *Homo erectus* fossil (Aziz et al., 1996) Unfortunately, this results in only partially preserved middle cranial fossae for almost all specimens and prevents the use of complete endocasts (Holloway, 1981).

There are two opposing positions on whether there is a single species present in Africa and Asia and referred to as *Homo erectus sensu lato* which is considered to be highly variable in cranial form due to climatic adaptations (Anton, 2003). These geographical 'morphs' are considered highly variable if not more so, than observed in modern humans (Harvati & Weaver, 2006). To this end, in Research aim 2, I compared the *Homo erectus sensu lato* sample to a broad global representation of modern human endocrania and statistically tested if the variation in *Homo erectus sensu lato* to determine whether the variation was as great or greater than a global modern *Homo sapiens* sample. I did not find a similar degree of variation as observed in modern *Homo sapiens*, but small sample size likely played a role in affecting the statistical robustness of results (Pearson

et al., 2021). The absence of the Zhoukoudian endocrania and access to Indonesian Ngadong *Homo erectus* samples reduced the potential sample considerably and future inclusion of Ngadong *Homo* erectus specimens would enable a more robust analysis of the variation present in *Homo erectus sensu lato*.

I did find differences in the temporal lobe between African *Homo ergaster* and Javanese *Homo erectus* which share a similar average absolute endocranial size but differed in the temporal lobe proportions. For example, Javanese *H. erectus* had longer and wider temporal lobes relative to total brain size compared to African *H. ergaster* which had shorter and narrower temporal lobes (Pearson et al., 2021). These findings suggest different patterns of cerebrocranial organisation and species-specific variation which was furthered examined in Research Aim 5 (Pearson and Polly, 2024). These findings are relevant to the discussion of potential sociobehvaioural and ecological differences between African *Homo ergaster* and Javanese *Homo erectus* (Pearson and Polly, 2024).

Early paleoanthropological investigations into the origins of modern humans were extensively conducted in the Indonesian islands by Eugene Dubois who believed the 'missing link' between early hominins and humans would be found in Southeast Asia. The fossil evidence provided by Dubois's discoveries included several key *Homo erectus* fossils from the Trinil site along the banks of the Solo River in Central Java including and neurocranial vault and femur recovered between 1891 to 1892 (Swisher et al., 2000). The islands in Indonesia have since yielded many more fossils of *Homo erectus* at sites of Ngangdong, Sangiran, Sambungmacan with other specimens of *Homo erectus* recovered from the cave site of Zhoukoudian in China but unfortunately these Chinese specimens were not recovered after World War II but research quality casts remain for study (Wood, 1984; Stringer, 1984).

More fossil *Homo* species have been discovered throughout in island Southeast Asia including *Homo floresiensis* on the Indonesian island of Flores (Brown et al., 2003) and *Homo luzonensis* from the Philippines (Détroit et al., 2019). There is now clear evidence for a high degree of migration and mobility of populations of different species of the genus *Homo* throughout this region (Norton et al., 2010; Teixeira et al., 2021; Demeter et al., 2022)

The early fossil specimens of *Homo ergaster* are represented by several partial crania which often do not have the facial skeleton preserved or only a partial facial skeleton. There is often damage to the cranial base associated post-mortem and potentially affected by geological conditions related to taphonomic processes during fossilisation. The most complete specimen of *Homo erectus senso lato* is that of an adolescent male skeleton KNM-WT 15000 or the 'Nariokotome boy' which has an impressive 85% of the skeleton preserved (Walker & Leakey, 1993a).

The dating of East African fossil sites is secure combining evidence from biostratigraphy, paleomagnetic correlation and direct radioisotopic dating of the volcanic tuffs which can be correlated from site to site. Through these dating techniques, the oldest East African *Homo ergaster* specimens are attributed to those from the Koori Fora sites (Cartmill & Smith, 2009). The dating in Java and China is incredibly problematic and highly debated (Rizal et al., 2020; Norton et al., 2020), The insecure dating of many fossils for *Homo ergaster* and *Homo erectus* is related to poor archaeological excavation notes at the time compared to the current level of precision in recording exact location of fossil specimens within a excavation site (Cartmill & Smith, 2009). The dating of many Javanese sites has taken a considerable time to unravel and slowly provides more stable and reliable dating estimates. In general, fossil specimens from East Africa attributed

to *Homo ergaster* are dated to between 1.8 to 1 million years ago (Herries et al., 2020; Cartmill & Smith, 2009).

In contrast, the Javanese fossil specimens have a longer duration in this region and are dated to approximately 1.6 million years ago to 100,000- 50,000 years ago (Rizal et al., 2020). There are noted differences in the cranial form between Javanese *Homo erectus* and African *Homo ergaster* and a general increase in endocranial size evident in specimens from Zhoukoudian in China (Cartmill & Smith, 2009).

The differences between Asian and African specimens have provided support for what is now generally recognised, as *Homo ergaster* restricted to Africa (Groves & Mazak, 1975) and a separate species, *Homo erectus*, present in Southeast Asia and China (Stringer, 1984; Wood 1984). There is still a precedent for an argument for a single species with geographically recognised 'morphs' attributed to *Homo erectus senso lato* which largely based on adaptational changes acquired during migration and gene flow between populations migrating from one environmental zone to another such as might be expected *Homo erectus senso lato* leaving the African forests and open woodlands to the vast tropical rainforests of Southeast Asia (Rightmire, 1990; Anton, 2004).

In modern humans, the argument of Allen and Bergman Rules are applied to body form and limb proportions related to optimal thermal regulation rules of surface area to volume ratios (Cartmill & Smith, 2009). The paleoneurological research by Falk (1990) on the 'radiator brain hypothesis with optional cranial form and blood supply also investigated more recently using thermodynamic and cranial form modelling by Bruner (2015; 2021). In support for African *Homo ergaster* possessing a body form as expected under body and limn proportions for modern *Homo sapiens* in similar environments, evidence from the adolescent Narikotome skeleton suggests long

limb proportions with a narrower thorax which is consistent with present day African hunter-gatherer populations in similar environmental zones (Bogin, 1999; Cartmill and Smith, 2002; Harvati & Weaver, 2006; Howells, 1989).

In general, African and Javanese fossil *Homo erectus senso lato* specimens share a wider cranial base at the mastoid region, prominent sagittal keeling which is more pronounced in Javanese specimens with flattened parietal bones (Cartmill and Smith, 2002; Pearson et al., 2021). If the thermoregulation rules for optional brain function under warm and exposed environments is applied, the further prominence of these cranial features in Javanese *Homo erectus* versus African *Homo ergaster* are not consistent with the optimal brain-blood draining and cooling conditions Falk, 1990). In paleoneurology, this challenges the single species concept where defined physiological adaptations became more extreme under contrasting paleoenvironments with neither African nor Javanese cranial form fits the optimal thermoregulation requirements.

A further complexity to a single species concept, is the further development of stone tool industries in Africa where and there were no changes to the stone tool industry in Asia until the appearance of *Homo sapiens* (Swisher et al., 2000). For example, lithic tools produced by Javanese *Homo erectus* are of the Oldowan type which was shared with the earlier fossil hominins *Homo habilis* and species in *Australopithecus* and *Paranthropus*.

In contrast, African *Homo ergaster* which predates the Asian species shared some overlap with *Homo habilis* but where the relatively simple Oldowan type persisted until more advanced techniques including the Achuelan industry appeared in Africa approximately 1.2 million years but this change in tool technology never appears in Java or sites associated with *Homo erectus* in Asia known as the Wallace Line (Swisher et al., 2000). Therefore, in Asia, unlike Africa, there is a continuation of the Oldowan lithic industry which still provides a puzzle for archaeologists and

palaeoanthropologists attempting to determine why the stone tool manufacture never changed in Asia until the appearance of *Homo sapiens* but went through several phases of development in Africa at the same time (Swisher et al., 2000)).

The findings from Research Aim 2, provides the first estimation of the temporal lobe volume in fragmentary fossil remains and especially in African *Homo ergaster* and Javanese *Homo erectus*. The long-held debates surrounding relative and absolute brain size similarities between these taxa offered an opportunity to examine whether or not there were species-specific differences in relative temporal lobe size as noted by Pearson et al. (2021) and further investigated by Pearson and Polly (2024). It it worth noting that Research Aims 1, 2, 4 and 5 likely relate to associated cerebral reorganisation where the brain and cranium are influenced by sociobehavioural complexities, environmental factors and changes over time to cerebrocranial form.

Future research directions in paleoneurology, should include the use of subset metrics from the middle cranial fossae developed to predict temporal lobe volume in other fragmentary fossils species and may prove useful in determining species-specific differences and relevance to cerebral reorganisation (Pearson & Polly, 20024). The implications of this second Research Aim 2, include the use of fragmentary fossil specimens in larger datasets to allow more statistically robust conclusions in hominin and anthropoid brain evolution. The wider implication of this research includes not only the application to human and nonhuman primate fossils for investigation of cerebral reorganisation in an evolutionary context but also should be considered for extension into the mammalian fossil record and comparisons between different mammalian orders and not just within primates through fragmentary fossil remains.

8.4. Research Aim 3: Re-assessing modern human temporal lobe volume compared to other anthropoids: Implications and future directions

In this thesis, Research Aim 3 re-assessed whether modern humans had disproportionately large temporal lobes compared to other extant anthropoids using a larger sample size, updated imaging techniques and more advanced phylogenetic comparative methods.

Two decades ago, Rilling and Seligman (2002) proposed that modern humans had larger than expected temporal lobes for an ape or monkey of its size. The relationship between brain size and body mass is a complex one as Grabwoski (2016) noted when determining if larger body size in human evolution was related to an increase in absolute brain size and the nature of that scaling relationship. In research conducted by Pearson et al. (2023a), a re-assessment of this landmark study by Rilling & Seligman (2002) was warranted and included a larger sample size of modern human in-vivo MRI (Marcus et al., 2007), the same nonhuman primate in-vivo MRI sample, the adoption of direct volumetric calculations from within the MRI and no interpolation between manually segmented regions of the brain.

The re-assessment also used phylogenetic comparative methods and additional random sampling aided with the robustness of the statistical tests. Pearson et al. (2023a) did not find modern humans had as great or greater than expected temporal lobe size and that they fit within the trend for anthropoid temporal lobe evolution. It is clear from the study by Rilling and Seligman (2002) that the evidence at hand indicated a larger than expected temporal lobe for modern humans but through the acquisition of a larger sample size and greater variation for modern humans and the similar but more recent phylogenetic comparative methods provides a solid foundation for the

understanding that modern humans are not particularly unique among anthropoid primates but rather are within the expected evolutionary trend for temporal lobe evolution.

The findings and discussion of Research Aim 1 and 3, the temporal lobe boundaries have been redefined during the past two decades with increased sensitivity and accuracy of MRI scans and cadaver dissections and, in particular, advances in cytoarchitectural studies (Sherwood et al., 2017). This has allowed further definition of the supero-posterior border of the temporal lobe which has been indefinable without MRI or dissections and no reliable external sulcal features to define this boundary (Pearson et al., 2020; Pearson et al., 2023a; Rilling, 2023). Regardless of the informative response by Rilling (2023), the findings of the reassessment of the Rilling and Seligman (2002) study remain unchanged but future direction might apply more current definitions of the temporal lobe to examine whether or not there is a real disproportionate difference in modern humans compared to other extant anthropoids which was not the findings in Research Aim 3 and in Pearson et al. (2023) where such slight differences are unlikely to affect the statistical results in Pearson et al. (2023).

Future research avenues should be the investigation as to whether other lobes of the brain in modern humans are as great or greater than expected for anthropoid primates. For example, the frontal lobes are frequently inferred to be larger in *Homo sapiens* but there are few robust statistical studies examining in-vivo MRI of the prefrontal and frontal cortices to examine whether these regions are relatively larger or not in modern humans and how they compare to other anthropoid primate species (Riling et al., 2006).The restriction of investigations to modern humans and selected primate species is likely due to difficulty in obtaining in vivo nonhuman primate MRI from a wider range of species. The increased number of studies examining relative brain regions would enable a more complete understanding of cerebral divisions in anthropoids and a more

thorough consideration of how, and in which species, cerebral reorganisation of different cerebral regions is more substantial.

The implication of Research Aim 3, is that by re-assessing a pivotal study of by Rilling and Seligman (2002) and the long-standing assumption that modern humans had disproportionately large temporal lobe sizes which went un-replicated for two decades where further research into the fossil hominin record was conducted without prior confirmation or replication of assumptions beforehand. In terms of future research avenues, there is a need for more investigations into the other regions of the brain across many extant and extinct anthropoid primate species to fully determine the relative size of different brain regions to each other and how these may, or may not, change between modern humans and to other anthropoid primates. The broader implication of these findings would be to better understand in brain regions are unique or not in modern humans and the evolutionary implications of brain changes for palaeoanthropology. There is a wider need to conduct similar studies in other mammalian taxa to then understand the position of primate temporal lobe size in the context of mammalian evolution and not just human or primate evolution.

8.5. Research Aim 4: Determining relative temporal lobe size the Cercopithecoidea and effects of socio-behavioural and palaeoenvironmental change over time: Implications and future directions

In this thesis, the fourth research aim was to examine the relative differences of temporal lobe to brain size in fossil and extant old-world monkeys and whether cerebral reorganisation may be associated with socio-behavioural shifts and palaeoenvironmental changes over 40 million years of old-world monkey evolution.

Primates are some of the most socially complex mammals. Extant anthropoids display many different socio-behavioural complexities associated with brain evolution (Barton, 2006). The recent research by Pearson & Polly (2023b) is the first comprehensive study undertaken into the evolution of the temporal lobes relative to brain size in stem-anthropoids and old-world monkeys. The temporal lobes are multimodal association cortex and functionally not restricted to just speech and comprehension of language but also in non-human primates, facial recognition, memory-related tasks, auditory and visual processing. Initial research by Radinksy (1978) and Falk (1978) proposed larger temporal lobes in living old world monkeys than fossil species but no substantial quantification of changes to relative temporal lobe size were conducted.

The social brain hypothesis (Dunbar, 1998) proposes that absolute brain size is restricted by group size. This certainly seems the case in extant baboons and macaques where living in larger groups has resulted in a larger brain than monkeys living in smaller groups (Meguerditchiana et al., 2002). However, the environmental hypothesis proposes brain size is influenced by diet and foraging habits as well as environmental habitat (Clutton-Brock, 1980). There are distinct differences in behaviour in primates who are habitually arboreal and rely on low-frequency calls to carry through dense rainforest compared to terrestrial savannah-dwelling primates with greater visual acuity and reliance on both visual and auditory cues to locate group members (Seyfarth 1987; Strier 2017).

The anatomical adaptations from an arboreal to terrestrial lifestyle is evident in extant and fossil anthropoid primates. For example, the Miocene fossil cercopithecoid, *Victoriapithecus macinnesi*, exhibits skeletal and cranial morphology compatible with a semi-terrestrial primate like an extant mangabey (Benefit, 1999; Gonzales et al., 2015). I did find an increase in absolute brain size among stem-anthropoids compared to extant cercopithecines, but the relative temporal lobe

size differed between early stem-anthropoids with a 1-1 scaling with brain size in later extinct cercopithecoids and living cercopithecines (Pearson & Polly, 2023). These changes observed in the Cercopithecoidea, indicate that cerebral reorganisation of the temporal lobe relative to other regions of the brain potentially plays an important role in anthropoid brain evolution. Additionally, the shift between smaller relative temporal lobes to scaling with brain size occurred during the middle Miocene and was apparent in the first semi-terrestrial fossil cercopithecoid, *Victoriapithecus macinnesi* (Benefit.2002).

The implications for comparing late Eocene stem-anthropoids to extant cercopithecines is best considered within the context of the 40-million-year timescale and the varying palaeoenvironmental changes that occurred in Africa during this time. For example, the cranial and post-cranial anatomy of the stem-anthropoids from Fayum site in Egypt are very similar to extant arboreal monkeys that inhabit dense tropical and moist rainforests such as existed during the Late Eocene-to Early Oligocene transition in the Fayum. Postcranial anatomy suggests a major shift in the evolutionary trajectories in Oligocene stem-catarrhine *Aegyptopithecus zeuxis* which was sexually dimorphic and considered a semi-arboreal species (Simons, 1995; Simons et al., 2007).

In transitioning from dense tropical rainforests to more open woodland, stem-catarrhines increased absolute brain size and temporal lobe size showed trend of scaling with brain size increase. The further transition to open Savannah and scrub woodland such as inhabited by baboons and macaques presently, required an increase in brain size associated with larger group sizes and more socio-behavioural complexity. For example, sexual dimorphism is present in stem-catarrhine *Aegyptopithecus zeuxis* that with the development of sagittal and nuchal crests and larger mandibles in males but also is common in species consuming tough, fibrous food sources

like observed in extant *Gorilla*. However, Grabowski et al. (2023) recently suggested that the digestive costs associated with folivory led to relatively smaller absolute brain sizes in primates compared to frugivorous or omnivorous species. If this is the case, fossil species like *Aegyptopithecus zeuxis* have an important role in understanding the complexities of increased sociality and dietary adaptations.

Future directions for examining relative temporal lobe to brain size are multifaceted. Future comparisons with neotropical monkeys are warranted to determine whether temporal lobe size scales with brain size or, as extinct platyrrhines inhabited a very similar environment to extant platyrrhines, whether the temporal lobe remains relatively small for brain size as found in stem-anthropoids from the tropical rainforest of the Late Eocene in Africa (Pearson & Polly, 2023b). If the adaptation to changing environments were a driver behind cercopithecoid temporal lobe and brain evolution, then the extant and fossil neotropical monkeys should retain similar relative temporal lobe to brain size without the environmental changes to drive socio-behavioural differences between extinct and extant taxa.

Further implications from this research study by Pearson & Polly (2023b) include the application to other mammalian taxa and anthropoid primate species. The adaptations to climatic changes are very relevant for current conservation measures and a better understanding of anthropoid brain evolution and plasticity would enable planning for conservation measures in threatened species in light of how easily they may, or may not, be adaptable to altering environmental conditions.

8.6. Research Aim 5: Temporal lobe evolution and changes to temporal lobe proportions in hominids: Implications and future directions.

In this thesis, the fifth research aim was to examine the evolutionary shifts in temporal lobe size and temporal lobe proportions in extant hominids and fossil hominins.

In paleoneurology and palaeoanthropology more generally, the focus of human brain evolution has remained with the conflation of brain size and cognitive capacity (Falk, 1980; 1992). Sherwood and Gomez-Robles (2012) argued that the human brain has high levels of plasticity which enable cerebral reorganisation to take place and, in turn, changes in temporal lobe size but also temporal lobe proportions where longer/shorter or wider/narrower temporal lobes played a distinctive role in the differences between early fossil hominins *Australopithecus-Paranthropus* clade and the extant species of the genus *Pan*. Differences in temporal lobe proportions also indicated that even though modern humans and fossil *Homo sapiens* have larger absolute brain sizes, the relative size of the temporal lobe to brain size does not indicate modern humans possess larger temporal lobes but may in fact be slightly smaller than other hominin taxa.

In paleoanthropology, it is still common to compare modern humans and extant great apes as acting as homologues for fossil hominins where the most closely related species genetically to humans such as chimpanzees and bonobos are often studied in light of human evolution. In this thesis, Research Aim 5 argues for the inclusion of the hominin clade to be studied within the broader evolutionary context of great ape brain and temporal lobe evolution. In terms of cerebral reorganisation and the evolution of the temporal lobe, Pearson & Polly (2024) noted most substantial changes to the relative temporal lobe size and temporal lobe proportions occurred in fossil hominin species of genus *Australopithecus*, *Paranthropus* and extant species of the genus *Pan* rather than later fossil *Homo* or extant *Homo sapiens* Paleoneurological studies are

increasingly focusing on comparative neuroanatomy and cerebral reorganisation in the genus *Pan* and *Homo* (Bryant & Pruess, 2018; Rilling, 2012; Falk, 2014).

The recent study by Pearson & Polly (2024) suggests that the extant great apes including *Homo sapiens* fit within the general trend of hominid temporal lobe evolution, and it is the changes to temporal lobe proportion and not size which define and differentiate species. The choice of comparative taxa when examining socio-behaviour in non-human apes often focuses on chimpanzees or less frequently, bonobos. However, there are considerable differences in morphology, behaviour and social organisation in bonobos which is not present in chimpanzees despite the close genetic relationship. For example, among chimpanzees, there are further specialisations of behaviour and social organisation between subspecies and different environments which each subspecies inhabits. Marchant (2012) suggested an evolutionary divergence between chimpanzees and bonobos approximately 2.3 million years ago, while the last common ancestor of the *Pan* and *Australopithecus-Paranthropus* clade was assumed to split about 5 million years ago. This divergence and specialisations unique to different chimpanzee subspecies and bonobos suggests the behaviour observed in these taxa may not reflect the last hominin ancestor and caution is warranted in comparing socio-behaviour in extant *Pan* to fossil hominins.

In this thesis, Research Aim 5 addressed the comparison of fossil hominins by direct comparison with extant hominids including extant *Homo sapiens*. Investigations of the relative and absolute temporal lobe volumes indicated changes relative to total brain size with the greatest differences in temporal lobe proportions occurring in extant *Pan* and extinct *Australopithecus - Paranthropus* clades. Pearson & Polly (2024) examined these changes in temporal lobe size and shifts in proportions within the context of three primate evolutionary brain hypotheses: the social brain (Dunbar, 1998), environmental (Clutton-Brock, 1980) and functional craniology (Moss &

Young, 1960) hypotheses. The consideration of brain evolution within the scope of just one of these hypotheses does not provide a thorough understanding of the mechanisms behind cerebrocranial evolution and cerebral reorganisation. In the context of temporal lobe evolution, it was evident that no singular hypothesis was a clear driver behind temporal lobe evolution but that primate brain evolution and cerebrocranial evolution and cerebral reorganisation is best examined by a combination of all three hypotheses (Pearson & Polly, 2024).

The implications of Research Aim 5, suggest a less 'anthrocentric' focus on human evolution is warranted with further investigations into cerebral reorganisation in the other brain regions including the frontal, parietal and occipital lobes to provide a more comprehensive understanding of human and nonhuman primate brain evolution and how the brain has changed throughout evolution and the potential roles of cranial form, sociality, environmental and ecological factors.

Future directions for this line of research should include a more extensive sample of great apes with the inclusion of fossil taxa the subfamily Ponginae where there are extinct taxa including *Sivapithecus* and *Gigantopithecus* which provide suitable study comparison with extant *Pongo* as conducted recently on dietary differences by Louys et al. (2021). Further investigations of putative fossil apes from Europe would also be suitable if the necessary middle cranial fossae are preserved and metrics can be collected to predict temporal lobe volume. The position of the human clade within the context of great ape evolution suggests that fossil hominins are not necessarily unique compared to other great apes but are within the generalised evolutionary trend for hominid brain and temporal lobe evolution.

8.7. Conclusion

In this thesis, I have argued that modern humans fit within the general trend of temporal lobe evolution anthropoid primates. To this end, five research aims were developed to quantify and assess temporal lobe evolution and middle cranial fossae changes in extant and extinct anthropoid primates with an evolutionary context of 40 million years.

In Research Aim 1 (Chapter 3), the first quantitative assessment of the association between the anthropoid temporal lobe of the brain and middle cranial fossae of the skull and to provide the first statistical prediction of temporal lobe size from the middle cranial fossa by developing seven linear metrics with application for fragmentary fossil remains (Pearson et al., 2020).In Research Aim 2 (Chapter 4), the first application of predicted temporal lobe volume from fragmentary fossil material and the first assessment cerebral reorganisation of the cerebrocranial temporal regions in extant *Homo sapiens* and species-specific changes between African *Homo ergaster* and Javanese *Homo erectus* (Pearson et al., 2021). Research Aim 3 (Chapter 5) provided a reassessment of foundational study in extant anthropoid temporal lobe volume but included a larger sample size, updated imaging methods and phylogenetic comparative analysis to determine that extant Homo sapiens did not have disproportionately large temporal lobe volumes but rather were within the general anthropoid trend (Pearson et al., 2023a).

In Research Aim 4 (Chapter 6), I applied statical multiple regressions from the seven linear metrics to predict a singular temporal lobe volume and provide the first assessment of relative temporal lobe size to brain size in stem-anthropoids, stem-catarrhines, stem-coleopteroids, extinct and extant cercopithecines determining that relative temporal lobe volume increased with brain size in extant and extinct cercopithecines and extinct cercopithecoids associated with shifts in the

paleoenvironment and sociobehavioural trends observed in semi-terrestrial and terrestrial quadrupedal old-world monkeys (Pearson & Polly, 2023b).

In Research Aim 5 (Chapter 7), the absolute, relative brain and temporal lobe size and relative temporal lobe proportions within the family Hominidae and tribe Hominini to provide the first prediction of relative temporal lobe size and proportional changes in extant great apes and fossil hominins and examined within the context of three primate evolutionary brain hypotheses: the social brain (Dunbar, 1998), environmental (Clutton-Brock, 1980) and functional craniology (Moss & Young, 1960) with conclusions that no singular hypothesis can address temporal lobe evolution in the Hominidae nor exclusively the tribe Homini but that the greatest changes in relative temporal lobe size and proportions occurred in extant *Pan* and extinct *Australopithecus* - *Paranthropus* taxa potentially associated with the last common ancestor of the human lineage and that extant *Homo sapiens* fit within the general trend for hominid relative and proportional changes to the cerebrocranial temporal regions (Pearson & Polly, 2024).

In this thesis, I have shown that modern humans and fossil hominins fit within the general trend of cerebrocranial temporal region evolution as other extinct and extant anthropoid taxa which confirms the inclusion of human paleoneurology within the broader context of primate paleoneurology and that modern humans and fossil hominins do not represent a particularly unique clade within anthropoid primate evolution. A shift is needed in biological anthropology to consider paleoanthropology within the much broader context of primate evolution. In this thesis, I have shown that the successful application of virtual anatomy techniques and phylogenetic comparative methods has a strong potential for future application of similar approaches to the study of other cerebrocranial regions and assessment of cerebral reorganisation in primate evolution with broader application to other mammalian taxa.

8.8. References

Anton, S.C., 2003. Natural history of *Homo erectus.* Am. J. Phys. Anthropol. Suppl. 37, 126–170.

Anton, S.C., Swisher, C.C.I., 2001. Evolution and variation of cranial capacity in Asian *Homo erectus*. In: *A Scientific Life: Papers in Honor of Professor Dr. Teuku Jacob*, (ed.) Indriati, E. Bigraf Publishing, Yogyakarta, Indonesia. pp. 25–39.

Amunts, K., & Zilles, K. (2012) Architecture and organizational principles of Broca's region, Trends in Cognitive Sciences, 16:8.

Ardesch, D. J., Scholtens, L. H., Longchuan, L., Preuss, T. M., Rilling, J. K., & van den Heuvel, M. P. (2019). Correction for Ardesch et al., Evolutionary expansion of connectivity between multimodal association areas in the human brain compared with chimpanzees. Proceedings of the National Academy of Sciences of the United States of America, 116(19), 9680.

Avery, M. D., (1995) Southern savannas and Pliestocene hominid adaptations: the micromammalian perspective, In: Paleoclimate and Evolution with Emphasis on Human Origins, (Eds) Vbra, E.S., Denton, G.H., Partridge, T.C., Buckle, L.H.), Yale University Press, London, UK, New Haven, USA, pp 459-478.

Aziz, F., Baba, H., Watanabe, N., 1996. Morphological study on the Javanese *Homo erectus* Sangiran 17 skull based upon a new reconstruction. *Geological Res. Develop. Centre Paleontology Series* , 8, 11–25.

Baab, K.L., (2008). The taxonomic implications of cranial shape variation in *Homo erectus*. J. Hum. Evol. 54, 827–847.

Barton, R.A. (2006) Primate brain evolution: Integrating comparative, neurophysiological, and ethological data. *Evol Anthropol* 15:224 –236.

Balzeau, A., Grimaud-Hervé, D., Détroit, F., Holloway, R.L., Combès, B., Prima, S., (2013) First description of the Cro-Magnon 1 endocast and study of brain variation and evolution in anatomically modern *Homo sapiens*, *Bull. Mém. Soc. Anthropol*. Paris, 25, 1-18.

Barton, R.A., (2006) Primate Brain Evolution: Integrating Comparative, Neurophysiological, and Ethological Data, Evol Anthropol,15:224 –236.

Bastir, M., & Rosas, A. (2006). Correlated variation between the lateral basicranium and the face: A geometric morphometric study in different human groups. Archives of Oral Biology, 51(9), 814–824. https:// doi.org/10.1016/j.archoralbio.2006.03.009

Bastir, M., & Rosas, A. (2016). Cranial base topology and basic trends in the facial evolution of *Homo*. Journal of Human Evolution, 91, 26–35.

Bastir, M., Rosas, A., Gunz, P., Pena-Melian, A., Manzi, G., Harvati, K., … Hublin, J. J. (2011). Evolution of the base of the brain in highly encephalized human species. Nature Communications, 2, 588. https:// doi.org/10.1038/ncomms1593

Bastir, M., Rosas, A., & Kuroe, K. (2004). Petrosal orientation and mandibular ramus breadth: Evidence for an integrated petroso-mandibular developmental unit. American Journal of Physical Anthropology, 123(4), 340–350. https://doi.org/10.1002/ajpa.10313

Bastir, M., Rosas, A., Lieberman, D. E., & O'Higgins, P. (2008). Middle cranial fossa anatomy and the origin of modern humans. The Anatomical Record, 291(2), 130–140. https://doi.org/10.1002/ar.20636

Bastir, M., Rosas, A., Stringer, C., Cuetara, J. M., Kruszynski, R., Weber, G. W., et al. (2010). Effects of brain and facial size on basicranial form in human and primate evolution. *Journal of Human Evolution*, 58(5), 424–431.

Benefit, B.R (1999) *Victoriapithecus*: The key to Old World monkey and catarrhine origins. Evol Anthropol 155–174

Benefit. B.R, McCrossin, M. (2002) The Victoriapithecidae: Cercopithecoidea. In: *The Primate Fossil Record*, (ed) Hartwig, W.C. Cambridge University Press, Cambridge, UK, pp. 241–253

Binkofski, F., Amunts, K., Stephan, K. M., Posse, S., Schormann, T., Freund, H. J., et al. (2000). Broca's region subserves imagery of motion: a combined cytoarchitectonic and fMRI study. Human Brain Mapping, 11, 273–285.

Bokde, A. L., Teipel, S. J., Schwarz, R., Leinsinger, G., Buerger, K., Moeller, T., & Hampel, H. (2005). Reliable manual segmentation of the frontal, parietal, temporal, and occipital lobes on magnetic resonance images of healthy subjects. Brain Research. Brain Research Protocols, 14(3), 135–145.

Borden, N. M., Forseen, S. E., & Stefan, C. (2016). Imaging anatomy of the human brain a comprehensive atlas including adjacent structures. Demos Medical Publishing

Braunsdorf, M, Blazquez-Freches G, RoumazeillesL, Eichert N, Schurzad M, Uithol S, Bryant, KL, Rogier B., Mars, RB (2021) Does the temporal cortex make us human? A review of structural and functional diversity of the primate temporal lobe. *Neuroscience & Biobehavioral Reviews.*

Brown, P., (2004) A new small-bodied hominin from the late Pleistocene of Flores, Indonesia., *Nature*, 431:7012, 1055-1061.

Bruner, E. (2015) Functional craniology and brain evolution. In *Human Paleoneurology*, Bruner E. (ed.) Springer, Switzerland. pp 57-94.

Bruner, E. (2017) Language, paleoneurology, and the fronto-parietal system. *Frontiers in Human Neuroscience,* 11(349): 1-5.

Bruner, E., Pereira-Pedro, A.S., Bastir, M., (2017) Patterns of morphological integration between parietal and temporal areas in the human skull. *J. Morphol*. 278, 1312–1320.

Bruner, E., (2021) Evolving human brains: Paleoneurology and the fate of Middle Pleistocene, *Journal of Archaeological Method and Theory*, 28, 76–94.

Bruner, E. (2017) The fossil evidence of human brain evolution. In J. H. Kaas (Ed.), *Evolution of nervous systems volume 4: The evolution of the human brain: Apes and other ancestors, Vol. 4*, Amsterdam, Boston: Elsevier Inc, pp. 63-92.

Bruner, E., Grimaud-Hervé, D., Wu, X., de la Cuétara, J. M., & Holloway, R. (2015). A paleoneurological survey of *Homo erectus* endocranial metrics. *Quaternary International*, 368, 80–87.

Bruner E., Holloway R.L (2010) A bivariate approach to the widening of the frontal lobes in the genus *Homo*. J Hum Evol 58:138-146.

Bryant, K. L., & Preuss, T. M. (2018). A comparative perspective on the human temporal lobe. In E. Bruner, N. Ogihara, & H. C. Tanabe (Eds.), Digital Endocasts: From skulls to brains. Tokyo: Springer Japan KK., pp. 239–258.

Cartmill, M., & Smith, F. (2009) The Human Lineage, Wiley-Blackwell: Hoooboken, New Jersey.

Charvet, C.J. & Finlay, B.L., (2012) 'Embracing covariation in brain evolution: large brains, extended development, and flexible primate social systems', In: Progress in Brain Research, (eds.) Hofman, M.A., & and Falk, D. Vol. 195

Clutton-Brock, T. H., & Harvey, P.H. (1980). Primates, Brains, and Ecology. Journal of Zoology 190 (3):309–323.

Coleman, M.N., & Colbert, M.W. (2010) Correlations between auditory structures and hearing sensitivity in non-human primates. Journal of Morphology, 271:5, 511-532.

Crinion, JT, Matthew A. L-R, Warburton, EA, Howard, D. Wise, RJS, (2003) Temporal lobe regions engaged during normal speech comprehension, Brain, 126, 1193-1201.

Damasio, H. (2005). *Human Brain Anatomy in Computerized Images*, 2nd edition, Oxford University Press, New York, NY, USA.

Dean, C.E. (2008) 'Growth processes in the cranial base of hominoids and their bearing on morphological similarities that exist in the cranial base of Homo and Paranthropus' in Evolutionary History of the 'Robust' Australopithecines, (ed) Grine, F. E., New Brunswick, New Jersey: Transaction Publishers, pp. 107- 112.

Demeter, F., Zanolli, C., Westaway, K.E. et al. (2022) A Middle Pleistocene Denisovan molar from the Annamite Chain of northern Laos. *Nat Commun* 13, 2557.

Détroit, F., Mijares, A.S., Corny, J. et al. (2019) A new species of *Homo* from the Late Pleistocene of the Philippines. *Nature* 568, 181–186.

Dominy, N J. & Lucas, P. W. (2001) Ecological importance of trichromatic vision to primates, Nature 410 (6:826): 363–366.

Dominy NJ (2004) Color as an indicator of food quality to anthropoid primates: ecological evidence and an evolutionary scenario. In: Ross CF, Kay R (eds) Anthropoid Origins: New Visions. Kluwer, Academic/Plenum Publishers, New York, pp 615–644.

Durband, A.C., Kidder, J.H., Jantz, R.L., 2005. A multivariate examination of the Hexian calvaria. Anthropol. Sci. 113, 147–154.

Dunbar, R. I. M. (1993). Coevolution of neocortical size, group size and language in humans. Behavioral and Brain Sciences 16 (4): 681-735.

Dunbar, R.I.M., (1998) The social brain hypothesis. Evolutionary Anthropology, 6 (5): 178–190.

Dunbar, R.I.M., (2009) The social brain hypothesis and its implications for social evolution, Annals of Human Biology, 36:5, 562-572.

Elton, S. (2012) Impacts of environmental change and community ecology on the composition and diversity of the southern African monkey fauna from the Plio-Pleistocene to the present, In *African Genesis: perspectives on hominin evolution*, (eds) Reynolds, S.C. and Gallagher A., Cambridge, UK. Cambridge University Press, pp-471-486.

Falk, D., Zollikofer, C.P.E., Ponce de León, M., Semendeferi, K., Alatorre Warren, J.L. & Hopkins, W.D. (2018) Identification of in vivo sulci on the external surface of eight adult chimpanzee brains: implications for interpreting early hominin endocasts. *Brain, Behavior and Evolution*, 91(1), 45–58.

Falk, D., (2014) Interpreting sulci on hominin endocasts: old hypotheses and new findings, *Frontiers in Human Neuroscience*, 8:134, doi: 10.3389/fnhum.2014.00134.

Falk, D., (2008) 'Enlarged Occipital/Marginal Sinuses and Emissary Foramina: Their significance in hominid evolution', In: *Evolutionary History of the 'Robust' Australopithecines*, (ed.) Grine, F. E., New Brunswick, New Jersey: Transaction Publishers, pp. 85-96.

Falk, D., Hildebolt, C., Smith, K., Morwood, M.J., Sutikna, T., Brown, P., Jatmiko, Saptomo, E.W., Brunsden, B., & Prior, F., (2005) The brain of LB1, *Homo floresiensis*, *Science*, New Series, 308: 5719, pp. 242-245.

Falk, D. (1978). Brain evolution in Old World monkeys. *American Journal of Physical Anthropology,* 48(3), 315–319.

Falk, D., Redmond, J.C. Jr., Guyer, J., Conroy, G.C., Recheis, W., Weber, G.W., & Seidler, H., (2000) Early hominid brain evolution: a new look at old endocasts, *Journal of Human Evolution*, 38, 695–717.

Falk D. (199) Brain evolution in *Homo*: The "radiator" theory. Behavioral and Brain Sciences. 13(2):333-344.

Falk, D., (1980) Hominid brain evolution: The approach from paleoneurology, Yearbook of Physical Anthropology, 23:93-107.

Falk, D (1992) *Braindance: New Discoveries About Human Brain Evolution*, Henry Holt: New York.

Indriati, E., Swisher 3rd, C.C., Lepre, C., Quinn, R.L., Suriyanto, R.A., Hascaryo, A.T., Grun, R., Feibel, C.S., Pobiner, B.L., Aubert, M., Lees, W., Anton, S.C., (2011) The age of the 20 meter Solo River terrace, Indonesia and the survival of *Homo erectus* in Asia. PloS One 6, e21562.

Kobayashi, Y., Matsui, T., & Ogihara, N. (2018). Inferring cortical subdivisions based on skull morphology. In Digital Endocasts, Springer KK, Tokyo, Japan. pp. 33-46.

Kochiyama, T., Ogihara, N., Tanabe, H. C., Kondo, O., Amano, H., Hasegawa, K., & Akazawa, T. (2018). Reconstructing the Neanderthal brain using computational anatomy. Scientific Reports, 8(1), 6296.

Kubo, D., Tanabe, H. C., Kondo, O., Ogihara, N., Yogi, A., Murayama, S., & Ishida, H. (2014). Cerebellar size estimation from endocranial measurements: an evaluation based on MRI data. In T. Akazawa, N. Ogihara, H. C. Tanabe, & H. Terashima (Eds.), Dynamics of learning in Neanderthals and modern humans, Vol. 2. Tokyo: Springer. pp. 209–215

Fleagle, J.G. (2013) Primate Adaptation and Evolution, 3rd edition, San Diago, London; Academic

Press.

Frost, S. R., Marcus, L. F., Bookstein, F. L., Reddy, D. P., & Delson, E. (2003). Cranial allometry, phylogeography, and systematics of large bodied papionins (primates: Cercopithecinae) inferred from geometric morphometric analysis of landmark data. The Anatomical Record Part A, 275(2), 1048–1072.

Gilbert, C. C. (2011). Phylogenetic analysis of the African papionin basicranium using 3-D geometric morphometrics: The need for improved methods to account for allometric effects. American Journal of Physical Anthropology, 144(1), 60–71.

Gilbert, C. C., Frost, S. R., Pugh, K. D., Anderson, M., & Delson, E. (2018) Evolution of the modern baboon (Papio hamadryas): A reassessment of the African Plio-Pleistocene record. Journal of Human Evolution, 122, 38–69.

Gomez-Robles, A., Smaers, J.B., Holloway, R.L., Polly, P.D., & Wood, B.A., (2017) Brain enlargement and dental reduction were not linked in hominin evolution, *PNAS*, 114:3, 468–473.

Gonzales, LA, Benefit, B.R, McCrossin, M.L, Spoor F. (2015) Cerebral complexity preceded enlarged brain size and reduced olfactory bulbs in old world monkeys. Nature Comm 6:75-80.

Grabowski, M. (2016) Bigger brains led to bigger bodies? The correlated evolution of human brain and body size. *Curr. Anthropol* 57(2):174-196.

Grabowski, M., Kopperud, B.T., Tsuboi, M., Hansen, T.F. (2023) Both Diet and Sociality Affect Primate Brain-Size Evolution, *Systematic Biology*, 72: 2, 404–418.

Groves, C.P. & Mazak, V. (1975) An approach to the taxonomy of the Hominidae: Gracile Villafranchian hominids in Africa. Casopis pro Mineralogii A Geologii, 20:225-246.

Groves, C.P. (2001) Primate Taxonomy Washington and London; Smithsonian Institution Press.

Harris, L.J (1993) Handedness in apes and monkeys: some views from the past. In: Primate Laterality: Current Behavioural Evidence of Primate Asymmetries. Ward, J.P & Hopkins, W.D (eds), Springer: New York

Harirngton A, Silcox MT, Yapuncich GS, Boyer DM, Bloch JI (2016) First virtual endocasts of adapiform primates. J Hum Evol 99:52-78.

Harvati, K., Weaver, T.D. (2006). Human cranial anatomy and the differential preservation of population history and climate signatures. *Anat. Rec. A Discov. Mol. Cell. Evol. Biol*. 288, 1225–1233.

Harvey, P.H, Krebs, J.R (1990) Comparing brains. *Science* 249:150–156.

Herries, A.I.R., Martin, J.M., Leece, A.B., Adams, J.W., Boschian, G., Joannes-Boyau, R., Edwards, T.R., Mallett, T., Massey, J., Murszewski, A., Neubauer, S., Pickering, R., Strait, D.S., Armstrong, B.J., Baker, S., Caruana, M.V., Denham, T., Hellstrom, J., Moggi-Cecchi, J., Mokobane, S., Penzo-Kajewski, P., Rovinsky, D.S., Schwartz, G.T., Stammers, R.C., Wilson, C., Woodhead, J., Menter, C., (2020) Contemporaneity of *Australopithecus*, *Paranthropus*, and early *Homo erectus* in South Africa. *Science*, 368 (6486), 7293.

Holloway, R.L., (1981) The Indonesian *Homo erectus* brain endocasts revisited. *Am. J. Phys. Anthropol.* 55, 503–521.

Holloway, R. L. (1983). Human paleontological evidence relevant to language behavior. *Hum Neurobiol*, 2(3), 105–114.

Holloway, R. L. (2018). On the making of endocasts: The new and the old in paleoneurology. In: *Digital Endocasts* (eds.) Bruner, E., Ogihara, N., & H. C. Tanabe, H.C., Tokyo: Springer Japan KK, pp.

Lieberman, D. E., Pearson, O. M., & Mowbray, K. M. (2000). Basicranial influence on overall cranial shape. Journal of Human Evolution, 38(2), 291–315.

Lieberman, D. E., Ross, C. F., & Ravosa, M. J. (2000). The primate cranial base: Ontogeny, function, and integration. American Journal of Physical Anthropology, 31, 117–169.

Lieberman, D. E. (2011). The evolution of the human head. Cambridge, Massachusetts. London, England: The Belknap Press of Harvard University Press.

Louys, J., Zaim, Y., Rizal, Y., Aswan, Puspaningrum, M., Trihascaryo, A., Price, G.J., Petherick, A., Scholtz,, E., & DeSantis, L.R.G. (2021) Sumatran orangutan diets in the Lat Pleistocene as inferred from dental microwear texture analysis, Quaternary International, 603: 74-81.

Malone, N., Fuentes, A. & White F.J. (2012). Variation in the Social Systems of Extant Hominoids: Comparative Insight into the Social Behavior of Early Hominins. International Journal of Primatology 33:1251-1277.

Maddison, W. P., & Maddison, D.R. (2021). Mesquite: a modular system for evolutionary analysis. (Version 3.70), Retrieved from http://www.mesquiteproject.org

Marchant, L. (2002). 'Behavioural Diversity in Chimpanzees and Bonobos', In: Behavioural Diversity in Chimpanzees and Bonobos, (eds.) by Boesch, C. & Hohmann, G. Cambridge University Press, pp. 4-5.

Marcus, D. S., Wang, T. H., Parker, J., Csernansky, J. G., Morris, J. C., & Buckner, R. L. (2007). Open access series of imaging studies (OASIS): Cross-sectional MRI data in young, middle aged, nondemented, and demented older adults. Journal of Cognitive Neuroscience, 19(9), 1498–1507.

Martins, E. P., & Hansen, T. F. (1997). Phylogenies and the comparative method: A general approach to incorporating phylogenetic information into the analysis of interspecific data. American Naturalist, 149: 646–667.

Matsuzawa, T. (2008) Primate Foundations of Human Intelligence: A View of Tool Use in Nonhuman Primates and Fossil Hominids. In: Matsuzawa, T. (eds) Primate Origins of Human Cognition and Behavior. Springer, Tokyo. https://doi.org/10.1007/978-4-431-09423-4_1.

McCarthy, R. C. (2001). Anthropoid cranial base architecture and scaling relationships. Journal of Human Evolution, 40(1), 41–66.

McCarthy, R. C. (2004). Constraints on Primate Craniofacial Growth and Architecture. (Doctor of Philosophy). The George Washington University.

McHenry, H.M. (2012) Origin and diversity of early hominin bipedalism, In: African Genesis: perspectives on hominin evolution, (eds) Reynolds, S.C., Gallagher A., Cambridge, UK. Cambridge University Press, pp 205-222.

Meguerditchiana A, Marie, D., Margiotoudi, K., Roth, M.., Nazarian, A. J-L, Claidière N., (2002) Baboons (*Papio anubis*) living in larger social groups have bigger brains. *Evol Hum Behav*, 42:30–34.

Mitteroecker, P., Gunz, P., Bookstein, F.L., (2005). Heterochrony and geometric morphometrics: a comparison of cranial growth in *Pan paniscus* versus *Pan troglodytes*. *Evol. Dev*. 7 (3), 244–258

Moss, M.L., Young, R.W., (1960). A functional approach to craniology. *Am J Phys Anthrop* 18:281-292.

Murray, E.A, Bussey, T.J, Saksida, L.M., (2007) Visual perception and memory: a new view of the medial temporal lobe function in primates and rodents. *Ann Rev Neurosci* 30:99–122.

Neubauer, S., Gunz, P., Scott, N. A., Hublin, J. J., & Mitteroecker, P. (2020). Evolution of brain lateralization: A shared hominid pattern of endocranial asymmetry is much more variable in humans than in great apes. *Sci Adv*, 6(7).

Nolte, J. (2009) *The Human Brain: An Introduction to its Functional Anatomy*, 6th edition., Mosby Elsevier, Philadelphia, USA.

Norton, C.J., Gao, X., Liu, W., Braun, D.R., Wu, X., (2010) Central-East China- A Plio-Pleistocene Dispersal Corridor: the current state of evidence for hominin occupations. In: *Asian Paleoanthropology: from Africa to China and beyond*, *Vertebrate Paleobiology and Paleoanthropology Series*. Norton, C.J., Braun, D.R. (eds.), Springer Dordrecht, Heidelberg, London, New York, pp. 159–168.

Pearson, A., Polly, P. D., & Bruner, E. (2020). Is the middle cranial fossa a reliable predictor of temporal lobe volume in extant and fossil anthropoids? American Journal of Physical Anthropology, 172, 698–713.

Pearson, A, Polly P.D, Bruner, E (2021) Temporal lobe evolution in Javanese *Homo erectus* and African *Homo ergaster*: Inferences from the cranial base. Quat. Int 603:5-21.

Pearson, A., Bruner, E., & Polly, P.D (2023a) Updated imaging and phylogenetic comparative methods reassess relative temporal lobe size in anthropoids and modern humans, *Am J Biol Anthropol*. 1–9.

Pearson, A., & Polly, P. D. (2023b). Temporal lobe evolution in extant and extinct Cercopithecoidea. *Journal of Mammalian Evolution*, 30, 683–694. https://doi.org/10.1007/s10914-023-09664-6.

Pearson, A., & Polly, P.D (2024) Temporal lobe evolution in Hominidae and the origin of human lobe proportions, *Am J Biol Anthropol.*

Pope, G.G. (1995) The influence of climate and geography on the biocultural evolution of the far eastern hominids, In*: Paleoclimate and Evolution with Emphasis on Human Origins*, (Eds) Vbra, E.S., Denton, G.H., Partridge, T.C., Buckle, L.H.), Yale University Press, London, UK, New Haven, USA, pp-493-506.

Powell, L.E., Isler, K., Barton, R.A. (2017) Re-evaluating the link between brain size and behavioural ecology in primates. Proc. R. Soc. B, 284: 1765.

Radinsky L (1974) The fossil evidence of anthropoid brain evolution. *American Journal of Physical Anthrop*ology, 41:15–28.

Richtsmeier, J. T., & Flaherty, K. (2013). Hand in glove: Brain and skull in development and *dysmorphogenesis. Acta Neuropathologica*, 125(4), 469–489.

Rightmire G.P. (1990) *The Evolution of Homo erectus*. Cambridge University Press, Cambridge.

Rightmire, G.P. (1986) Stasis in *Homo erectus*? Stasis in *Homo erectus* defended, *Paleobiology* 12, 324–325.

Rilling, J.K. (2014) Comparative primate neurobiology and the evolution of brain language systems, Current Opinion in Neurobiology, 28:10–14.

Rilling, J. K. (2006). Human and nonhuman primate brains: Are they allometrically scaled versions of the same design? Evolutionary Anthropology, 15, 65–77.

Rilling, J. K., & Seligman, R. A. (2002). A quantitative morphometric comparative analysis of the primate temporal lobe. Journal of Human Evolution, 42(5), 505–533.

Rilling, J.K., & Insel, T.R (1999) The primate neocortex in comparative perspective using magnetic resonance imaging. *J Hum Evol*, 37(2):191–223.

Rizal, Y., Westaway, K.E., Zaim, Y., van den Bergh, G.D., Bettis 3rd, E.A., Morwood, M.J., Huffman, O.F., Grun, R., Joannes-Boyau, R., Bailey, R.M., Sidarto, Westaway, M.C., Kurniawan, I., Moore, M.W., Storey, M., Aziz, F., Suminto, Zhao, J.X., Aswan, Sipola, M.E., Larick, R., Zonneveld, J.P., Scott, R., Putt, S., & Ciochon, R.L. (2020) Last appearance of *Homo erectus* at Ngandong, Java, 117,000-108,000 years ago. *Nature*, 577, 381–385.

Rosas, A., Pena-Melian, A., Garcia-Tabernero, A., Bastir, M., & De La Rasilla, M. (2014). Temporal lobe sulcal pattern and the bony impres- sions in the middle cranial fossa: The case of the el Sidron (Spain) neandertal sample. The Anatomical Record, 297(12), 2331–2341.

Sansalone, G., Allen, K., Ledogar, J., Ledogar, S., Mitchell, D.R., Profico, A., Castiglione, S., Melchionna, M., Serio, C., Mondanaro, A., Raia, P., & Wroe, S., (2020) Variation in the strength of allometry drives rates of evolution in primate brain shape, Proc. R. Soc. B, 287.

Semendeferi, K., & Damasio, H. (2000). The brain and its main anatomical subdivisions in living hominoids using magnetic resonance imaging. Journal of Human Evolution, 38(2), 317–332.

Simons, E (1995) Egyptian Oligocene primates: a review. *Yearb Phys Anthropol*, 38:199–238.

Simons, EL, Seiffert, ER, Ryan TM, & Attia Y (2007) A remarkable female cranium of the early Oligocene anthropoid *Aegyptopithecus zeuxis* (Catarrhini, Propliopithecidae). *Proc Natl Acad Sci USA*, 104(21):8731–8736.

Stephan, H. (1972) Evolution of primate brains: a comparative anatomical investigation, In: Tuttle, R. (Ed.) The Functional and Evolutionary Biology of Primates, Aldine-Atherton, Chicago, pp. 155-174.

Stephan, H., Frahm, H., & Baron, G. (1981). New and revised data on volumes of brain structures in insectivores and primates. Folia Primatologica, 35, 1–29.

Sherwood, C.C., & Gomez-Robles, A., (2017) Brain plasticity and human evolution, *Annu. Rev. Anthropol*., 46, 399–419.

Strier, K. B. (2017) *Primate Behavioural Ecology*, 5th edition, Routledge, New York, NY, USA.

Stringer, C. (1984) The definition of *Homo erectus* and the existence of the species in Africa and Europe, CFS, 69:131-143.

Swisher, C.C. III, Curtis, G.H., & Lewin, R. (2000) Java Man. Scribner: New York, London, Toronto, Sydney, Singapore.

Tattersall, I., (2007) *Homo ergaster* and its Contemporaries, In: Handbook of Paleoanthropology, Henke, W., Tattersall, I., Hardt, T. (eds.), Springer, Berlin, pp. 1633–1654.

Teixeira, J.C., Jacobs, G.S., Stringer, C. et al. (2021) Widespread Denisovan ancestry in Island Southeast Asia but no evidence of substantial super-archaic hominin admixture. Nat Ecol Evol, 5, 616–624.

Wood, B. (1984) The origin of *Homo erectus*, CFS, 69:99-111.

Van Minh, N., & Hamada, Y. (2017). Age-related changes of sulcal imprints on the endocranium in the Japanese macaque (Macaca fuscata). *American Journal of Physical Anthropology*, 163(2), 285–294.

Zollikofer, C.P.E. and De León, M.S.P. (2013), Pandora's growing box: Inferring the evolution and development of hominin brains from endocasts. *Evol. Anthropol*., 22: 20-33.

APPENDIX A- EXTANT ANTHROPOID TAXA STUDIED

1. Introduction

In this thesis, the extant anthropoid primates studied follow the classification systems of Groves (2001) and Fleagle (2013) where the Order Primates is divided into Semiorders Strepsirrhini and Haplorrhini and the suborder Anthropoidea where the Tarsiiformes are excluded from this thesis with focus on anthropoids. In the following sections, I describe the distribution, morphological, ecological and behavioural attributes of the extant anthropoids studied throughout this dissertation. Unless noted otherwise, descriptions are my own observations.

2. Infraorder Platyrrhini

The infraorder Platyrrhini classification Groves (2001) and Fleagle (2013) where the Order Primates is divided into Semiorders Strepsirrhini and Haplorrhini and the suborder Anthropoidea with the infraorder Platyrrhini including the neotropical monkeys inhabiting South and Central America with the taxonomic classification below including the species studied indicated in bold. A general description at subfamily rank is provided below.

Order Primates (Linnaeus, 1758)

Suborder Haplorrhini (Pocock, 1918)

Infraorder Platyrrhini (Saint-Hilarie, 1812)

Family Cebidae (Bonaparte, 1831)

Subfamily Saimiriinae (Miller, 1924)

Genus *Saimiri* (Voigit, 1831)

***Saimiri sciureus* (Linnaeus, 1758)**

Subfamily Cebinae (Bonaparte, 1831)

Genus *Sapajus* (Kerr, 1792)

***Sapajus apella* (Silva, 2001)**

2.1. Genus *Sapajus*

The genus *Sapajus* includes eight species which are also known commonly as the 'robust' or 'untufted' capuchins (Groves, 2001).

2.1.1. *Sapajus apella*

The common name for *Sapajus apella* the Guinean brown capuchin. This species of capuchin is found throughout Columbia, Venezuela, and Brazil with the limits of their range extending through the Amazon Forest in the northern and southern regions of the Amazonian Delta, and into Venezuela in the south-eastern and eastern limits of the Zona dos Colas where a transitional zone of deciduous forest and scrub provide the western extent of their distribution around the interfluvial areas of the Rios Negro and Solimoes and the Rios Madeira Pueblo (Mittermier, Rylands & Wilson, 2013).

Morphologically, Guinean brown capuchins are medium-sized diurnal, semi-terrestrial neotropical monkeys. This species has a stocky torso, broad head with minimal facial prognathism face, and short limbs but possess a semi-prehensile tail and highly dexterous digits. The presence of sexual dimorphism is noted by Mittermier, Rylands & Wilson (2013) with slight variation in weight in adult males (~3.5 kg) compared to females (~2.4 kg). The pelage is long and noticeably darker on the limbs, tail than the body which does have a defined dorsal stripe. The is deep brown with longer black hairs forming the 'tuft' on the top of the head resulting in a blunt profile (Figure 2.1.).

The habitat of *Sapajus apella* is variable with the species found from 700 - 1000 metres above sea level in lowland submontane and montane forests of the Guinean and Brazilian central and eastern Amazon basin and the Delta region of the Amazon River (Mittermier, Rylands & Wilson, 2013). Brown Guinean capuchin also occurs in seasonally inundated forests flooded forests, mangrove and palm forests to savannas and open-canopied babassu palm forests (Mittermier, Rylands & Wilson, 2013).

The diet of the Guinean brown capuchin is noticeably influenced by the wet and dry seasons and resource availability (Mittermier, Rylands & Wilson, 2013). During the wet season, the diet consists of mostly of fruit (~ 70%) but during the dry season, thick-husk palm nuts are predominately consumed (~50%) with stone tool-and-anvil techniques employed to crack open these hard nut husks with foraging supplemented by some fruit (~30%), leaves, flowers, pith, and stem. With the capuchins also eat small animal prey consisting of 10% - 20% of their diet and approximately 12% comprising succulent leaf parts (Mittermier, Rylands & Wilson, 2013). The Amazon Shield has low forest productivity resulting in a group home range a between as 30 - 70 hectares and daily movements of the capuchins is much longer during the wet season when foraging is more plentiful and greater distances are travelled in source of preferred fruit (Mittermier, Rylands & Wilson, 2013).

Mittermier, Rylands & Wilson (2013) note that social group organisation includes a single dominant adult male with group size between 10-20 individuals including up to five adult females. Females reach sexual maturity at approximately five years, but males take longer and do not reach maturity until eight years (Mittermier, Rylands & Wilson, 2013). Infants are born singuallrly (not into litters or multiple births) with a noted rapid neonatal growth in the first eight weeks after birth followed by a slowing stage and interestingly for a male-dominated species, the adult males appear

directly involved in infant care and are noted to be very tolerant of the infants and juveniles in their group (Mittermier, Rylands & Wilson, 2013).

Figure 2.1-1. An image of *Sapajus apella* from the Canberra National Zoo and Aquarium, Australia © Alannah Pearson.

2.2. Genus Saimiri

The genus *Saimiri* includes seven species and are commonly known as the squirrel monkey (Groves, 2001).

2.2.1. *Saimiri sciureus*

Saimiri sciureus is commonly known as the Guinean squirrel monkey. This species of neotropical monkey inhabit Guiana and Northern Brazil, specifically regions of with the northern Amazon River from the Rios Negro and Demini to the eastern limits at the Rio Pindare and a southern extent of the distribution to the upper reaches of the Rio Xingu (Mittermier, Rylands & Wilson, 2013). Morphologically, these monkeys are small-bodied with noticeably longer hind-limbs than forelimbs and do possess a semi-prehensile tail. The head appears relatively larger and

more rounded than the capuchins and there is no significant sexual dimorphism. In general, males are very slightly larger (~950g) than females (~850g) (Mittermier, Rylands & Wilson, 2013). The pelage appears greyish to buff-coloured with yellow-fawn forelimbs, hands and feet and a distintly pink face with black muzzle and top of the head. These monkeys also have markedly white brow arches and white ear tufts.

The habitat of *Saimiri sciureus* is quite variable with extensions from mature forest, lowland rainforest and seasonally inundated forests mangrove and swamp forests (Mittermier, Rylands & Wilson, 2013). The diet of the Guinean squirrel monkey is variable and like the Brown capuchin is dependent on wet and dry seasons of the neotropics. Mittermier, Rylands & Wilson (2013) discuss the diet as consisting mostly of insects, fruit, flowers, nectar, seeds, gums, some small lizards and bird eggs. There is a noted higher consumption of insects during the dry season (~74%) compared to the wet season (~54%) when more time was spent on foraging for fruit and seeds which are more plentiful during dry season but this results in less time engaging in social behaviour compared to the wet season (Mittermier, Rylands & Wilson, 2013). In general, *Saimiri sciureus* has a large home range is between 110-123 ha and little difference noted in travelling through range between wet or dry seasons (Mittermier, Rylands & Wilson, 2013). Regardless of the season, the travelling time and use of the range does not differ with changes to food sources.

The social organisation of *Saimiri sciureus* differs from the capuchins, *Sapajus apella.* with a large female-dominated multimale, multifemale groups with between 44-55 individuals (Mittermier, Rylands & Wilson, 2013). Females reach sexual maturity at much earlier than males at approximately 2 years with males not reaching sexual maturity until much later around years with an extended subadult interval (Mittermier, Rylands & Wilson, 2013). Further, a single infant is born with care for infants shared between female members of the group and unlike *Sapajus*

apella, squirrel monkey males do not appear to share interest in parental care (Mittermier, Rylands& Wilson, 2013).

Figure 2.2-1. An image of *Saimiri sciureus* from Mogo Zoo, Australia © Alannah Pearson.

3*. Infraorder Catarrhini*

The Infraorder Catarrhini includes the old-world monkeys, small and great apes inhabiting Africa, Asia, and isolated parts of Europe. Taxonomic classification follows the description below with species studied indicated in bold.

Order Primates (Linnaeus, 1758)

Suborder Haplorrhini (Pocock, 1918)

Infraorder Catarrhini (Saint-Hilarie, 1812)

Superfamily Cercopithecoidea (Gray, 1821)

Family Cercopithediae (Gray, 1821)

Subfamily Cercopithecinae (Gray, 1821)

Tribe Papioini (Burnett, 1828)

Genus *Macaca* (Lacepede, 1799)

***Macaca mulatta* (Zimmerman, 1780)**

Genus *Papio* (Erxleben, 1777)

***Papio anubis* (Lesson, 1827)**

Genus *Cercocebus* (Saint-Hilarie, 1812)

***Cercocebus atys* (Audebert, 1797)**

Superfamily Hominoidea (Gray, 1825)

Family Hylobtaidae (Gray, 1870)

Genus *Hylobates* (Illiger, 1811)

***Hylobates lar* (Linnaeus, 1771)**

Family Hominidae (Gray, 1825)

Subfamily Ponginae (Elliot, 1912)

Genus *Pongo* (Lacepede, 1799)

***Pongo pygmaeus* (Linnaeus, 1760)**

Pongo abelii (Lesson, 1827)

Subfamily Homininae (Gray, 1825)

Genus *Gorilla* (Saint-Hilaire, 1853)

***Gorilla gorilla* (Savage, 1847)**

Genus *Pan* (Oken, 1816)

***Pan troglodytes* (Blumenbach, 1799)**

***Pan paniscus* (Schwarz, 1929)**

Genus *Homo* (Linnaeus, 1758)

***Homo sapiens* (Linnaeus, 1758)**

3.1. Genus *Macaca*

The genus *Macaca* includes twenty-two recognised species and commonly known as macaques (Groves, 2001).

3.1.1. *Macaca mulatta*

The common name for *Macaca mulatta* is the rhesus macaque which have a very broad distribution inhabiting regions from southern and Southeast Asia from Nepal, Bangladesh, India, north-east China to Myanmar. Morphologically, *Macaca mulatta* is a medium-sized old-world monkey but unlike most cercopithecines, there is minimal sexual dimorphism with females only slightly smaller (~6 kg) than males (~9 kg) (Zinner, Fickenscher & Roos, 2013). The rhesus macaque pelage of the body varies from golden-brown to orange with a black crown of the head, back of the neck and cheeks but the face has pinkish, red to brown skin pigmentation without hair.

Macaca mulatta has very variable habitat but some populations are more arboreal in forested regions compares to non-forested regions where populations are more are semi-terrestrial with the habitat extending from sea level to as high an elevation as 2000 metres above sea level (Zinner, Fickenscher & Roos, 2013). The habitat is highly variable with environments from deciduous forests and scrub, evergreen forests and montane forests to tidal swamps but also within human occupied areas and co-habitation with humans among urban, rural areas and temples (Zinner, Fickenscher & Roos, 2013). Despite variable habitats, rhesus macaques have extensive home ranges of approximately 194 hectares which overlap with other groups and often result in antagonism with different areas of the home range are used seasonally dependent on resource availability (Zinner, Fickenscher & Roos, 2013). Noted by Zinner, Fickenscher & Roos (2013)

the diet of this species is variable including fruit, seeds and flowers to foliage such as leaves, bark, shoots, stems and but also gums and fungi and some animal matter supplementation from insects crab, crayfish to fish and bird eggs.

The social organisation of *Macaca mulatta* comprises large multimale, multifemale groups with males only slightly more dominant than females with females reach sexual maturity at approximately 4 years while males do not reach sexual maturity until several years later at approximately 6 years (Zinner, Fickenscher & Roos, 2013). Infants are born singular and weakened quite quickly within three months but there is an extended nursing stage that may continue for as long as one year (Zinner, Fickenscher & Roos, 2013).

Figure 3.3.1-1. Image of *Macca mulatta* (Zinner, Fickenscher & Roos, 2013).

2.2. Genus *Papio*

The genus *Papio* includes six species which are commonly known as baboons (Groves, 2001).

3.2.1. *Papio anubis*

Papio anubis is commonly named the olive baboon is a terrestrial old-world monkey attributed to the subfamily Cercopithecine. *Papio anubis* is located throughout the northern savannas of Mali, Guinea and Sierra Leone with a western distribution extending to Eritrea and western Ethiopia and the southern limits along the north and eastern borders of Democratic Republic of Congo and northwest Tanzania. There are also isolated populations found in the Tibesti, Ennedi and Air Mastiffs in the Sahara (Zinner, Fickenscher & Roos, 2013).

Morphologically, *Papio anubis* similar to many cercopithecines are very sexually dimorphic with males much larger (~26kg) than females (~16kg) (Zinner, Fickenscher & Roos, 2013). *Papio anubis* is diurnal and terrestrial with a noticeably long-snout and longer forelimbs than hind limbs and pelage which is olive-brown coloured in both sexes and also black hands and feet with the tail often long but carried upward and bent over the back (Zinner, Fickenscher & Roos, 2013). There are ischial callosities in both sexes and noticeable sexual swelling in females.

The habitat of *Papio anubis* is very broad and extends from semi-desert, open savanna to scrub and open forests and into rainforests with elevations up to 2500 metres above sea level and into human cultivated farmlands (Zinner, Fickenscher & Roos, 2013). The diverse habitat is also reflected by a largely omnivorous and frugivorous diet which is sustained by opportunistic foraging where diet varies depending on the habitat and seasonal fluctuations but includes fruit, leaves, flowers, tubers, roots and grasses, bark, fungi and seeds with additional faunal matter including invertebrates, lizards, birds and even small mammals and small primates (Zinner, Fickenscher & Roos, 2013).

The social organisation of Papio anubis comprises large multimale, multifemale groups (~20-120 individuals) with a single dominant male with females reaching sexual between four to

seven years old and males reaching sexual maturity later at approximately seven to ten years old (Zinner, Fickenscher & Roos, 2013). Infants are born throughout the year but only one infant at a time and during breeding times, males and females form a temporary courtship during mating and females are observed to form alliances with other males which may serve to protect offspring during male-male aggression and reduce infanticide risk (Zinner, Fickenscher & Roos, 2013). Additionally, females form dominance hierarchies with high-ranking mothers support their daughters during intragroup conflicts with female dominance hierarchies inheritable from mother to daughter with a dominant female line potentially remaining stable over several generations (Zinner, Fickenscher & Roos, 2013).

Figure 3.2. An image of *Papio anubis* (Zinner, Fickenscher & Roos, 2013).

3.3. Genus *Cercocebus*

The genus *Cercocebus* comprises seven species commonly known as mangabeys (Groves, 2001).

3.3.1. *Cercocebus atys*

Cercocebus atys is commonly known as the sooty mangabey is a semi-terrestrial and arboreal quadrupedal old-world monkey attributed to the subfamily Cercopithecine. *Cercocebus atys* is located throughout southwest Senegal, Guinea-Bissau and extending to west and southeast Guinea, Sierra Leone, Liberia, Western Ivory Coast with the eastern limits of the distribution at the Nzo-Sassandra River system (Zinner, Fickenscher & Roos, 2013). Morphologically, *Cercocebus atys* is diurnal and mostly terrestrial and less sexually dimorphic than other mangabey species with females (~6.3kg) smaller than males (~ 10.5kg) with pelage colouring generally grey with darker hands and feet and dark greyish-pink face with paler, long whiskers on the cheeks(Zinner, Fickenscher & Roos, 2013).

The habitat for *Cercocebus atys* includes primary and secondary forest types, dry swamp to mangrove estuaries, savanna to tropical evergreen forests and occasionally into human cultivated farmlands (Zinner, Fickenscher & Roos, 2013). Diet consists primarily of fruit, seeds, leaves and flowers (~98.7%) with only a small amount of faunal matter (~1.3%) but observations of populations located in the Tai Forest National Park include a much higher proportion of faunal matter (~26%) than other populations located elsewhere (Zinner, Fickenscher & Roos, 2013).

Social organisation in *Cercocebus atys* comprises of very large multimale-multifemale groups with single a dominant male (~120 individuals) with sexual maturity in the wild is uncertain but captive females are observed at approximately five years old with a single infant born and in the wild there are distinct breeding seasons with females copulating both with the dominant male but also subordinate males (Zinner, Fickenscher & Roos, 2013). Females are observed to form closely related dominance hierarchies with other females, but adult males are always dominant to females (Zinner, Fickenscher & Roos, 2013).

Figure 3.3.-1 An image of *Cercocebus atys* © Adrien Groul https://www.inaturalist.org/observations/153509104

3.4. Genus *Hylobates*

The genus *Hylobates* is more commonly known as the lar gibbons have five recognised species (Groves, 2001).

3.4.1 *Hylobates lar*

Hylobates lar is commonly known as the lar gibbon or the white-handed gibbon is a small ape species which is located throughout the island of Sumatra, Indonesia, the Malay Peninsula, Malaysia and extending into Myanmar and Thailand (Chivers, 2013). Morphologically, *Hylobates lar* diurnal, arboreal brachiating small apes habitually with no discernible sexual dimorphism with females minimally smaller (~5kg) than males (~6kg) (Chivers, 2013).

Hylobates lar possess the same adaptions as other small apes with extreme elongation of the upper limbs arms and a specialised wrist to allow for brachiation with reduced lower limbs resulting in an awkward bipedal locomotion along branches but also on occasionally on the ground.

Unlike other small ape species of *Nomacus* or *Hoolcok*, the pelage colouring in *Hylobates lar* is not sex or age-related differences with male or female colouring black or buff-coloured but both sexes have white hands and feet, naked black skin on the face surrounded by white coloured ring.

Hylobates lar inhabit a variable environment from lowland forests, deciduous and evergreen forests, wet evergreen but also peat-swamp forests below 1200 metres above sea level. (Chivers, 2013). Diet is somewhat variable with there is a preference is for seasonal sweet ripe fruit when during the wet season but during the cool dry season, diet becomes more diversified to include younger leaves, flowers and buds and also can include the faunal matter and of bird eggs (Chivers, 2013).

Social organisation for *Hylobates lar* is generally a bonded pair with offspring in the social group but the species may also form polyandrous groups with a single adult female and two adult males and monogamous pairing or polyandrous may occur over the lifetime of a female with sexual maturity reached earlier for females (~9 years) than males (~10 years) with single infant births and considerable time spent on postnatal care (Chivers, 2013). Infant care is mostly conducted by the female, but older siblings and the male may assist at times with infants able to brachiate by nine months and are weaned by approximately two years with adult females able to have offspring every three to five years (Chivers, 2013).

Figure 3.4.1. An image of *Hylobates lar* from Melbourne Zoo © Alannah Pearson.

3.5. Genus *Pongo*

The genus *Pongo* is commonly known as the orangutan is a great ape with three recognised species (Groves, 2001; Nater et al., 2017).

3.5.1. *Pongo pygmaeus*

Pongo pygmaeus is commonly known as the Bornean orangutan and is located in regions throughout Malaysia and Indonesia but more specifically in fragmented forested areas of north and eastern Borneo in Sabah State, extending into western Borneo in South Sarawak State and in Indonesian Borneo in Northwest Kalimantan, East Kalimantan, southwest and Central Kalimantan provinces of Indonesia (Williamson, Maisels & Groves, 2013). Morphologically, *Pongo pygmaeus* are large-bodied diurnal, semi-arboreal great apes with elongated forelimbs for suspensory feeding and employing a clinging and grasping locomotion with hands and feet used interchangeably

during both feeding and locomotion. Compared to other orangutan species, *Pongo pygmaeus* stockier and much heavier and exhibits more extreme sexual dimorphism with males (~47.5kg) larger than females (~37.5kg) and 'flanged' males who have undergone a secondary maturation process with substantially increased body mass (~72.5kg) (Williamson, Maisels & Groves, 2013). The pelage in *Pongo pygmaeus* darker brown-reddish with longer hair and flanged males developing large, dark skinned cheek pads and a prominent throat sac and unlike Sumatran orangutan species there is no prominent beard or moustache.

Habitat for *Pongo pygmaeus* includes fragmented forests separated by impassable mountains and rivers natural barriers with mature riverbank, freshwater swamp, peat-swamp, lowland forests up to elevations of 500 metres above sea level and are also found in young and secondary forests and less frequently in montane forests (Williamson, Maisels & Groves, 2013). Diet is predominantly fruit but supplemented with seeds, flowers, shoots and bark while infrequently small vertebrates with seasonal fluctuations affecting fruit abundance which is worsened by the El Nino La Niña oscillations across the tropical eastern Pacific Ocean leading to prolonged drought and consumption the inner bark of trees and harder seeds while wet monsoon seasons provide an abundance fruit, succulent seeds and allow for the accruing fat reserves to sustain individuals during food scarcity (Williamson, Maisels & Groves, 2013).

Social organisation is mostly solitary with adult males semi-solitary and a large home range that overlaps with more than one adult female which may have up to one or two dependent offspring (Williamson, Maisels & Groves, 2013). A single infant is weaned at approximately five years where they become increasingly independent are still associated with their mother until eight years old or more in which both male and female offspring will disperse from the natal group. Sexually mature and dominant flanged males use 'long call' vocalisation to alert females and other

males in the area to their location in which the dominant flanged male does not tolerate other flanged males and unflanged males are known to avoid flanged males but still gain access to females for mating (Williamson, Maisels & Groves, 2013).

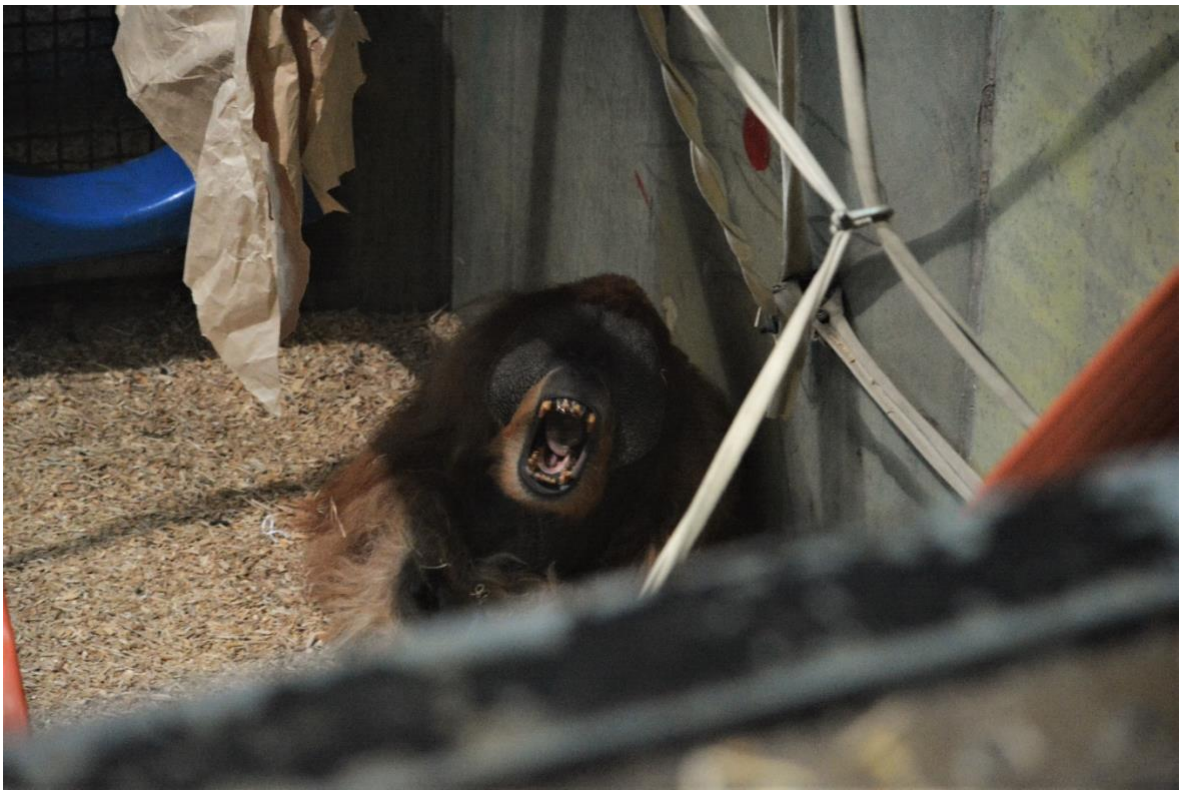

Figure 3.5.1. An image of flanged male *Pongo pygmaeus* from Melbourne Zoo © Alannah Pearson.

3.6. Genus *Gorilla*

The genus *Gorilla* has recognised two species *Gorilla gorilla* (Western Gorilla) with two subspecies the Cross River Gorilla (*Gorilla gorilla diehli*) and the Western Lowland Gorilla (*Gorilla gorilla gorilla*), while *Gorilla beringei* (Eastern gorilla) has two subspecies the Mountain gorilla (*Gorilla beringei beringei*) and the Eastern lowland gorilla (*Gorilla beringei graueri*) (Groves, 2003).

3.6.1. *Gorilla gorilla*

Gorilla gorilla is commonly known as the Western gorilla and is located in southern Cameroon, south-western Central African Republic, Equatorial Guinea, Gabon, Republic of Congo, and North Angola (Williamson, Maisels & Groves, 2013). Morphologically, *Gorilla gorilla* exhibits significant sexual dimorphism with males (~168kg) larger compared to females (~65kg) (Williamson, Maisels & Groves, 2013).The pelage is brown-black except for a completely black naked face, hands and feet and in older adult males, the chest has brownish hair and the midback turns greyish-white (commonly known as a 'silverback') and some adult males may have chestnut coloured hair on the crown of the head. Adult males develop secondary sexual characteristics including large *masseter* and *temporalis* muscles which attach to large sagittal crests, possess large canine teeth and incisors.

Habitat of *Gorilla gorilla* include lowland forest types from open and closed canopies, moist and seasonally inundated forests, vast swamplands at below 500 metres above sea level (Williamson, Maisels & Groves, 2013). Diet consists primarily of ripe succulent fruits and herbaceous vegetation including leaves, stems and shoots and during dry seasons when fruit is scarce, protein-rich mature leaves are supplemented (Williamson, Maisels & Groves, 2013).

Social organisation in this species consists of cohesive group with a single dominant adult male, multiple females and their offspring and occasionally immature males (~16 individuals) with females reaching sexual maturity (~10 years) but males are much later (~18 years) and infants are born singularly and there is a long period of postnatal care until an infant is weaned at approximately five years old (Williamson, Maisels & Groves, 2013).

Figure 3.6.1. An image of adult male *Gorilla gorilla* from Mogo Zoo © Alannah Pearson.

3.7. Genus *Pan*

The genus *Pan* consists of two extant species *Pan paniscus* commonly known as the bonobo and *Pan troglodytes* known as the Common Chimpanzee (Groves, 2001).

3.7.1. Pan troglodytes

Pan troglodytes is known as the common chimpanzee and located across wide band across central Africa including southeast Cameroon, southwestern and eastern Central African Republic, extending into the Democratic Republic of the Congo west of the Ubangi River, Equatorial Guinea, Gabon, northern and eastern Democratic Republic of the Congo, regions of southeastern Nigeria, western and central Cameroon, southwestern South Sudan, western Uganda, Rwanda, Burundi and western Tanzania, and into southern Senegal, Guinea-Bissau Liberia, Sierra Leone, Ivory Coast, Liberia and Ghana (Williamson, Maisels & Groves, 2013). Morphologically, Pan troglodytes

exhibit sexual dimorphism with males (~49kg) larger than females (~35kg) (Williamson, Maisels & Groves, 2013). The pelage is long and black but can become grey on the rump in older adults and both sexes may have bald crown with age. The hands, feet, face and ears are naked pinkish-skin which may darken with age and there are distinct brow ridges.

Habitat in *Pan troglodytes* varied mature, moist and closed-canopies, lowland, submontane, montane, secondary swamp and gallery forests and extending into dry forest, open woodland and savanna (Williamson, Maisels & Groves, 2013). Diet is varied as *Pan troglodytes* is an noted opportunistic forager with most subspecies engaging in some form of coordinated social hunting of small primate prey including red colobus monkeys, termite nest foraging and stone tools use to open hard-husked seeds but generally, the species is frugivorous with leaves, stems, flowers, bark, honey, fungi, bird eggs, invertebrates and faunal matter consumed Williamson, Maisels & Groves, 2013).

Social organisation consists of a large multimale-multifemale group (~35 or more individuals) with fission-fusion society employed during food abundance or shortages with sexual maturity occurring in females and males at approximately 15 years and males dominant to females and infants are born singularly and not weaned until five years where until then they are dependent on adults (Williamson, Maisels & Groves, 2013).

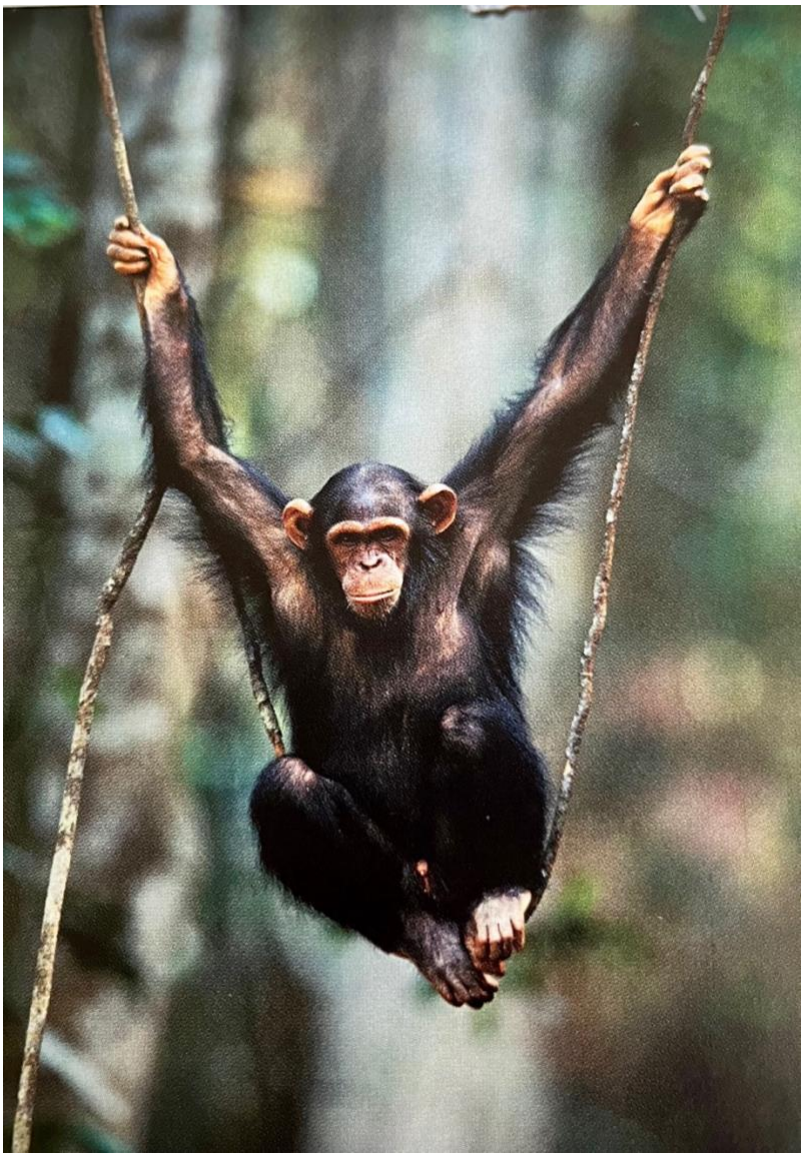

Figure 3.7.1. An image of *Pan troglodytes* from Williamson, Maisels & Groves (2013).

3.7.2. *Pan paniscus*

Pan paniscus commonly called the bonobo is located in the Central Democratic Republic of Congo in a basin formed by the bend in the Congo River which is the north and western extent of the distribution, to the east by Lualaba River and to the Kasai/Sankuru Rivers in the south where these major waterways are a natural barrier separating *Pan paniscus* from *Pan troglodytes* and *Gorilla gorilla* on the other side (Groves, 2001). Morphologically, Pan paniscus exhibits moderate sexual dimorphism compared to Pan troglodytes with males (~39.5kg) larger than females (~31kg)

(Williamson, Maisels & Groves, 2013). *Pan paniscus* is similar in appearance to *Pan troglodytes* but for some notable exceptions including longer more gracile limbs, slenderer trunk, a rounded head that appears to be relatively smaller than *Pan troglodytes* and pelage which is black throughout with black hands, feet and face with the exception of pinkish lips.

Pan paniscus inhabit closed, moist and mixed, mature and secondary forests and also seasonally inundated swamp forests and extending mosaic forest, dry forest, marshy grasslands even and savanna open-woodlands (Williamson, Maisels & Groves, 2013). Diet is predominately frugivorous with leaves, stems, new shoots, flowers, seeds, bark, fungi and aquatic plants supplemented with the consumption of invertebrates, faunal matter including and small primates (Williamson, Maisels & Groves, 2013).

Social organisations consist of fission-fusion society like *Pan troglodytes* and groups are medium-to-large multimale- multifemale (~20 individuals) with sexual maturity in females later (~14 years) later than males (~10 years) and infants are born singularly and not weaned until approximately five years old (Williamson, Maisels & Groves, 2013). There is no specific breeding season, and copulation is a daily occurrence, and adult males are known to form friendly pair-relationships with unrelated adult females to form coalitions to support each other against other individuals. Adult females are considered co-dominant to males but there is usually a dominant male which mates with the females and female hierarchy determines male social hierarchy (Williamson, Maisels & Groves, 2013).

Figure 3.7.2.2. An image of *Pan paniscus* (Williamson, Maisels & Groves, 2013).

3.8. Genus *Homo*

The genus *Homo* comprises only one extant species. The ecological descriptions provided follow Fleagle (2013) and Bogin (2005).

3.8.1. *Homo sapiens*

Homo sapiens commonly known as modern humans and are the only extant species of the genus *Homo* with a unique distribution for great apes which extends across every continent in a global distribution. Morphologically, *Homo sapiens* are slightly sexually dimorphic with larger body mass in males (~62.5kg) than in females (~57.5kg) (Fleagle, 2013). The body is absent of thick hair except on the head and pubic regions in both sexes with males developing facial hair and more body hair at puberty and there is no facial prognathism with the face tucked well beneath the brow ridges and *Homo sapiens* utilise obligate bipedalism. Skin colour is variable between populations and is largely dependent on melanin absorption through darker skin colouring in

equatorial regions where more direct sunlight is received and paler skin tones north of the equator where there is less exposure to direct sunlight (Bogin, 2005). Melanin is necessary to synthesise vitamin D and in populations in the Arctic regions where there are slightly darker skin tones are related to the consumption of higher vitamin D marine resources (Bogin, 2005). Limb proportions are strongly correlated with Allen and Bergman rules where physiological adaptations for longer limbs and a narrower trunk in equatorial regions to increase body cooling by drawing heat away from the core and into the limbs while shorter limbs and a stockier trunk occurs in colder regions to maintain heat within the core and prevent heat loss through the limbs (Bogin, 2005).

Diet in *Homo sapiens* is omnivorous with the consumption a variety of food sources from domesticated flora and fauna where the development of agriculture has allowed for the fast processing of food sources and a greater reliance more recently, on pre-processed food sources which have a higher calorie and salt and may be associated with the development of obesity in some populations (Fleagle, 2013).

Figure 3.8.1 An image of modern *Homo sapiens.* Image © Alannah Pearson.

APPENDIX B- EXTINCT ANTHROPOID TAXA STUDIED

1. Introduction

In this thesis, the extinct anthropoid primates studied follow the classification systems of Groves (2001), Hartwig (2002) and Fleagle (2013) where the Order Primates is divided into Semiorders Strepsirrhini and Haplorrhini and the suborder Anthropoidea where the Tarsiiformes are excluded from this thesis with focus on anthropoids. The following sections provide a context for extinct specimens studied throughout this dissertation with fossil site descriptions, site dating and the associated fossil anthropoid classifications attributed to recovered fossil remains. In the later sections, I provide the morphological and endocranial descriptions of the fossil anthropoids studied throughout this dissertation. Unless noted otherwise, descriptions are my own observations.

2. *Fossil Site Descriptions*

The following section describes the key fossil sites associated with the fossil specimens studied in this thesis and includes a wide geographical range and geological timespan with sites from Africa, South America, Southeast Asia, Middle East and Europe dated to between 40 million years ago to 30 thousand years ago.

2.1 Rio Gallegos

The Rio Galleogos site dates from the Middle Miocene (~16.5 million years ago) from the Santa Cruz Formation located on the Atlantic coast of southern Argentina, South America. Deposits dated to the Santacrucian (Early Miocene) are located on the banks of the Rio Gallegos

River near the town of Rio Gallegos, southern Argentina and give the site its namesake. Fossil primate material recovered from these deposits include a partial cranium, mandibular remains and a partial skeleton attributed to the stem-platyrrhine, *Homunclus patagonicus* (Fleagle & Tejedor, 2002).

2.2. Gaiman

The Gaiman site includes deposits dated from the Colhuehuapian Land Mammal Age (Early Miocene) and is located near Gaiman in Chubut Province, Argentina, South America. Fossil primate material recovered from the site includes a very damaged but mostly complete skull, several mandibular fragments, numerous isolated teeth and a talus which are attributed to the stem-platyrrhine, *Dolichocebus gaimensis* (Fleagle & Tejedor, 2002).

2.3. Sacanana

The site of Sacanana includes deposits dating to the Colhuehuapian (Early Miocene) and is located in northern Chubut, Argentina, South America. The fossil primate material recovered from the site includes a mostly complete skull attributed to the stem-platyrrhine, *Tremacebus harringtoni* (Fleagle & Tejedor, 2002).

2.4. Fayum

The Fayum Depression is a rich bearing fossil site located on expansive eroded eastern edge of the Sahara Desert in Egypt. The site provides a sequence of fossiliferous sedimentary deposits which contain an exceptional record of early mammalian evolution in Africa from the Late Eocene and Early Oligocene. The primate fossil material has been recovered from the Jebel Qatrani Formation with deposits that date from the Late Eocene to the Early Oligocene (Beard,

2002; Rasmussen, 2002). The fossil primate material which has been recovered from three levels of the Jebel Qatrani Formation include the uppermost levels (Quarries M, I) with stem-anthropoids attributed to *Apidium phiomense*, and stem-catarrhines attributed to *Aegyptopithecus zeuxis* and *Parapithecus grangeri*. The middle level deposits (Quarries G, V) contain many intermediate or transitional species and the lowest deposits in the sequence (Quarries E and L-41) date from the Late Eocene to Early Oligocene with fossil primates attributed to the stem-anthropoids *Catopithecus browni* and *Proteopithecus sylviae* (Beard, 2002; Rasmussen, 2002).

2.5. Maboko Island

Maboko Island site contains highly fossiliferous deposits located on Maboko Island, Lake Victoria in Kenya and dated to the Middle Miocene. Fossil primate remains that have been recovered include hundreds of dental and cranial elements, a nearly complete cranium and postcranial remains attributed to the fossil cercopithecoid, *Victoriapithecus macinnesi* (Benefit, 2002).

2.6. Lateoli

The site of Lateoli is located on the Serengeti Plains in northern Tanzania, approximately 40 km south of the other fossil site Olduvai Gorge (Schwartz & Tattersall, 2003). Fossil remains recovered from the deposits include a mostly complete calvaria and maxilla and part of the nasal region which is known as LH-18 and was recovered in-site from the surface of overlying Ngaloba Beds and attributed to fossil *Homo sapiens* where the dating of the Ngaloba Beds is approximately 120 thousand years ago based on the adjacent tuff and supported by U-series dating of the fossil bone which yielded a date range between 129 -108 000 years ago (Schwartz & Tattersall, 2003).

The archaeological context of the site is associated with stone tools from the Middle Stone Age assemblage (Schwartz & Tattersall, 2003).

2.7. Swartkrans

The Swarrtkrans site is a breccia-filled cavity located approximately 10km northwest of Krugcrsdorp, Gauteng Province in South Africa and about 2km from the other fossil bearing-site of Sterkfontein (Shwartz & Tattersall, 2005), The dating of the site has proved difficult with a solution-filled cavity with a complicated taphonomic history of infill and subsequent collapse. There are two recognised sections to the site with a pink breccia known as the Outer Cave and the stratified brown breccia partial- filled Inner Cave while the Outer Cave consists of breccias accumulated over different time periods, while the pink breccia which is fossil hominin-bearing is an isolated 'hanging remnant' that has adhered to the northern wall of the cave and undercut by an erosional surface (Shwartz & Tattersall, 2005). Swartkrans Members 1-3 is faunally estimated to date between approximately l.8-1.5 million years ago with fossil remains attributed to *Paranthropus* hominin species (Shwartz & Tattersall, 2005) and to fossil papionin species *Dinopithecus ingens* (Jablonski, 2002).

2.8. Taung

Taung is a fossil bearing site which is fissure filled by flowstones and located at the Northern Lime Company Works approximately 10km south-west of Taung, Northern Cape, South Africa (Shwartz & Tattersall, 2005). Fossil remains recovered from the deposits are attributed to *Australopithecus* hominin species (Shwartz & Tattersall, 2005) and fossil papionin *Papio angusticeps (idolzi*) (Jablonski, 2002).

2.9. Sterkfontein

The site of Sterkfontein is an in-filled cavity of dolomitic limestone and located approximately 10km Northwest of Krugersdorp, Gauteng province, South Africa (Shwartz & Tattersall, 2005). Fossils remains recovered from the site are attributed to s *Australopithecus* and *Paranthropus* from Member 4 and a juvenile cranium attributed to *Homo erectus* (Herries et al., 2020; Schwartz & Tattersall, 2005). The deposits of Member 4 are dated to proximately 2.0-1.7 million years ago (Shwartz & Tattersall, 2005) and there are two archaeological assemblages present in the site with earlier Oldowan lithics and later Acheulean artefacts recovered from Member 5 (Shwartz & Tattersall, 2005),

2.10. West Turkana

West Turkana is a fossil collecting region located to the west of Lake Turkana, northern Kenya and Omo Shungura, Ethiopia (Shwartz & Tattersall, 2005). Dating has relied on the geochemical correlation of tuffs which correspond to the Ethiopian Shungura Formation sequence of fluvial sediments. Fossils recovered from the site have been attributed to *Australopithecus from the* Nachukui Formation and *Paranthropus aethiopicus* from Lomekwi I below an ash fall which corresponds to Shungura Tuff D dated to approximately 2.50 million years ago (Shwartz & Tattersall, 2005). The archaeological context includes Oldowan lithic assemblages recovered throughout the Nachukui Formation but there is no evidence directly linking any of the stone tools with a specific early hominin species (Shwartz & Tattersall, 2005).

2.11. Koobi Fora

The site of Kooobi Fora consists of an area east of Lake Turkana, northern Kenya and extending south along the eastern shore of Lake Turkana from Ileret in the north to Allia Bay in

the south (Shwartz & Tattersall, 2002; 2005). Initial dating problems were encountered with series of lacustrine and fluvial deposits interspersed with numerous volcanic tuffs and complex local faulting. Koobi Fora is now known to have three stratigraphically contiguous members (the Burgi, KBS and Okotc) which span from 2.7-1.4 million years ago. Fossil remains recovered from the site have been attributed to *Paranthropus boiesi*, *Homo habilis* and *Homo ergaster* (Shwartz & Tattersall, 2002; 2005).

2.12. Olduvai Gorge

The site of Olduvai Gorge is situated on the Serengeti Plains approximately 50km north of Lake Eysai where the gorge cuts through recent deposits (Shwartz & Tattersall, 2002). The fossil bearing strata rest on a lava base and is consist of a series of volcanic tufts and lacustrine, fluviatile and wind-blown deposits which are numbered Beds 1-5 (Shwartz & Tattersall, 2002). Fossil hominin remains recovered from this site are attributed to is *Paranthropus boiesi* (Shwartz & Tattersall, 2005).

2.13. Broken Hill (Kabwe)

The Broken Hill (Kabwe) mine site is located in Zambia, southern Africa. The former mine site includes two dolomitic limestone hills containing lead and zinc ore which were tunnelled and discovered to be highly fossiliferous (Shwartz & Tattersall, 2002). Fossil remains from the site include the Kabwe skull and femur which were recovered from the deepest deposits but mining destroyed the original cave site (Shwartz & Tattersall, 2002). The fossil hominin remains recovered from the site are attributed to *Homo heidelbergensis* (Shwartz & Tattersall, 2003).

2.14. Mugharet-es Skhul

The Mugharet-es Skhul rock shelter site is located on the western slope of Mount Carmel overlooking the Wadi-el Mughara region in the Middle East where the site ispenetrated by many hollowed caves set deep into limestone escarpment (Shwartz & Tattersall, 2003). The smallest of these caves is the rock shelter site known as Mugharet-es Skhul which site includes several archaeological layers of lithics, worked fossil mammal bones and at least ten deliverable burials (Shwartz & Tattersall, 2003). The fossil material recovered from the site includes and a well-preserved skull and some postcranial material which are attributed to *Homo sapiens* (Shwartz & Tattersall, 2003).

2.15. Tabun Cave

Tabun Cave site cave is located in the Wadi-el Mughara region on the western flank of Mount Carmel range, approximately 9km south of Haifa, Israel (Shwartz & Tattersall, 2003). The skeletal material includes a fragmentary cranium, and partial postcranial elements of a small individual presumed to be female which are attributed to *Homo neanderthalensis* (Shwartz & Tattersall, 2003).

2.16. La Ferrassie

The site of La Ferrassie is located just in the Dordogne region, France with site consisting of a rock shelter with three levels of deposits dated to the Aurignacian period and skeletal remains recovered between the Aurignacian layers and a lower layer dated to the Mousterian (Shwartz & Tattersall, 2003). Fossil hominin remains recovered are attributed to *Homo neanderthalensis* (Schwartz & Tattersall, 2003).

2.17. La Chapelle-aux-Saints

The site of La Chapelle-aux-Saints is located near the village bearing its namesake in France where site is a hollowed limestone cave containing a calcareous clay and fallen debris from the cave ceiling (Shwartz & Tattersall, 2003). Fossil hominin remains recovered are attributed to *Homo neanderthalensis* (Schwartz, & Tattersall, 2003).

2.18. Sangrian

The site of Sangiran is located on the Jemoro River, a tributary of the Solo River in Central Java, Indonesia (Schwartz & Tattersall, 2002).The site deposits consist of river sandstone, conglomerates and volcanic tuffs corresponding to the skeletal bearing layers of site of Trinil (Schwartz & Tattersall, 2002). Fossil hominin remains recovered are a calotte and femur attributed to *Homo erectus* (Schwartz & Tattersall, 2002).

2.19. Liang Bua

The site of Liang Bua consists of a large limestone cave located near the Liang Bua village, Flores, Indonesia where the deposits of the cave site include a deep pit in a ‘wash-off’ area which yielded stegadon faunal remains and hominin skeletal material of several individuals which attributed to *Homo floresiensis* (Brown et al., 2004).

2.20. Cro-Magnon

The site of Cro-Magnon is located in the Dorodogne region, France where the site is a rock shelter infilled by landfall but with recognisable fossil hominin occupation layers and evidence of deliberate burial for skeletal remains of five adults and an infant with The stratigraphic layers contemporaneous with glacial faunal remains from the Upper Pleistocene (Schwartz & Tattersall,

2003). The fossil hominin remains recovered are attributed to *Homo sapiens* (Schwartz & Tattersall, 2002).

3. Descriptions of Stem-Anthropoids

The stem-anthropoids are classified under the Suborder Haplorrhini and Infraorder Anthropoidea and includes extinct taxa from the Late Eocene to Late Oligocene from Africa. The taxonomic classification system is detailed below with species studied in this thesis are indicated in bold. In the following sections, I describe the morphological and endocranial attributes of the stem-anthropoids studied throughout this dissertation. Unless noted otherwise, descriptions are my own observations.

Order Primates (Linnaeus, 1758)

Suborder Haplorrihini (Pocock, 1918)

Infraorder Anthropoidea (Mivart, 1864)

Family Parapithecidae, (Schlosser, 1918)

Genus *Apidium* (Osborn, 1908)

***Apidium phiomense* (Osborn, 1908)**

Genus *Parapithecus* (Schlosser, 1910)

***Parapithecus grangeri* (Simons, 1974)**

Family Proteopithecidae (Simons, 1997)

Genus *Proteopithecus*, (Simons, 1989)

***Proteopithecus sylviae* (Simons, 1989)**

3.1. Genus *Apidium*

The genus *Apidium* is represented by three extinct species. Fossil specimens attributed to the genus *Apidium* consist of partial crania, cranial fragments, and mandibular and dental remains. Similar to many stem-anthropoids, the dental formulae are 2.1.3.3 and the P2 is smaller relative to P3-4 than in the genus *Parapithecus*. Cranial material suggests a complete postorbital closure and relatively large olfactory bulbs cranial size (Beard, 2002).

3.1. *Apidium phiomense*

The type specimen for *Apidium phiomense* is AMNH-1-3370, a left dentary fragment preserving the crowns of P_4-M_3. The species has been recovered from the Fayum Depression, Egypt in the upper part of the Jebel Qatrani Formation dated to the Early Oligocene. Generally, morphology of *Apidium phiomens*e suggests it is larger than either *Apidium moustafai* or *Apidium bowni* and has relatively longer M_3 than observed in other two species of the genus *Apidium* (Beard, 2002).

In this thesis, the specimen of *Apidium phiomens*e studied was DPC-9867 and description of the endocranial morphology included post-deformational damage anteroposteriorly and the endocranial cavity breccia filled which resulted potential damage to the bone on the internal surface of the endocranium with poor convolutional details throughout. The middle cranial fossae show deformational damage to the bone surface, but it is narrow mediolaterally and wider posteriorly. The orbital foramen is present and there is shallow depression where the temporal pole is located. The petrous part of the temporal bone is angled toward the region of the auditory meatus and is narrower mediolaterally and longer anteroposteriorly. The specimen is broken posteriorly to the auditory meatus and the mastoid region. The orbits are likely affected by deformational

compression of the cranial vault, but the orbits appear large with a relatively wide interorbital space. There is minimal cranial base flexion, which is consistent with a quadrupedal primate, but no determination can be made as to whether or not *Apidium phiomens*e was an obligate arboreal quadruped.

3.2. Genus *Parapithecus*

The genus *Parapithecus* is represented by two extinct species. Fossil specimens attributed to the genus *Parapithecus* consist of mandibular, postcranial, dental, and fragmentary cranial remains which indicate the genus *Parapithecus* had a relatively shortened face compared to *Apidium* which may relate to the observed reduction of incisors. The cheek teeth are similar to *Apidium* but *Parapithecus* has relatively larger P_2 than *Apidium*.

3.2.1. *Parapithecus grangeri*

The type specimen of *Parapithecus grangeri* is the specimen CGM-26912 comprising the left dentition and P_1-M_1. *Parapithecus grangeri* has been recovered from the Fayum Depression, Egypt from upper part of the Jebel Qatrani Formation and dated to the Early Oligocene. Generally, the morphology of *Parapithecus grangeri* suggests it is larger than *Parapithecus fraasi* and uniquely, *Parapithecus grangeri* entirely lacks the lower incisors (Beard, 2002).

In this thesis, the specimen of *Parapithecus grangeri* studied was DPC-18651. The endocranial morphology of DPC-18651 was partially affected by breccia infill that was removed virtually to examine the internal surface of the cranium. The right middle cranial fossa is intact and well-preserved with evidence from a narrow and shallow hollow for the temporal pole, but other convolutional details are not well preserved on the endocranial surface. The dorsum sellae is partially intact with a large orbital foramen. The foramen ovale is positioned deep near the petrous

part of the temporal bone which relatively long and narrow and steeply curves towards the auditory meatus. The middle cranial fossa is relatively narrow posteriorly and wider anteriorly. The specimen exhibits a short, broad face with no visible canines. The premolars and molars are large and there is evidence of a significant postorbital constriction. The orbits are large with a narrow interorbital space and the snout is only partially preserved but suggests a strong and robust facial skeleton.

3.3. Genus *Proteopithecus*

The genus *Proteopithecus* is represented by one extinct species which was studied here.

3.3.1. *Proteopithecus sylviae*

The type specimen for *Proteopithecus sylviae is* CGM-41886 represented by a left maxillary fragment preserving the crowns of M^{1-3} and the left P^2. *Proteopithecus sylviae* has been recovered from the Fayum Depression, Egypt from Quarry L-41 and the lower part of the Jebel Qatrani Formation and dated to the Late Eocene. Generally, the morphology of *Proteopithecus sylviae* indicates a relatively small anthropoid primate similar in size to the fossil eosimiid, *Bahinia pondaungensis* but the postcranial anatomy suggests a similarity to small platyrrhines (Beard, 2002; Simons & Seiffert, 1999). Craniodentally the dental formula is 2:1:3:3 with relatively larger canines suggesting sexual dimorphism and while the maxillaryP^2 is relatively smaller to P^{3-4} , the mandibular remains indicate that a P_2 that is relatively larger to P_{3-4} (Beard, 2002).

In this thesis, the specimen of *Proteopithecus sylviae* studied was DPC-14095 with the specimen affected considerably by deformational and geological compression factors with the endocranial cavity affected by matrix infill and a broken but positioned foramen magnum making interpretation of the middle cranial fossae difficult. However, the left middle cranial fossa was

well preserved with a deep hollow for the temporal pole and the orbital foramen is present but the dorsum sellae is affected by defamation processes. The dental arcade appears to have shifted posteriorly and is now positioned beneath the greater wings of the sphenoid. The foramen ovale and carotid canal are present, but the majority of the petrous bone is heavily worn on the surface likely by geological processes and interpretation of this region is challenging.

4. Description of Stem-Platyrrhines

The stem-platyrrhines are classified under the Suborder Haplorrhini and Infraorder Platyrrhini which includes extinct taxa from the Early to Middle Miocene from South America. The taxonomic classification system is detailed below with species studied indicated in bold. In the following sections, I describe the morphological and endocranial attributes of the stem-platyrrhines studied throughout this dissertation. Unless noted otherwise, descriptions are my own observations.

Order Primates (Linnaeus, 1758)

Suborder Haplorrhini (Pocock, 1918)

Infraorder Platyrrhini (Saint-Hilarie, 1812)

Family Atelidae (Gray, 1925)

Subfamily Pitheciinae (Mivart, 1865)

Tribe Homunculini (Ameghino, 1894)

Genus *Homunculus* (Ameghino, 1894)

***Homunculus patagonicus* (Ameghino, 1894)**

Family Cebidae (Bonaparte, 1831)

Subfamily Cebinae (Bonaparte, 1831)

Subfamily Saimiriinae (Miller, 1924)

Genus *Dolichocebus* (Kraglievich, 1951)

***Dolichocebus gaimanensis* (Kraglievich, 1951)**

Subfamily Aotinae (Elliot, 1931)

Genus *Tremacebus* (Hershkovitz, 1974)

***Tremacebus harringtoni* (Rusconi, 1933)**

4.1. Genus *Homunculus*

The genus *Homunculus* is represented by one extinct species.

4.1.1. *Homunculus patagonicus*

The type specimen for *Homunculus patagonicus* is MACN-A-12498 represented by a right mandibular fragment with a complete symphysis and recovered from the Rio Gallegos site from the Santa Cruz Formation from southernmost Santa Cruz Province, Argentina and dated to the Early Miocene and early Middle Miocene. Generally, the morphology of *Homunculus patagonicus* includes mandibular, postcranial, and cranial material with relatively small lower canines and incisors and series of substantial shearing crests. The facial skeleton has a prominent snout and relatively deep face with moderately sized orbits and narrow interorbital space, while the cranium is globular (Fleagle & Tejedor, 2002).

In this thesis, the specimen of *Homunculus patagonicus* is studied was MPV-3501 and the specimen was affected by matrix infill, which was virtually removed but there is also deformational affects mediolaterally. The right middle cranial fossa was the best-preserved region for study. There is a distinct and shallow hollow for the temporal pole. The dorsum sellae is present but only partially intact. There is no closure of the orbits, leaving the greater wings, lesser wings of the sphenoid absent. The orbital foramen is large. The petrous part of the temporal bone is

steeply angled towards the auditory meatus. The foramen ovale is positioned far back in the middle cranial fossa. There are deep sulcal impressions in the posterior cranial fossa for the cerebellum and deep sinus drainage. The orbits are large, and snout is robust with prominent canines, potentially indicating sexual dimorphism. There is a distinct post- orbital constriction which may be exaggerated due to potential mediolateral compression and deformation of the cranium.

4.2. Genus *Dolichocebus*

The genus *Dolichocebus* is represented by one extinct species and will be discussed below.

4.2.1. *Dolichocebus gaimanensis*

The type specimen for type specimen for *Dolichocebus gaimanensis* is MACN-14128 represented by an edentulous and distorted cranium. The fossil remains were recovered from Caiman, Chubut Province. Argentina and dated to the Early Miocene. Morphologically, the cranium of *DoIicliocccbus gaimanensis* indicates a medium-sized platyrrhine with the cranium possessing moderate-sized orbits with a narrow interorbital region and a relatively narrow braincase, which is not distorted (Fleagle & Tejedor, 2002).

In this thesis, the specimen of *Dolichocebus gaimanensis* studied was MACN-14128. The right side middle cranial fossa was best preserved for study. The orbital foramen and the foramen ovale and carotid canal are present. The petrous part of the temporal bone is fragmented potentially due to deformational processes and has shifted away from where it joins the wall of the temporal bone. There is a shallow depression for the temporal pole. The middle cranial fossa appears to be short anteroposteriorly and broad mediolaterally. There is clear convolution details present on the endocranium. The orbits are very large, and there is an intermediate interorbital space. The snout

is short and broad, and the cranium rounded with strong temporal lines and potential cresting. The foramen magnum is positioned far back on the cranium indicative of a quadrupedal primate.

4.3. Genus *Tremacebus*

The genus *Tremacebus* is represented by one extinct species.

4.3.1. *Tremacebus harringtoni*

The type specimen of *Tremacebus harringtoni* is FLM-619 represented by a relatively complete and undistorted cranium. The fossil remains were recovered from Sacanana, Chubut Province, Argentina and dated to the Early Miocene. Morphologically, the cranium of *Tremacebus harringtoni* has a broad snout with relatively large orbits and a wide interorbital region not dissimilar to the extant nocturnal platyrrhine, *Aotus* (Fleagle & Tejedor, 2002).

In this thesis, the specimen studied of *Tremacebus harringtoni* was FML-619. The specimen is short and broad, with a large face and considerably large orbits. There is a wide interorbital space. The left middle cranial fossa was best preserved for study but was affected by adhering matrix which was removed virtually. There is a slight hollow for the temporal pole. The dorsum sellae is present but only partially intact and the orbital foramen is present. The petrous part of the temporal bone is only partially preserved but is relatively long and the greatest width of the cranium appears to be at the mastoid region. There is evidence of an auditory bullae rather than a tympanic tube. There are minimal convolutional details preserved on the endocranial surface.

5. *Description of Stem-Catarrhines*

Stem-catarrhines are classified under the Suborder Haplorrhini and Infraorder Catarrhini and include extinct taxa from the Early to Late Oligocene from Africa. The taxonomic classification is detailed below with species studied indicated in bold. In the following sections, I describe the morphological and endocranial attributes of the stem-catarrhines studied throughout this dissertation. Unless noted otherwise, descriptions are my own observations.

Order Primates (Linnaeus, 1758)

Suborder Haplorrhini (Pocock, 1918)

Infraorder Catarrhini (Saint-Hilaire, 1812)

Family Propliopithecidae (Strauss, 1961)

Genus *Aegyptopithecus* (Simons, 1965)

***Aegyptopithecus zeuxis* (Simons, 1965)**

Family Oligopithecidae (Kay and Williams, 1994)

Genus *Catopithecus* (Simons, 1989)

***Catopithecus browni* (Simons, 1989)**

5.1. Genus *Aegyptopithecus*

The genus *Aegyptopithecus* consists of one extinct species.

5.1.1. *Aegyptopithecus zeuxis*

The type specimen of *Aegyptopithecus zeuxis* is CGM- 26901 represented by a left mandible with P_4–M_2. The fossil remains were recovered from the Fayum Depression in the upper sequence of the Jebel Qatrani Formation and date to the early Oligocene (Rasmussen, 2002). Morphologically, *Aegyptopithecus zeuxis* was a large and robust stem-catarrhine with an estimated

body size similar to extant gibbons and howler monkeys (Simons, 1965; Kay et al., 1981; Simons & Rasmussen, 1991). There are several cranial specimens of *Aegyptopithecus* indicating a robust facial skeleton with broad interorbital space and the temporal lines converge above the orbits in males forming a prominent, sagittal crest.

In this thesis, there were several specimens of *Aegyptopithecus zeuxis* studied with a broad basicranium with the posterior carotid foramen entering the auditory bulla fairly far back (as in extant *Alouatta*) and there is a large promontory canal. The endocasts of *Aegyptopithecus zeuxis* indicates relatively smaller frontal lobes than any extant anthropoid but relatively larger olfactory bulbs (Radinsky, 1975; Simons, 1993). The endocast shape is low and elongated but there are only slight convolutions observable.

5.2. Genus *Catopithecus*

The genus *Catopithecus* consists of one extinct species.

5.2.1. *Catopithecus browni*

The type specimen of *Catopithecus browni* is CGM-41885 and represented by a right mandible preserving the P3–M_3. Fossil remains have been recovered from the Fayum Depression, Egypt in the lower sequence of the Jebel Qatrani Formation, Quarry L-41 and dated to Late Eocene (Rasmussen, 2002). Morphologically, *Catopithecus browni* is a small-bodied primate with an unfused mandibular symphysis. Dentally, the canines project and there is indication of sexual dimorphism. Postcranially, *Catopithecus* is also very ancestral with Seiffert et al. (2000) comparing resemblance between the humerus of *Catopithecus* and propliopithecines where *Catopithecus* is indicative of a more generalised arboreal quadruped. Cranially, the facial skeleton is relatively deep and projecting with the snout much broader than that of any extant anthropoid

or strepsirrhine. The orbits are relatively small and there is a broad interorbital region. The cranial vault appears relatively small, and a braincase is relatively smaller than more recent extinct and extant anthropoids. On the neurocranium, the temporal lines converge to form a sagittal crest that stretches towards the posterior of the cranial vault where there is also nuchal cresting. The ectotympanic is platyrrhine-like with an angular form rather than a tubular one observed in extant catarrhines. Unfortunately, all the known crania of *Catopithecus* are considerably affected by geological or deformation processes (Rasmussen, 2002).

In this thesis, the specimen of *Catopithecus browni* studied was DPC-11388**.** The specimen is considerably damaged by both deformational processes and geological compression. Despite this, the virtual endocranium was accessible with the left middle cranial fossa the best preserved for study. From observation, the dorsum sellae is present although matrix infill has caused some disruption to the endocranial surface. There is a shallow depression for the temporal pole. The petrous part of the temporal bone is fragmented but there is evidence of the carotid canal and foramen ovale. The ectotympanic tube appears to be angular and there is potentially the presence of an auditory bullae. There are no convolution details visible on the endocranial surface. The orbits appear relatively small. The canines are large suggesting sexual dimorphism, and the posterior position of the foramen magnum is consistent with an arboreal quadrupedal anthropoid.

6. Description of Early Fossil Cercopithecoids

Early fossil cercopithecoids are classified under the Suborder Haplorrhini and Infraorder Catarrhini and include extinct taxa from the Middle Miocene from Africa. The taxonomic classification is detailed below with species studied indicated in bold. In the following sections, I describe the morphological and endocranial attributes of the fossil cercopithecoids studied throughout this dissertation. Unless noted otherwise, descriptions are my own observations.

Order Primates (Linnaeus, 1758)

Suborder Haplorrhini (Pocock, 1918)

Infraorder Catarrhini (Saint-Hilaire, 1812)

Superfamily Cercopithecoidea (Gray, 1821)

Family Victoriapithecidae (von Koenigswald, 1969)

Genus *Victoriapithecus* (von Koenigswald, 1969)

***Victoriapithecus macinnesi* (von Koenigswald, 1969)**

6.1. Genus *Victoriapithecus*

The genus *Victoriapithecus* comprises one extinct species.

6.1.1. *Victoriapithecus macinnesi*

The type specimen of *Victoriapithecus macinnesi* is KNM-MB 1 and is represented by a partial mandible with fossil remains of this species recovered from Napak, Uganda; Maboko Formation, Kenya, Tugen Hills Sequence, Kenya and are dated to the Middle Miocene (Benefit & McCrossin, 2002). Morphologically, the skull of *Victoriapithecus* has a lower neurocranium relative to length and width which is uncommon for Miocene apes and a less flexed cranial base with longer a mid-cranial region and the temporal lines converge with orbits that are taller than wide. (Benefit & McCrossin, 2002). From this cranial morphology *Victoriapithecus* closely resembles the stem-catarrhine *Aegyptopithecus* (Simons, 1987).

In this thesis, the specimen of *Victoriapithecus macinnesi* studied was the inverted virtual endocast of KNM-MB-29100. The cranium is well preserved with only partial damage between the facial skeleton and neurocranium. From observation, the left middle cranial fossa was determined to be best preserved for study. The dorsum sellae is partially present and there is deep

hollow for he temporal pole. The orbital foramen is present and intact. The temporal bone is well preserved with the petrous part more angled towards the auditory meatus. The petrous part of the temporal bone is long anteroposteriorly and narrow mediolaterally but broadens posteriorly. There are strong convolution details on the internal plane of the temporal bone and in the posterior cranial fossa there is evidence of deep hollow for the cerebellum a deep impression of sinus drainage. The anterior cranial fossa is present and displays a large hollow for the olfactory bulb. Generally, the middle cranial fossa is long and narrow and angled anteroposteriorly towards the orbital regions which is consistent with a or arboreal terrestrial quadrupedal anthropoid where there appears to be minimal cranial base flexion.

7. Descriptions of Extinct Cercopithecines

Extinct cercopithecines are classified under the Suborder Haplorrhini and Infraorder Catarrhini and Superfamily Cercopithecoidea and include extinct taxa from the Early Pliocene to the Late Pleistocene in Africa. The taxonomic classification is detailed below with species studied indicated in bold. In the following sections, I describe the morphological and endocranial attributes of the fossil cercopithecines studied throughout this dissertation. Unless noted otherwise, descriptions are my own observations.

Order Primates (Linnaeus, 1758)

Suborder Haplorrhini (Pocock, 1918)

Infraorder Catarrhini (Saint-Hilaire, 1812)

Superfamily Cercopithecoidea (Gray, 1821)

Family Cercopithecidae (Gray, 1821)

Subfamily Cercopithecinae (Gray, 1821)

Tribe Papionini (Burnett, 1828)

Subtribe Papionina (Burnett, 1828)

Genus *Papio* (Erxleben, 1777)

***Papio angusticeps (izodi)* (Gear, 1926)**

Genus *Dinopithecus* (Broom, 1937)

***Dinopithecus ingens* (Broom, 1937)**

7.1. Genus *Papio*

The genus *Papio* comprises three recognised extinct species. A consolidation into *Papio izoldi* of all small species of *Papio* recognised from South Africa (*P. izodi, P. wellsi and P. angusticeps*) was advocated by Szalay & Delson (1979) and is followed here.

7.1.1. *Papio angusticeps (izodi)*

The type specimen of *Papio angusticeps (izodi)* ***is*** AD 992, represented by a badly damaged female cranium. Fossil remains have been recovered from Taung, Sterkfontein, Kromdraai, Cooper's Cave, and Haasgat Cave, South Africa and all are dated to the Late Pleistocene (Jablonski, 2002). Morphologically, *Papio angusticeps (izodi)* has a well-developed supraorbital torus. Dentally specimens are indistinguishable from *Parapapio* species but are rendered cranially distinct by the concavity and steep drop in the orbital profile.

In this thesis, several specimens of *Papio angusticeps (izodi)* were studied including CO-100 which will be described. The specimen is a partial cranium missing the right side but the left side the cranium is intact. The left middle cranial fossa was best preserved for study and dorsum sellae is present and intact. The olfactory bulb region is intact, and the orbital foramina are large and present. The foramen ovale is positioned quite far back along the petrous part of the temporal bone. The petrous part of the temporal bone is short anteroposteriorly and broad mediolaterally.

There are clear convolution details on the internal surface of the temporal and parietal bones. There is deep hollow for the temporal pole. The relative position of the middle cranial fossa is consistent with a quadrupled primate and there appears to be low cranial base flexion. The face is long anteroposteriorly with a pronounced, long snout and broad mediolaterally. There are large canines suggesting sexual dimorphism and the orbits are large with a narrow interorbital region. This is similar to extant *Papio*.

7.2. Genus *Dinopithecus*

The genus *Dinopithecus* comprises one extinct species.

7.2.1. *Dinopithecus ingens*

The type specimen for *Dinopithecus ingens* is SB 7, a partial mandible with damaged dentition with fossil remains have been recovered from Swartkrans, South Africa and are dated to the mid-Pliocene (Jablonski, 2002). Morphologically, *Dinopithecus ingens* is one of the largest cercopithecoids and exceeded in overall size only by *Theopithecus oswaldi* from the Late Pleistocene with the genus *Dinopithecus* a very large and sexually dimorphic papionin with a large and robust skull (Jablonski, 2002). There is the presence of strong masticatory and nuchal muscles and the temporal lines merge in both sexes which, in males form sagittal and nuchal crests. The supraorbital torus is robust, and the interorbital region is relatively broad (personal observation).

The specimen studied was SK-554 which is intact and has a long projecting snout. The face is narrow and there is intermediate post orbital constriction. The left middle cranial fossa was best preserved for study but there is partial breakage throughout the sphenoid and postorbital regions. The middle cranial fossa shows strong convolutions details and has a deep but narrow hollow for the temporal pole. The petrous part of the temporal bone is broad with the foramen ovale located

towards the front of the middle cranial fossa. The foramen magnum is positioned far back in the skull relative to face and there appears to be minimal cranial base flexion consistent with a large, quadrupedal primate.

8. Description of Extinct Hominins

Extinct hominins are classified under the Suborder Haplorrhini and Infraorder Catarrhini and Family Hominidae and the Subfamily Homininae and include extinct taxa from the Early Pliocene to the Late Pleistocene in Africa, Asia, Middle East, and Europe. The taxonomic classification is detailed below with species studied indicated in bold. In the following sections, I describe the morphological and endocranial attributes of the fossil hominins studied throughout this dissertation. Unless noted otherwise, descriptions are my own observations.

Order Primates (Linnaeus, 1758)

Suborder Haplorrhini (Pocock, 1918)

Infraorder Catarrhini (Saint-Hilaire, 1812)

Superfamily Hominoidea (Gray, 1825)

Family Hominidae (Gray, 1825)

Subfamily Homininae (Gray, 1825)

Genus *Australopithecus* (Dart, 1925)

***Australopithecus africanus* (Dart, 1925)**

Genus *Paranthropus* (Broom, 1938)

***Paranthropus aethiopicus* (Arambourg & Coppens, 1968)**

***Parapanthropus boiesi* (Leakey, 1959)**

Genus *Homo* (Linnaeus, 1758)

***Homo habilis* (Leakey, 1964)**

***Homo erectus* (Dubois, 1892)**

***Homo ergaster* (Groves & Mazak, 1975)**

***Homo floresiensis* (Brown, 2004)**

***Homo heidelbergensis* (Schoetensack, 1908)**

***Homo neanderthalensis* (King, 1864)**

***Homo sapiens* (Linnaeus, 1758)**

8.1. Genus *Australopithecus*

The genus *Australopithecus* comprises six recognised extinct species.

8.1.1. *Australopithecus africanus*

The type Specimen of *Australopithecus africanus* is the Taung cranium of a child. Fossil remains have been recovered from Taung, Makapansgat and Sterkfontein, South Africa and dated to approximately 3 – 2 million years ago (Schwartz & Tattersall, 2005). Morphologically, *Au. africanus* crania are more globular with less neurocranial cresting than observed in other species of *Australopithecus* or in *Paranthropus* (Schwartz & Tattersall, 2005). The face is relatively prognathic with bony pillars framing the nasal aperture. The dental remains indicate that the post-canine teeth are relatively larger than in *Au. afarensis* but not as disproportionally large as observed specimens attributed to the genus *Paranthropus* (Schwartz & Tattersall, 2005).

In this thesis, the specimen of *Australopithecus africanus s*tudied was STS-5 and STS-71 According to Holloway and Broadfield (2004), the specimens attributed to *Au. africanus* are noted to have endocrania with the presence of a large a rostral beck in the frontal lobe while the temporal poles project forward and deep into the middle cranial fossa. There are often poorly retained convolution details but there is evidence for the trigeminal nerve root, the middle meningeal artery,

partial evidence for of the auditory nerve and the carotid canal via the foramen laceum (Holloway & Broadfield, 2004).

8.2. Genus *Paranthropus*

The genus *Paranthropus* comprises three recognised extinct species.

8.2.1. *Paranthropus aethiopicus*

The type Specimen of *Paranthropus aethiopicus is* Omo-18-18 and represented by an edentulous mandible with fossil remains have been recovered from West Turkana, Kenya and Omo Shungura, Ethiopia and dated to 2.7 – 2.3 million years ago (Schwartz & Tattersall, 2005). Morphologically, the cranial base is unflexed and the face is 'dished' with laterally flaring zygomatic arches. The dentition has large anterior teeth relative to post-canine teeth when compared to the hyper-condition observed in *P. robustus* and *P. boisei* (Schwartz & Tattersall, 2005).

In this thesis, the *Paranthropus aethiopicus* specimen studied was KNMWT-17000. From observation, there is slight distortion to the right temporal lobe which is displaced superiorly and some of the cranial base is missing. Consistent with the findings by Holloway and Broadfield (2004), the frontal lobe is narrow and pointed with the presence of the frontal beck similar to OH5 but in generally, there is poor cortical bone preservation. According to Holloway and Broadfield (2004) in the posterior cranial fossa, the right sigmoid sinus is considerably larger than the left deemed indicative that the sagittal sinus flow was probably towards the right rather than the left (Holloway & Broadfield, 2004).

8.2.2. *Paranthropus boiesi*

The type specimen of *Paranthropus boiesi is* OH5 and represented by a complete cranium including dentition. Fossil remains attributed to this species have been recovered from, Olduvai Gorge, Koobi Fora, West Turkana, Kenya; Omo, Shungura, Ethiopia and dated to 2.3 – 1.4 million years ago (Schwartz & Tattersall, 2005). Morphologically, the crania are noted to have a 'dished' face with high and anteriorly flared zygomata and sagittal and nuchal crests. Dentally, there is extreme post canine megodontia and highly molarised premolars (White, 2002).

In this thesis, the specimen of *Paranthropus boiesi* studied was OH5 and KNMER-406. From observation, the middle cranial fossa is affected by some damage to the sphenoid bones on both sides and generally there is a lack of convolution details on the endocranial surface and as a result, the temporal, parietal and occipital lobes lack any distinct sulcal details. The specimen KNM-ER 406 was affected by matrix infill which was virtually removed. The right middle cranial fossa was determined as the best for study. On the right, there is presence of a hollow for the temporal pole which is deep. The petrous part of the temporal bone is partially intact and curved towards the auditory meatus. The foramen magnum is positioned low and slightly towards the posterior of the cranium. Generally, the orbits are rounded with a narrow interorbital space and the cranium appears to be relatively shortened anteroposteriorly.

8.3. Genus *Homo*

The genus *Homo* comprises at least ten extinct species.

8.3.1. *Homo habilis*

The type Specimen of *Homo habilis* is OH7, represented by a juvenile mandible. Fossil remains attributed to this specimen have been recovered from the sites of Omo and Hadar,

Ethiopia; Olduvai Gorge, Tanzania; East Lake Turkana, Kenya; and Sterkfontein, South Africa and dated to approximately 2.33 - 1.6 million years ago (Schwartz, & Tattersall, 2003) On average, the absolute endocranial capacity is larger than that observed in *Australopithecus* specimens but smaller than *Homo ergaster* (Pearson & Polly, 2024). There is the presence of a supraorbital torus and the upper face is wider than the midface breadth. Dentally, the premolars are smaller than *Australopithecus* and *Paranthropus* and more consistent with species of the genus *Homo*. (Schwartz &Tattersall, 2003).

The specimen studied of *Homo habilis* included KNM-ER 1813 and is described here. The right temporal pole and some of the left cerebellar lobe and frontal lobe are missing. The convolution details are not very clear except for the lateral sulcus anteriorly. There is a slight protuberance left Broca's region, but it is uncertain that it will be asymmetrical since the right side is missing. The meningeal veins are visible. The base of the left temporal lobe indicates that the presence of the middle meningeal vessels via the foramen spinosum before tripartite bifurcations occurred posteriorly, anteriorly, and dorsally.

The specimen KNM-1805 has a relatively complete and undistorted temporal lobe, and anterior rostral beck. Most of the convolutional details are missing except for in the temporal lobes where the inferior temporal sulcus is discernible. The meningeal vessels entering through the foramen spinosum before branching into a recurved anterior division to provide meningeal vessels coursing posteriorly and dorsally over the posterior portion of the frontal lobe. An inferior-posterior division of the middle meningeal provided a small number of vessels to be lower parietal and occipital bones (Holloway & Broadfield, 2004).

8.3.2. *Homo ergaster*

The type specimen of *Homo ergaster* is KNM-ER 992 represented by an adult mandible. Fossil remains have been recovered from Koobi Fora and West Turkana, Kenya; Olduvai Gorge, Tanzania; Swartkrans, South Africa and Dmanisi, Republic of Georgia and dated to approximately 1.8 – 1.6 million years ago (Dunsworth & Walker, 2002). Morphologically, African *Homo ergaster* has smaller cheek teeth compared to *Australopithecus* or *Homo habilis* and a slenderer mandible. The cranial capacity is larger than in earlier hominins and characterised by thinner bones than in Asian *Homo erectus* and s cranium that is long and low with sagittal keeling, projecting brow ridges and a prominent occipital torus and a broad facial skeleton (Dunsworth & Walker, 2002; Schwartz & Tattersall, 2003).

In this thesis, the specimens studied included KNM-ER 3733**.** This specimen is attributed to an adult female based on the less robust cranial morphology. The cranium is partially complete with minimal distortion to the right middle cranial fossa. The endocranial surface of the cranial base in may have undergone erosional processes which affect the clarity of the convolutional details. The temporal poles project anteriorly, and the petrous pyramid appears large and positioned superiorly to the posterior cranial fossae. Unfortunately, the sellae turcica is too distorted to describe whether the angle or position is similar to extant *Homo sapiens*. The specimen KNM-ER 3883 is a partial cranium with much of the facial skeleton not preserved. The endocranial surface of the cranial base displays some distortion affecting the left middle cranial fossa with distortion more noticeable when comparing the left and right side with the dorsum sellae positioned slightly to the right. Although the KNM-ER 3883 is a mostly complete cranium, the internal bony surface in a similar condition to KNM-ER 3733 with erosion of the internal table of bone making identification of cerebral convolutions difficult. The position of the anterior temporal

pole suggests the temporal lobe would likely have projected anteriorly. Despite the sparse meningeal pattern on the endocast, the bifurcation pattern is similar to KNM-ER 3733. The specimen OH-9 is A partial calvarium with the right-side of the neurocranium incomplete. The facial skeleton is not preserved but the fragmentary neurocranial vault indicates a rounded but defined supraorbital torus and a noticeable postorbital constriction. The endocranial surface of the cranial base in OH 9 is well preserved, however, the posterior cranial fossa is incomplete with the lesser wing of the sphenoid and the dorsum sellae on the right side not preserved. There appears a mild distortion to the anterior temporal pole of the right middle cranial fossa, however, when viewed inferiorly, cranial base deformation, if present, is very mild and is likely associated with the broken occipital and surrounding areas of the foramen magnum. The endocranial surface of the greater wing of the sphenoid near the left anterior temporal pole appears to be enlarged compared to the right, with possible rotation and inferior torsion to the temporal lobe.

8.3.3. *Homo erectus*

The type specimen of *Homo erects* is Trinil 2, adult partial cranium (Dunsworth & Walker, 2002). Fossil remains have been recovered from Narmada, India; Hexian, Gongwangling (Lantian), Zhoukoudtan, Jianshi and Yunxian, China; Sambungmachavn, Solo, Trinil, Ngandong, Modjokcrto and Sangiran, Indonesia and dated to 1.6 million years ago 50,000 years ago (Schwartz & Tattersall, 2003). Morphologically, the crania are long and low with greatest cranial breadth toward base. The frontal bone has a pronounced supraorbital torus, supratoral sulcus and a frontal keel. There is a significant degree of postorbital constriction compared to *Homo sapiens*.

The specimens representing *Homo erectus* studied here include Sambungmacan 3. The specimen is a calotte with articulated fragments of the cranial base but no facial skeleton. The endocranial surface of the cranial base is well preserved but very incomplete with the greater and

lesser wings of the sphenoid incomplete and no perseveration of the temporal pole. The right petrous bone is completely preserved while the left is partially complete.

The specimen Sangiran 2 is also a calotte without a facial skeleton and only a small section of the arched supraorbital torus retained and displays a well-defined postorbital constriction. The cranial base is only partially preserved with no sphenoid preserved but the supramastoid region of the temporal bone appears robust and broad when viewed posteriorly. There are preserved greater and lesser wings of the sphenoid with the left and right petrous bones of the middle cranial fossa is partially preserved and the squamous and mastoid portions of the temporal bone. The right petrous bone is incomplete and undistorted with a small part of the greater wing of the sphenoid articulated.

The specimen Sangiran 4 is a partial calvarium and maxillae fragment, The calvarium is large with the partial neurocranium showing thick cranial bones. The he temporal bones have prominent mastoid processes and sharp, defined nuchal planes. The endocranial surface of the cranial base is well-preserved and cracked but the foramen magnum, posterior cranial fossa, and dorsum sellae are complete. Unfortunately, most of the greater and lesser wings of the sphenoid are incomplete but the anterior margin of the greater wing of the sphenoid is retained but temporal pole is reliably clear.

The specimen Sangiran 17 is the most complete specimen of Javanese *Homo erectus* and is large cranium with a partial but very prognathic facial skeleton and robust supraorbital tori, well-defined nuchal region, and a prominent mastoid process. The endocranial surface of the cranial base is well preserved and without apparent distortion. The middle cranial fossa is mostly preserved with complete squamous and petrous bones, dorsum sellae, a partial sellae turcica and articulated anterior margin of the greater wings of the sphenoid.

8.3.4. *Homo floresiensis*

The type specimen of *Homo floresiensis is* LB1, represented by a cranium and postcranial material and fossil remains have been recovered from Laing Bua cave, Flores, Indonesia and dated to 100,000 to 50,000 years ago (Brown et al., 2004). Morphologically, *Homo floresiensis* has unique dental, cranial, and postcranial morphology that is most similar to early *Homo* from East Africa rather than *Homo sapiens* or Asian *Homo erectus* (Aiello, 2010; Jungers, 2013). The estimated cranial capacity is small and resembles *Australopithecus* or early *Homo* and postcranial elements suggest a small stature of one metre in height Brown et al., 2004).

In this thesis, the specimen studies of *Homo floresiensis* is LB1. The middle cranial fossa is intact, and the left middle cranial fossa best preserved for study. There is a shallow depression for the temporal pole. The petrous part of the temporal bone is positioned at a sharp angle towards the auditory meatus, but this may be exacerbated to some extent by the defamation and damage to the cranium. Mediolaterally, there is evidence of breakage to the petrous bone. The foramen ovale is positioned anteriorly in the cranial base and the orbital foramen is present. Unfortunately, there is damage to the lesser wings of the sphenoid opening the middle cranial fossa to the anterior cranial fossae and damage to the dorsum sellae. There are well-preserved convolutional impressions on endocranial surface of middle cranial fossa and the temporal bone. The foramen magnum is positioned towards the middle of the skull indicating a bipedal posture and the cranium is broadest at the mastoid regions with minimal postcranial constriction. The face is short and flat, positioned below the orbital ridges but this might be exacerbated by defamation processes.

8.3.5. *Homo heidelbergensis*

The type Specimen of *Homo heidelbergensis* is the Mauer mandible, a nearly complete mandible missing premolars and first two left molars and lacking a chin (Schwartz & Tattersall, 2002). Fossil remains have been recovered from Heidelberg, Germany; Kabwe, Southern Africa; Bodo in Eastern Africa; Petralona in Greece and possibly Dali, China and dated to 700 000–130 000 years ago (Schwartz & Tattersall, 2002). Morphologically, cranial similarities between the African and European fossils are noticeable. The cranium is characterised by a larger cranial capacity, divided brow ridges and compared to *Homo erectus*, *Homo heidelbergensis* has smaller teeth and a mandible with a broader ramus and a deeper corpus but lacking a chin.

In this thesis, the specimens of *Homo heidelbergensis* studied included Bodo. The endocranium is somewhat distorted but retains the frontal portion with anterior and dorsal regions of the right parietal lobe, most of the left temporal pole and a small portion of the right temporal pole. The right temporal pole is rotated anteriorly relative to the left side causing an anterior displacement of the right temporal lobe. There is similarity to Kabwe fossil frontal lobes is noted by (Broadfield and Holloway, 2004).

The specimen Kabwe is an almost complete cranium missing only a small section of the right is occipital and parietal lobs. The preservation of the internal table of bone is very good and shows good sulcal and meningeal details. The middle meningeal vessels are thick entering the skull via out the foramen spinosum and small branches along the inferior temporal lobe. The middle branch of the middle meningeal vessel is thick and ascends slightly posterior to the coronal suture. There are very large brow ridges, a rounded and protruding occipital lobes and the low vault resembles Amud and Ngangdong (Holloway & Broadfield, 2004).

8.3.6. *Homo neanderthalensis*

The type specimen of *Homo neanderthalensis* is Feldhofer 1 and represented by a calotte (Schwartz & Tattersall, 2002). Fossil remains have been recovered from Mount Carmel, Israel; and throughout Europe and dated to 300,000 to 35,000 years ago (Schwartz & Tattersall, 2002). Morphologically, *Homo neanderthalensis* has a prognathic face with an unusually large nasal region and large arching brow ridges over the orbits. The cranium is rounded with a prominent 'bun' posteriorly and flattened parietal bones. The brain is absolutely and relatively large. Postcranially, the limbs are robust with shortened distal elements.

In this thesis, the specimens of *Homo neanderthalensis* studied include Tabun 1. This specimen has a prominent frontal crest and appears that the frontal lobes were fairly far forward over the orbital cones and were separated by wide, deep depression around the cribriform plate. The right transverse sinus is much larger than the left and it appears to have diverged higher. The sigmoid sinuses are deep and run behind and beneath the petrosal bones which are broad

The specimen Gibraltar 1 most of the right side preserved including the frontal, temporal and some of the parietal, occipital and cerebellar lobes. The left side is partially missing with some pf the left occipital lobe present and the medial temporal lobe and pole. The cranial base is mostly intact middle prefrontal region is broader on the right than the left but petalias cannot be verified (Holloway and Broadfield, 2004).

The specimen of La Chapelle-Aux Saints is an almost complete endocranium missing portions of the cranial base, the orbital part of the frontal lobe, medial portions of the temporal lobe poles and the brainstem. The shape is long, low and broad and resembles other western European Middle Pleistocene specimens such as Gibraltar. The convolutional details are poor and

those of the meningeal vessels. The lateral sulcus is present at the apex but it is harder to observe posteriorly.

The specimen of La Ferrassie 1 is an almost complete cranium missing portions of the prefrontal orbital part of the frontal lobe, the left orbital portion of Broca's cap, the middle temporal poles, the foramen magnum region. There are no reliable convolution details except in the inferior aspect of the temporal lobes. The occipital lobes protrude posteriorly most likely due to the occipital bun trait in Neanderthals. The meningeal vessels are not elaborate and are only visible mostly on the right side. The pattern appears to be similar to that observed in La Chapelle-aux Saints.

The specimen La Quina 5 is a small cranium assumed to be a female individual. The endocranium lacks most of the cranial base. There are not reliable convolutions details preserved on the endocranial surface,

8.3.7. *Homo sapiens*

There is no type specimen for *Homo sapiens*. Fossil remains have been recovered from Jebel Irhoud, Morocco; Omo Kibish Formation, Ethiopia; Herto in the Middle Awash region, Ethiopia; Mount Carmel, Israel; Cro-Mignon, France, and dated to 300,000 years ago to 10, 000 years coinciding with the last glacial maximum (Schwartz & Tattersall, 2002). Morphologically, fossil *Homo sapiens* possess relatively and absolutely smaller dentition, a vertical mandibular ramus and a chin, with a shortened and retracted face that is positioned beneath reduced brow ridges and high vertical forehead and postcranially, the skeleton tends towards more gracile limb structure and proportions (Smith, 2002).

In this thesis, specimens of extinct *Homo sapiens* included Cro-Magnon 1. The specimen is an edentulous individual but the endocranium is clear and retains convolution details and right Broca's Cap is large, but the left is missing (Holloway & Broadfield, 2004)

References

Beard, K.C. (2002) Basal anthropoids, In: *The Primate Fossil Record*, Hartwig, W.C., (ed.). Cambridge University Press, Cambridge, UK. pp. 133-149.

Benefit, B.R., & McCrossin, M.L. (2002) The Victoriapithecidae, Cercopithecoidea, In: *The Primate Fossil Record*, Hartwig, W.C., (ed.). Cambridge University Press, Cambridge, UK. pp.241-253.

Brown, P., Sutikna, T., Morwood, M. J., Soejono, R. P., Saptomo, E. W., & Due, R. A. (2004). A new small-bodied hominin from the Late Pleistocene of Flores, Indonesia. *Nature*, 431(7012), 1055-1062.

Dunsworth, H., & Walker, A. (2002) Early Genus *Homo*, In: *The Primate Fossil Record*, Hartwig, W.C., (ed.). Cambridge University Press, Cambridge, UK. pp.419-435.

Fleagle, J.G., & Tejedor, M. F., (2002) Early platyrrhines of southern South America, In: *The Primate Fossil Record*, Hartwig, W.C., (ed.). Cambridge University Press, Cambridge, UK. pp.161-173.

Herries, A. I., Martin, J. M., Leece, A. B., Adams, J. W., Boschian, G., Joannes-Boyau, R., ... & Menter, C. (2020). Contemporaneity of *Australopithecus*, *Paranthropus*, and early *Homo erectus* in South Africa. *Science*, 368(6486), eaaw7293.

Holloway, R.L., & Broadfield, D.C.(2004*) The Human Fossil Record, Brain Endocasts: The Paleoneurological Evidence, Volume 3*; Wiley-Liss; Hoboken, New Jersey, USA.

Jablonski, N.G. (2002) Fossil Old World Monkeys: The late Neogene radiation, In: *The Primate Fossil Record*, Hartwig, W.C., (ed.). Cambridge University Press, Cambridge, UK. pp.255-299.

Rasmussen, D.T. (2002) Early catarrhines of the African Eocene and Oligocene, In: *The Primate Fossil Record*, Hartwig, W.C., (ed.). Cambridge University Press, Cambridge, UK. pp. 203-240.

White, T.D. (2002) Earliest hominids, In: *The Primate Fossil Record*, Hartwig, W.C., (ed.). Cambridge University Press, Cambridge, UK. pp. 407-417.

Schwartz, J.H., & Tattersall, I. (2002) *The Human Fossil Record, Terminology and Craniodental Morphology of Genus Homo (Europe*), Volume 1; Wiley-Liss; Hoboken, New Jersey, USA.

Schwartz, J.H., & Tattersall, I. (2003) *The Human Fossil Record: Craniodental Morphology of Genus Homo (Africa and Asia), Volume* 2; Wiley-Liss; Hoboken, New Jersey, USA.

Schwartz, J.H., & Tattersall, I. (2005) *The Human Fossil Record, Craniodental Morphology of Early Hominids (Genera Australopithecus, Paranthropus, Orrorin), and Overview, Volume 4*; Wiley-Liss; Hoboken, New Jersey, USA.

Simons, E.L., & Seiffert, E.R. (1999) A partial skeleton of *Proteopithecus sylviae* (Primates: Anthroppoidea): first associated dental and postcranial remains of an Eocene anthropoidean, *Comptes rendus de l'Academie des sciences, Paris*. 329, 921-927.

Smith, F. H. (2002) Migrations, radiations and continuity: patterns in the evolution of Middle and Late Pleistocene humans', In: *The Primate Fossil Record,* Hartwig, W.C., (ed.). Cambridge University Press, Cambridge, UK. pp.437-456.

APPENDIX C- SPECIMEN SAMPLE AND COLLECTION IDENTIFICATIONS

1. Magnetic Resonance Imaging (MRI) Samples

The anonymised human in-vivo MRI samples are provided with known sex, collection ID and Collection Access Source. The non-human primate in-vivo MRI samples are included with known sex, Collection ID, and the Collection Access Source. Both collections of in-vivo human and non-human primate MRI have originally been published with appropriate ethic protocols (Marcus et al., 2009; Rilling & Insel, 1999).

Table 1. Human and non-human primate MRI sample with collection IDs and MRI source, taxon and sex of the specimens.

ID	TAXON	SEX	Collection ID	Collection Access
7	*Homo sapiens*	M	OASIS	Open Access Series of Imaging Studies
9	*Homo sapiens*	F	OASIS	Open Access Series of Imaging Studies
12	*Homo sapiens*	M	OASIS	Open Access Series of Imaging Studies
17	*Homo sapiens*	M	OASIS	Open Access Series of Imaging Studies
18	*Homo sapiens*	M	OASIS	Open Access Series of Imaging Studies
29	*Homo sapiens*	M	OASIS	Open Access Series of Imaging Studies
37	*Homo sapiens*	M	OASIS	Open Access Series of Imaging Studies
43	*Homo sapiens*	M	OASIS	Open Access Series of Imaging Studies
49	*Homo sapiens*	F	OASIS	Open Access Series of Imaging Studies
54	*Homo sapiens*	F	OASIS	Open Access Series of Imaging Studies
55	*Homo sapiens*	F	OASIS	Open Access Series of Imaging Studies
59	*Homo sapiens*	F	OASIS	Open Access Series of Imaging Studies
61	*Homo sapiens*	F	OASIS	Open Access Series of Imaging Studies
63	*Homo sapiens*	M	OASIS	Open Access Series of Imaging Studies
69	*Homo sapiens*	M	OASIS	Open Access Series of Imaging Studies
74	*Homo sapiens*	M	OASIS	Open Access Series of Imaging Studies
77	*Homo sapiens*	F	OASIS	Open Access Series of Imaging Studies
90	*Homo sapiens*	M	OASIS	Open Access Series of Imaging Studies
97	*Homo sapiens*	M	OASIS	Open Access Series of Imaging Studies
101	*Homo sapiens*	M	OASIS	Open Access Series of Imaging Studies
104	*Homo sapiens*	F	OASIS	Open Access Series of Imaging Studies

105	*Homo sapiens*	M	OASIS	Open Access Series of Imaging Studies
107	*Homo sapiens*	M	OASIS	Open Access Series of Imaging Studies
108	*Homo sapiens*	M	OASIS	Open Access Series of Imaging Studies
111	*Homo sapiens*	M	OASIS	Open Access Series of Imaging Studies
117	*Homo sapiens*	M	OASIS	Open Access Series of Imaging Studies
125	*Homo sapiens*	F	OASIS	Open Access Series of Imaging Studies
126	*Homo sapiens*	M	OASIS	Open Access Series of Imaging Studies
131	*Homo sapiens*	M	OASIS	Open Access Series of Imaging Studies
140	*Homo sapiens*	F	OASIS	Open Access Series of Imaging Studies
156	*Homo sapiens*	F	OASIS	Open Access Series of Imaging Studies
162	*Homo sapiens*	F	OASIS	Open Access Series of Imaging Studies
236	*Homo sapiens*	F	OASIS	Open Access Series of Imaging Studies
294	*Homo sapiens*	F	OASIS	Open Access Series of Imaging Studies
295	*Homo sapiens*	F	OASIS	Open Access Series of Imaging Studies
310	*Homo sapiens*	F	OASIS	Open Access Series of Imaging Studies
313	*Homo sapiens*	F	OASIS	Open Access Series of Imaging Studies
379	*Homo sapiens*	F	OASIS	Open Access Series of Imaging Studies
392	*Homo sapiens*	F	OASIS	Open Access Series of Imaging Studies
397	*Homo sapiens*	F	OASIS	Open Access Series of Imaging Studies
93I	*Saimiri sciureus*	F	NCBR	National Chimpanzee Brain Resource
93M	*Saimiri sciureus*	M	NCBR	National Chimpanzee Brain Resource
S105	*Saimiri sciureus*	M	NCBR	National Chimpanzee Brain Resource
S104	*Saimiri sciureus*	M	NCBR	National Chimpanzee Brain Resource
Andy	*Sapajus apella*	M	NCBR	National Chimpanzee Brain Resource
Binkey	*Sapajus apella*	F	NCBR	National Chimpanzee Brain Resource
Diva	*Sapajus apella*	F	NCBR	National Chimpanzee Brain Resource
Vincent	*Sapajus apella*	M	NCBR	National Chimpanzee Brain Resource
RUL-1	*Macaca mulatta*	M	NCBR	National Chimpanzee Brain Resource
RJE-1	*Macaca mulatta*	F	NCBR	National Chimpanzee Brain Resource
153C	*Macaca mulatta*	M	NCBR	National Chimpanzee Brain Resource
REG3	*Macaca mulatta*	M	NCBR	National Chimpanzee Brain Resource
FYF	*Cercocebus atys*	M	NCBR	National Chimpanzee Brain Resource
FSO	*Cercocebus atys*	M	NCBR	National Chimpanzee Brain Resource
FFK	*Cercocebus atys*	F	NCBR	National Chimpanzee Brain Resource
FWJ	*Cercocebus atys*	M	NCBR	National Chimpanzee Brain Resource
140M	*Papio cynocepahlus*	M	NCBR	National Chimpanzee Brain Resource
B263	*Papio cynocepahlus*	M	NCBR	National Chimpanzee Brain Resource
Bosandjo	*Pan paniscus*	M	NCBR	National Chimpanzee Brain Resource
Brian	*Pan paniscus*	M	NCBR	National Chimpanzee Brain Resource
Lorel	*Pan paniscus*	F	NCBR	National Chimpanzee Brain Resource
Jill	*Pan paniscus*	F	NCBR	National Chimpanzee Brain Resource

Laz	*Pan troglodytes*	M	NCBR	National Chimpanzee Brain Resource
Kengee	*Pan troglodytes*	F	NCBR	National Chimpanzee Brain Resource
Lulu	*Pan troglodytes*	F	NCBR	National Chimpanzee Brain Resource
Merv	*Pan troglodytes*	M	NCBR	National Chimpanzee Brain Resource
Jimmy	*Pan troglodytes*	M	NCBR	National Chimpanzee Brain Resource
Mary	*Pan troglodytes*	F	NCBR	National Chimpanzee Brain Resource
Kinyani	*Gorilla gorilla*	F	NCBR	National Chimpanzee Brain Resource
Kekla	*Gorilla gorilla*	M	NCBR	National Chimpanzee Brain Resource
Molek	*Pongo pygmaeus*	M	NCBR	National Chimpanzee Brain Resource
Minyak	*Pongo pygmaeus*	M	NCBR	National Chimpanzee Brain Resource
Mentubar	*Pongo pygmaeus*	M	NCBR	National Chimpanzee Brain Resource
Hati	*Pongo pygmaeus*	F	NCBR	National Chimpanzee Brain Resource
Buddy	*Hylobates lar*	M	NCBR	National Chimpanzee Brain Resource
Sunny	*Hylobates lar*	M	NCBR	National Chimpanzee Brain Resource
Cleo	*Hylobates lar*	F	NCBR	National Chimpanzee Brain Resource
Cherokee	*Hylobates lar*	F	NCBR	National Chimpanzee Brain Resource

2. Computed Tomography (CT and uCT) Samples and Collections

The extant human ex-vivo cranial Computed Tomography (CT) samples are provided with known sex, Collection ID and the Collection Access Source. The non-human primate ex-vivo cranial Micro-Computed Tomography and Computed Tomography (CT and u-CT) samples are provided with known Sample ID, assigned taxonomy, known sex, Collection ID and the Collection Access Source.

Table 2. The human and non-human primate CT samples with collection IDs and CT source, taxon, and sex of the specimens.

ID	Taxon	Sex	Collection ID	Collection Source	Collection Access
30568	*Saimiri scirueus*	F	MCZ	Harvard Natural History Museum	Morphosource.org
30569	*Saimiri scirueus*	M	MCZ	Harvard Natural History Museum	Morphosource.org
30572	*Saimiri scirueus*	M	MCZ	Harvard Natural History Museum	Morphosource.org
43484	*Saimiri scirueus*	M	MCZ	Harvard Natural History Museum	Morphosource.org
271005	*Sapajus apella*	M	UNSM	Smithsonian Natural History Museum	Smithsonian Natural History Museum
241397	*Sapajus apella*	M	UNSM	Smithsonian Natural History Museum	Smithsonian Natural History Museum
241395	*Sapajus apella*	M	UNSM	Smithsonian Natural History Museum	Smithsonian Natural History Museum
1067	*Sapajus apella*	F	PRICT	Kyoto Primate Research Centre	Morphosource.org
241396	*Sapajus apella*	F	UNSM	Smithsonian Natural History Museum	Smithsonian Natural History Museum
1068	*Sapajus apella*	F	PRICT	Kyoto Primate Research Centre	Morphosource.org
19982	*Cercocebus atys*	M	MCZ	Harvard Natural History Museum	Morphosource.org
25626	*Cercocebus atys*	M	MCZ	Harvard Natural History Museum	Morphosource.org
62639	*Cercocebus atys*	F	MCZ	Harvard Natural History Museum	Morphosource.org
604	*Cercocebus atys*	F	PRICT	Kyoto Primate Research Centre	Morphosource.org
26475	*Macaca mulatta*	M	MCZ	Harvard Natural History Museum	Morphosource.org
61414	*Macaca mulatta*	M	MCZ	Harvard Natural History Museum	Morphosource.org
1160	*Macaca mulatta*	M	PRICT	Kyoto Primate Research Centre	Morphosource.org
361	*Macaca mulatta*	M	PRICT	Kyoto Primate Research Centre	Morphosource.org

362	*Macaca mulatta*	M	PRICT	Kyoto Primate Research Centre	Morphosource.org
363	*Macaca mulatta*	M	PRICT	Kyoto Primate Research Centre	Morphosource.org
1462	*Macaca mulatta*	F	PRICT	Kyoto Primate Research Centre	Morphosource.org
1463	*Macaca mulatta*	F	PRICT	Kyoto Primate Research Centre	Morphosource.org
1464	*Macaca mulatta*	F	PRICT	Kyoto Primate Research Centre	Morphosource.org
1465	*Macaca mulatta*	F	PRICT	Kyoto Primate Research Centre	Morphosource.org
1466	*Macaca mulatta*	F	PRICT	Kyoto Primate Research Centre	Morphosource.org
1467	*Macaca mulatta*	F	PRICT	Kyoto Primate Research Centre	Morphosource.org
162899	*Papio anubis*	M	UNSM	Smithsonian Natural History Museum	Smithsonian Natural History Museum
51380	*Papio anubis*	M	ANHM	American Natural History Museum	Morphosource.org
351	*Papio anubis*	M	PRICT	Kyoto Primate Research Centre	Morphosource.org
397476	*Papio anubis*	F	UNSM	Smithsonian Natural History Museum	Smithsonian Natural History Museum
83515	*Hylobates lar*	F	UNSM	Smithsonian Natural History Museum	Smithsonian Natural History Museum
112711	*Hylobates lar*	F	UNSM	Smithsonian Natural History Museum	Smithsonian Natural History Museum
115502	*Hylobates lar*	F	UNSM	Smithsonian Natural History Museum	Smithsonian Natural History Museum
253539	*Hylobates lar*	F	UNSM	Smithsonian Natural History Museum	Smithsonian Natural History Museum
253599	*Hylobates lar*	F	UNSM	Smithsonian Natural History Museum	Smithsonian Natural History Museum
307759	*Hylobates lar*	F	UNSM	Smithsonian Natural History Museum	Smithsonian Natural History Museum
260590	*Hylobates lar*	F	UNSM	Smithsonian Natural History Museum	Smithsonian Natural History Museum
104438	*Hylobates lar*	M	UNSM	Smithsonian Natural History Museum	Smithsonian Natural History Museum
111970	*Hylobates lar*	M	UNSM	Smithsonian Natural History Museum	Smithsonian Natural History Museum
115501	*Hylobates lar*	M	UNSM	Smithsonian Natural History Museum	Smithsonian Natural History Museum
124024	*Hylobates lar*	M	UNSM	Smithsonian Natural History Museum	Smithsonian Natural History Museum
241423	*Hylobates lar*	M	UNSM	Smithsonian Natural History Museum	Smithsonian Natural History Museum
307752	*Hylobates lar*	M	UNSM	Smithsonian Natural History Museum	Smithsonian Natural History Museum
307756	*Hylobates lar*	M	UNSM	Smithsonian Natural History Museum	Smithsonian Natural History Museum
153822	*Pongo pygmaeus*	F	UNSM	Smithsonian Natural History Museum	Smithsonian Natural History Museum

145309	*Pongo pygmaeus*	F	UNSM	Smithsonian Natural History Museum	Smithsonian Natural History Museum
145306	*Pongo pygmaeus*	F	UNSM	Smithsonian Natural History Museum	Smithsonian Natural History Museum
145302	*Pongo pygmaeus*	F	UNSM	Smithsonian Natural History Museum	Smithsonian Natural History Museum
145300	*Pongo pygmaeus*	F	UNSM	Smithsonian Natural History Museum	Smithsonian Natural History Museum
142186	*Pongo pygmaeus*	F	UNSM	Smithsonian Natural History Museum	Smithsonian Natural History Museum
142185	*Pongo pygmaeus*	F	UNSM	Smithsonian Natural History Museum	Smithsonian Natural History Museum
142199	*Pongo pygmaeus*	M	UNSM	Smithsonian Natural History Museum	Smithsonian Natural History Museum
142188	*Pongo pygmaeus*	M	UNSM	Smithsonian Natural History Museum	Smithsonian Natural History Museum
145305	*Pongo pygmaeus*	M	UNSM	Smithsonian Natural History Museum	Smithsonian Natural History Museum
145304	*Pongo pygmaeus*	M	UNSM	Smithsonian Natural History Museum	Smithsonian Natural History Museum
145303	*Pongo pygmaeus*	M	UNSM	Smithsonian Natural History Museum	Smithsonian Natural History Museum
145301	*Pongo pygmaeus*	M	UNSM	Smithsonian Natural History Museum	Smithsonian Natural History Museum
582726	*Gorilla gorilla*	F	UNSM	Smithsonian Natural History Museum	Smithsonian Natural History Museum
252580	*Gorilla gorilla*	F	UNSM	Smithsonian Natural History Museum	Smithsonian Natural History Museum
252577	*Gorilla gorilla*	F	UNSM	Smithsonian Natural History Museum	Smithsonian Natural History Museum
220060	*Gorilla gorilla*	F	UNSM	Smithsonian Natural History Museum	Smithsonian Natural History Museum
176216	*Gorilla gorilla*	M	UNSM	Smithsonian Natural History Museum	Smithsonian Natural History Museum
176209	*Gorilla gorilla*	M	UNSM	Smithsonian Natural History Museum	Smithsonian Natural History Museum
174716	*Gorilla gorilla*	M	UNSM	Smithsonian Natural History Museum	Smithsonian Natural History Museum
174715	*Gorilla gorilla*	M	UNSM	Smithsonian Natural History Museum	Smithsonian Natural History Museum
174714	*Gorilla gorilla*	M	UNSM	Smithsonian Natural History Museum	Smithsonian Natural History Museum
174712	*Gorilla gorilla*	M	UNSM	Smithsonian Natural History Museum	Smithsonian Natural History Museum
9338	*Pan paniscus*	F	RMCA	Royal Museum of Central Africa	Museum National d'historie naturelle
11352	*Pan paniscus*	F	RMCA	Royal Museum of Central Africa	Museum National d'historie naturelle
26963	*Pan paniscus*	F	RMCA	Royal Museum of Central Africa	Museum National d'historie naturelle
27002	*Pan paniscus*	F	RMCA	Royal Museum of Central Africa	Museum National d'historie naturelle
27698	*Pan paniscus*	F	RMCA	Royal Museum of Central Africa	Museum National d'historie naturelle

26991	*Pan paniscus*	F	RMCA	Royal Museum of Central Africa	Museum National d'historie naturelle
26989	*Pan paniscus*	F	RMCA	Royal Museum of Central Africa	Museum National d'historie naturelle
20882	*Pan paniscus*	F	RMCA	Royal Museum of Central Africa	Museum National d'historie naturelle
26939	*Pan paniscus*	M	RMCA	Royal Museum of Central Africa	Museum National d'historie naturelle
26960	*Pan paniscus*	M	RMCA	Royal Museum of Central Africa	Museum National d'historie naturelle
26996	*Pan paniscus*	M	RMCA	Royal Museum of Central Africa	Museum National d'historie naturelle
27005	*Pan paniscus*	M	RMCA	Royal Museum of Central Africa	Museum National d'historie naturelle
29064	*Pan paniscus*	M	RMCA	Royal Museum of Central Africa	Museum National d'historie naturelle
27696	*Pan paniscus*	M	RMCA	Royal Museum of Central Africa	Museum National d'historie naturelle
220064	*Pan troglodytes*	F	UNSM	Smithsonian Natural History Museum	Smithsonian Natural History Museum
220063	*Pan troglodytes*	F	UNSM	Smithsonian Natural History Museum	Smithsonian Natural History Museum
174710	*Pan troglodytes*	F	UNSM	Smithsonian Natural History Museum	Smithsonian Natural History Museum
174707	*Pan troglodytes*	F	UNSM	Smithsonian Natural History Museum	Smithsonian Natural History Museum
174701	*Pan troglodytes*	F	UNSM	Smithsonian Natural History Museum	Smithsonian Natural History Museum
220327	*Pan troglodytes*	M	UNSM	Smithsonian Natural History Museum	Smithsonian Natural History Museum
220326	*Pan troglodytes*	M	UNSM	Smithsonian Natural History Museum	Smithsonian Natural History Museum
220065	*Pan troglodytes*	M	UNSM	Smithsonian Natural History Museum	Smithsonian Natural History Museum
176228	*Pan troglodytes*	M	UNSM	Smithsonian Natural History Museum	Smithsonian Natural History Museum
174704	*Pan troglodytes*	M	UNSM	Smithsonian Natural History Museum	Smithsonian Natural History Museum
24	*Homo sapiens*	F	Morton	Morton Collection University Pennsylvania	University Pennsylvania
670	*Homo sapiens*	F	Morton	Morton Collection University Pennsylvania	University Pennsylvania
920	*Homo sapiens*	F	Morton	Morton Collection University Pennsylvania	University Pennsylvania
1559	*Homo sapiens*	F	Morton	Morton Collection University Pennsylvania	University Pennsylvania
1698	*Homo sapiens*	F	Morton	Morton Collection University Pennsylvania	University Pennsylvania

1702	*Homo sapiens*	F	Morton	Morton Collection University Pennsylvania	University Pennsylvania
59	*Homo sapiens*	M	Morton	Morton Collection University Pennsylvania	University Pennsylvania
45	*Homo sapiens*	M	Morton	Morton Collection University Pennsylvania	University Pennsylvania
3	*Homo sapiens*	M	Morton	Morton Collection University Pennsylvania	University Pennsylvania
920	*Homo sapiens*	F	ULAC	Universität Leipzig Anatomie Institut	NESPOS Archive
13	*Homo sapiens*	F	ULAC	Universität Leipzig Anatomie Institut	NESPOS Archive
39	*Homo sapiens*	M	ULAC	Universität Leipzig Anatomie Institut	NESPOS Archive
66	*Homo sapiens*	F	ULAC	Universität Leipzig Anatomie Institut	NESPOS Archive
217	*Homo sapiens*	F	ULAC	Universität Leipzig Anatomie Institut	NESPOS Archive
218	*Homo sapiens*	F	ULAC	Universität Leipzig Anatomie Institut	NESPOS Archive
225	*Homo sapiens*	F	ULAC	Universität Leipzig Anatomie Institut	NESPOS Archive
316	*Homo sapiens*	F	ULAC	Universität Leipzig Anatomie Institut	NESPOS Archive
318	*Homo sapiens*	F	ULAC	Universität Leipzig Anatomie Institut	NESPOS Archive
319	*Homo sapiens*	F	ULAC	Universität Leipzig Anatomie Institut	NESPOS Archive
324	*Homo sapiens*	F	ULAC	Universität Leipzig Anatomie Institut	NESPOS Archive
343	*Homo sapiens*	F	ULAC	Universität Leipzig Anatomie Institut	NESPOS Archive
814	*Homo sapiens*	F	ULAC	Universität Leipzig Anatomie Institut	NESPOS Archive
955	*Homo sapiens*	M	ULAC	Universität Leipzig Anatomie Institut	NESPOS Archive
954	*Homo sapiens*	M	ULAC	Universität Leipzig Anatomie Institut	NESPOS Archive
909	*Homo sapiens*	M	ULAC	Universität Leipzig Anatomie Institut	NESPOS Archive
904	*Homo sapiens*	M	ULAC	Universität Leipzig Anatomie Institut	NESPOS Archive
813	*Homo sapiens*	M	ULAC	Universität Leipzig Anatomie Institut	NESPOS Archive
812	*Homo sapiens*	M	ULAC	Universität Leipzig Anatomie Institut	NESPOS Archive
335	*Homo sapiens*	M	ULAC	Universität Leipzig Anatomie Institut	NESPOS Archive
308	*Homo sapiens*	M	ULAC	Universität Leipzig Anatomie Institut	NESPOS Archive

307	*Homo sapiens*	M	ULAC	Universität Leipzig Anatomie Institut	NESPOS Archive
12	*Homo sapiens*	M	ULAC	Universität Leipzig Anatomie Institut	NESPOS Archive
16	*Homo sapiens*	M	ULAC	Universität Leipzig Anatomie Institut	NESPOS Archive
19	*Homo sapiens*	M	ULAC	Universität Leipzig Anatomie Institut	NESPOS Archive
57	*Homo sapiens*	M	ULAC	Universität Leipzig Anatomie Institut	NESPOS Archive
58	*Homo sapiens*	M	ULAC	Universität Leipzig Anatomie Institut	NESPOS Archive
60	*Homo sapiens*	M	ULAC	Universität Leipzig Anatomie Institut	NESPOS Archive
210	*Homo sapiens*	M	ULAC	Universität Leipzig Anatomie Institut	NESPOS Archive
213	*Homo sapiens*	M	ULAC	Universität Leipzig Anatomie Institut	NESPOS Archive
223	*Homo sapiens*	M	ULAC	Universität Leipzig Anatomie Institut	NESPOS Archive
235	*Homo sapiens*	M	ULAC	Universität Leipzig Anatomie Institut	NESPOS Archive
257	*Homo sapiens*	M	ULAC	Universität Leipzig Anatomie Institut	NESPOS Archive
258	*Homo sapiens*	M	ULAC	Universität Leipzig Anatomie Institut	NESPOS Archive
33	*Homo sapiens*	M	ULAC	Universität Leipzig Anatomie Institut	NESPOS Archive

3. Computed Tomography (CT and µCT) Extinct Samples and Collections

The extinct ex-vivo cranial Computed Tomography (CT) extinct of hominin specimens and ex-vivo cranial Micro-Computed Tomography (u-CT) extinct nonhuman primate specimens provided with Specimen IDs, assigned taxonomy, Sample Collection and Collection Access Source.

Table 3. The extinct human and non-human primate CT samples with collection IDs and CT source, taxon, and of the specimens.

ID	Taxon	Collection ID	Collection	Access Agreement
CRM 1	*Homo sapiens*	Cro-Magnon 1	NESPOS Archive	NESPOS
Mladec 1	*Homo sapiens*	Mladec 1	NESPOS Archive	NESPOS
Singa 1	*Homo sapiens*	Singa 1	Vienna Digital Fossil Hominid Archive	Vienna
Skhul 5	*Homo sapiens*	Skhul V	American Museum Natural History	NESPOS
LH18	*Homo sapiens*	LH-18	Vienna Digital Fossil Hominid Archive	Vienna
Gibraltar 1	*Homo neanderthalensis*	NHMUK-PA-EM-3881	Natural History Museum	NHM
La Ferrassie 1	*Homo neanderthalensis*	MNHN	Museum National d'historie naturelle	MNHN
La Chapelle	*Homo neanderthalensis*	MNHN	Museum National d'historie naturelle	MNHN
Tabun 1	*Homo neanderthalensis*	NHMUK-PA-EM-3640	Natural History Museum	NESPOS
La Quina 5	*Homo neanderthalensis*	NMHN	Museum National d'historie naturelle	NMNH
Kabwe	*Homo heidelbergensis*	NHMUK-PA-E-686	Natural History Museum	NHM
Bodo	*Homo heidelbergensis*	Vienna	Vienna Digital Fossil Hominid Archive	NESPOS
KNMER-3883	*Homo ergaster*	KNM	National Museums of Kenya	KNMN
KNMER-3733	*Homo ergaster*	KNM	National Museums of Kenya	KNMN
OH9	*Homo ergaster*	KNM	National Museums of Kenya	KNMN
Sangiran2	*Homo erectus*	SMF	Senckenberg Museum Frankfurt	SMF
Sangiran4	*Homo erectus*	SMF	Senckenberg Museum Frankfurt	SMF

Sangiran17	*Homo erectus*	ANUBAC	Australian National University Biological Anthropology Collection	ANU
Sm3	*Homo erectus*	NESPOS	American Museum Natural History	NESPOS Archive
LB1	*Homo floresiensis*	ANUBAC	Australian National University Biological Anthropology Collection	ANU
KNM-ER-1805	*Homo habilis*	KNM	National Museums of Kenya	KNMN
KNM-ER-1813	*Homo habilis*	KNM	National Museums of Kenya	KNMN
OH5	*Paranthropus boiesi*	OH	Vienna Digital Fossil Hominid Archive	NESPOS Archive
KNM-ER-406	*Paranthropus boiesi*	KNM	National Museums of Kenya	KNMN
KNM-WT-17000	*Paranthropus aethiopicus*	KNM	National Museums of Kenya	KNMN
STS-5	*Australopithecus africanus*	STS-5	Vienna Digital Fossil Hominid Archive	NESPOS
STS-71	*Australopithecus africanus*	STS-71	Vienna Digital Fossil Hominid Archive	NESPOS
DMNH-SK-554	*Dinopithecus ingens*	DMNH	Distong Museums of South Africa	Morphosource.org
DMNH-CO-135	*Papio angusticeps*	DMNH	Distong Museums of South Africa	Morphosource.org
DMNH-CO-100	*Papio angusticeps*	DMNH	Distong Museums of South Africa	Morphosource.org
CGM-40327	*Aegyptopithecus zeuxis*	CGM	Cairo Geological Museum	Morphosource.org
CGM-85785	*Aegyptopithecus zeuxis*	CGM	Cairo Geological Museum	Morphosource.org
DPC-1208	*Aegyptopithecus zeuxis*	DPC	Duke Lemur Center Divison of Fossil Primates	Morphosource.org
DPC-5401	*Aegyptopithecus zeuxis*	DPC	Duke Lemur Center Divison of Fossil Primates	Morphosource.org
DPC-18651	*Parapithecus grangeri*	DPC	Duke Lemur Center Divison of Fossil Primates	Morphosource.org
KNM-MB-29100	*Victoriapithecus macinnesi*	KNM-MB	University College London, National Museums of Kenya	UCL & KNMN
DPC-9867	*Apidium phiomense*	DPC	Duke Lemur Center Divison of Fossil Primates	Morphosource.org
DPC-11388	*Cateopithecus browni*	DPC	Duke Lemur Center Divison of Fossil Primates	Morphosource.org
DPC-14095	*Proteopithecus sylviae*	DPC	Duke Lemur Center Divison of Fossil Primates	Morphosource.org
MPV-3501	*Homunculus patagonicus*	MPV	Museo Argentino de Ciencias Naturales	Morphosource.org
FMI-619	*Tremacebus harringtoni*	FML	Museo de Fundacion Miguel Lillo	Morphosource.org